

**SONIC FATIGUE TOLERANCE OF GLASS  
FILAMENT STRUCTURE:  
EXPERIMENTAL RESULTS**

*J. A. HAYES*

\*\*\* Export controls have been removed \*\*\*

This document is subject to special export controls and each transmittal to foreign governments or foreign nationals may be made only with prior approval of Vehicle Dynamics Division (FDD), Air Force Flight Dynamics Laboratory, Wright-Patterson AFB, Ohio 45433.

## FOREWORD

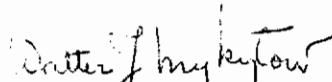
The research in this report was performed by North American Aviation, Inc., Columbus Division, Columbus, Ohio, for the Aero-Acoustics Branch, Vehicle Dynamics Division, Air Force Flight Dynamics Laboratory, Wright-Patterson Air Force Base, Ohio, under Contract AF 33(615)-2683, Evaluation of Sonic Fatigue Tolerance of Glass Filament Structures. This is part of a continuing effort to develop and establish the tolerance levels in terms of sound pressure levels for fiber reinforced structures applicable to many classes of flight vehicles and is part of the Research and Technology Division, Air Force Systems Command's exploratory development program.

The work was conducted under Project 1471, Aero-Acoustic Problems, Task 147101, Sonic Fatigue, with Mr. R.C.W. van der Heyde, as project engineer. The work started 15 May 1965 and ended 15 July 1966. The project leader was Mr. J.A. Hayes, assisted by Mr. M. Fife who conducted the tests, Mr. C. Maines who performed the structural optimization of the glass fiber panels, and Mr. A.M. Federico who performed the metallurgical examination of the failed aluminum control panels.

Others who contributed were Mr. J. Sanborn of the Structural Composites Group, NAA-Columbus, who produced the Pilot Test Program glass fiber panels, and Mr. Darwin Hardin of the Flexible Company, Loudonville, Ohio, who was responsible for the production test panels.

The manuscript was released by the authors in July 1966.

This technical report has been reviewed and is approved.

  
WALTER J. MYKYTOW

Asst. for Research & Technology  
Vehicle Dynamics Division  
AF Flight Dynamics Laboratory

## ABSTRACT

Sonic Fatigue experimental test results on a series of sixty flat rectangular glass fiber sandwich test panels are presented and discussed. The panels were of the fluted core (corrugated) type, had nominal overall dimensions of 24" x 30" x 0.45", and a nominal surface weight of one pound per square foot. The fluted core glass fabric (181 and 151 S glass) was of the integrally woven variety. A vacuum process was employed to impregnate the glass cloth with resin. Twenty each of three types of panel were sonic fatigue tested using a discrete frequency siren, five identical panels at four different sound pressure levels, to provide three S-N (Sound Pressure Level Vs. Cycles to Failure) plots. Twenty aluminum skin-stringer panels of the same overall dimensions and surface weight were similarly tested for control.

# Contrails

## TABLE OF CONTENTS

<u>SECTION</u>		<u>PAGE</u>
I	INTRODUCTION	1
II	SUMMARY	3
III	PILOT TEST PROGRAM	4
	1. Discussion	4
	2. Aluminum Control Panel Design	4
	3. Test Fixture Design and Evaluation	5
	4. Aluminum Control Panel Discrete Frequency Tests	7
	5. Aluminum Control Panel Broad Band Siren Tests	8
	6. Type I Glass Fiber Panel Preliminary Design	8
	7. Type I Glass Fiber Panel Discrete Frequency Tests	9
	8. Type II Glass Fiber Panel Preliminary Design	10
	9. Type II Glass Fiber Panel Discrete Frequency Tests	10
	10. Type III Glass Fiber Panel Preliminary Design	10
	11. Type III Glass Fiber Panel Discrete Frequency Tests	11
	12. Conclusions	11
IV	ALUMINUM CONTROL PRODUCTION PANEL TESTS	
	1. Discussion	13
	2. Panel Modal Response Characteristics	14
	3. Modal Damping Measurements	15
	4. Panel Stress vs. Frequency Response Data	16
	5. Non-Linearity Effects	17
	6. Panel SPL vs. Cycles to Failure Data	17
	7. Sound Field Measurements	18
	8. Failure Analysis	18
	9. Conversion to Random S-N Data	19
V	TYPE I GLASS FIBER PRODUCTION PANEL TESTS	
	1. Discussion	25
	2. Panel Design	25
	3. Panel Modal Response Characteristics	25
	4. Panel Stress vs. Frequency Response Data	26
	5. Modal Damping Measurements	27
	6. Panel SPL vs. Cycles to Failure Data	27
	7. Sound Field Measurements	28
	8. Failure Analysis	28

## TABLE OF CONTENTS (Cont'd)

<u>SECTION</u>		<u>PAGE</u>
VI	TYPE II GLASS FIBER PRODUCTION PANEL TESTS	29
	1. Discussion	29
	2. Panel Design	29
	3. Panel Modal Response Characteristics	29
	4. Panel Stress vs. Frequency Response Data	30
	5. Modal Damping Measurements	30
	6. Panel SPL vs. Cycles to Failure Data	30
	7. Failure Analysis	30
VII	TYPE III GLASS FIBER PRODUCTION PANEL TESTS	31
	1. Discussion	31
	2. Panel Design	31
	3. Panel Modal Response Characteristics	31
	4. Panel Stress vs. Frequency Response Data	31
	5. Modal Damping Measurements	32
	6. Panel SPL vs. Cycles to Failure Data	32
	7. Failure Analysis	32
VIII	CONCLUSIONS AND RECOMMENDATIONS	33
	APPENDIX A - Test Set-up and Instrumentation	127
	APPENDIX B - Glass Fiber Panels Structural Optimization	135
	APPENDIX C - Glass Fiber Panels Manufacturing Data	148
	APPENDIX D - Fluted Core Glass Fiber Flight Vehicle Structural Applications	154
	REFERENCES	126

# Contracts

## LIST OF FIGURES

<u>FIGURE NO.</u>	<u>TITLE</u>	<u>PAGE</u>
1	Aluminum Control Panel Original Design	36
2	Aluminum Control Panel Final Design	37
3	Sonic Fatigue Test Fixture - Original Design	38
4	Sonic Fatigue Test Fixture - Final Design	39
5	Test Fixture Response at Position 1 (150 db)	40
6	Test Fixture Response at Position 2 (150 db)	41
7	Test Fixture Response at Position 1 with Weights (150 db)	42
8	Control Panel Response Position 21 (150 db)	43
9	Panel C1X Strain Gage Locations	44
10	Panel C1X No. 2 Strain Gage Response at 140 db and 160 db SPL	45
11	Strain Gage Locations Control Panel C2X	46
12	Panel C2X No. 3 Strain Gage Response at 150 db SPL	47
13	Panel C2X No. 5 Strain Gage Response at 150 db SPL	48
14	Typical Broad Band Siren Noise Spectrum 165 db SPL O/A	49
15	Panel C3X after Broad Band Siren Test	50
16	Type I Glass Fiber Panel - Original Design	51
17	Type I Glass Fiber Panel - Strain Gage Locations	52
18	Panel Type I - No. 1 Strain Gage Response	53
19	Panel Type I - No. 3 Strain Gage Response (145 db)	54
20	Strain Gage Locations Type II Glass Fiber Panel	55
21	Panel Type II Mid Panel Strain Gage E1 Response	56
22	Panel Type II Mid Panel Strain Gage E2 Response	57
23	Panel Type II Mid Panel Strain Gage E3 Response	58
24	Panel Type II Corner Strain Gage C1 Response	59
25	Panel Type II Corner Strain Gage C2 Response	60
26	Panel Type II Corner Strain Gage C3 Response	61
27	Panel Type II Mid Panel Displacement vs. SPL	62
28	Type II Glass Fiber Panel after Failure	63
29	Glass Fiber Panel Type III Strain Gage Location	64
30	Glass Fiber Panel Type III Gage No. 1 Response (165 db)	65
31	Strain Gage Locations Production Control Panels	66
32	Skin-Stringer Panel, Common Mode Shapes	67
33	Aluminum Control Panel Mode Shapes - Sub-Panels First Mode	68
34	Control Panel No. 24 Mid-Bay Third Mode (189 Hz.)	69
35	Typical Control Panel Stress vs. Frequency Response 140 db (gage position 2)	70
36	Typical Control Panel Stress vs. Frequency Response 145 db (gage position 2)	71
37	Typical Control Panel Stress vs. Frequency Response 150 db (gage position 2)	72

# Contrails

## LIST OF FIGURES (Cont'd)

<u>FIGURE NO.</u>		<u>PAGE</u>
38	Typical Control Panel Stress vs. Frequency Response 155 db (gage position 2)	73
39	Stress Response Data Control Panel No. 25 - Effects of "Oilcan"	74
40	Control Panel Stress Response Showing Influence of Stringer Rotation	75
41	Control Panel Sound Pressure vs. RMS Stress (No. 2 Gage)	76
42	Aluminum Control Panels SPL vs. Cycles to Failure Plot	77
43	Control Panel Failing Stress vs. Cycles to Failure	78
44	Microphone Locations in Siren Test Section	79
45	Typical Control Panel Microphone and Strain Gage Oscilloscope Traces	80
46	Narrow Band Analysis of #4 Microphone Noise (140 db)	81
47	Narrow Band Analysis of #4 Microphone Noise (150 db)	82
48	Narrow Band Analysis #2 Strain Gage Data (140 db)	83
49	Narrow Band Analysis of #2 Strain Gage Data (150 db)	84
50	Cross-sectional View of Control Panel AF-111 Adhesive Bond Line	85
51	Control Panel Typical Skin Failures	86
52	Skin-Stringer Attachment - Improved Design	87
53	Random S-N Curve for 7075-T6 Alclad	88
54	Glass Fiber Production Test Panel Sectional Views	89
55	Type I Glass Fiber Panel Mode Shapes	90
56	Accelerometer Locations for Panel Deflection Measurements	91
57	Type I Panel Deflection vs. SPL in Flute Direction	92
58	Type I Panel Deflection vs. SPL, Transverse Flute Direction	93
59	Type I Panel-Mid Panel Deflection vs. SPL	94
60	Type I Panel Frequency Response Characteristics (Gage Position #1)	95
61	Type I Panel Frequency Response Characteristics (Gage Position #2)	96
62	Typical Type I Panel Amplitude Decay Trace	97
63	Type I Panels SPL vs. Cycles to Failure Plot	98
64	Glass Fiber Panel S-N Curves	99
65	Microphone and Strain Gage Oscilloscope Traces - Type I Panels	100
66	Type I Panel Cross-Section after Failure	101
67	Type II Panel Deflection vs. SPL Flute Direction	102
68	Type II Panel Deflection vs. SPL, Transverse Flute Direction	103
69	Type II Panel - Mid Panel Deflection vs. SPL	104
70	Type II Panel Frequency Response Characteristics	105

# Contrails

## LIST OF FIGURES (Cont'd)

<u>FIGURE NO.</u>		<u>PAGE</u>
71	Type II Panels - SPL vs. Cycles to Failure Plot	106
72	Type II Panel - Cross Section of Top Doubler Edge after Failure	107
73	Type III Panel Deflection vs. SPL in Flute Direction	108
74	Type III Panel Deflection vs. SPL, Transverse Flute Direction	109
75	Type III Panel - Mid Panel Deflection vs. SPL	110
76	Type III Panel Frequency Response Characteristics	111
77	Type III Panels SPL vs. Cycles to Failure Plot	112
78	Typical Type III Mid Panel Failure	113
79	Type III Panel Flute Line Failure - Close-up View	114
80	Simplified Block Diagram of Siren Test Set-up	130
81	View of Sonic Fatigue Test Fixture with Glass Fiber Panel Installed	131
82	Dynamic Strain Gage Circuit	132
83	Typical HE-141 Strain Gage Grid Failure	133
84	Test Set-up Panel Mode Shape and Damping Measurements	134
85	Lifting Surface Optimization Program Box Beam	143
86	Aluminum Control Panel Cross Section	143
87	Box Beam Glass Fiber Panel, Load and Bending Moment Diagrams	144
88	Glass Fiber Panel - Lower Surface and Core Dry Fabric Lay-up	149
89	Glass Fiber Panel - Upper Surface Dry Fabric Lay-up	150
90	Glass Fiber Panel - Caul Tool	151
91	Glass Fiber Panel - Resin Pouring	152
92	Diagram of Vacuum Impregnation System	153
93	Fluted Core Glass Fiber Wing and Tail Boom Sectional Views (OV-10A)	155



# Contrails

## LIST OF TABLES

<u>TABLE NO.</u>	<u>TITLE</u>	<u>PAGE</u>
I	Aluminum Control Panel Sonic Fatigue Test Results	115
II	Control Panel Hardnesses Data	116
III	Control Panel Hardnesses Data	116
IV	Type I Glass Fiber Panels - Sonic Fatigue Test Results	117
V	Type I Glass Fiber Panels - Damping Data	118
VI	Type I Glass Fiber Panels Stress Summary	119
VII	Type II Glass Fiber Panels - Damping Data	120
VIII	Type II Glass Fiber Panels - Sonic Fatigue Test Results	121
IX	Type II Glass Fiber Panels Stress Summary	122
X	Type III Glass Fiber Panels - Damping Data	123
XI	Type III Glass Fiber Panels Sonic Fatigue Test Results	124
XII	Type III Glass Fiber Panels Stress Summary	125
XIII	IBM 7090 Lifting Surface Optimization Program Input and Output Data	145
XIV	IBM 7090 Lifting Surface Optimization Program Output Data	146
XV	IBM 7090 Lifting Surface Optimization Program Output Data	147

# *Contrails*

## SECTION I

### INTRODUCTION

Recent advances in the state-of-the-art of composite filamentary technology in general, and glass fiber composites in particular, have led to the latter being seriously considered for flight vehicle structural applications. Reference (1) and (2). The promise of lower weight, lower cost, lower radar detection, easier maintainability, superior corrosion resistance, and ready repair of damage in the field, compared with metal structures, has recently led to proposals for an all glass fiber COIN aircraft from Convair, Goodyear and Columbus Division of North American Aviation.

Developments in resin technology allowing the use of glass fiber composites for high temperature applications, are expected eventually to permit the use of such composites in supersonic aircraft, where high noise and temperature environments may be significant factors in the design of the structure. The increasing use of high powered lift fans for VTOL aircraft has resulted in very high discrete frequency sound pressure levels of the order of 170 db in structural areas adjacent to the fans. These levels in combination with thermal problems of hot gas-driven fans constitute a severe environment for which composite structures may prove the only solution.

While research and development of more advanced composites utilizing Boron, Carbon and other recently developed filaments is proceeding rapidly, glass fiber reinforced composites are more likely to be employed in flight vehicles on a significant scale in the immediate future. The program reported herein is therefore designed to provide basic sonic fatigue tolerance experimental test data and design criteria for glass fiber flight vehicle structure.

The majority of glass fiber flight vehicle structural applications to date have been dictated by radar transparency considerations. These applications have required the use of simple laminated-skin moulded structures typical of many radomes. These structures are generally lightly loaded and have a relatively low structural efficiency. For primary load bearing structure, such as a wing box or spar, the low Young's Modulus, coupled with a relatively linear stress-strain relationship (low elongation) of glass fiber composites tends to preclude buckling of skin panels at high loads. This makes sandwich construction mandatory in order to achieve the necessary structural stiffness.

The most commonly used glass fiber sandwich is honeycomb. A corrugated fluted core glass fabric in which the face sheets and cores are interwoven was developed some years ago by the Raymond Development Industries under the name of "Raypan". This offers an alternate sandwich

# Contrails

construction which has advantages over honeycomb for some applications. With highly loaded skins the core helps carry part of the load, making for a more efficient structure. The facing material and core are integral, requiring a break in the glass filaments for separation, whereas face and core of honeycomb rely entirely on a secondary adhesive line contact bond. Fluted core provides better skin to skin shear transfer through the diagonal truss core compared with honeycomb core. Fluted core is more readily formed over small radii (across the flute direction) than honeycomb core. Honeycomb construction tends to be lighter for some low stress buckling applications. It is easier to manufacture and inspect since the cores are precured before the skins are bonded. Some aircraft structural applications of glass fiber fluted core are briefly discussed in Appendix D.

Three glass fiber fluted core sandwich configurations were selected for sonic fatigue testing and evaluation. The first configuration selected had a hollow (unstabilized) core, while the second and third configurations were foam stabilized. An aluminum control panel of the same surface weight (1 lb./ft.<sup>2</sup>) was used for comparative testing. The data presented in this report are intended for use in the development of sonic fatigue design techniques for this type of glass fiber sandwich construction. The data will be used in the development of a series of Sonic Fatigue Engineering Design Charts for these and similar composite sandwich constructions, for use in glass fiber flight vehicle design.

NOTE: All sound pressure levels in this report are in reference to  $2 \times 10^{-5}$  Newtons/meter<sup>2</sup> (0.0002 dynes/cm<sup>2</sup>).

## SECTION II

### SUMMARY

Three types of glass-fiber reinforced plastic sandwich construction were investigated in an experimental sonic fatigue test program designed to provide basic sonic fatigue resistivity experimental test data for such construction. A literature search, (Volume 1 of this report), was made of glass fiber reinforced flight vehicle structural technology, with particular emphasis on flight vehicle structural applications. This search revealed a multiplicity of glass fiber applications to flight vehicles. These were mainly in secondary structure such as radome fairings where solid laminate construction was used. The search also showed a dearth of information on specific glass fiber sonic fatigue applications. Because of the low Young's Modulus of glass fiber solid laminates (less than one third that of aluminum), sandwich construction is mandatory for many structural applications to achieve the necessary stiffness. Three types of fluted core (diagonal truss flutes at 60°) were selected for evaluation, one design with hollow flutes and the other two designs with polyurethane foam filled flutes. An aluminum skin-stringer panel with a surface weight of approximately 1 lb/ft.<sup>2</sup> was used as a control. The glass fiber panels were first optimized for end load carrying capability and found to be lighter than the control panel. A pilot sonic fatigue test program was conducted to evaluate proposed panel designs. The control panel was modified as a result of this program by the addition of stringer end plates to improve torsional restraint of the stringers. The glass fiber panel designs were finalized and a choice of discrete frequency siren sonic fatigue testing was made for all panels in the program.

A total of twenty sonic fatigue test panels, five each at four different discrete frequency sound pressure levels were required to establish sound pressure level vs. cycles to failure data. The control panel sound pressure test levels were 140 db, 145 db, 150 db, 155 db. The control panels approached infinite life at 140 db SPL and failed in approximately 6 minutes at 155 db SPL. The corresponding sound pressure test levels for the glass fiber panels were 155-156 db, 157.5 db, 160 db and 163 db. The majority of the glass fiber panels approached infinite life at 155-156 db and failed in 3-5 minutes at 163 db SPL.

The glass fiber panels exhibited high damping and excellent sonic fatigue resistivity compared with the control panel. The Type III glass fiber panel design (Zerocel foam-filled core at 151-S glass fabric weave) was superior in sonic fatigue resistivity to the other two glass fiber panel designs employing 181-S glass fabric weave.

## SECTION III

### PILOT TEST PROGRAM

#### 1. DISCUSSION

The literature review phase of this program

showed that there are as yet no satisfactory analytical techniques for designing fluted core structures for sonic fatigue applications available at present. Accordingly, it was concluded that an experimental approach using a Pilot Test Program was needed to evolve satisfactory sonic fatigue test panel designs for production testing.

#### Pilot Test Program Objectives

The principal objectives of this program were:

- (a) To evolve three satisfactory glass fiber fluted core (corrugated) sonic fatigue test panel design configurations to be designated Type I, Type II, and Type III for comparative testing with an aluminum control panel of the same surface weight (1 lb/ft.<sup>2</sup>) and overall dimensions (24" x 30").
- (b) To determine whether broad band or discrete frequency testing should be employed for production panels.
- (c) To evaluate test fixture design and test set-up and instrumentation.
- (d) To determine a suitable range of SPL test levels for each group of test panels.
- (e) To examine modal response characteristics of each proposed test panel design, and identify critical frequencies.
- (f) To determine optimum location of strain gages.
- (g) To investigate panel failure modes and verify failure detection methods.

#### 2. ALUMINUM CONTROL PANEL DESIGN

A number of aluminum sonic fatigue test panel designs were considered for use as a control panel.

These included aluminum honeycomb sandwich, bonded beaded, chemi-milled waffle grid, and skin-stringer construction. A skin-stringer

7075-T-6 Aluminum design was selected as the most suitable design for this program for the following reasons:

- (a) Skin-stringer construction is currently considered to be by far the most representative of the majority of aluminum flight vehicle structures.
- (b) More experimental sonic fatigue test data are available for this type of structure than for any other.
- (c) Skin-stringer construction is more readily analyzed from a sonic fatigue aspect than sandwich designs such as aluminum honeycomb.
- (d) Skin-stringer construction can be more readily modified structurally or repaired during preliminary test evaluation to alter its potential fatigue life, e.g., by change of skin gage, whereas bonded or chem-milled panels are difficult to repair or modify after assembly.

#### Original Design

The general arrangement of this panel is shown on Figure 1. The design is typical of most current conventional aircraft structures, the aspect ratio of the bays being quite commonly found in fuselage, flap, aileron and empennage trailing edge structures. The 0.040" Z stiffeners are bonded and riveted to the 0.032" skins. All materials are 7075 T-6 Alclad. Overall dimensions are 24" x 30" and the weight is 5 lb. The 1/4 inch stringer tie-in bolts were used to replace the rivets originally specified when the latter worked loose after a few preliminary frequency sweeps at low SPL's. Further frequency sweeps at higher sound pressure levels showed that stringer rotation was excessive and further modifications were necessary.

#### Modified Final Design

The modified final design, which was also adapted for production testing is shown on Figure 2. The 1/2 inch bolts were removed and small gusset plates were added to provide better stringer-end tie-in, and limit torsional vibration of the stringers. These plates proved effective, but did not entirely eliminate stringer rotation. The addition of the gusset plates increased the panel nominal weight from 5 lb. to 5.25 lb.

### 3. TEST FIXTURE DESIGN

The design objectives for the test fixture were:

# Contrails

- (a) To provide a single fixture capable of accommodating all test panel designs in the program without the need for changing and attachments.
- (b) To provide test panel and fixity approximating that to be employed in the sonic fatigue investigations on similar size test panels in the RTD Sonic Fatigue Facility.
- (c) To be compatible with siren test section of Columbus Division of NAA sonic fatigue test facility.

## Origin Test Fixture Design

A general arrangement of this design is shown on Figure 3. A 36" x 56" x 3/8" thick structural steel plate with a 24" x 36" rectangular hole forms the base, to which are bolted steel edge members. The aluminum "picture frame", Figure 3, was in turn bolted to the steel angle edge members. Test panels were attached to the picture frame nut plates by 3/16" bolts at 2" spacing.

During preliminary evaluation of this design, it became obvious that fixture modes were intruding into the control panel response and detuning was necessary. It was decided to add heavy edge reinforcing in the form of a bolted-on frame of channel section structural steel members.

## Final Test Fixture Design

The final version of the test fixture design is shown on Figure 4. The 50 lb. lead weights were added to eliminate the first bending mode of the vertical channel-section edge members. Due to a number of aluminum "picture frame" failures in the corner welds, Figure 3, it was decided to discontinue welding corners and assemble the frame as four separate edge members, Figure 4. This proved quite satisfactory and did not appear to alter end fixity significantly.

## Test Fixture Evaluation

The original test fixture design, Figure 3, was installed in the discrete frequency siren test facility and the first aluminum control panel No. C-1-X was mounted in it. During initial frequency sweeping at low SPL's, it was immediately apparent from stroboscopic examination that the fixture and the test panel were both unsatisfactory. The fixture was modified as shown on Figure 4, however, the 50 lb. weights were not included at this stage. The 1/4 inch bolts were added to the control panel, Figure 1.



A total of some twenty-seven accelerometer locations were used to probe the fixture and panel response. Two important frame accelerometer locations, positions 1 and 2, are shown on Figure 4. Typical accelerometer frequency response data from these positions, with the test panel removed, are shown on Figures 5 and 6 respectively, for 150 db SPL. The large peak at 60 Hz, Figure 5, was at first thought to be a 60 Hz instrumentation fault, however, it was later identified as first bending mode of the vertical channel section fixture edge reinforcement. The effect of adding 50 lb. weights is shown on Figure 7 where this peak virtually disappears.

Figure 8 shows accelerometer location 21 (mid sub-panel) frequency response at 150 db.

#### 4. ALUMINUM CONTROL PANEL DISCRETE FREQUENCY TESTS

##### Frequency Sweep Tests Panel C-1-X

A total of six Budd type C12-121 strain gages were affixed to panel No. C-1-X as shown on Figure 9. Typical stress vs. frequency response data for strain gage #2 (mid-panel position) are shown for 140 db and 160 db on Figure 10. A large number of stress-frequency sweeps were performed on this panel and the stress response data showed multimodal response characteristics typical of this construction. During the latter part of the frequency sweep tests the 1/4 inch bolts periodically worked loose and had to be re-tightened. This was no doubt due to the large stringer rotation.

##### Failure Tests - Panel C-1-X

Upon completion of the stress frequency response tests, the panel was subjected to a discrete frequency SPL of 160 db at 155 Hz. Failure occurred at a stringer heel, Figure 1, after some ten minutes running i.e.,  $9.28 \times 10^4$  cycles. Torsional rotation of the stringer was the primary cause of failure.

##### Frequency Sweep Tests - Panel C-2-X

The second aluminum control panel No. C-2-X was modified by the addition of gusset plates, Figure 2. Eight strain gages were affixed to this panel as shown on Figure 11, and stress vs. frequency data recorded on tape for SPL's of 145 db and 150 db.

Typical response data for gage #3 and gage #5 for 150 db SPL are shown on Figures 12 and 13, respectively. Stroboscopic examination of panel mode shapes showed that the two critical modes corresponded to sub-panel in-phase (upper frequency) and sub-panel anti-phase (lower frequency) response. The frequency separation of these modes

was only of the order of 10 Hz.

## Failure Tests - Panel C-2-X

Upon examination of the stress response data, it was decided to use the upper (in phase) frequency for failure test. Considerable difficulty was encountered in holding the panel on the desired resonant frequency since this shifted gradually downwards from 160 Hz to 150 Hz in the course of the test. There was evidence of increasing "oilcan" in the sub-panels as the test progressed. The panel failed after 41 minutes and 8 seconds at resonance at 145 db. The mean resonant frequency was 155 Hz, corresponding  $3.82 \times 10^5$  cycles to failure. Failure occurred in the skin adjacent to a stringer heel. This test showed the effectiveness of the gusset plates in preventing excessive stringer rotation, and the design was adopted for production. The multi-modal response characteristics of this panel clearly indicated that broad band testing was desirable.

## 5. ALUMINUM CONTROL PANEL BROAD BAND SIREN TESTS

The third aluminum control panel, No. C-3-X, which was identical in all respects to panel No. C-2-X, was strain gaged at eight locations as for panel No. C-2-X and the stress response data from each gage recorded on tape for a series of test runs at 140 db, 145 db, 150 db, 155 db, and 160 db, in the broad band siren facility. Typical siren sound test spectrum for an O/A SPL of 165 db is shown on Figure 14; sound spectra for lower levels were similar. Panel C-3-X was run for 10 minutes at 155 db O/A SPL in the broad band siren without sign of failure. The sub-panel in-phase mode was evident from a stroboscopic examination of the panel motion, however, many other significant modes were also observed. The panel failed across #3 strain gage after a further 40 minutes running at 160 db. Failure (Figure 15) was identical to that of Panel No. C-2-X.

## 6. TYPE I GLASS FIBER PANEL PRELIMINARY DESIGN

The general arrangement of this panel is shown on Figure 16. The panel is made up of an integrally woven fluted core of 181-S glass, both flutes and skin having a nominal finished thickness of .010". Polypropylene triangular mandrels are used to keep the flutes in shape during resin impregnation and pre-cure phase. These are later removed to give a hollow fluted core. The upper and lower outer skins consist of two plies of 181-S glass fabric\* layed up at  $45^\circ$  to the flute direction. The end closeout for the transverse-to-flute direction is shown on Figure 16, Section A-A, and for the parallel-to-flute direction, the flutes were cut off at  $60^\circ$  and the ends closed out using a secondary-bonded (3-ply) angle.

\*Nominal thickness 0.010" per ply.

Resin impregnation was via the vacuum bag technique using Jones Dabney EPIREZ-510 epoxy resin and APCO 320 catalyst. Further details of manufacture are given in Appendix C.

This panel was optimized for end load carrying capability,\*\*(See Appendix B). The finished weight was 4.54 lb. (2061 grms.), and the overall thickness was 0.455 inches.

## 7. TYPE I GLASS FIBER DISCRETE FREQUENCY TESTS

### Frequency Sweep Tests

A number of strain gages were affixed to this panel at locations shown on Figure 17. The panel was then subjected to constant SPL vs. frequency sweeps from 0 to 500 Hz at SPL's of 140 db, 145 db, 150 db, 155 db and 160 db. However, because of the fact that most of the gages failed during preliminary sweeps, it was not possible to obtain a complete set of data from all gages. The premature failure of the gages was found to be due to excessive strains in the glass fiber resulting from the relatively low tensile modulus ( $E \approx 3 \times 10^6$  psi) for this material. This was incompatible with the 5% elongation of the Budd Type C-12-141 gages, which were used successfully on the aluminum panels. Budd Type HE-141 gages (15% elongation) were substituted for all further glass fiber panels.

Typical stress vs. frequency response data for gage position 1 at 145 db, 150 db, 155 db, are shown on Figure 18.

Figure 19 shows similar data for gage position 3 at 145 db.

The first peak at approximately 60 Hz, Figure 18, is the panel-aluminum picture frame first mode, the second peak being the panel first mode, and the upper peak appears to be the fifth harmonic of the lower mode. The upper peak is not present on the response data from gage position 3 (in direction of flutes). This is to be expected since the panel has a much higher stiffness in the flute direction than occurs across the flute direction.

### Failure Tests

This panel was tested for 32 minutes and 24 seconds at SPL of 160 db, when failure occurred on the skin at the lower right hand corner, Figure 17. Failure was readily detected by a sudden drop out of resonance when the panel could not be retuned.

\*\*The panel edge design is not optimum for end loading, however, it was chosen to provide a "soft" edge in order to precipitate failure in the body of the panel. A primary panel edge failure was not considered desirable for these tests, since panel edge design was not the subject of the investigation.

## 8. TYPE II GLASS FIBER PANEL PRELIMINARY DESIGN

This panel was of similar construction to the Type I panel, Figure 17, however, polyurethane foam mandrels were used in place of the removable polypropylene mandrels of Type I. The foam mandrels were retained in place for flute stabilization. In order to compensate for the added weight of the foam, one glass fabric ply from the upper panel surface and one ply from the lower panel surface were omitted. The total number of edge plies of 181-S fabric was thus reduced from six to four. The finished panel weighed 4.20 lb. (1,900 grams). Overall thickness was 0.465".

## 9. TYPE II GLASS FIBER PANEL DISCRETE FREQUENCY TESTS

### Frequency Sweep Tests

A number of strain gages were affixed to this panel as shown on Figure 20. The panel was then subjected to constant SPL vs. frequency sweeps from 0 to 500 Hz at SPL's of 145 db, 150 db, and 155 db. Typical stress vs. frequency response data for these SPL's are given for mid-panel gages  $E_1$ ,  $E_2$ ,  $E_3$  on Figures 21, 22, 23, respectively, and similar data for panel corner gages  $C_1$ ,  $C_2$ ,  $C_3$ , are given on Figures 24, 25, 26, respectively. Measured stress levels in all four corners were approximately equal.

### Panel Deflection Tests

An accelerometer was placed at the mid-panel position and the mid-panel displacement as a function of sound pressure was measured for the panel first resonant mode. These data are presented on Figure 27.

The relatively low stiffness of the glass fiber material accounts for the large mid-panel displacements at the higher SPL's.

### Failure Tests

The Type II panel was tested to failure at 160 db SPL at its first mode. There was a sharp drop in resonant frequency after some 4 minutes and 10 seconds of running. The panel suffered delamination along its lower edge originating at the edge radius, Figure 28.

## 10. TYPE III GLASS FIBER PANEL PRELIMINARY DESIGN

The Type III glass fiber panel was of the same general construction as for Type I panel, Figure 16. The principal difference was the use of 151-S glass fabric (nominal ply thickness 0.007") instead of 181-S fabric. Four facing plies were used on both upper and

lower surfaces. These plies were laid up alternating at 45° to the flute direction. The panel overall thickness was 0.500" and the finished weight was 5.07 lb (2,303 grams).

## 11. TYPE III GLASS FIBER PANEL DISCRETE FREQUENCY TESTS

Strain gages were located on this panel at locations shown on Figure 29. The panel was subjected to constant SPL vs. frequency sweeps at 145 db, 150 db, 155 db, 160 db and 165 db. A typical stress vs. frequency plot for a 165 db sweep is shown on Figure 30. This panel suffered premature flute failure during a second sweep at 165 db. Examination of the failed flute showed that the finished skin to flute thickness ratio was approximately 3.5 to 1. It was clear that the flutes in this design required foam stabilization.

## 12. CONCLUSIONS

The following general conclusions were drawn from the Pilot Test Program results.

### Control Panel Design

The modified control panel design, Figure 2, was satisfactory for production testing. The modifications introduced a weight increase of approximately 0.25 lb.

### Type I Glass Fiber Panel Design

This design was generally satisfactory, however, the finished weight of 4.3 lb. was below the specified weight. ( $5 \pm .2$  lb.). Extra ply facings were needed to bring the panel to the required finished weight. There was some slight evidence of delamination along the sharp edge radius; a more generous edge radius was indicated.

### Type II Glass Fiber Panel Design

This design was clearly not satisfactory. The lower edge failure was due to insufficient edge thickness resulting from the trading of two edge plies of glass fabric for foam stabilizer. The effect of the sharp edge radius was also detrimental. The finished weight of 4.2 lb. (1,906 grams), was well below specified design weight.

### Type III Glass Fiber Panel Design

The obvious defect in this design was the lack of stabilization of the very thin flutes. The weight was satisfactory. It was concluded that foam stabilization should be used in this design for the production panels.

# Contrails

## Test Procedures

The multi-modal response characteristics of the aluminum control panels indicated that broad band testing should be used. However, the response characteristics of all three glass fiber panels indicated that a much higher range of SPL's would be needed for testing them than the levels required for the control panel, particularly when the former were modified and brought up to the desired weight. It was concluded that the Columbus Division NAA "Broad Band Siren Facility, had neither the required acoustic output, nor a sufficiently flat spectrum for testing the glass fiber panels. It was therefore decided to use the discrete frequency siren for all production testing.

## SECTION IV

### ALUMINUM CONTROL PRODUCTION PANEL TESTS

#### 1. DISCUSSION

A total of twenty sonic fatigue aluminum control panels was specified for production testing, five each at four different SPL's. The choice of five specimens was based on the relationship

$$\epsilon = 1 - N\beta^{N-1} + (N-1)\beta^N$$

for statistical confidence, where

$\epsilon$  = degree of assurance that at least  $100\beta$  percent of an infinite number of specimens will fail between the largest and shortest failure times encountered in a sample of size  $N$ . For  $N = 5$  and taking  $\beta = 50$  percent

$$\epsilon = 1 - 5(.5)^4 + 4(.5)^5$$

$$\epsilon = 80 \text{ percent.}$$

#### Selection of Test SPL's

The four discrete frequency SPL's selected were: 140 db, 145 db, 150 db and 155 db. A failure time not exceeding twenty hours was used as a criterion for determining the lowest test SPL (140 db). Failure times at the highest SPL (155 db) were of the order of 5-6 minutes.

#### Production Test Panels

All production test panels were made with gusset plate reinforcing of stringers, Figure 2. Due to some operator production problems with AF-111 adhesive, five production panels were rejected and had to be replaced. These problems are fully discussed in Part 8 of this section.

#### "Oilcan" Effects

All control panels were found to be particularly prone to "oilcan" effects. During production testing it was necessary to periodically stop the test and loosen all panel attach bolts to relieve "oilcan". The problem was particularly acute during a severe cold weather spell when overnight chilling of the siren test area frequently occurred. The effects of "oilcan" on panel response are discussed in detail in Part 2 of this section.

## Test Procedures

The test procedures followed were intended to ensure uniformity of and, as far as possible, to control all factors which might contribute to scatter. Two strain gage positions, (Pos. 2 and Pos. 3) Figure 31, were used for the majority of the production test panels. The effects of stringer rotational modes were investigated on some panels using strain gage positions 4 and 5. Frequency sweeps (0-500 Hz) were made on all test panels at the designated test SPL and where appropriate, at lower SPL's, before proceeding with fatigue testing. The panels did not respond significantly at frequencies above 400 Hz. For fatigue testing the panels were tuned for maximum response at gage position 2 or 3. When gage failures occurred, the panels were tuned using microphone response. Failure was readily detected by a sharp drop in resonant frequency. All panels failed on the skin at a stringer heel location, usually across gage position 2 or 3. Some panels showed evidence of AF-111 adhesive bond failure due to poor bonding. These panels were later replaced. Full details of the test set up and instrumentation are given in Appendix A.

## 2. PANEL MODAL RESPONSE CHARACTERISTICS

### Skin-Stringer Panel Modes

The response characteristics of skin-stringer panels have been analyzed by Y.K. Lin, Reference (3). Typical normal modes for continuous panels of this type are shown on Figure 32 (a), (b), (c).

Stroboscopic examination of control panel mode shapes under acoustic load in the siren showed that the predominant mode shapes were those shown on Figure 32 (d) and (e).

At times these modes interchanged producing a distinct low frequency beat. The sub-panel in-phase mode (all bays in phase) Figure 32 (b), was seldom to be found. This is no doubt connected with the fact that the free skin sub-panel width for the mid bay (#2) is greater than that for Bay #1 or Bay #3, Figure 32 (f); the sub-panels having a strong tendency to vibrate in antiphase. This condition is accentuated by the stringer torsional mode coupling.

The sub-panel in-phase mode was isolated during panel shake tests with a panel mounted on a stiff frame suspended from bungee cord, and driven by a pair of 50 lb. shakers, Figure 33. The sub-panel third mode for similar conditions is shown on Figure 34. Many other higher modes were identified during the shake tests, however, isolation of these modes was difficult. Modal frequencies for specific modes were in general somewhat lower in the shake test fixture than in the siren test fixture. This is accounted for by



some detail differences in the fixture designs, which affect panel edge fixity.

### 3. MODAL DAMPING MEASUREMENTS

Modal damping measurements were obtained from a number of control panels for various modes using the amplitude decay method. The percent critical damping  $C/C_0$  for a given mode is obtained from the simple relationship:

$$C/C_0 = \frac{0.110}{n}$$

where  $n$  = number of cycles to half amplitude. Decay curves in general tended to show interference from extraneous modes and slight variation in placement of an accelerometer pick-up was found to produce a marked change in the purity of the decay curve. There was significant variation in critical damping ratio for a given mode between individual panels and between individual bays of a given panel. The best decay curves were obtained by placing the accelerometer pick-up on the mid-bay and adding weights to the adjacent bays to prevent these bays from responding. Some improvement was also obtained in decay curve purity by using clamps to restrain the torsional motion of the stringers. Decay curves obtained by tapping of the panels did not show any significant improvement over those obtained by shaker excitation. The following damping ratios were found to be typical of the control panels.

- (a) Sub-panel in-phase (1st mode)  $C/C_0 = 0.009$
- (b) Sub-panel mid-bay (1st mode)  $C/C_0 = 0.014$   
-Outer bays clamped
- (c) Sub-panel mid-bay (1st mode)  $C/C_0 = 0.01$   
-Z stringer clamped
- (d) Sub-panel mid-bay (3rd mode)  $C/C_0 = .016$

*Considering the potential energy absorbed in weights & clamps, these values are of order 100%.*

The lower panel modes are lightly damped and it would appear that the AF-111 adhesive bonding contributes little to damping since the foregoing damping ratios are also typical of riveted (non-bonded) skin-stringer panels.

## 4. PANEL STRESS VS. FREQUENCY RESPONSE DATA

### Normal Control Panel Response

Selected stress vs. frequency data (gage position #2 or #3) for production control panels subjected to 140 db, 145 db, 150 db, and 155 db are presented on Figures 35 through 38, respectively. The upper resonant peak frequency in each stress vs. frequency plot, which corresponds with the adjacent sub-panel in-phase mode, Figure 2 (d) or (e), was used as the test frequency for fatigue testing of all control panels.

The exact shape of the principal resonant peaks at a given SPL and their frequencies, were found to vary significantly from panel to panel and from bay to bay in a given panel. This is no doubt due to some variation in panel manufacture between individual panels, to be expected in this type of construction. Minor variations in placement of strain gages on individual panels, together with difficulties in maintaining precise control of the airflow to the siren at panel resonance were additional factors affecting stress response at a given strain gage location on a panel.

### "Oilcan" Effects

The effects of "oilcan" on stress response are illustrated on Figure 39. The response with "oilcan" present shows a significant lowering of the critical resonant frequencies and the corresponding panel stresses at those frequencies. The degree of "oilcan" present in a given panel could be determined by running a frequency sweep at the test SPL, and comparing it with the original data obtained before commencement of the fatigue test. The primary cause of "oilcan" was found to be differential expansion or contraction of the test fixture relative to the test panel.

Some panels developed "oilcan" in one or more bays after a period of fatigue testing. This was readily relieved by loosening all attach bolts and rebolting after panel and frame temperatures had reached equilibrium. All control panels with the exception of panel #13 were free of "oilcan" built in at manufacture.

### Effects of Stringer Rotation

Figure 40 shows stress response vs. frequency data for gage positions #2 and #3 (panel skin) and the adjacent stringer response obtained from stringer gage positions #4 and #5, for applied SPL's of 140 db and 155 db. The strong influence of the stringer rotation is evident at the higher SPL. At the 140 db SPL, however, #3 (skin) gage response does not appear to be influenced by stringer rotation. This would indicate that panel mode shape was as shown on Figure 32 (e) for the 140 db sweep.

## 5. NON-LINEARITY EFFECTS

Typical stress vs. applied SPL is plotted for a control panel as shown on Figure 41. The 155 db point is omitted because of the large range of sound pressures.

Non-linearity factors based on mean square stress ratios of actual stress to linear stress are:

SPL db	Non-Linearity Factor ( $\lambda$ )
140	1
145	0.94
150	0.785
155	0.65

The SPL at which a given panel responds non-linearly is highly dependent on the amount of "oilcan" present, and possibly the membrane stresses built in during manufacture.

## 6. PANEL SPL VS. CYCLES TO FAILURE DATA

Table I shows sonic fatigue test results on all twenty-five production control panels. These results are plotted on an SPL vs. Cycles to Failure curve on Figure 42. The mean failing stresses shown, Table I, are those measured at gage positions #2 or #3, Figure 31, during failure tests. Most panels exhibited a gradual drop in resonant frequency and/or stress during test. The test frequency shown on Table I was that prevailing for the greater part of the test run. It should be noted that many frequency vs. stress sweeps were made on most panels at various SPL's, before and during fatigue testing.

The 140 db test level was selected on the basis of panel #5 data. This panel was later rejected after other panels showed no failure at 20 hours of test at this level. The control panels appear to approach infinite life at 140 db. Panel #12 which showed no failures after twenty hours testing at 140 db, SPL was retested at 155 db SPL and failed after 14 minutes testing at this level. All panels failed on the skin at a stringer heel location.

Figure 43 shows a reverse bending S-N curve for 7075-T-6 Alclad. The average of the peak values of failing stress, and cycles to failure (excluding rejected panels) from Table I for 140 db, 145 db, 150 db and 155 db SPL are also plotted on Figure 43.

These curves indicate that stress concentration factors operating at the test SPL's are:

SPL	Stress Concentration Factor
140 db	3
145 db	2.5
150 db	2.4
155 db	2.5

## 7. SOUND FIELD MEASUREMENTS

### Microphone Oscilloscope Traces

The sound field in the siren test section was continuously monitored during test at the four microphone positions, Figure 44. Microphone position #4 (mid-panel) was used as prime position for SPL measurement in all tests. Sound pressure levels measured at microphone positions #1 and #2 were generally within  $\pm 1.5$  db of those measured at microphone position #4. Corresponding SPL's measured at microphone position #3 (nearest siren) were usually 2 to 3 db higher than those measured at microphone position #4.

Typical oscilloscope traces of the microphone data are shown on Figure 45. The shape of these traces is determined not only by the harmonic content of the siren noise itself, but also by panel re-radiation effects. A 90 degree phase shift between microphone #4 trace and strain gage position #2 output, Figure 45, corresponds to the panel resonant response.

### Narrow Band Analysis

A number of narrow band analysis measurements (2 cycle filter) were made on microphone and strain gage data at all four test SPL's. Figure 46 shows a typical narrow band analysis plot at 140 db, for microphone position #4. The corresponding plot for 150 db SPL is shown on Figure 47. The increase in the harmonic content of the sound at the higher SPL's is evident. Similar results were obtained from other microphone positions.

A narrow band analysis plot for strain gage position #2 is shown on Figure 48 for 140 db SPL, and similar data for the 150 db SPL is shown on Figure 49. These plots show the predominantly sinusoidal response of the panels.

## 8. FAILURE ANALYSIS

### Normal Panel Failure

A typical AF-111 adhesive skin-stringer bond line is shown on Figure 50 (a), and a section through a typical skin failure is

shown on Figure 50 (b). The failure line generally followed that of the AF-111 adhesive\* and was initiated at the sharp edge of the adhesive bead, where there was an obvious line of stress concentration, Figure 51.

The control panel design does not specify precise width or location of the bonding strip of AF-111 adhesive between skin and stringer, and in some control panels the adhesive line did not extend much beyond the flat portion of the stringer heel.

## Rejected Panels

Panels #2, #5, #11, #15 and #18, Table I, were rejected because their failure times were well outside the normal scatter band for the remaining panels. Sections taken through four "good" and rejected panels showed no significant thickness variation in adhesive or aluminum thickness. All failures originated at the stress concentration of the adhesive bond line.

Table II shows Rockwell hardness readings taken on "good" and rejected panels. Table III shows results of a dimensional survey taken of the four panels sectioned. Lap shear tests of sample test pieces for "good" and rejected panels showed that adhesive shear stress failure values were well within AF-111 specification limits. This also applied to panel #9 which suffered a premature bond failure between skin and stringer resulting in a rivet line failure. Examination of the failed panel showed evidence of insufficient clamping pressure during adhesive cure. However, the lap shear control specimen for this panel was adequately clamped and gave good results. It was later established that a switch of operators was made during manufacture of panel #9, and that the new operator had not followed correct clamping procedure during adhesive cure. It was noted that in the initial series of production panels, the AF-111 adhesive did not extend much beyond the heel-skin junction leaving a significant stress concentration at this point. Accordingly, it was decided to extend the adhesive beyond this junction in all subsequent panels. A section through panel #20 with extended adhesive line is shown on Figure 52(a). The line of failure is still on the adhesive edge, however, the stress concentration factor is probably reduced. The fatigue life of these panels could be significantly improved by use of an additional doubler, Figure 52(b).

## 9. CONVERSION TO RANDOM S-N DATA

Excluding rejected panels, Table I, the average number of cycles to failure for the discrete frequency SPL's employed for the control panel tests were:

\*Panel No. 9 failed along rivet line after premature failure of AF-111 adhesive bond.

# Contrails

<u>SPL (db)</u>	<u>Average No. of Cycles to Failure N</u>
140	$1.06 \times 10^7$
145	$2.12 \times 10^6$
150	$4.5 \times 10^5$
155	$7.15 \times 10^4$

Using the method outlined in Reference (4), a rough estimate of the equivalent random sound pressure spectrum levels, corresponding to the above discrete frequency test SPL's, can be made. The 7075 T-6 Random S-N curve of Reference (4) is used and reproduced on Figure 53. A critical damping ratio  $\delta = 0.01$  is assumed. The non-linearity factor ( $\lambda$ ) values of page 17 are used. The multimodal factor  $\gamma$  is calculated for each discrete frequency test SPL as follows:

## 140 db SPL

From the stress vs. frequency response plot, Figure 35, two (2) stress peaks are assumed significant,

<u>Frequency</u>	<u>Stress</u>
143 Hz	4,400 psi
150 Hz	5,500 psi

$$\begin{aligned}\text{Total stress} &= \sqrt{(4.4)^2 + (5.5)^2} \text{ kpsi} \\ &= 7.05 \text{ kpsi}\end{aligned}$$

$$\text{For 150Hz, } \gamma = \frac{7.05}{5.5} = 1.28$$

## 145 db SPL

From stress vs. frequency response plot, Figure 36, significant stress peaks are assumed to be:

<u>Frequency</u>	<u>Stress</u>
150 Hz	6,500 psi
158 Hz	6,900 psi

$$\begin{aligned}\text{Total stress} &= \sqrt{(6.5)^2 + (6.9)^2} \text{ kpsi} \\ &= 9.48 \text{ kpsi}\end{aligned}$$

$$\text{For 158 Hz, } \gamma = \frac{9.48}{6.9} = 1.37$$

# Contrails

## 150 db

From stress vs. frequency response plot, Figure 37, significant stress peaks are assumed to be:

<u>Frequency</u>	<u>Stress</u>
135 Hz	4,900 psi
153 Hz	7,600 psi
162 Hz	8,100 psi

$$\begin{aligned}\text{Total stress} &= \sqrt{(4.9)^2 + (7.6)^2 + (8.1)^2} \text{ kpsi} \\ &= 12.13 \text{ kpsi}\end{aligned}$$

$$\text{For 162 Hz, } \gamma = \frac{12.13}{8.1} = 1.5$$

## 155 db

From stress vs. frequency response plot, Figure 38, significant stress peaks are assumed to be:

<u>Frequency</u>	<u>Stress</u>
158 Hz	12,200 psi
165 Hz	12,400 psi

$$\begin{aligned}\text{Total Stress} &= \sqrt{(12.2)^2 + (12.4)^2} \text{ kpsi} \\ &= 17.4 \text{ kpsi}\end{aligned}$$

$$\text{For 165 Hz, } \gamma = \frac{17.4}{12.4} = 1.4$$

# Contrails

If	$P_H$	=	Discrete sound pressure (psi)
	$P_R$	=	Random sound pressure (psi)
	$\sigma_H$	=	RMS sinusoidal stress (psi)
	$\sqrt{\sigma^2}$	=	RMS random equivalent stress (psi)
	$f$	=	Test frequency (discrete) Hz
	$\delta$	=	$C/C_0$ = percent critical damping

Then  $P_R$  may be calculated from the relationship:

$$P_R = P_H \frac{\sqrt{\sigma^2}}{\sigma_H} \div (\pi \delta f)^{1/2} \lambda \gamma$$

## 140 db SPL Discrete

For this SPL we have:

$f$	=	150 Hz
$N$	=	$1.06 \times 10^7$ cycles to failure
$P_H$	=	0.03 Psi
$\lambda$	=	1
$\gamma$	=	1.28
$\sigma_H$	=	$15,000 \times .707 = 10,600$ psi rms (Figure 53)
$\sqrt{\sigma^2}$	=	7,000 psi (Figure 53)
$P_R$	=	$0.03 \times \frac{7,000}{10,600} \div (\pi \times .01 \times 150)^{1/2} \times 1.28$
$P_R$	=	$\frac{0.03 \times 0.66}{2.78} = 0.007$ psi
$SPL_R$	=	127.5 db <sub>R</sub> Spectrum Level



## 145 db SPL Discrete

For this SPL we have:

$$\begin{aligned} f &= 158 \text{ Hz} \\ N &= 2.12 \times 10^6 \text{ cycles to failure} \\ P_H &= 0.052 \text{ psi} \\ \lambda &= 0.94 \\ \gamma &= 1.37 \\ \sigma_H &= 16,400 \times 0.707 = 11,600 \text{ psi rms (Figure 53)} \\ \sqrt{\sigma^2} &= 8,200 \text{ psi (Fig. 53)} \\ P_R &= 0.052 \times \frac{8,200}{11,600} \div (1.58 \pi)^{1/2} \times 0.94 \times 1.37 \\ P_R &= \frac{0.038}{2.86} = 0.013 \text{ psi} \\ \text{SPL}_R &= 133.0 \text{ db}_R \text{ Spectrum Level} \end{aligned}$$

## 150 db SPL Discrete

For this SPL we have:

$$\begin{aligned} f &= 162 \text{ Hz} \\ N &= 4.5 \times 10^5 \text{ cycles to failure} \\ P_H &= 0.1 \text{ psi} \\ \lambda &= 0.78 \\ \gamma &= 1.5 \\ \sigma_H &= 21,500 \times 0.707 = 15,200 \text{ psi rms (Figure 53)} \\ \sqrt{\sigma^2} &= 11,800 \text{ psi (Figure 53)} \\ P_R &= 0.1 \times \frac{11,800}{15,200} \div (\pi \times .01 \times 162)^{1/2} \times 0.78 \times 1.5 \\ P_R &= \frac{0.078}{2.64} = .03 \\ \text{SPL}_R &= 140 \text{ db}_R \text{ Spectrum Level} \end{aligned}$$

# Contrails

## 155 db SPL Discrete

For this SPL we have:

$$\begin{aligned} f &= 165 \text{ Hz} \\ N &= 7.15 \times 10^4 \text{ cycles to failure} \\ P_N &= 0.16 \text{ psi} \\ \lambda &= 0.65 \\ \gamma &= 1.4 \\ G_H &= 34,500 \times 0.707 = 24,400 \text{ psi rms (Figure 51)} \\ \sqrt{\delta^2} &= 18,500 \text{ psi} \\ P_R &= 0.16 \times \frac{18,500}{24,400} \div (\pi \times .01 \times 165)^{1/2} \times 0.65 \times 1.4 \\ P_R &= \frac{0.118}{2.07} = .058 \text{ psi} \\ \text{SPLR} &= 145.5 \text{ dB}_R \text{ Spectrum Level} \end{aligned}$$

## SECTION V

### TYPE I GLASS FIBER PRODUCTION PANEL TESTS

#### 1. DISCUSSION

A total of twenty-one Type I (hollow flute) sonic fatigue production test panels were tested in the discrete frequency siren. The first Type I panel made by the Flexible Company, Loudonville, Ohio for tooling and process try-out was tested at 155 db and failed in 36 min. 21 sec. This panel showed some evidence of edge delamination and resin starvation in the edge flutes. The panel was below minimum weight and it was apparent that the edge flute radius (.060") was inadequate. This panel was rejected and it was decided to increase edge flute radius to 0.25" on all subsequent panels. The resin starvation was due to failure to maintain sufficient vacuum during impregnation of the core. The finished weight of 4.78 lb. was due to a miscalculation in number of glass fabric plies required for the desired weight of 5.2 lb.\* An extra glass fabric facing sheet was added to the lower (outer) panel surface to achieve the desired weight. Some difficulty was experienced in maintaining weight tolerances with the latter ten of the twenty Type I production test panels (see Table 4). The Flexible Company was unable to offer any explanation for the overweight, however, the resin content of many of the overweight panels appears high in some panel edge areas.\*\* The problem did not recur on Type II or Type III panels.

#### 2. PANEL DESIGN

The general arrangement of the Type I Glass Fiber Production Test Panel is similar to the Type I original design, Figure 16, with the exception of edge flute radii and the number of glass fabric facing plies. A cross-sectional view of the panel is shown in Figure 54(a).

#### 3. PANEL MODAL RESPONSE CHARACTERISTICS

Mode Shapes - The significant modes for this panel were determined by mounting the panel in a stiff rectangular frame, horizontally suspended by a bungee cord suspension and driven by a pair of 50 lb. shakers (see Appendix A). These modes are illustrated on Figure 55. Mode shapes were also investigated by measuring panel accelerations at a number of locations along a vertical and horizontal line through the panel mid-point, with the panel installed in the siren test section, Figure 56.

\* Average aluminum panel weight.

\*\*A check on Type I panel flute and skin thickness, showed little variation between heavy and light panels, indicating most of the excess weight was in the panel edges.

# Contrails

The highest panel stresses were obtained in the transverse-to-flute direction at the mid-panel position (#1 gage Figure 55) when the panel was driven in its first mode. Specific modal frequencies in the shake test did not agree with those obtained in the siren test due to differences in edge fixity of the two installations.

Panel Deflections - Figure 57 shows zero to peak panel deflection along the flute direction for a range of sound pressure levels, with the panel tuned to first mode. Corresponding data for the transverse flute direction are given on Figure 58. Mid-panel deflection as a function of SPL for panel first mode resonance is shown on Figure 59. This panel goes non-linear at approximately 150 db SPL. The very large mid-panel deflection is evident and corresponds with the low Young's Modulus of the glass laminates ( $E = 2.33 \times 10^6$  psi for the transverse-to-flute direction). It should be noted that measured panel deflections on the panel center lines, Figure 56, show slightly larger deflections along the vertical panel axis than those at corresponding locations along the lateral panel axis. This is accounted for by the greater unsupported panel length in the vertical (flute) direction compared with the lateral (transverse-to-flute) direction. The lower inherent panel stiffness in the lateral direction is more than offset by the disparity in unsupported span lengths.

#### 4. PANEL STRESS VS. FREQUENCY RESPONSE DATA

All glass fiber production test panels were frequency swept from 0 to 400 Hz at the test SPL before testing to failure. SPL vs. Frequency Response plots were obtained for most panels from gage position #1 (mid-panel transverse) and gage position #2 (right side panel, transverse). Sweep rates were approximately 2 to 5 cycles per second per second, depending on sound pressure level. Measured stress levels at the principal resonant peaks were dependent on the degree of control exercised by the siren air supply operator when passing through resonance.

This was particularly noticeable when the siren was being operated at high SPL's, and plant air demand was at a peak. Repeat frequency sweeps were made on a number of panels at a constant SPL to check repeatability. Generally, stress levels at the resonant peaks tended to be slightly higher on the second sweep tending to a constant level at the third and subsequent sweeps.

Typical mid-panel Transverse Stress vs. Frequency Response Plots for a Type I panel are shown on Figure 60 for a sound pressure spectrum level of 155 db. A corresponding typical Frequency Response Plot for gage position #2 is shown on Figure 61. The double peak at approximately 130 Hz, Figure 61, does not denote two resonant peaks, but is due to siren air supply variation in passing through resonance.

## 5. MODAL DAMPING MEASUREMENTS

The critical damping ratios for the first and second panel modes were obtained from the Stress vs. Frequency Response Plots from gage position #1 and position #2 respectively, using the half-power bandwidth method. For the stress response plot, Figure 60, the half-power bandwidth for the panel first mode is  $\Delta f = 9$  Hz, while the resonant frequency  $f_0$  is 133 Hz.

$$\text{Critical Damping } C/C_0 = \frac{\Delta f}{2f_0} = \frac{9}{2 \times 133} = 0.034$$

Similarly for the stress response plot, Figure 61, the bandwidth for the panel second mode is  $\Delta f = 10$  Hz, while the resonant frequency is 308 Hz.

$$\text{Critical Damping } C/C_0 = \frac{\Delta f}{2f_0} = \frac{10}{2 \times 308} = 0.016$$

A summary of critical damping ratios for Type I panels, measured by the half-power bandwidth method from stress plots made at 155 db sound pressure spectrum levels, is given in Table V. Damping of the Type I glass fiber panels appears to be significantly higher than that of the control panels.

The Type I glass fiber panel critical damping ratios were also measured using the amplitude decay method. The panel was mounted in the siren test section and excited with a large loudspeaker at its first mode. A typical decay trace from an accelerometer at panel mid-point position is shown in Figure 62.

NOTE: The foregoing damping measurements include radiation damping effects which were not investigated.

## 6. PANEL SPL VS. CYCLES TO FAILURE DATA

These data are summarized on Table IV and plotted on Figure 63. The first Type I glass fiber panel tested failed on its edge flute, left side. Examination of this panel at failure showed that it became extremely hot over most of its surface during testing (estimated temperature 250°F). It was obvious that some cooling would be necessary for fatigue testing. Accordingly, it was decided to have a large cooling fan blowing on all subsequent panels during test. This maintained the panel surface temperature at approximately 120°F., or lower, except locally on failure areas where the temperature rose rapidly during failure. This was particularly noticeable at the 160 db and 163 db SPL test levels.

With the exception of Panel No. 1 which failed prematurely due to excessive heating, and Panel No. 9 whose failure was due to an aluminum frame failure, the remaining three panels tested at 155 db showed no damage after twenty hours running at this level. Panel No. 16 was retested at 163 db after com-

pletion of twenty hours at 155 db and failed in 2 minutes and 7 seconds at this level. These results indicate that the panels approach infinite life at 155 db. Increasing the SPL to 157.5 db produces a marked reduction in panel life to about 42 minutes (average).

A stress vs. cycles to failure summary for Type I panels is shown on Table VI. These S-N data are plotted on Figure 64. The average values of stress and cycles to failure do not include test points outside the normal scatter band.

## 7. SOUND FIELD MEASUREMENTS

Four microphones located inside the test section (see Figure 44) were used to monitor the sound field. An additional external microphone was added at the mid-panel position for tuning the panel after failure of the strain gages. This external microphone produced a clean sinusoidal signal compared with the internal microphones. The #4 microphone (mid-panel position) was used for setting SPL test levels on all panels. Sound Pressure Levels measured at microphone position #3 (nearest siren) were generally 2 db higher than those at microphone position #4. Sound Pressure Levels measured at microphone positions #1 and #3 were usually 1 db lower than those at position #4. Typical microphone and strain gage signals for Type I panel tests are shown on Figure 65. These are also typical of the Type II and III panels.

## 8. FAILURE ANALYSIS

The primary cause of failure of the Type I glass fiber panels was internal flute collapse resulting in inner skin flute line failures usually near the panel edge. A typical Type I panel failed section is shown on Figure 66. The sectioned failed panels were found to have a considerable amount of powdered resin and glass debris in the flutes. This was no doubt due to the severe flexing of the thin flutes during test, particularly at the higher sound pressure levels. Sections through unfailed panels, tested at 155 db, showed some debris in the flutes and strong evidence of resin starvation. Prolonged testing at the 155 db test level produced no external damage and appeared to have little effect on the panel. This was born out by re-testing panel No. 16 at 163 db SPL after completion of 20 hours at 155 db SPL. The failure time at the 163 db SPL was reduced from approximately 3 minutes to 2 minutes compared with panels tested only at 163 db SPL. The excessive disparity between skin and flute thickness in the Type I panel is a basic design weakness and does not permit the full potential of the hollow fluted core to be realized.

## SECTION VI

### TYPE II GLASS FIBER PRODUCTION PANEL TESTS

#### 1. DISCUSSION

A total of twenty Type II glass fiber production panels was sonic fatigue tested in the discrete frequency siren. A sound pressure spectrum level of 155 db was chosen for the lowest test level. Three panels tested at this level showed no signs of failure after twenty hours testing. Accordingly, it was decided to test the remaining two panels of the group at 156 db SPL; these panels failed in 5.5 and 7 hours respectively. Five each of the remaining Type II panels were tested at 157.5 db, 160 db, and 163 db SPL respectively. The Type II panels did not show any significant improvement in sonic fatigue resistivity over the Type I panels. While the foam stabilized flutes remained generally intact after testing, a majority of the panels suffered top and bottom edge doubler failures.

#### 2. PANEL DESIGN

The Type II glass fiber panel design is identical in all respects with that of the Type I panel, with the exception of the flutes which are foam stabilized. Zerocel polyurethane triangular foam mandrels (6 lb./ft.<sup>3</sup> density) were used to fill the core, and were retained in place during cure cycle. The extra weight of these foam mandrels was compensated for by the deletion of one 181-S glass fabric facing sheet from both the upper and lower panel surface. (see Figure 54(b)).

#### 3. PANEL MODAL RESPONSE CHARACTERISTICS

Mode Shapes. - The Type II glass fiber panels exhibit generally similar modal response characteristics to those of the Type I panels, Figure 55. The Type II panel first mode resonant frequency is approximately ten Hz below that of the Type I panel first mode frequency. This is in accord with the lower panel stiffness of the Type II panels to be expected from the deletion of two facing plies. The foam does not affect overall panel stiffness significantly.

Panel Deflections. - Figure 67 shows typical Type II panel deflected shapes in the in-flute direction for a number of SPL's. The mid-panel 0-Peak deflection of 1.34 inches for 155 db SPL compares with 0.88 inches for the Type I panel, and corresponds with the higher panel stiffness of the latter. Type II panel deflected shapes in the transverse-to-flute direction are shown on Figure 68. Mid-panel 0-Peak deflection vs. SPL is shown on Figure 69.

## 4. PANEL STRESS VS. FREQUENCY RESPONSE DATA

Test procedures for the Type II panel frequency sweep tests were identical with those for the Type I panels (Section III-4). Typical mid-panel transverse stress vs. frequency response plots for a Type II panel at 155 db SPL are shown on Figure 70.

## 5. MODAL DAMPING MEASUREMENTS

Critical damping ratios for the first and second panel modes were obtained from the Stress vs. Frequency Response Plots using the half-power bandwidth method and the amplitude decay method. A summary of critical damping ratios for the first and second modes of the Type II panels, derived from half-power bandwidth measurements is presented in Table VII. First mode critical damping from accelerometer decay trace measurements was:

$$C/C_0 = 0.037$$

## 6. PANEL SPL VS. CYCLES TO FAILURE DATA

These data are summarized on Table VIII and plotted on Figure 71. The majority of the Type II panels suffered top and bottom doubler failures in the transverse to flute direction. Some panels suffered edge hole tear-out due to aluminum frame failure. Testing of these panels was resumed with a replacement aluminum frame and extra large washers to provide adequate edge damping. A stress vs. cycles to failure summary for Type II panels is shown in Table IX. These S-N data are plotted on Figure 64.

## 7. FAILURE ANALYSIS

The Type II Panels exhibited a tendency to fail consistently along the top and/or bottom secondarily-bonded doubler (See Figure 72). A number of panels suffered from edge delamination near the doubler and outerface bond. There was no evidence of any AF-111 adhesive bond failure. The large deflections of the Type II panels, particularly at the higher SPL's produced considerable local flexing of the secondarily bonded doublers in the core end close-outs. The poor tie-in between doubler and flutes is a basic weakness in all three glass fiber panel designs. Examination of a number of the failed Type II panels showed evidence of mal-distribution of the resin within the panel cores.



## SECTION VII

### TYPE III GLASS FIBER PRODUCTION PANEL TESTS

#### 1. DISCUSSION

Twenty-one Type III sonic fatigue production test panels were tested in the discrete frequency siren. A sound pressure spectrum level of 156 db was used for the lowest test level, and all five panels tested at this level completed twenty hours testing without failure, indicating that the Type III panels approach infinite life at this level. At the highest sound pressure spectrum level of 163 db, the Type III panels failed in 5-6 minutes. The Type III panels, fabricated from 151-S glass cloth, and foam-filled as for Type II panels, were clearly superior in sonic fatigue resistivity to the Type I and II panels. They failed in a more consistent and satisfactory manner, and gave less scatter than either Type I or II. The quality of construction was generally better, judging by external appearance and examination of sections of failed panels.

#### 2. PANEL DESIGN

The Type III Panel Design is illustrated on Figure 54(c). The 151-S glass facing plies have a nominal finished moulded thickness of 0.007" compared with 0.010" for the 181-S glass. Three facing plies are used on the top (inside) surface of the panel and four on the bottom (outside) surface. The panel is otherwise identical in construction to the Type II panel.

#### 3. PANEL MODAL RESPONSE CHARACTERISTICS

Mode Shapes. - The modal response characteristics of the Type III panels are generally similar to that of Type I and II panels, Figure 55. The first panel mode frequency is approximately 125 Hz, compared with 130 Hz for Type I panels and 115 Hz for Type II panels.

Panel Deflections. - Figure 73 shows zero to peak panel deflection along the flute direction for 145 db, 150 db, and 155 db SPL. Similar data for the transverse flute direction are given on Figure 74. Mid-panel zero-peak deflection as a function of SPL for first mode panel resonance is shown on Figure 75. The Type III panels become non-linear at approximately 150 db SPL.

#### 4. PANEL STRESS VS. FREQUENCY RESPONSE DATA

The Type III panel transverse stress vs. frequency characteristics are shown for a typical panel on Figure 76. They are generally similar to those of the Type I and II panels.

## 5. MODAL DAMPING MEASUREMENTS

A summary of critical damping ratios for Type III panels, measured by the half-power bandwidth method from stress plots made at 155 db sound pressure spectrum level, is given on Table X. First mode critical damping from an accelerometer decoy trace was:

$$C/C_0 = 0.027$$

## 6. PANEL SPL VS. CYCLES TO FAILURE DATA

These data are summarized on Table XI and plotted on Figure 77. A stress vs. cycles to failure summary for Type III Panels is shown on Table XII. These S-N data are plotted on Figure 74.

## 7. FAILURE ANALYSIS

A typical Type III Mid-panel Failure is shown on Figure 78. The failure line in the flute direction was approximately four inches long when failure was detected. The panel was run for a few extra minutes to propagate the crack. A close-up view of a portion of this crack (approximately X40 magnification) is shown on Figure 79. The broken glass filaments are evident. Sections taken through a number of failed Type III panels showed that the flutes were generally intact. Discoloration of the Zerocel foam near the failure areas showed evidence of high local heating at failure despite the use of a large cooling fan throughout the test duration.

SECTION VIII

CONCLUSIONS AND RECOMMENDATIONS

CONCLUSIONS

Glass Fiber Panel Sonic Fatigue Resistivity.- The Type III Glass Fiber Panels were clearly superior in sonic fatigue resistivity to the Type I or Type II panels. Test results show that there is little to choose between the latter two designs from the sonic fatigue aspect. It is not clear whether the superiority of the Type III panels is due to the 151-S glass fabric weave characteristics (smaller yarn diameter and closer mesh weave), or to the generally better overall quality of these panels. While all three glass fiber panel designs show superior sonic fatigue resistivity to the aluminum skin-stringer control panel design, the latter is possibly a worse choice in metal construction for sonic fatigue applications. Aluminum honeycomb panels of the same surface weight could be expected to be superior to the skin-stringer panels under similar sonic loading.

*This is a question in view of damping of a panel in flight*

Test Procedures. - The selection of discrete frequency (1st panel mode) testing for the glass fiber panels and the relatively high range of sound pressure levels required for panel failure resulted in large panel deflections which could not be considered realistic in an actual flight vehicle design application. The techniques of composite design and construction permitting a radical reduction in the number of individual components in an airframe may result in some very large span unsupported sandwich skins, e.g., in a fuselage wing, or flap area. Excitation of these surfaces in their lower resonant modes by sonic loading, e.g., by large lift fans, may result in unacceptable deflections and stresses leading to sonic fatigue problems. The predominantly uni-modal response characteristics of the glass fiber panel designs in this program tend to justify the choice of discrete frequency testing, however, the particular panel size is possibly too small to be representative of many typical glass fiber fluted-core flight vehicle structural applications.

Damping measurements from all three glass fiber panel designs show that the percent critical damping was  $C/C_0 \approx 0.03$  for the panel 1st mode and  $C/C_0 \approx 0.015$  for the panel 2nd mode. The internal cross-sectional dimensions of the siren test section (12" x 48") are such that panel radiation damping <sup>does</sup> ~~may~~ contribute significantly to the measured values of damping. The measured damping ratios may therefore be somewhat optimistic.

*2nd Mode would not be noticeable*

Glass Fiber Panel Designs. - All three (3) glass fiber panel designs were deficient in a number of respects.

- (a) Ineffective tie-in between flutes and top and bottom secondarily bonded close-out doublers. This resulted in many premature panel failures due to doubler collapse.

- (b) Adverse flute-to-outer skin thickness ratios making for an imbalanced weight.

NOTE: This situation was brought about by the choice of integrally-woven fluted-core fabric rather than sewn-fluted-core (Uni-core) fabric. The former is normally supplied with flute and skin of the same thickness, i.e., the standard cloth thickness for the fabric specified, while the latter may be made of differing core and skin fabric thicknesses. The addition of many outer surface plies to reach the required panel weight is unrealistic. However, the integrally woven glass fabric bond between flutes and skin is generally considered superior to the stitched bond of the sewn core. For optimum design, unstabilized core should have a 1:1 flute-to-skin thickness ratio.\* With foam filled cores, a flute-to-skin thickness ratio no less than 1:3 is desirable.

Glass Fiber Panel Manufacturing Methods. - Examination of all three types of glass fiber production test panels in this program, both before and after test, showed that the majority of the panels were correctly made. The surface finish and quality were generally good. However, weight control of the Type I panels was only fair. Sections taken through these panels showed internal maldistribution of resin, particularly in the flutes. The AF-111 adhesive bonding of the panel close-out doublers was excellent in all cases, no doubler bond failures being recorded. It seems doubtful if the wet-resin vacuum bag technique for making fluted core composite sandwich structures can be developed to produce the necessary uniformity of resin content essential for weight and quality control. It is possible that the use of some of the newer pre-preg materials may provide a better solution.

Glass Fiber Mechanical Properties. - Due to the very large number of variables in glass fiber composite structural design, no "standard" composite laminates have been evolved; the individual fabric lay-up, resin, catalyst, cure cycle, etc., are chosen in a somewhat arbitrary manner for many applications. This has led to a multiplicity of configurations without adequate data on mechanical properties and fatigue characteristics of these configurations.

Sonic Fatigue Test Results. - The following general conclusion may be drawn from the sonic fatigue test results in this program.

- (a) Fluted core glass fiber construction can be expected to have generally excellent sonic fatigue resistivity provided that it is designed so that large panel lower modes are not significantly excited by the noise environment.

\*For standard 60 degree flute angle.

# Contrails

- (b) Better panel edge design and control of resin distribution in the panels would result in superior sonic fatigue resistivity than that demonstrated.
- (c) Foam stabilized flute construction, where flute to skin thickness ratios are no less than 1:3, is likely to prove superior to un-stabilized (hollow) flute construction for sonic fatigue applications.
- (d) Large temperature gradients near failure areas were due to the relatively high damping of the glass fiber panels, low thermal conductivity, and the poor heat radiation from the dark panel surface. Adequate cooling is essential in sonic fatigue testing of composite filamentary structures if heat damage to the resin system is to be avoided.

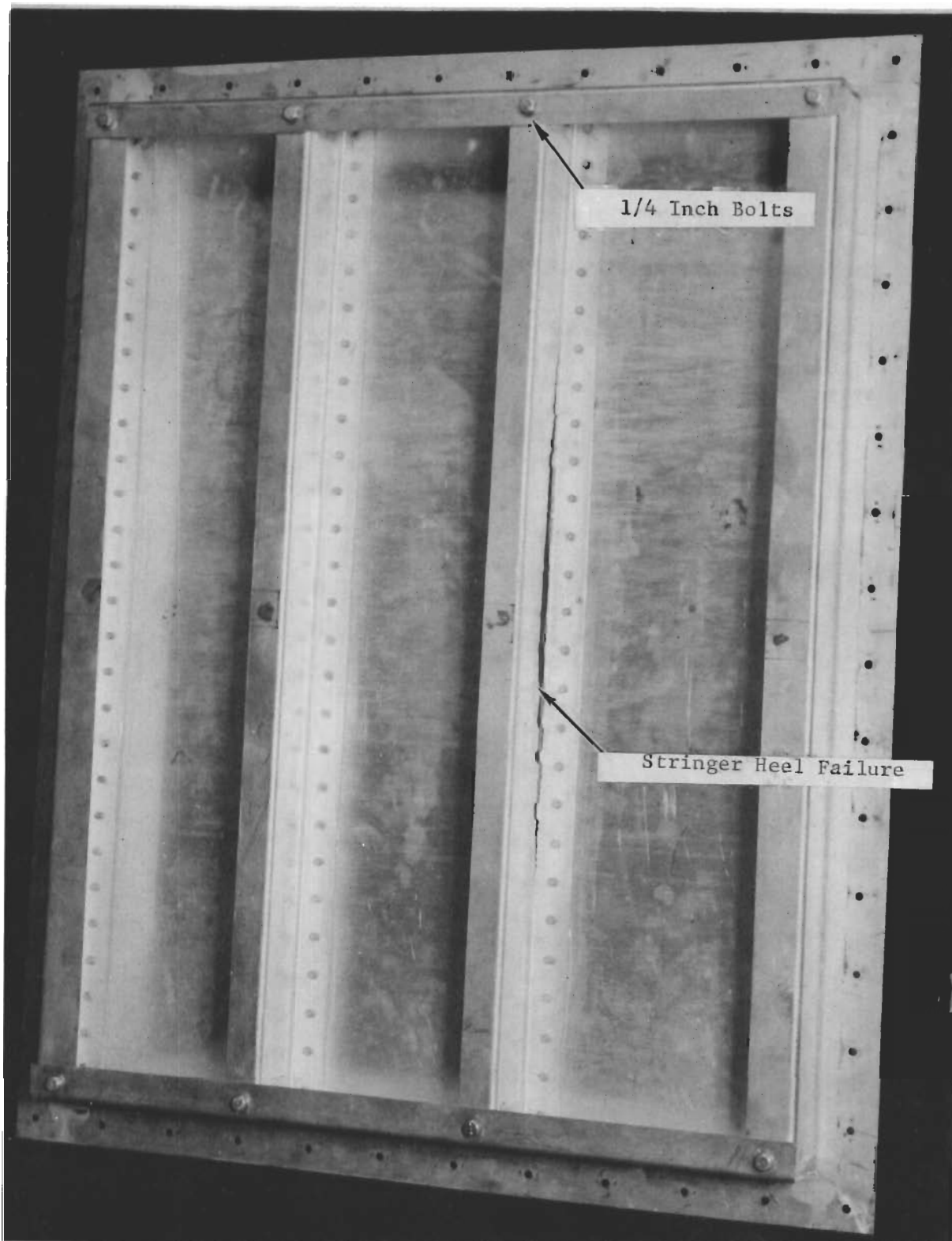


Figure 1. Aluminum Control Panel Original Design

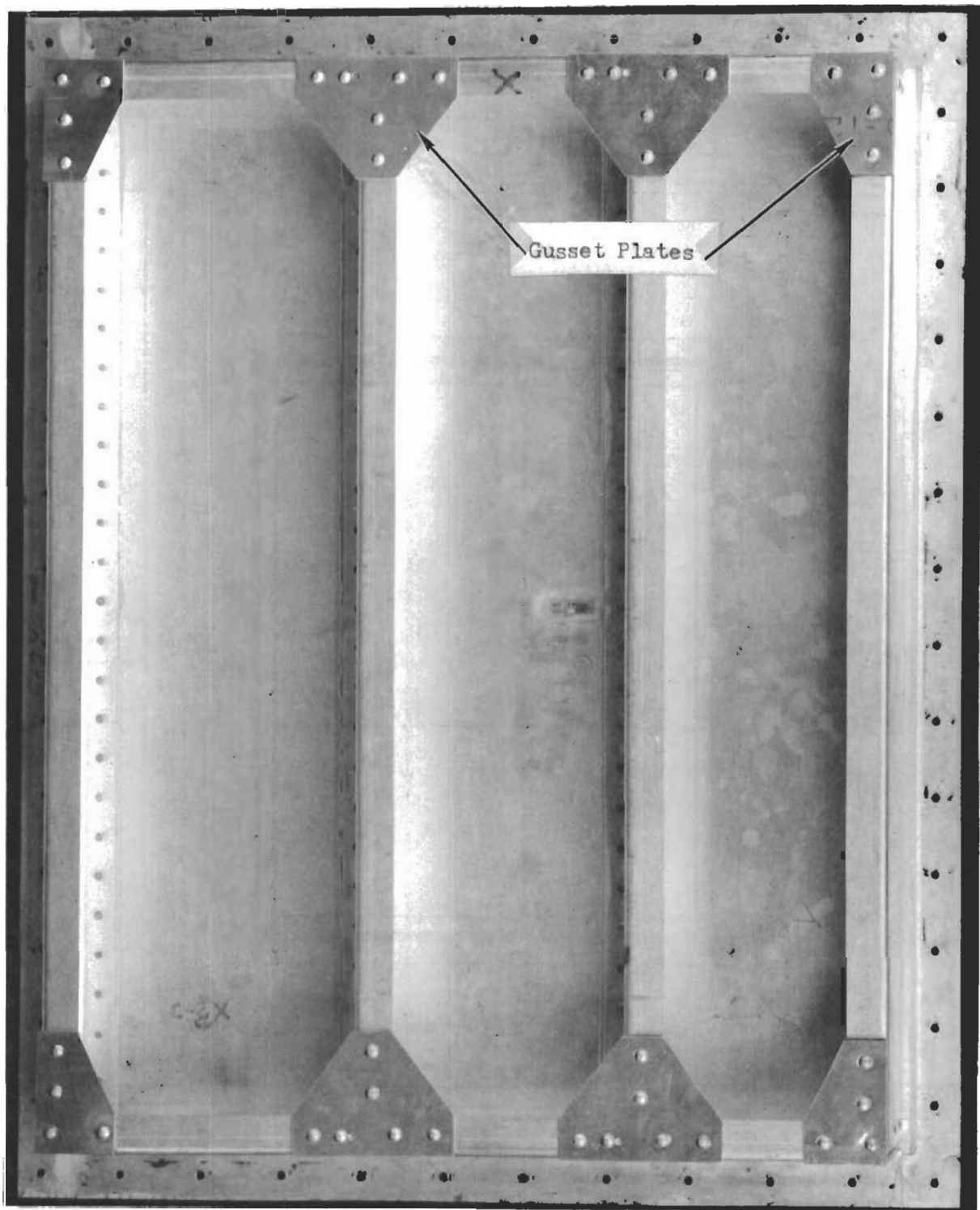


Figure 2. Aluminum Control Panel Final Design

# Contrails

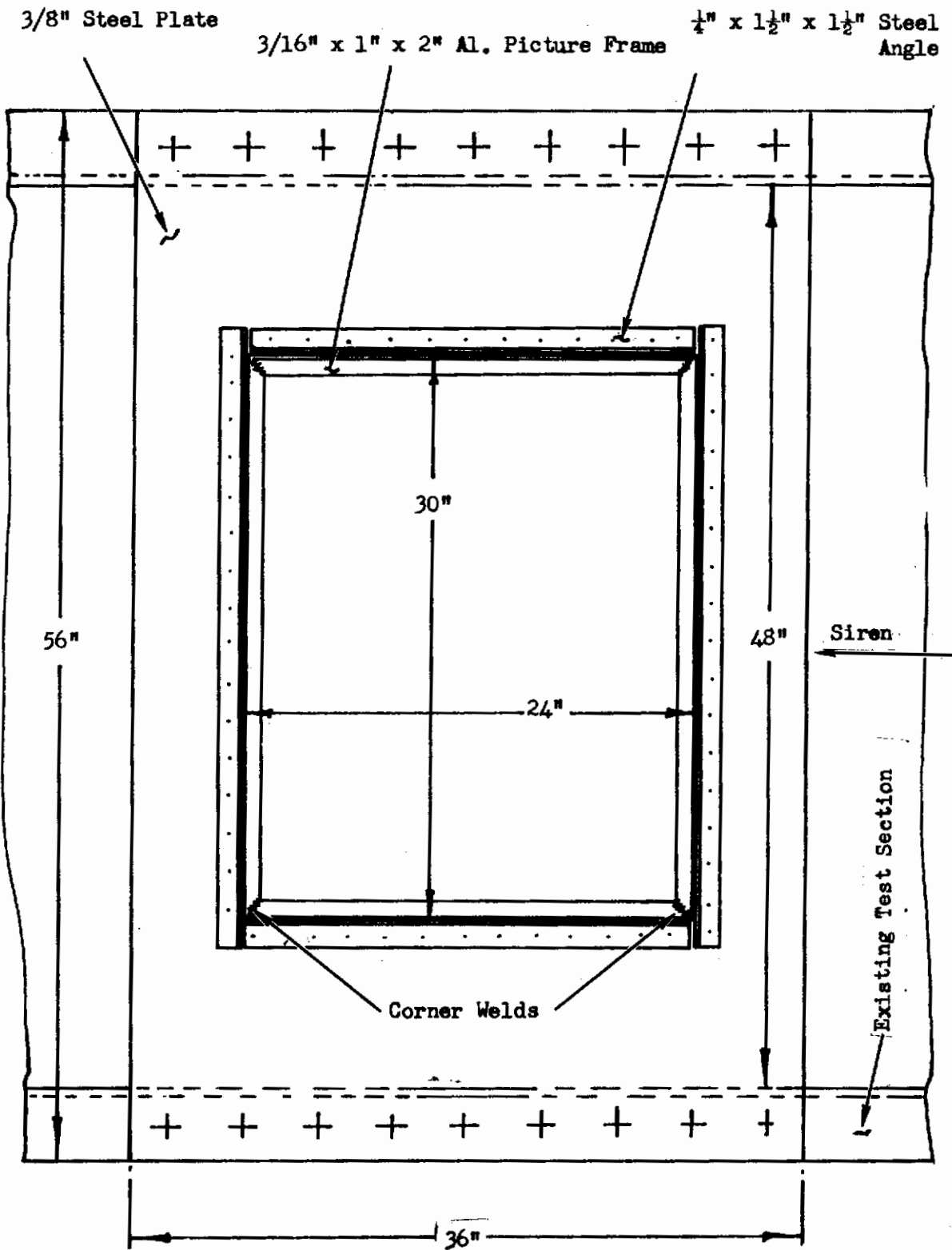


Figure 3. Sonic Fatigue Test Fixture - Original Design



# Contrails

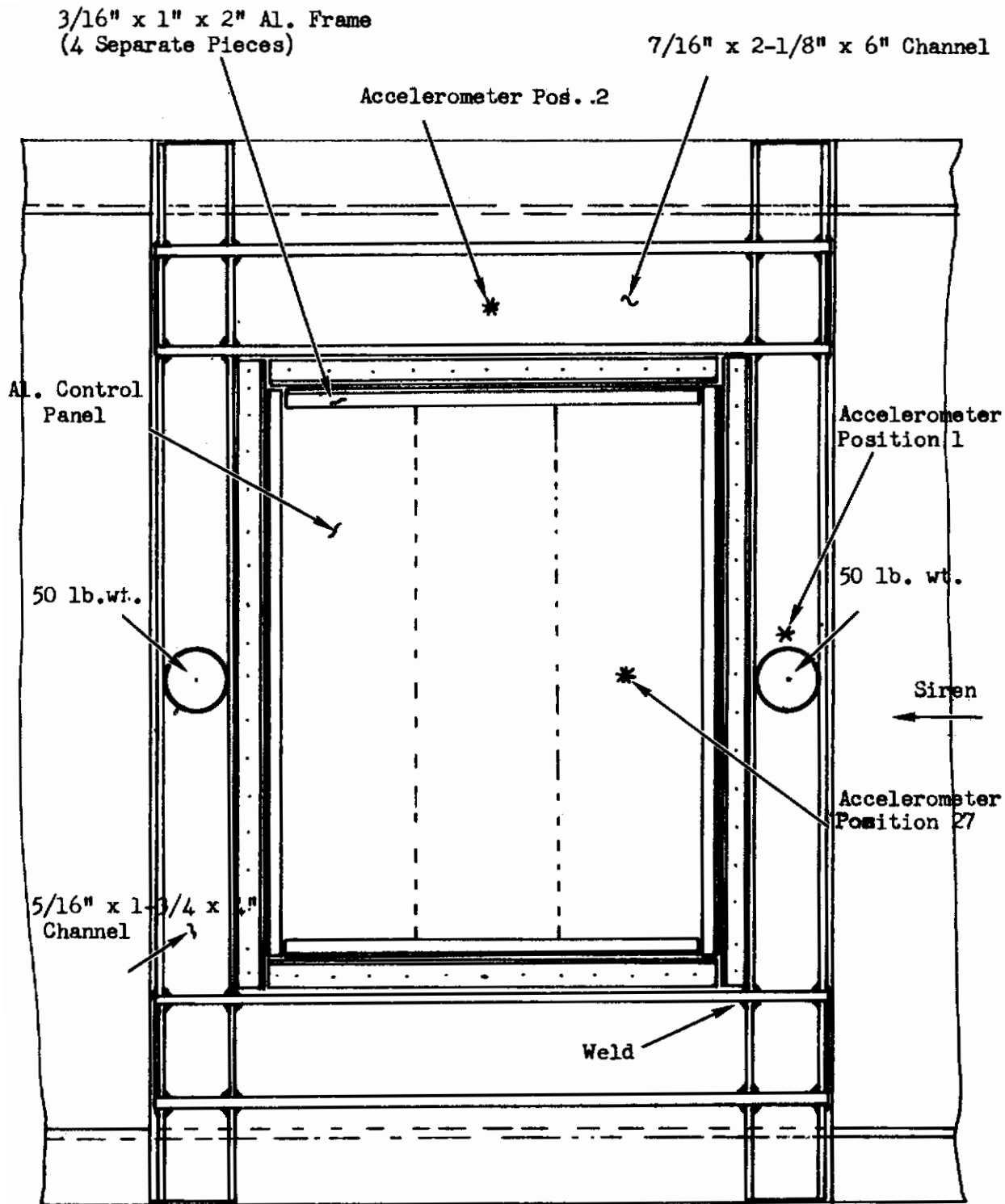


Figure 4. Sonic Fatigue Test Fixture - Final Design

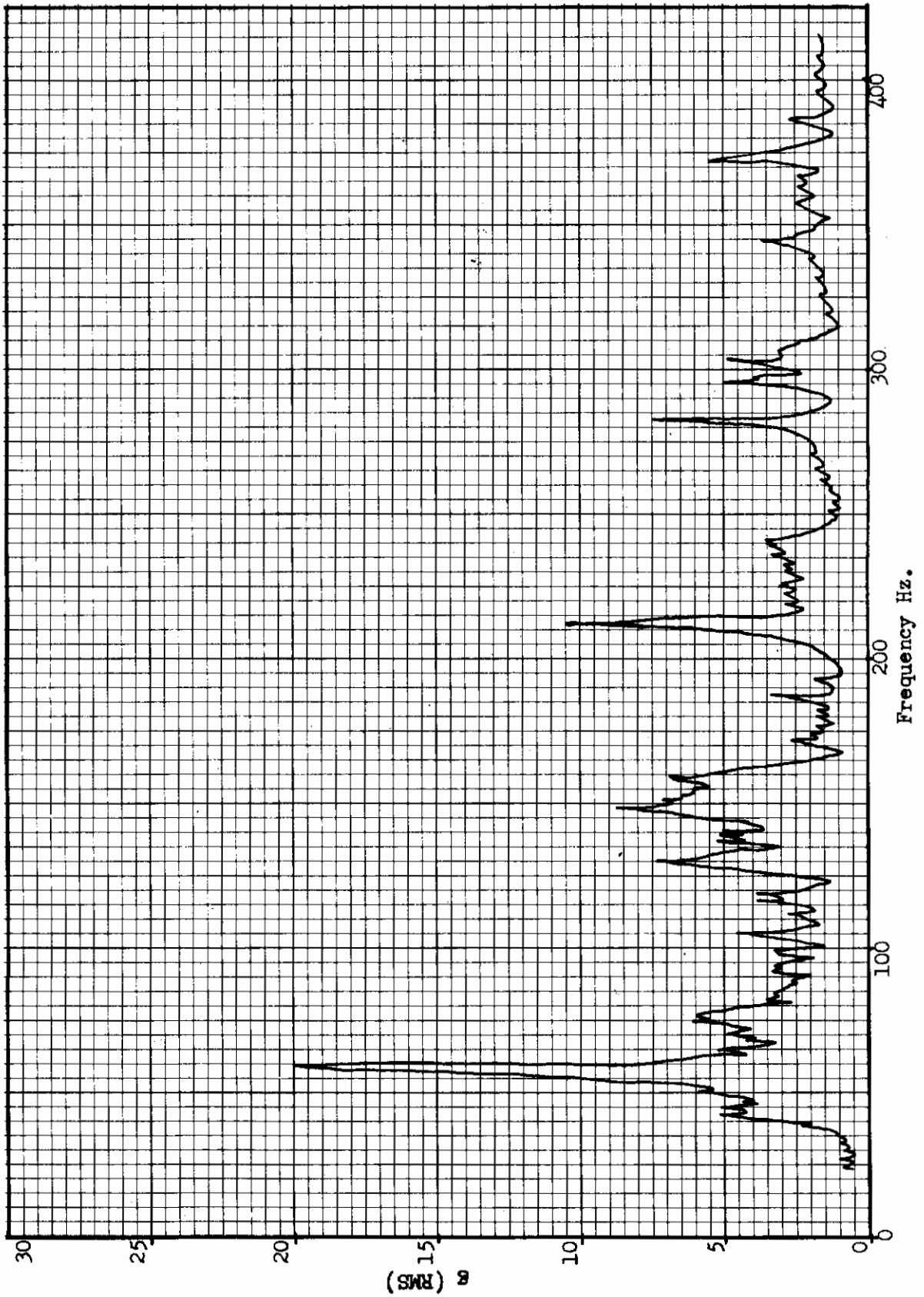


Figure 5. Test Fixture Response at Position 1 (150 db)

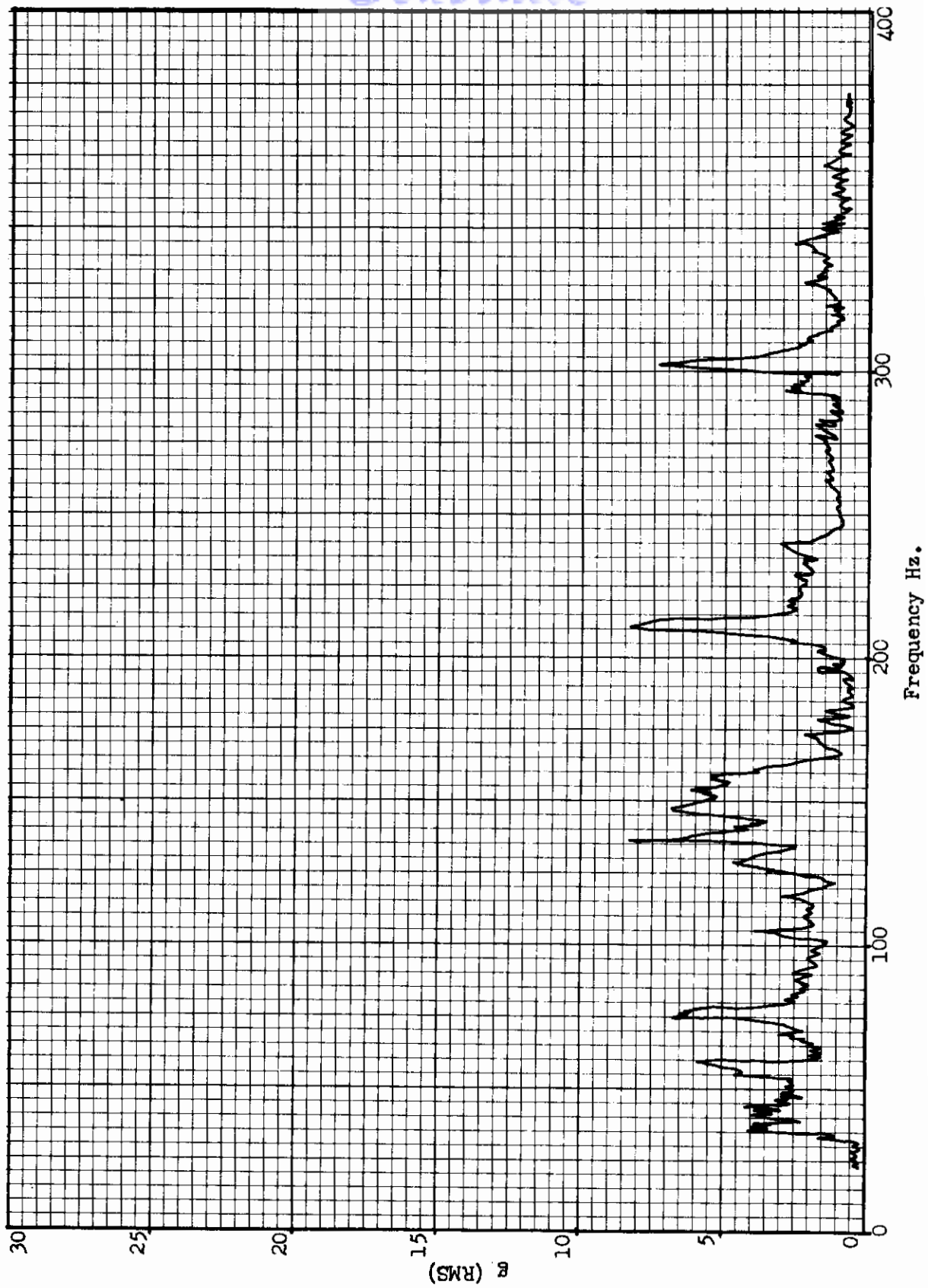


Figure 6. Test Fixture Response at Position 2 (150 db)

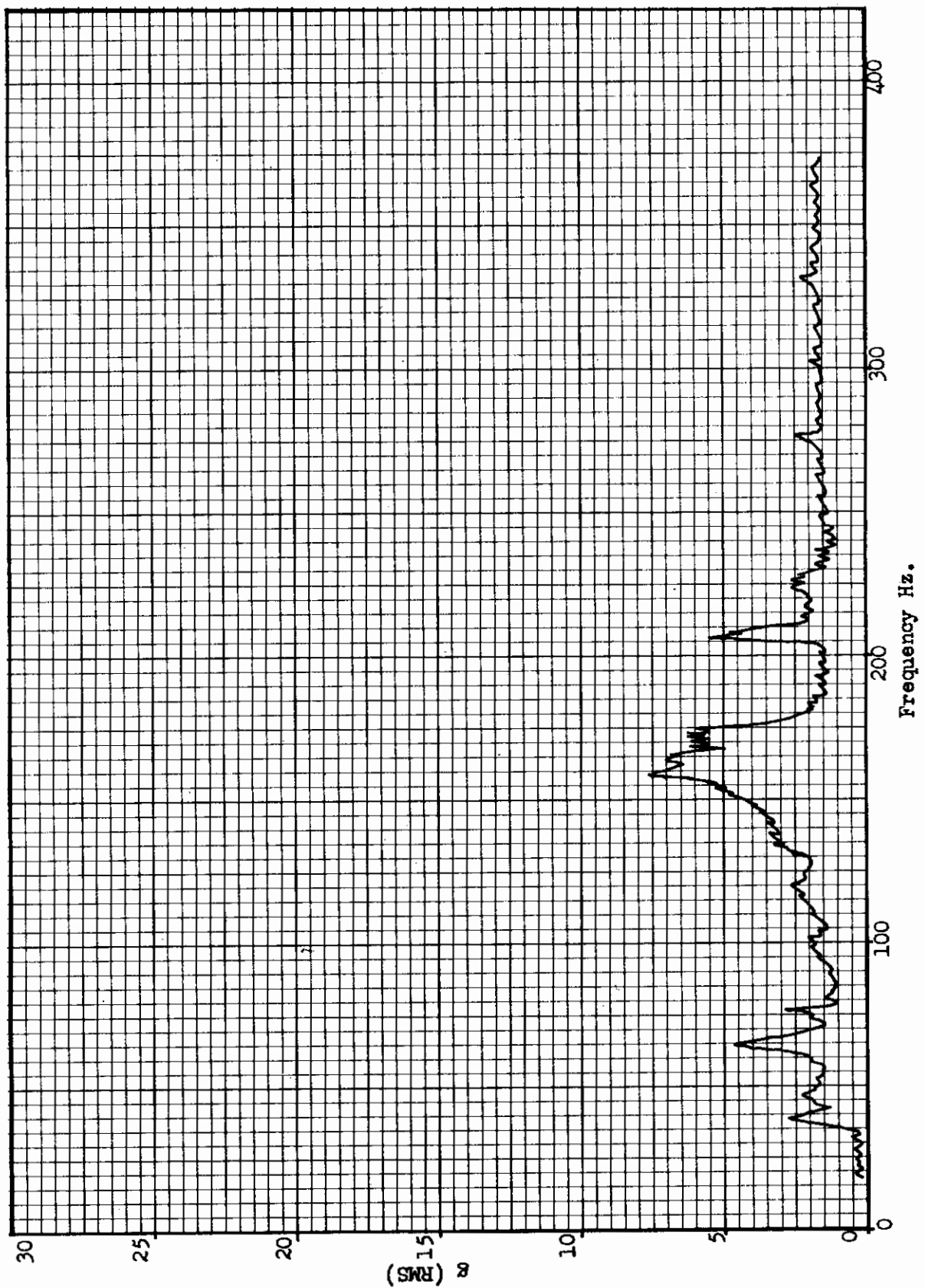


Figure 7. Test Fixture Response at Position 1 with Weights (150 db)

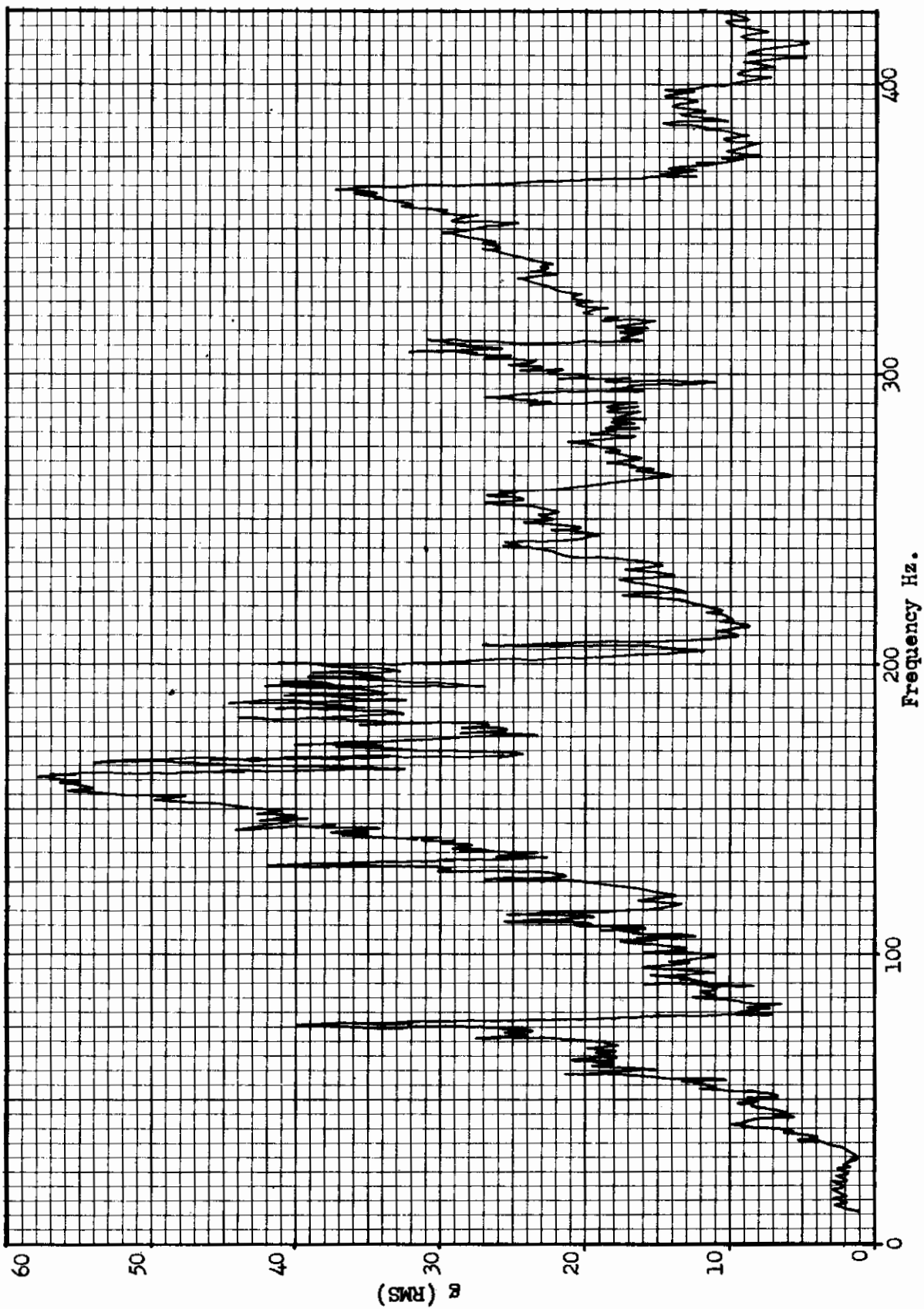


Figure 8. Control Panel Response Position 21 (150 db)

# Contrails

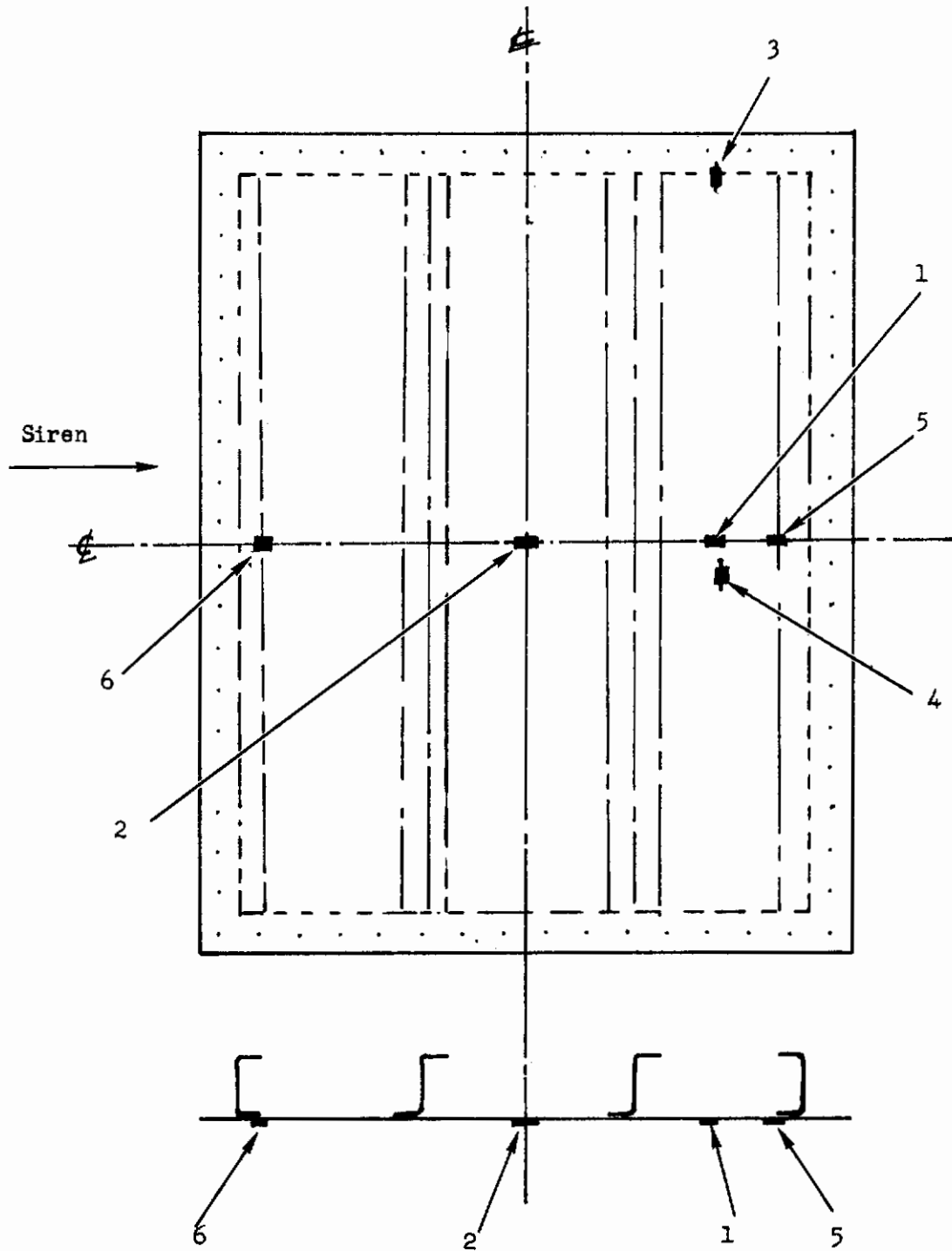


Figure 9. Panel CLX Strain Gage Locations

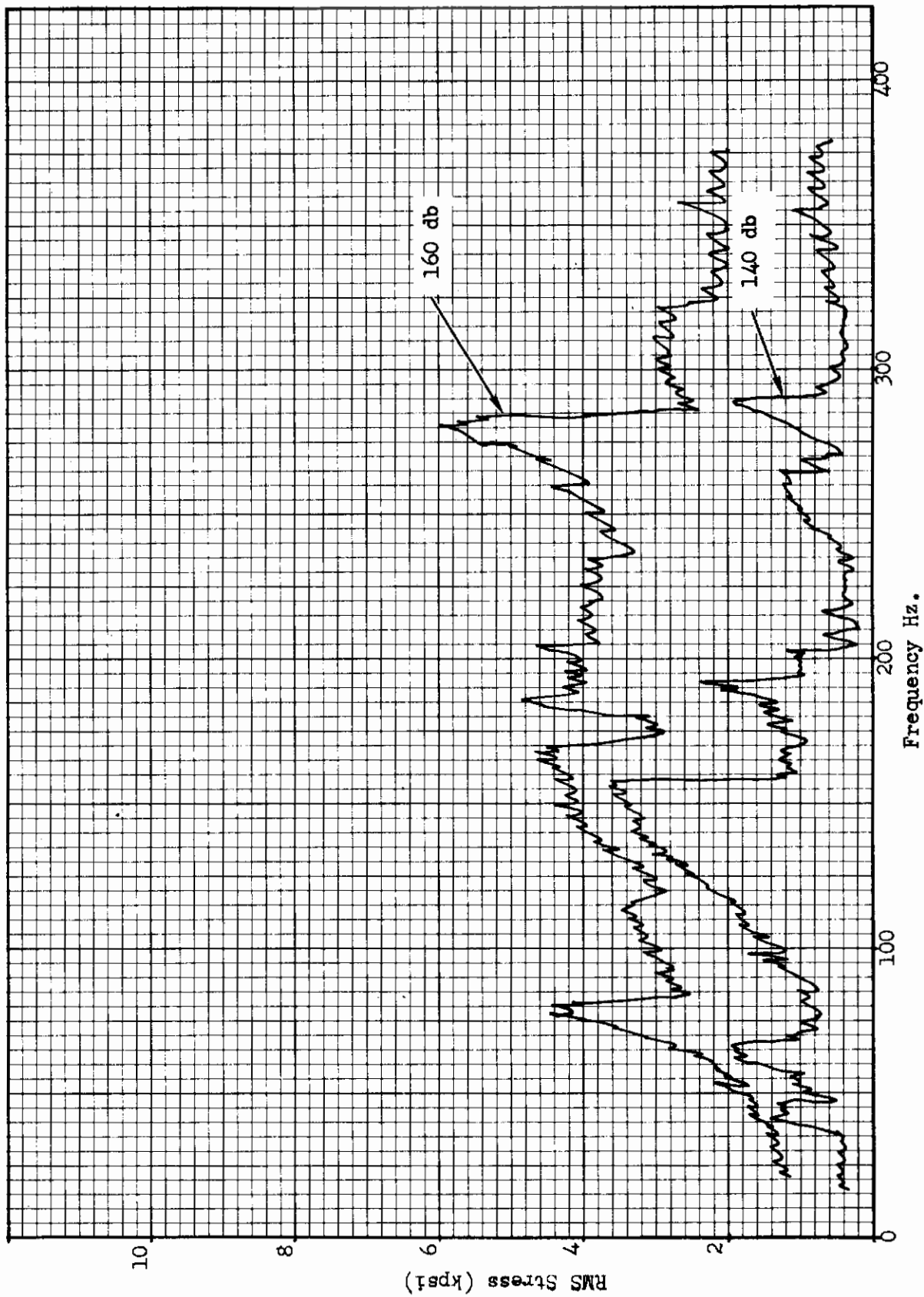


Figure 10. Panel C-1X No. 2 Strain Gage Response at 140 db and 160 db SPL

# Contrails

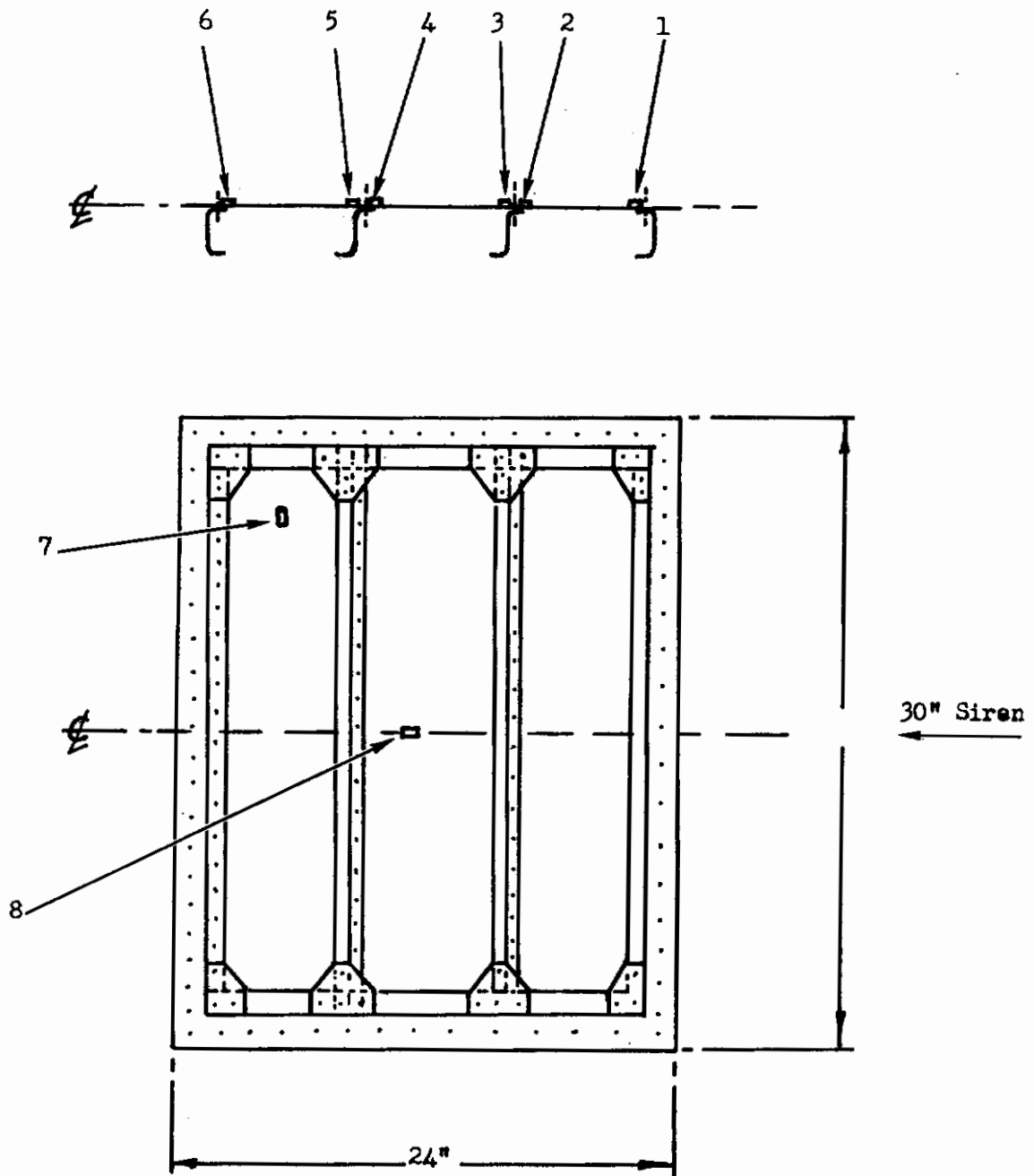


Figure 11. Strain Gage Locations Control Panel C-2X



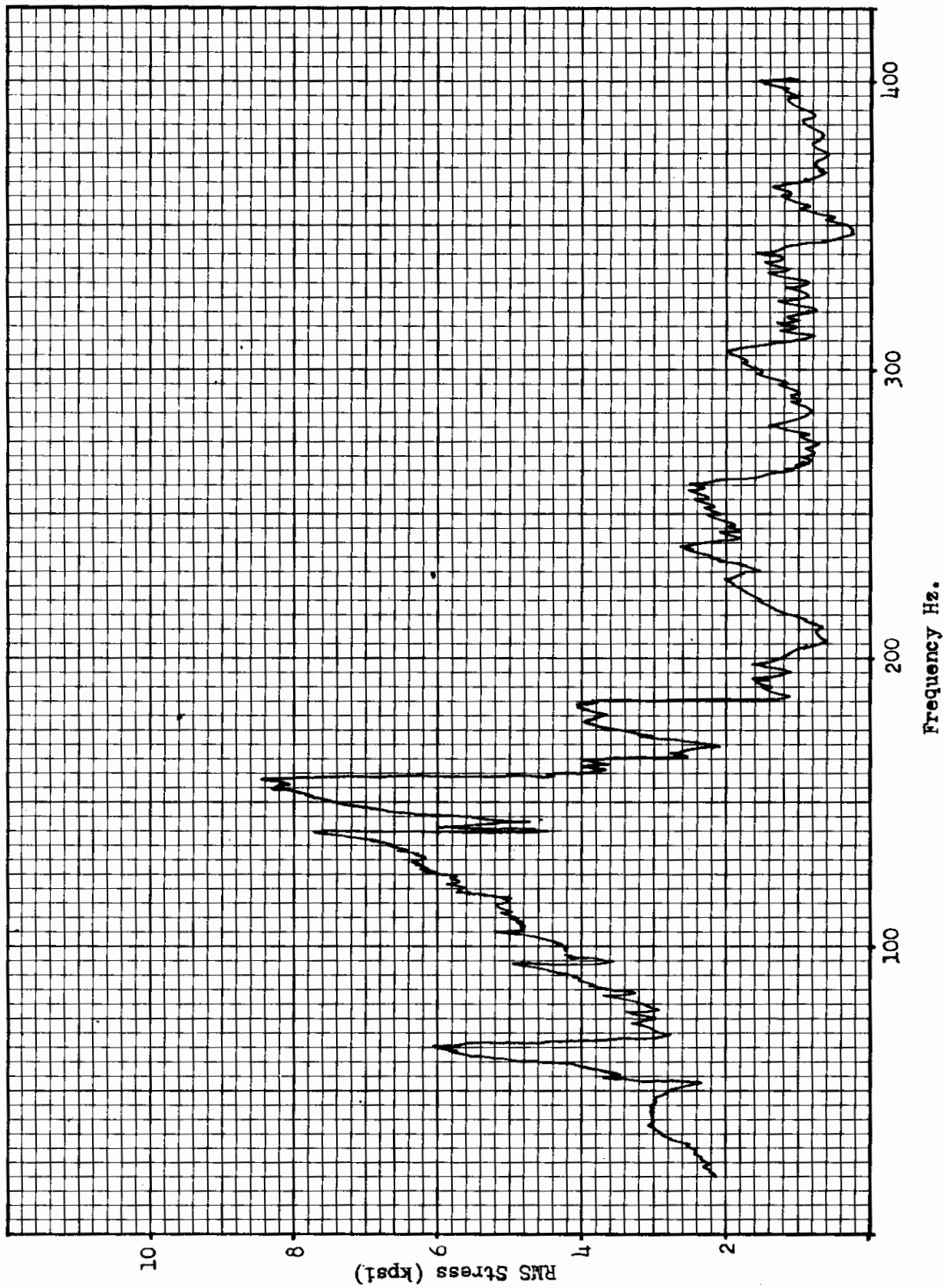


Figure 12. Panel C-2X No. 3 Strain Gage Response at 150 db SPL

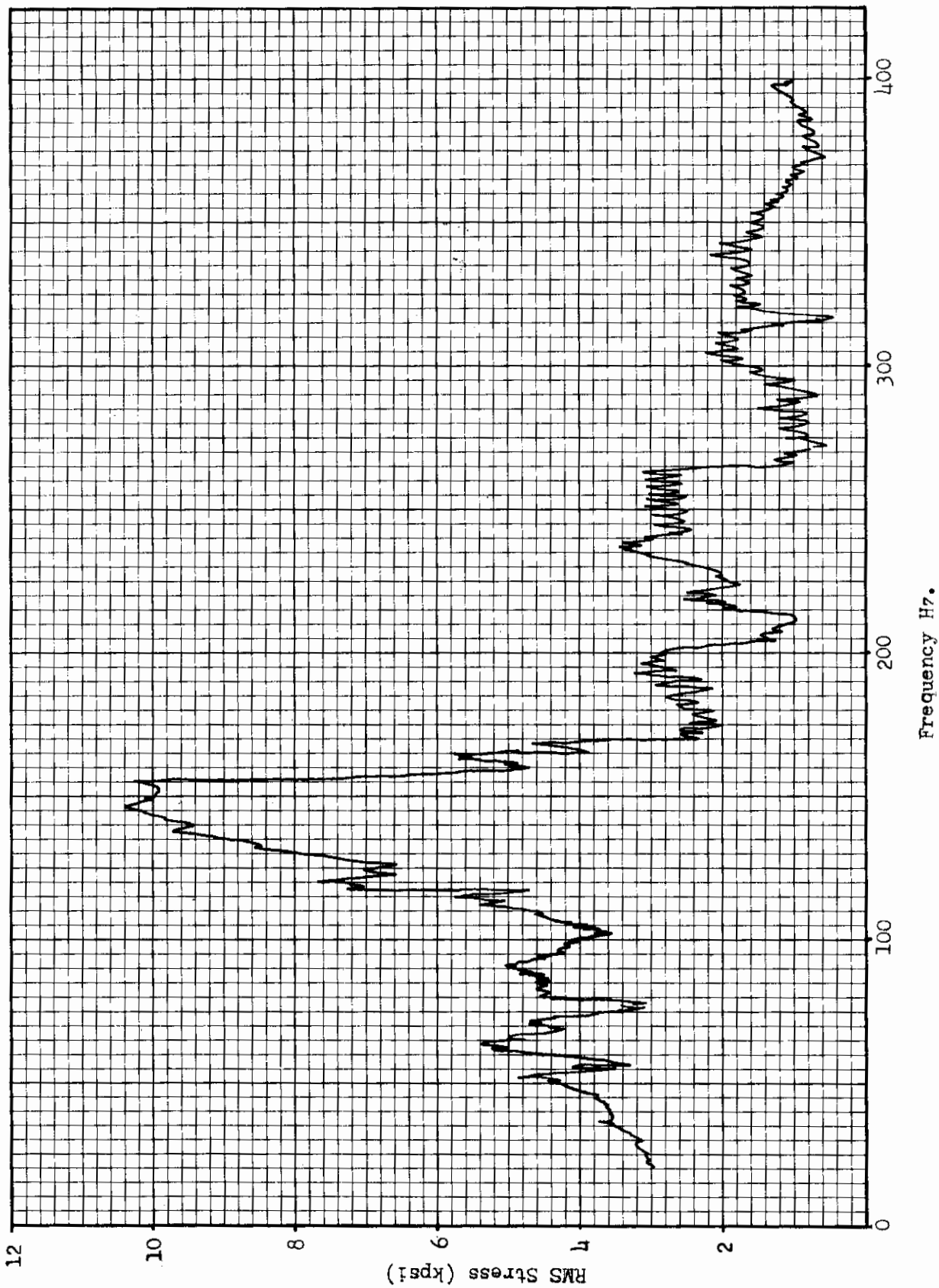


Figure 13. Panel C-2X No. 5 Strain Gage Response at 150 db SPL

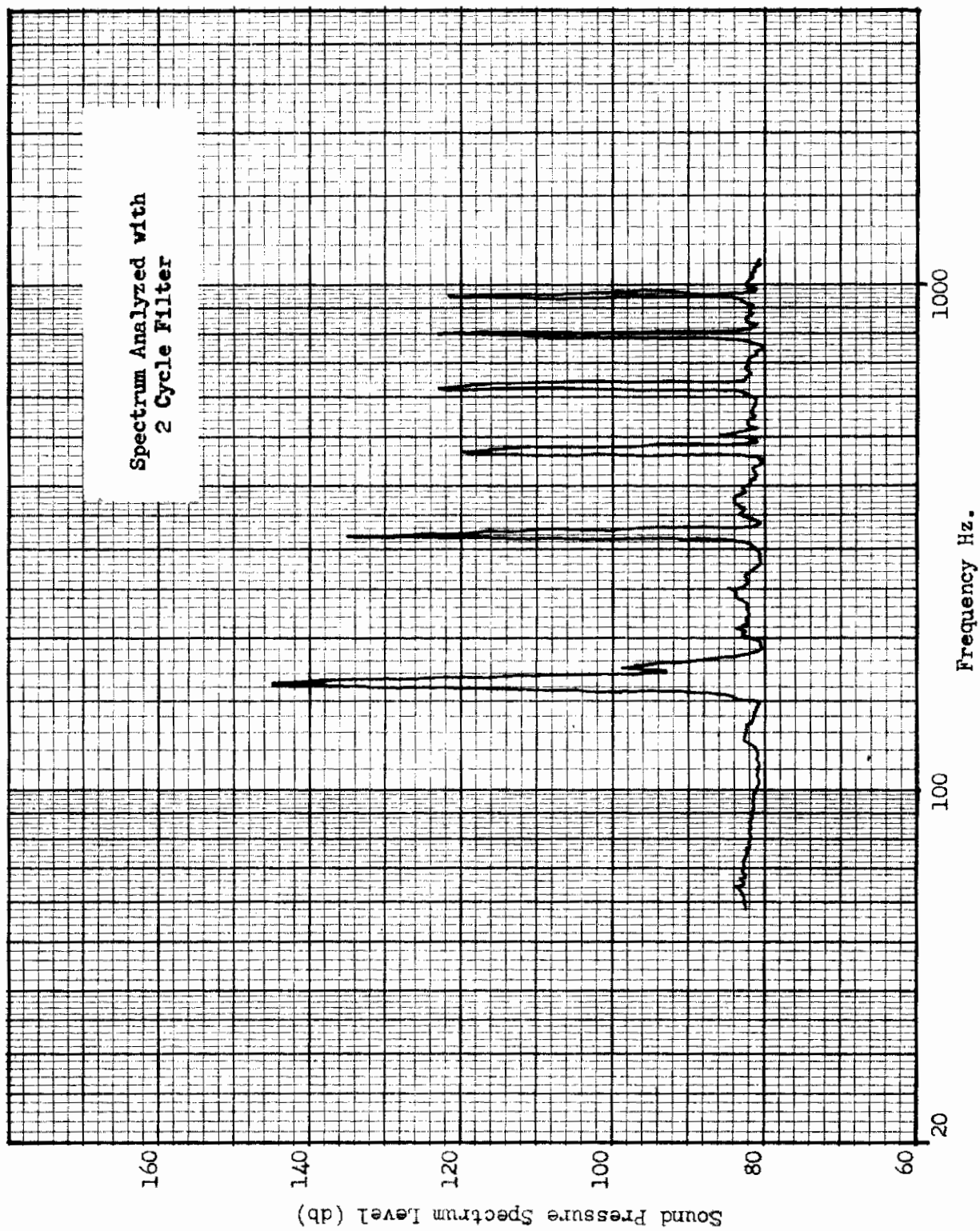


Figure 14. Typical Broad Band Siren Noise Spectrum 165 db SPL O/A

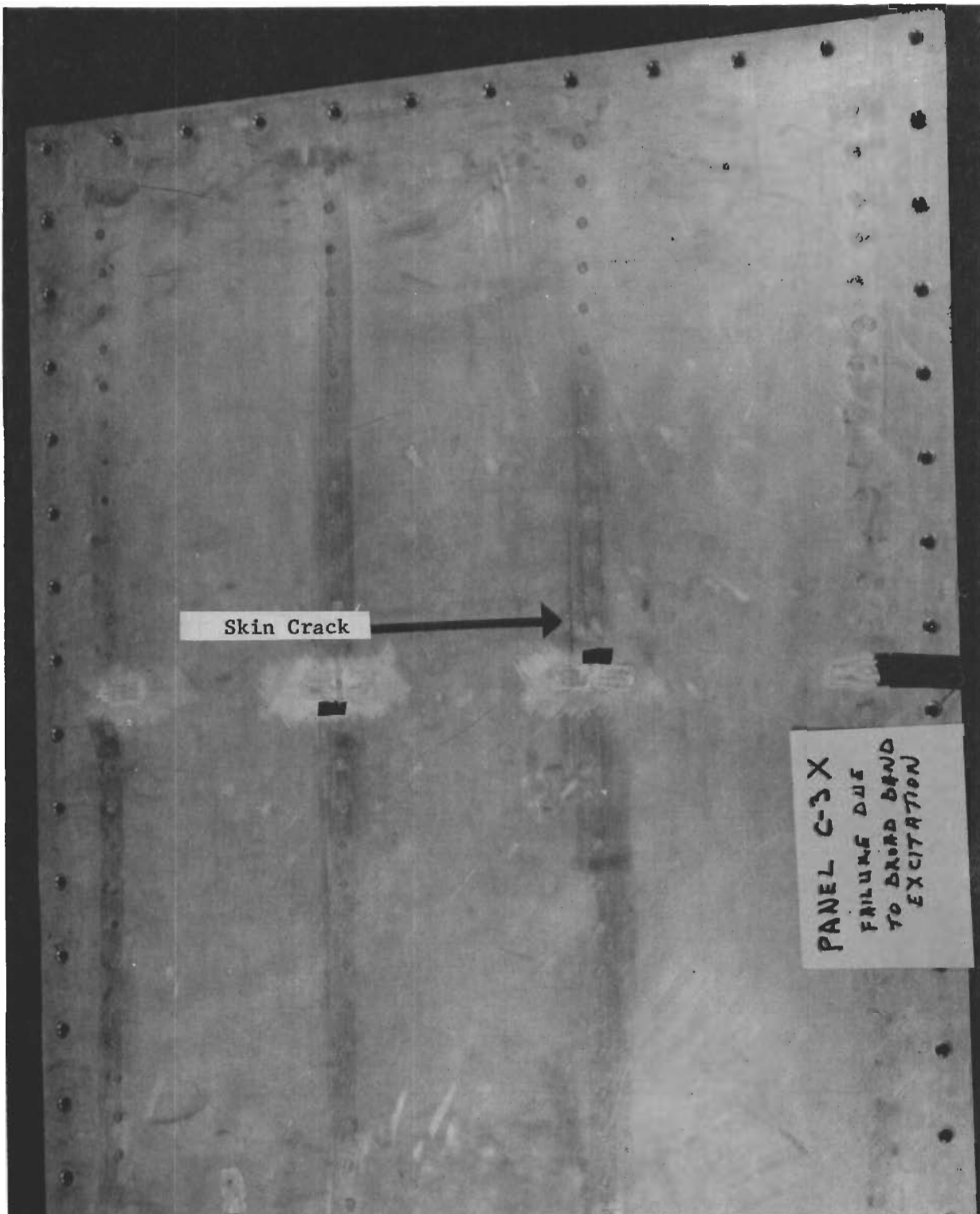


Figure 15. Panel C-3X after Broad Band Siren Test  
50

# Contrails

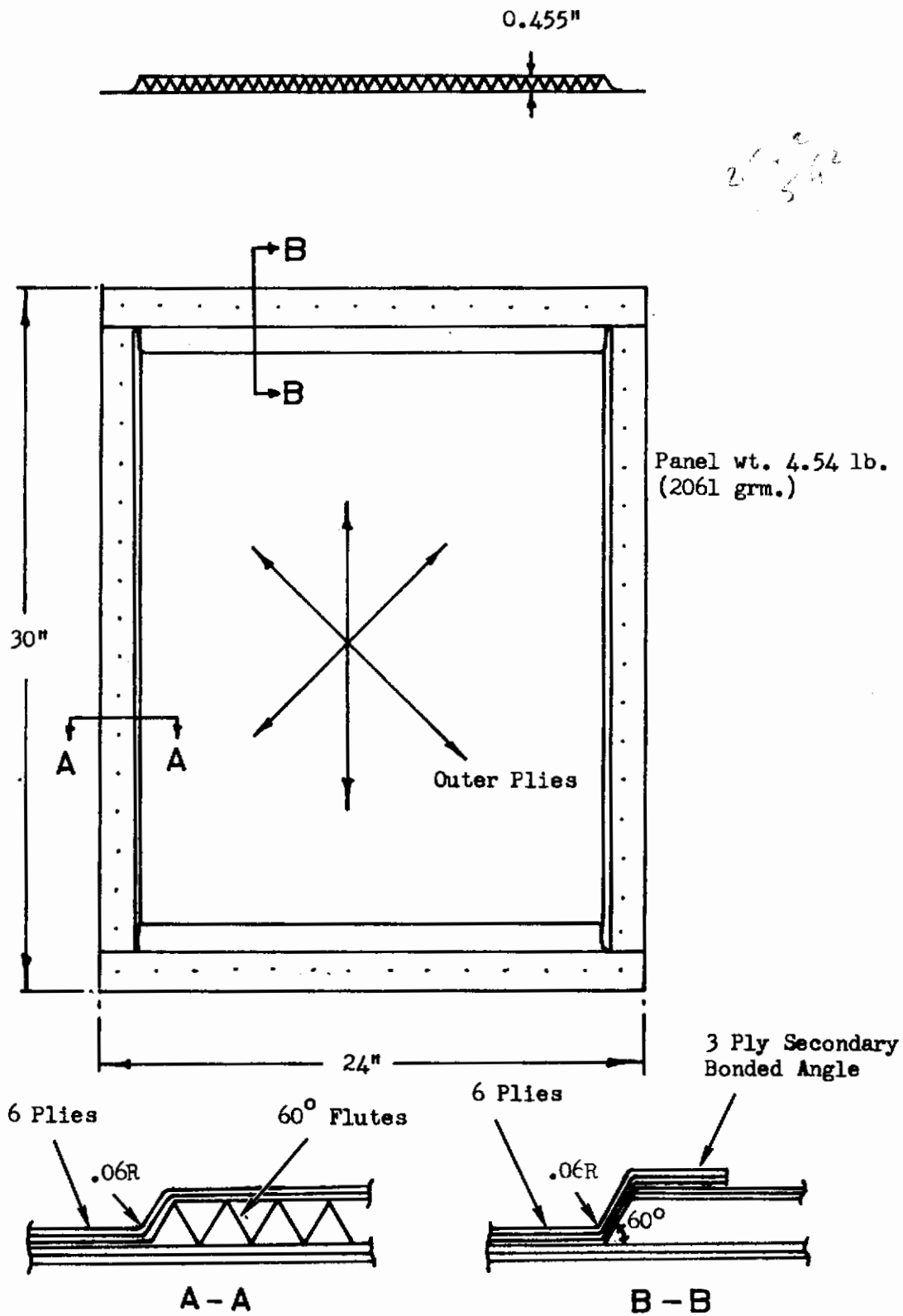


Figure 16. Type I Glass Fiber Panel - Original Design

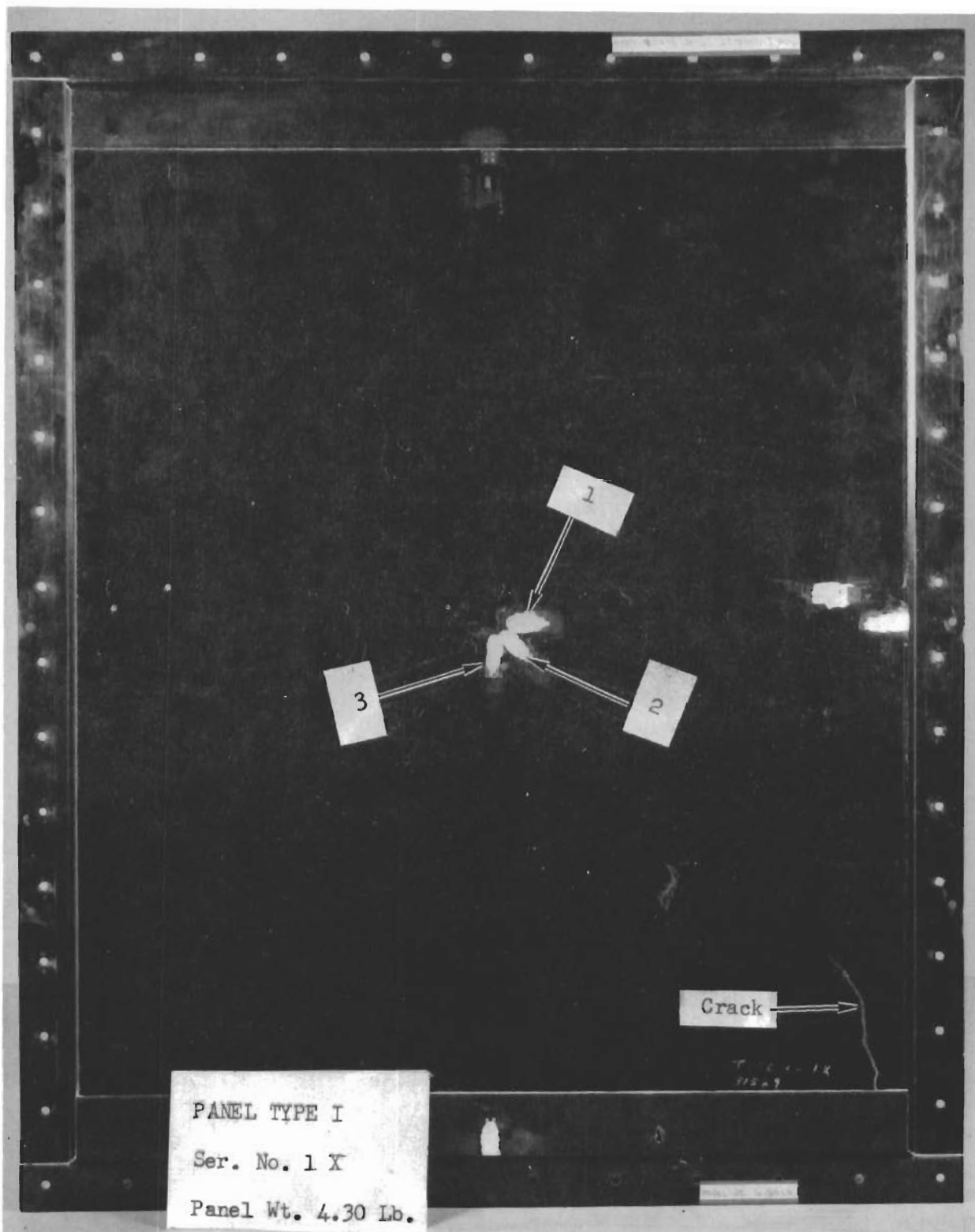


Figure 17. Type I Glass Fiber Panel - Strain Gage Locations

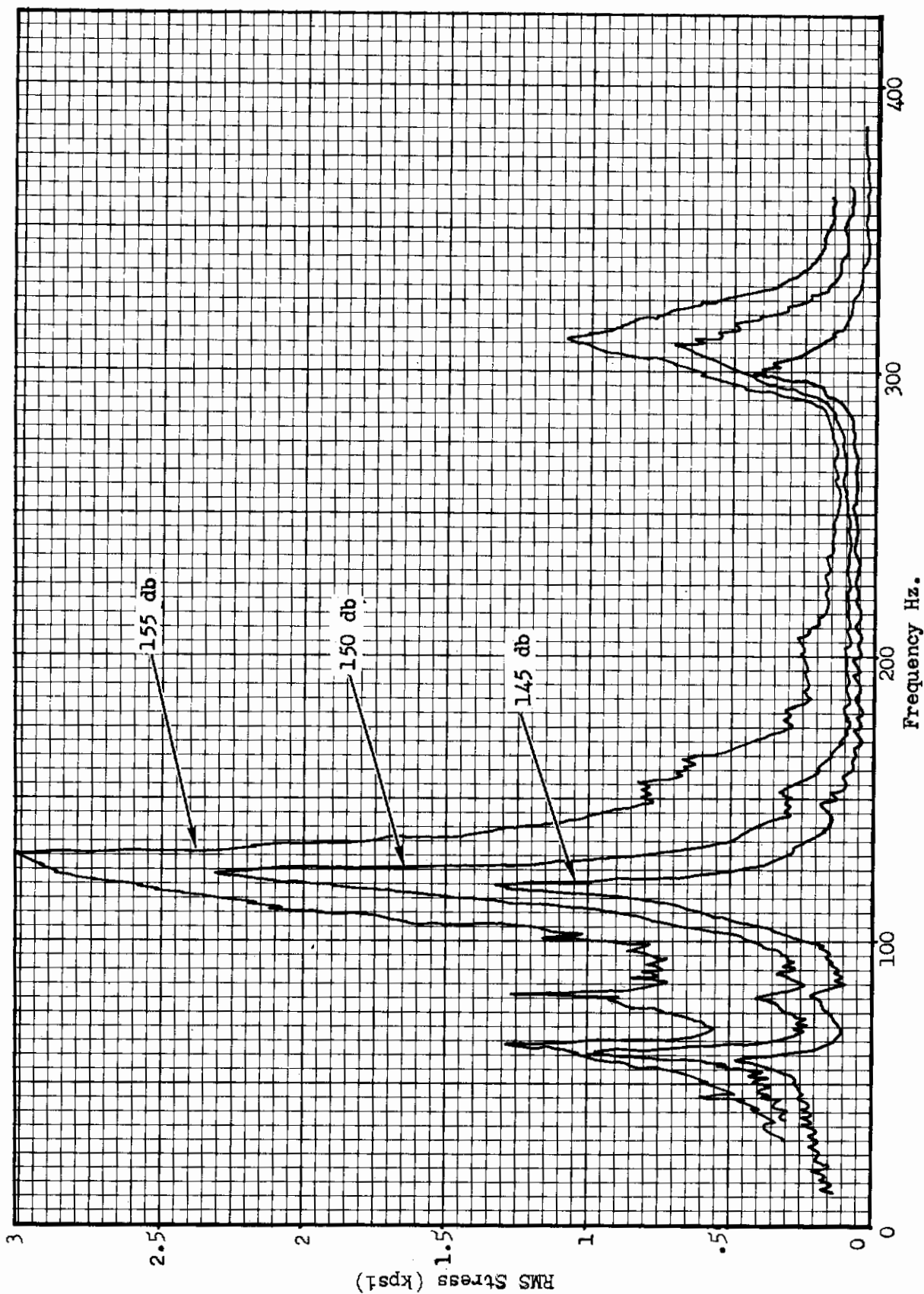


Figure 18. Panel Type I - No. 1 Strain Gage Response

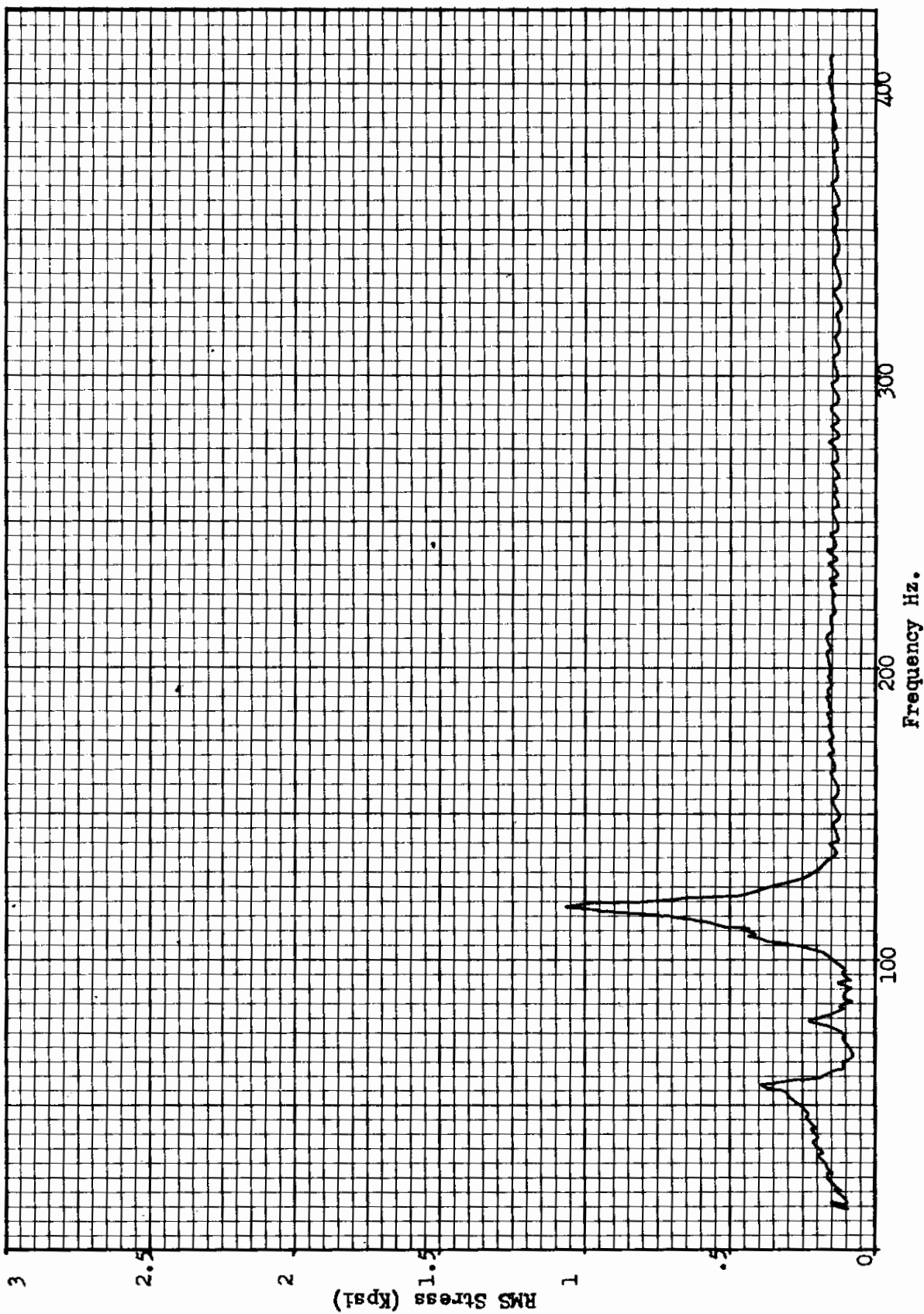


Figure 19. Panel Type I - No. 3 Strain Gage Response (145 db)



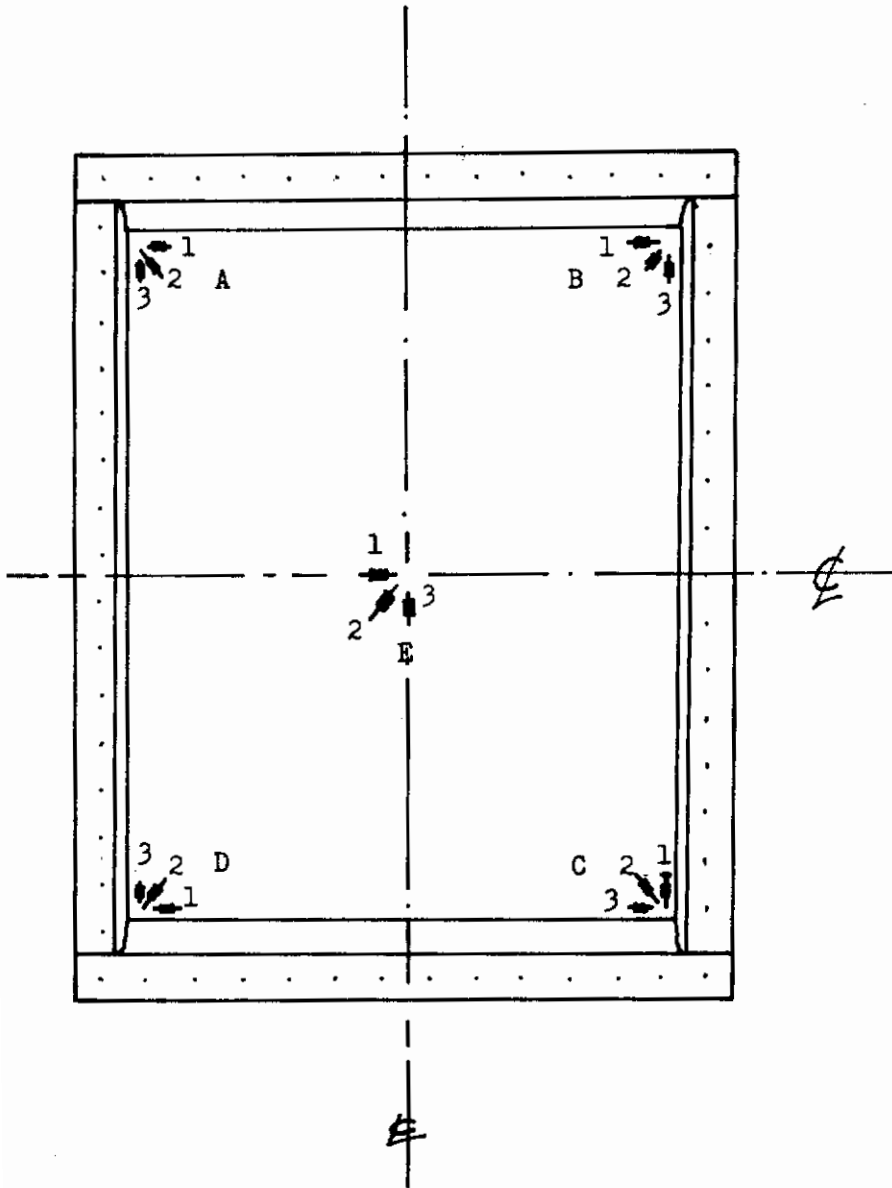


Figure 20. Strain Gage Locations Type II Glass Fiber Panel

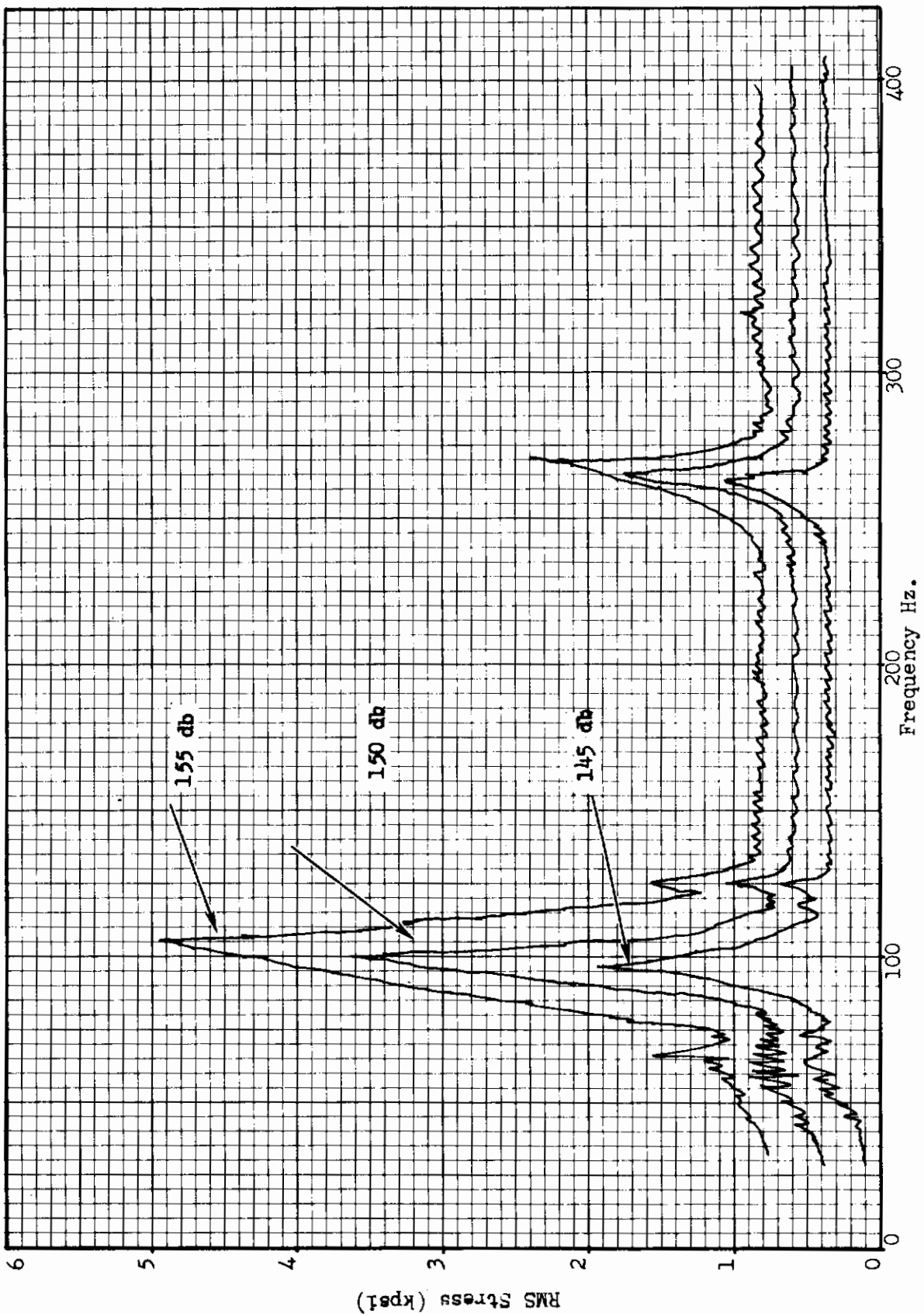


Figure 21. Panel Type II Mid Panel Strain Gage E<sub>2</sub> Response

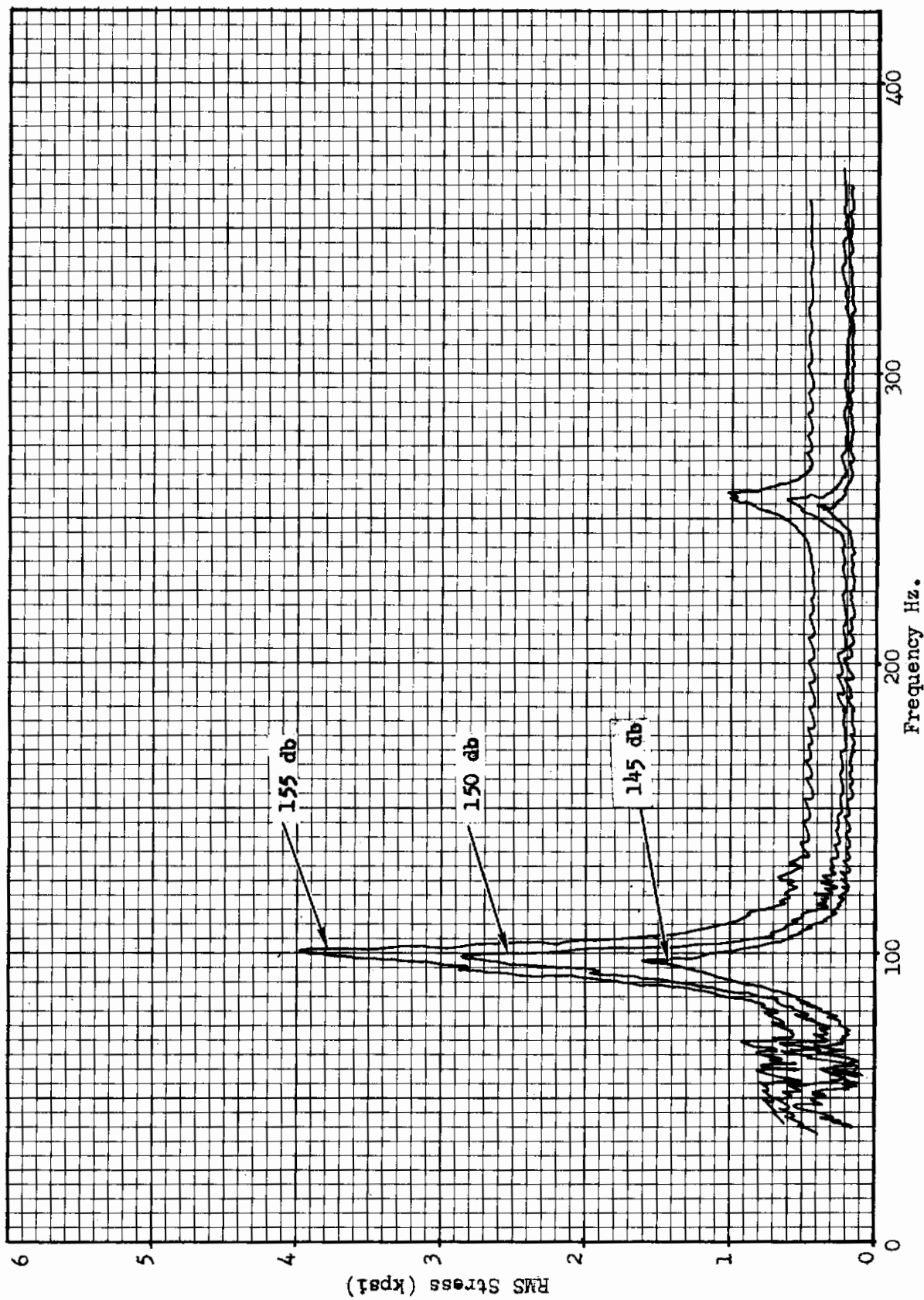


Figure 22. Panel Type II Mid Panel Strain Gage E<sub>2</sub> Response

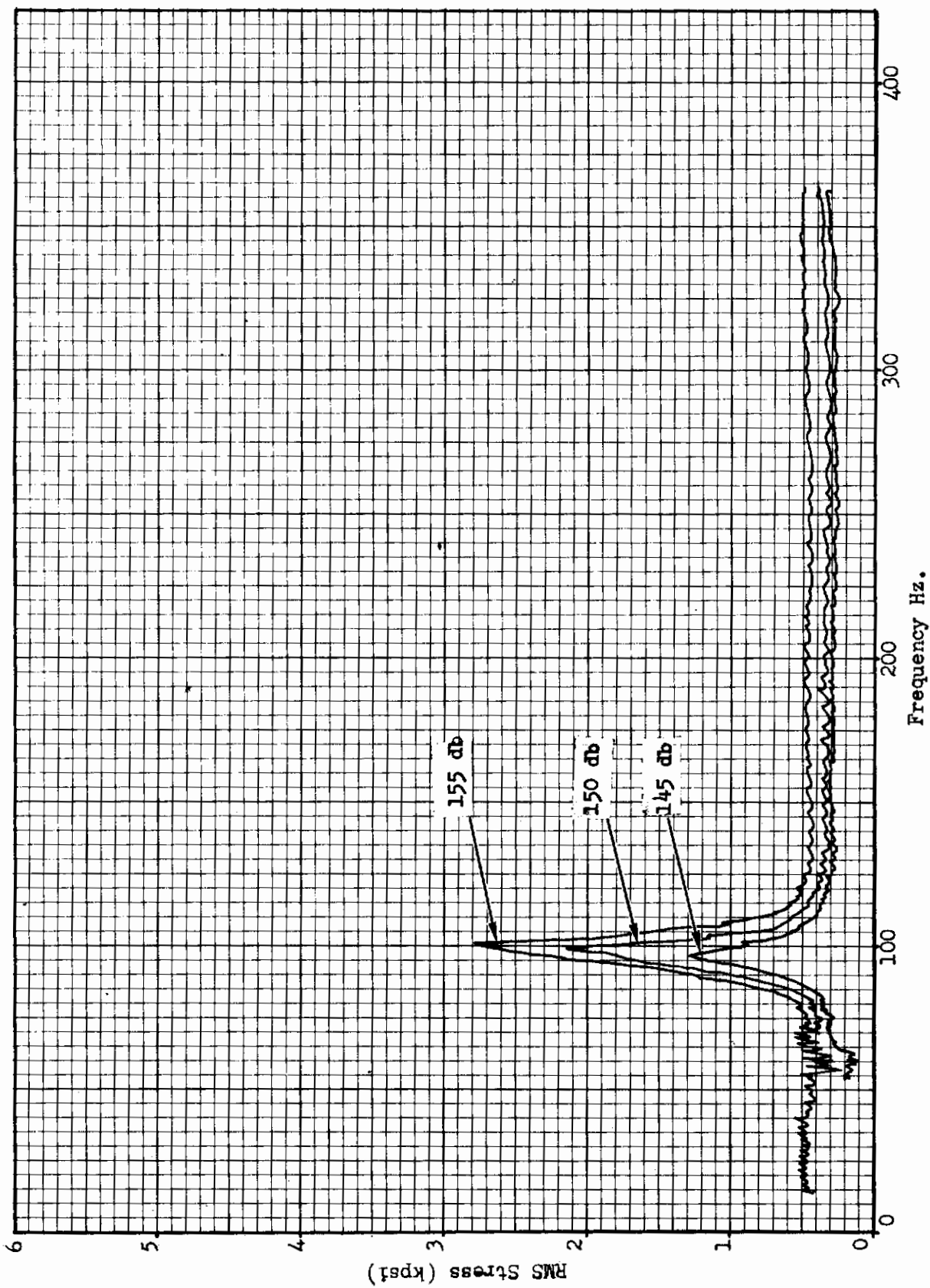


Figure 23. Panel Type II Mid Panel Strain Gage E<sub>3</sub> Response

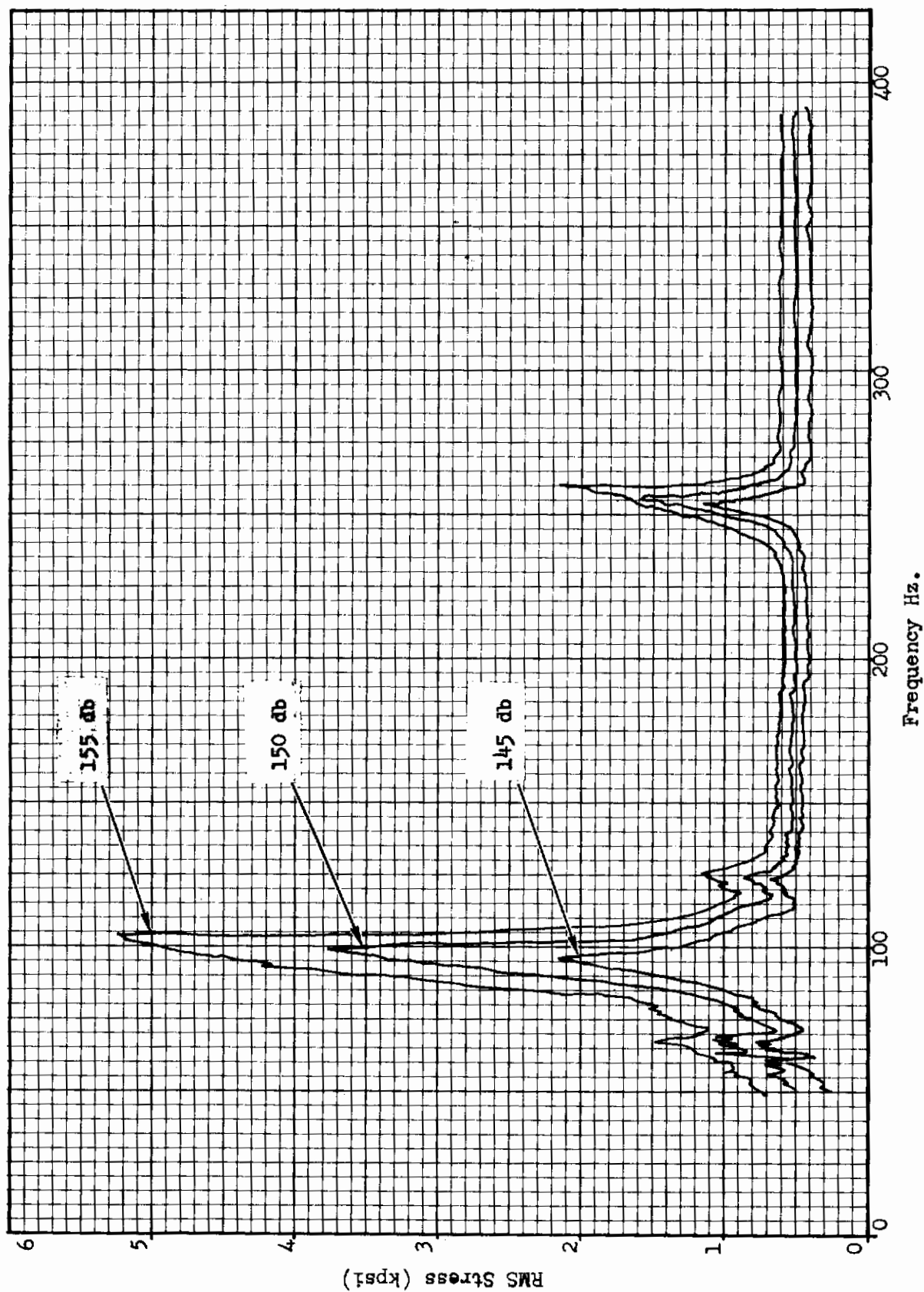


Figure 24. Panel Type II Corner Strain Gage C<sub>1</sub> Response

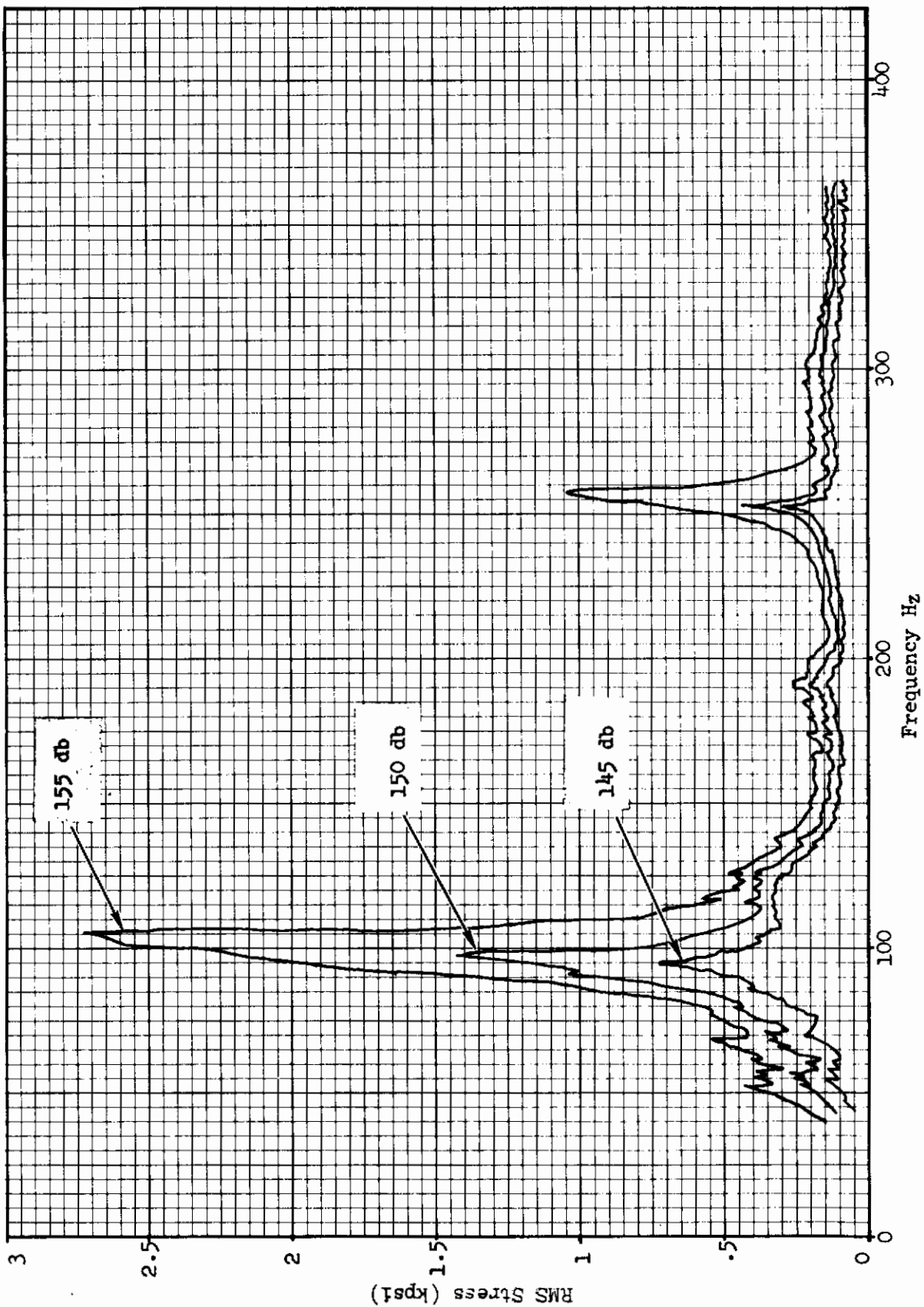


Figure 25. Panel Type II Corner Strain Gage C<sub>2</sub> Response

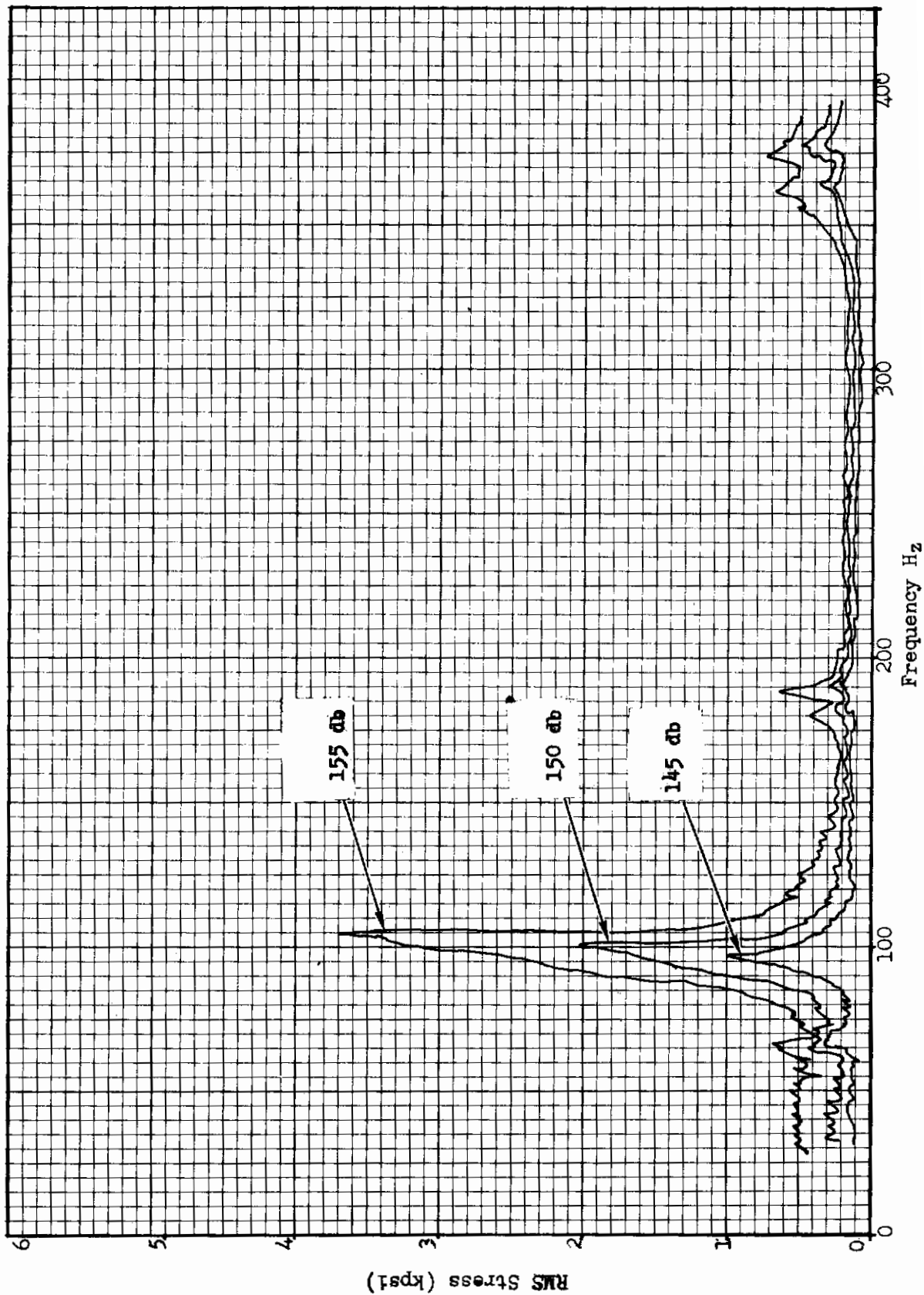


Figure 26. Panel Type II Corner Strain Gage C<sub>3</sub> Response

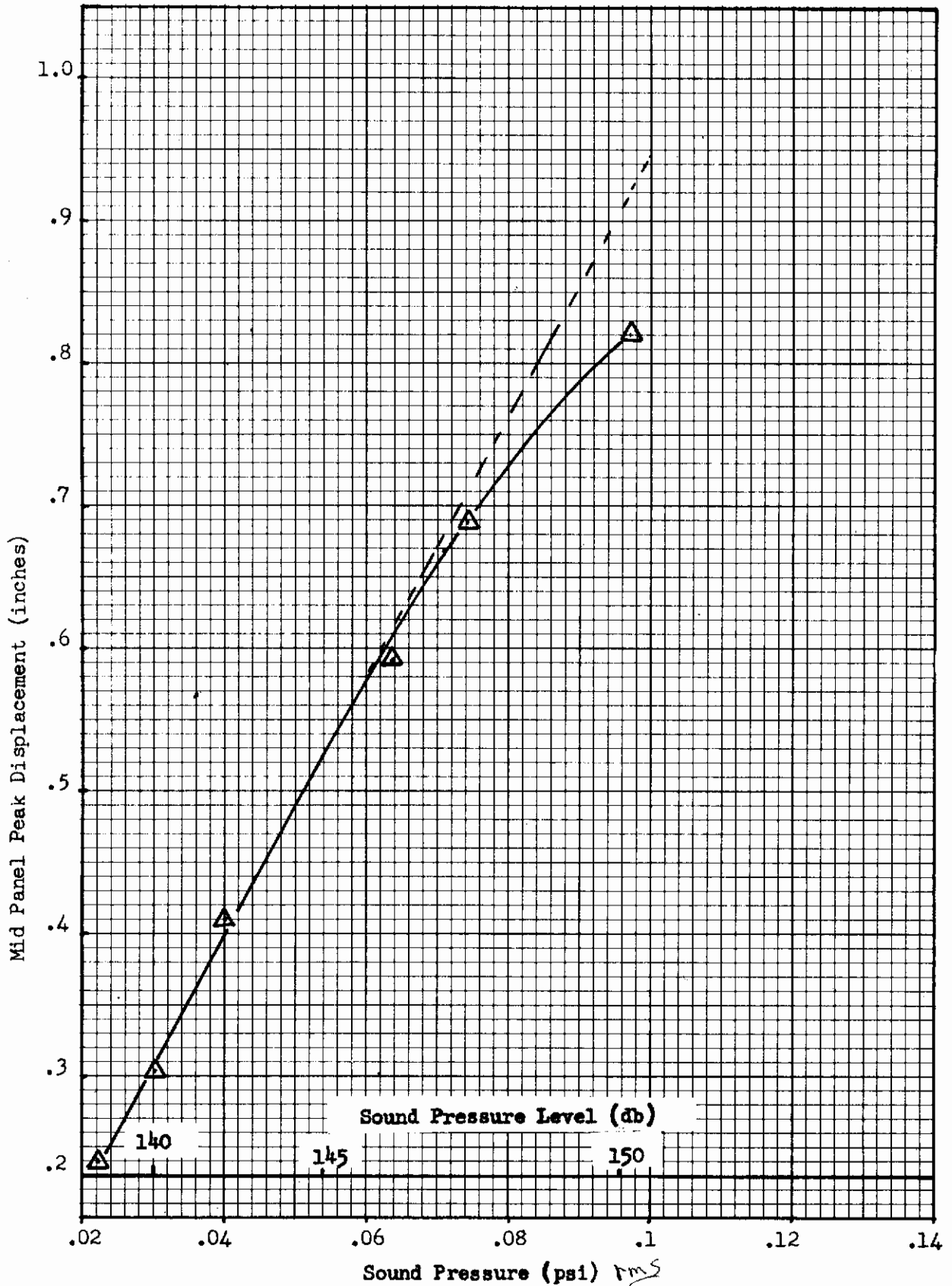


Figure 27. Panel Type II Mid Panel Displacement vs. SPL



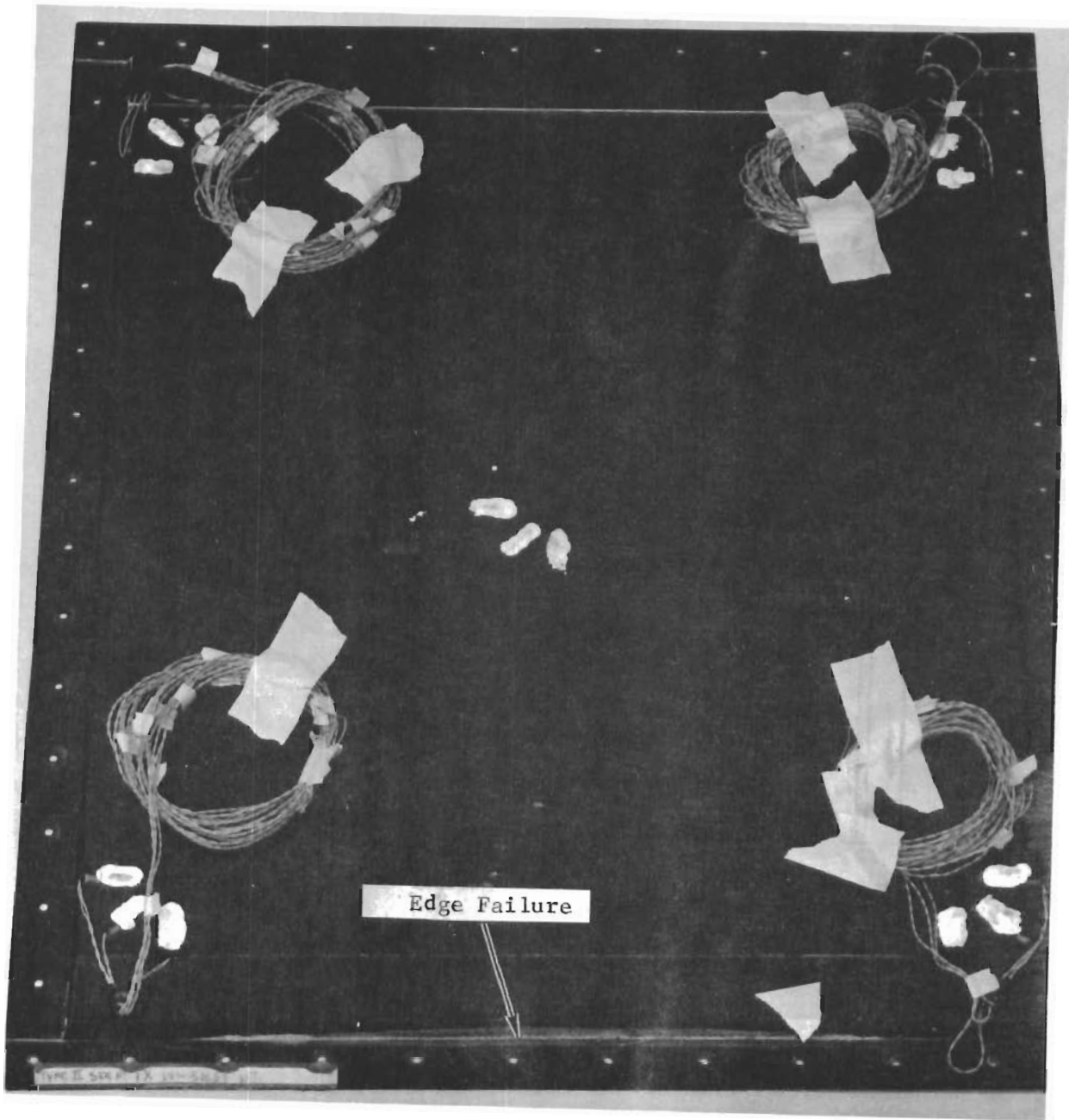


Figure 28. Type II Glass Fiber Panel after Failure

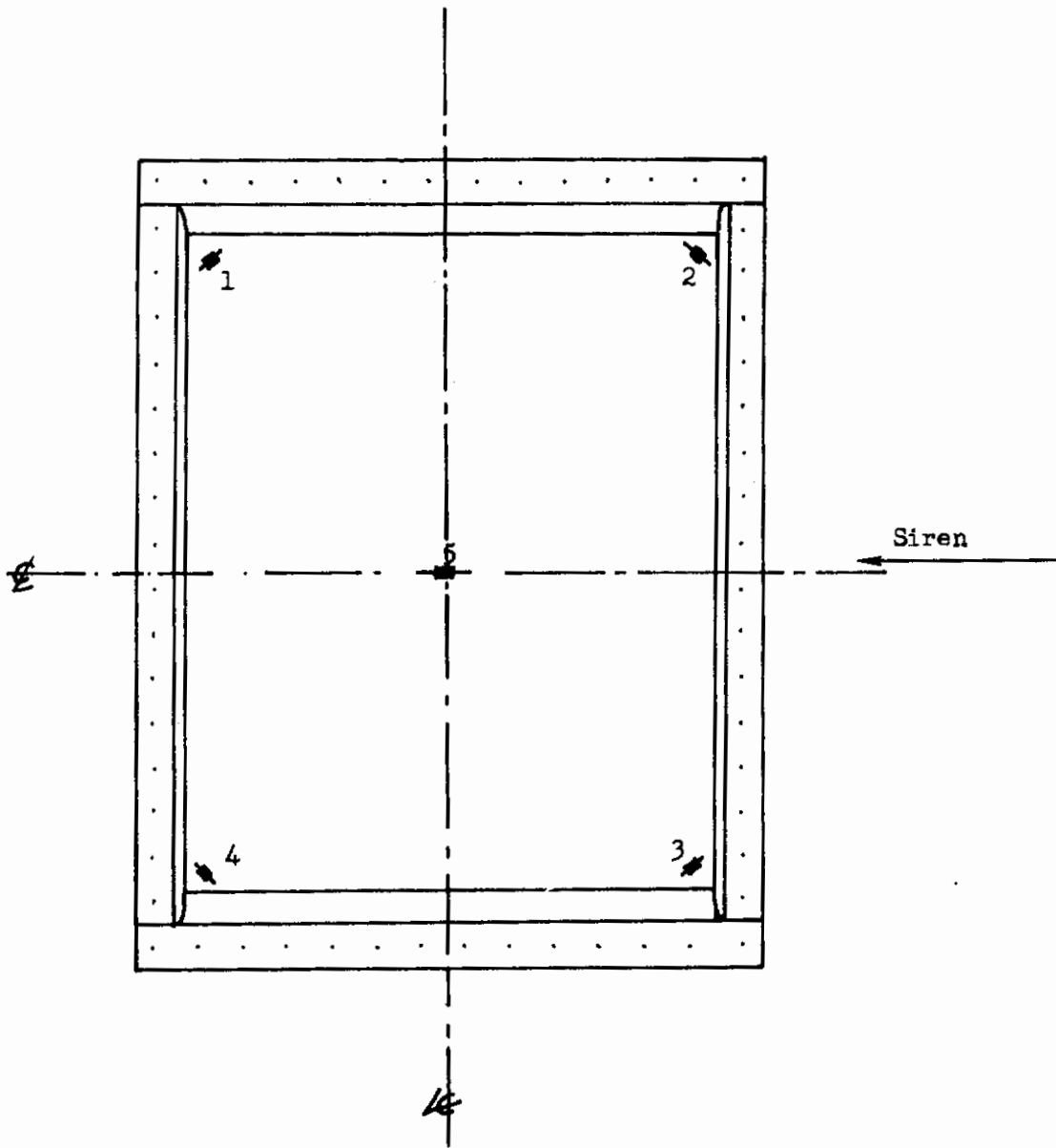


Figure 29. Glass Fiber Panel Type III Strain Gage Location

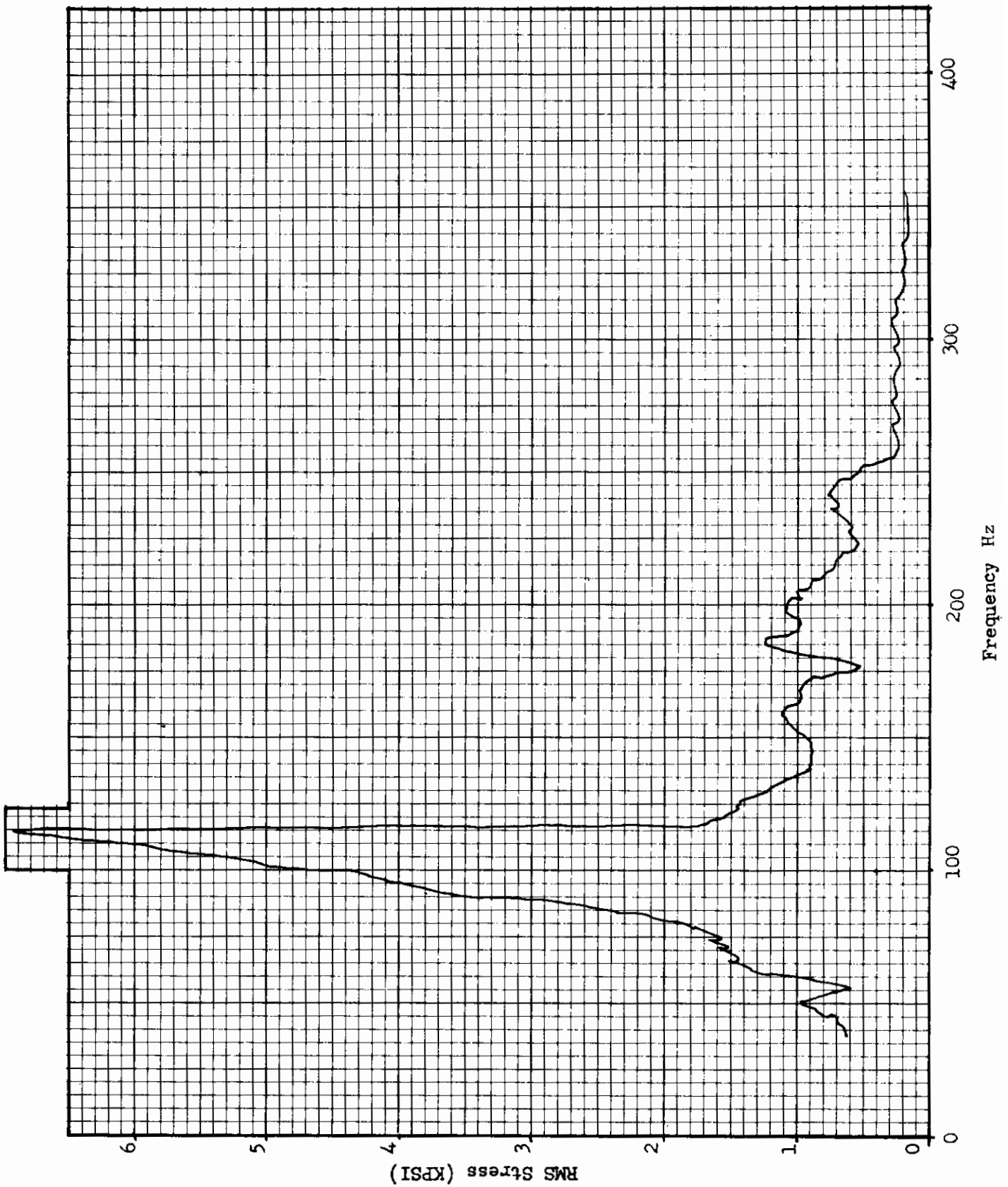


Figure 30. Glass Fiber Panel Type III Gage No. 1 Response (165 db)

# Contrails

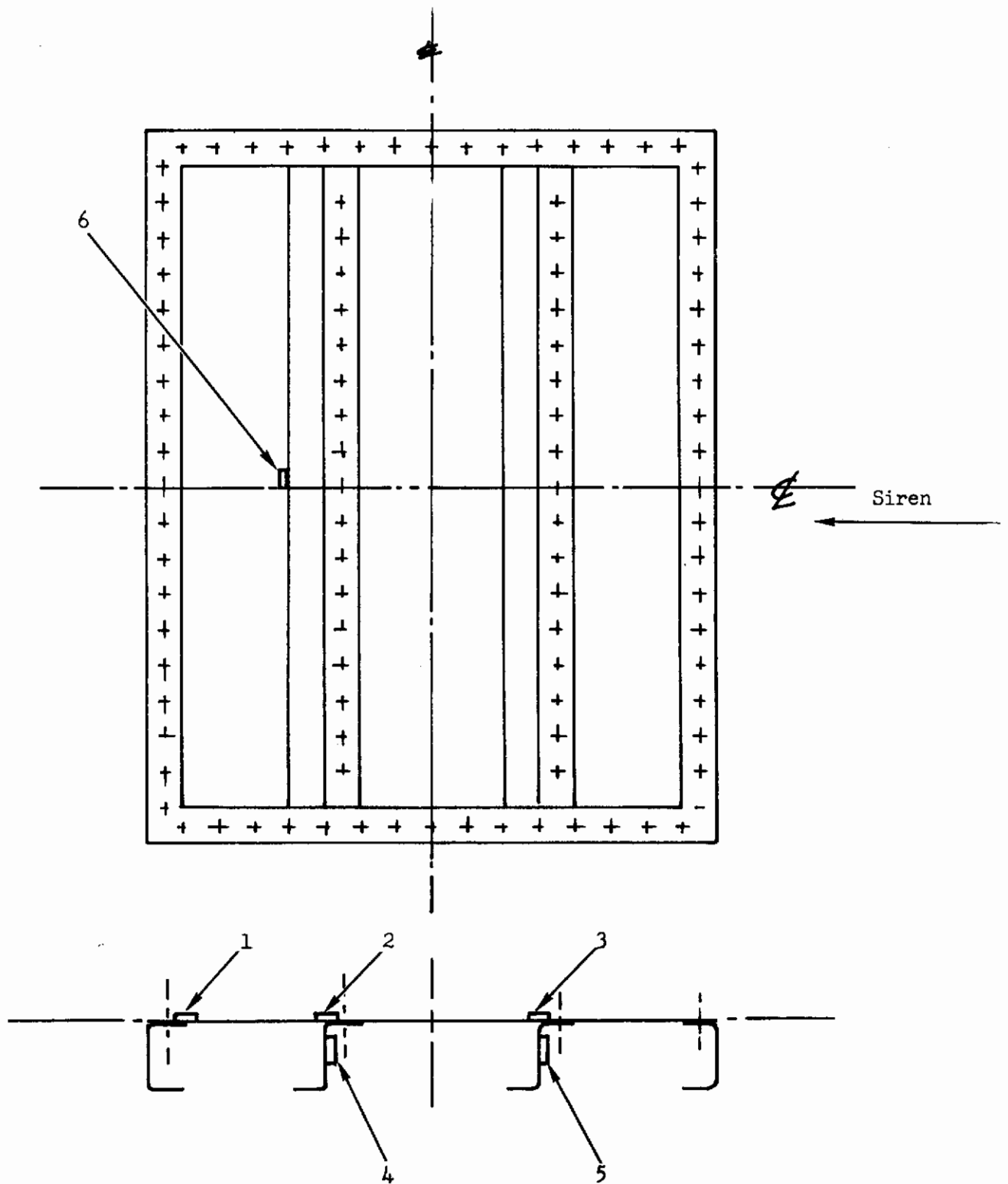


Figure 31. Strain Gage Locations Production Control Panels

# Contrails

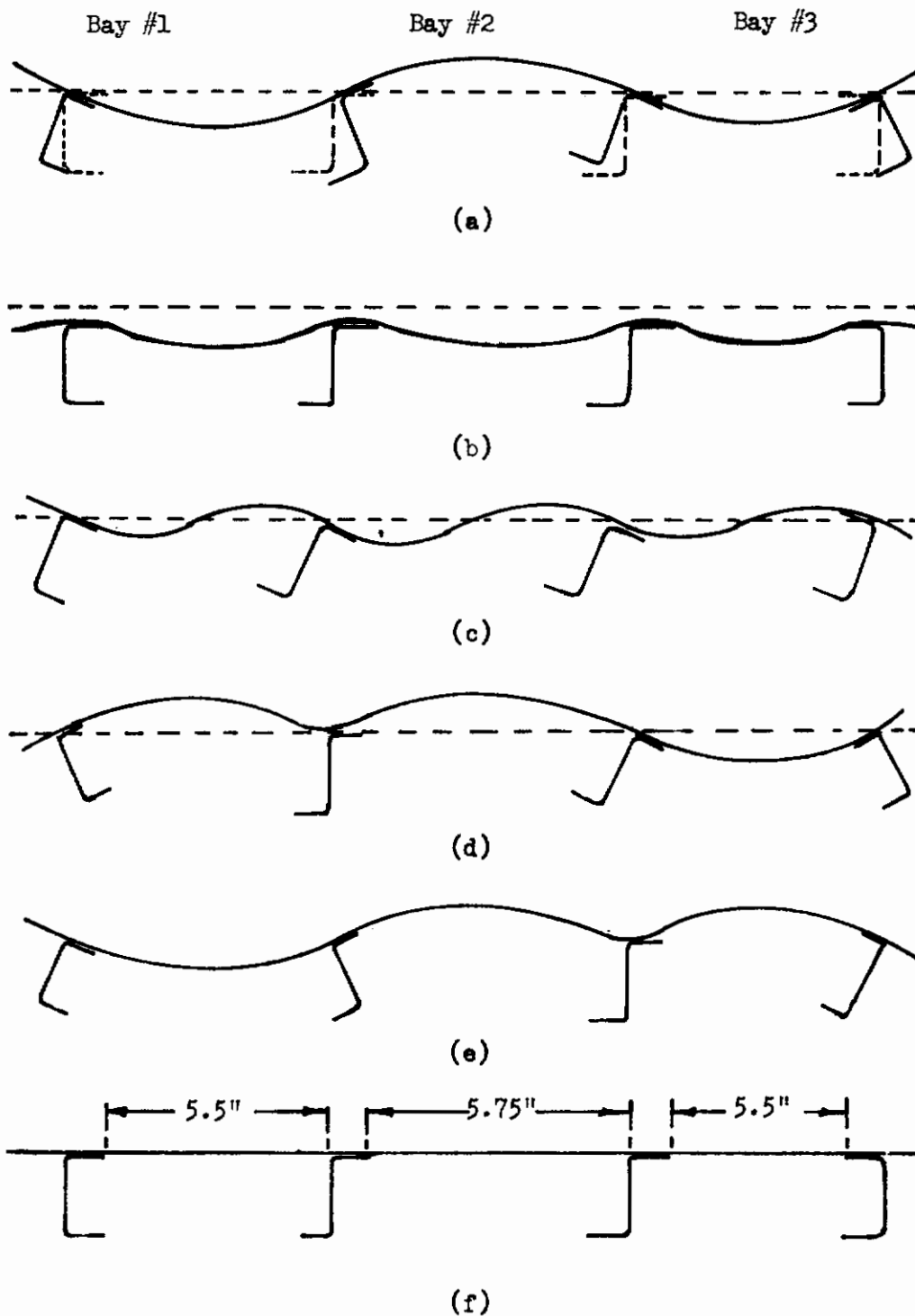
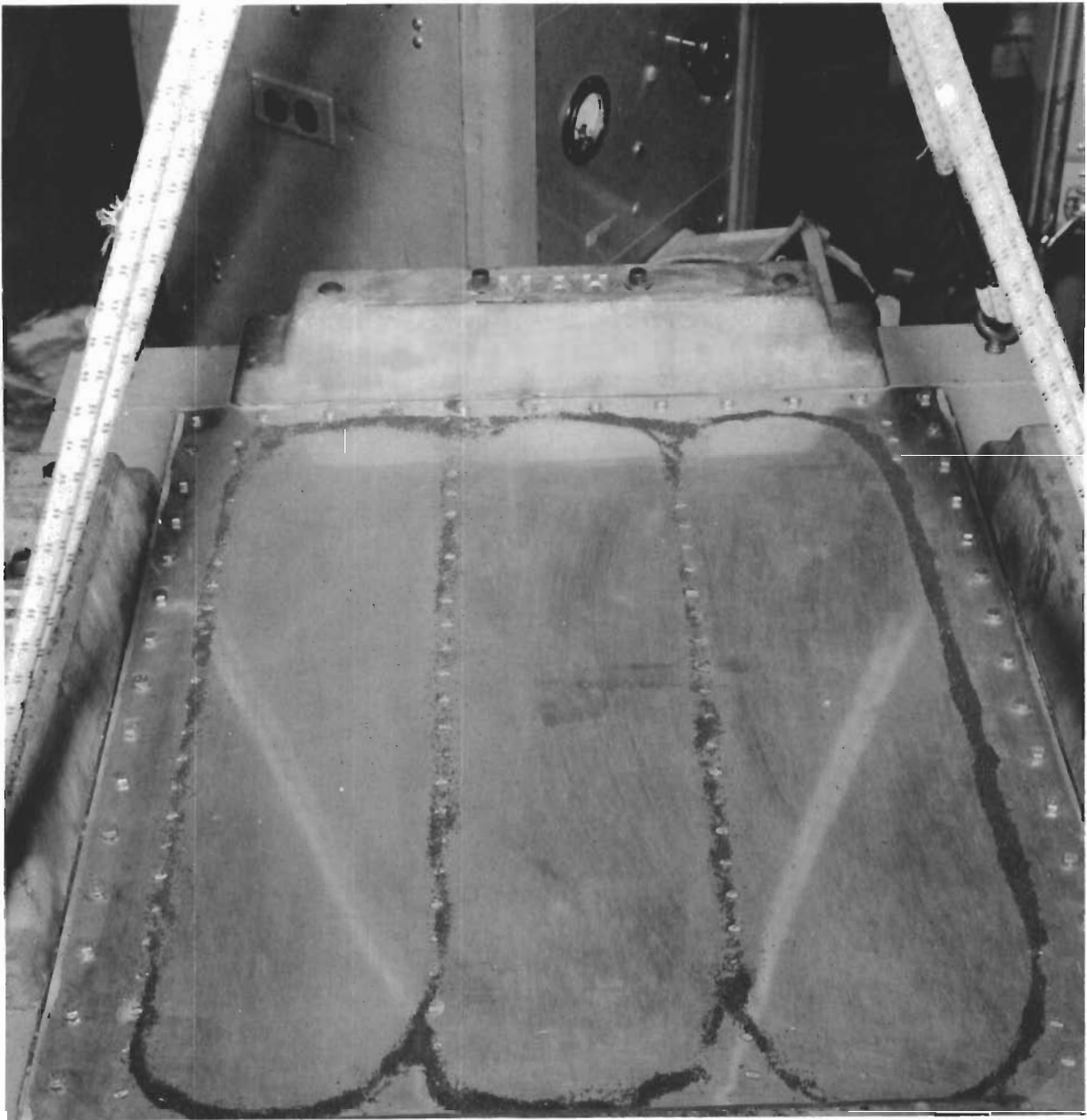


Figure 32. Skin-Stringer Panel, Common Mode Shapes



Subpanels in Phase 134 Hz (Panel #18)

Figure 33. Aluminum Control Panel Mode Shapes - Sub-Panels First Mode

# Contrails

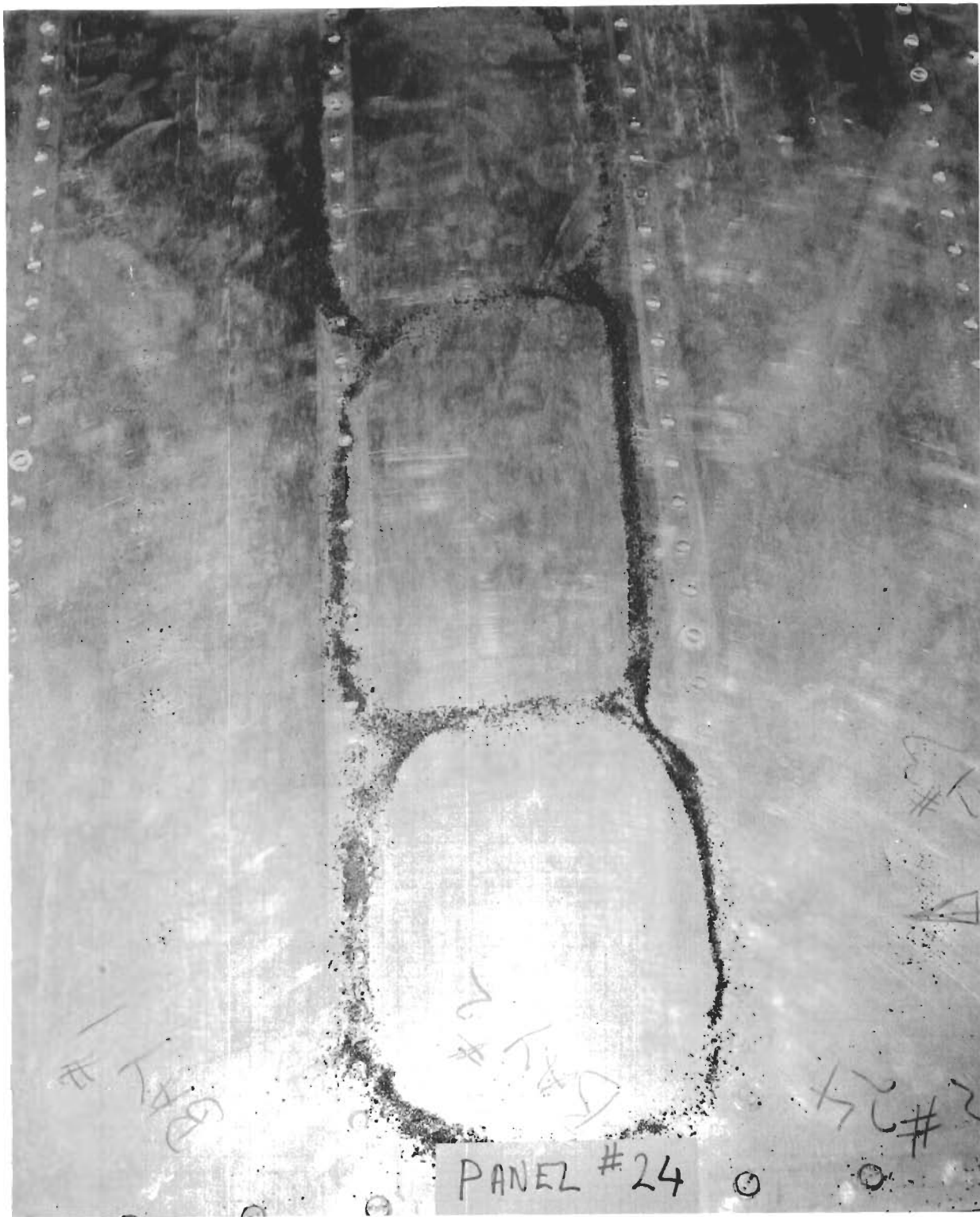


Figure 34. Control Panel No. 24 Mid-Pay Third Mode (189 Hz.)

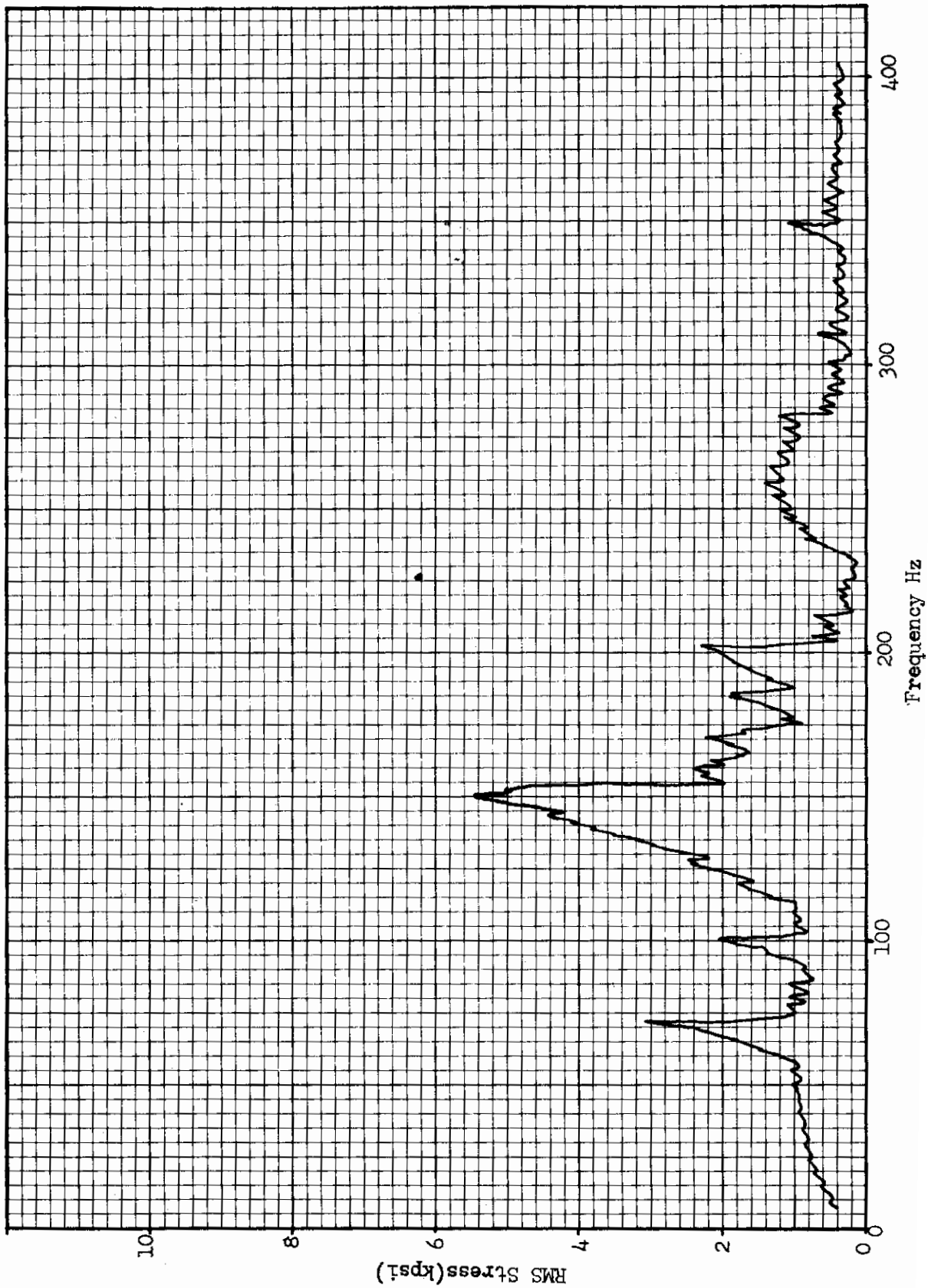


Figure 35. Typical Control Panel Stress vs. Frequency Response (140 db (Gage Position 2))



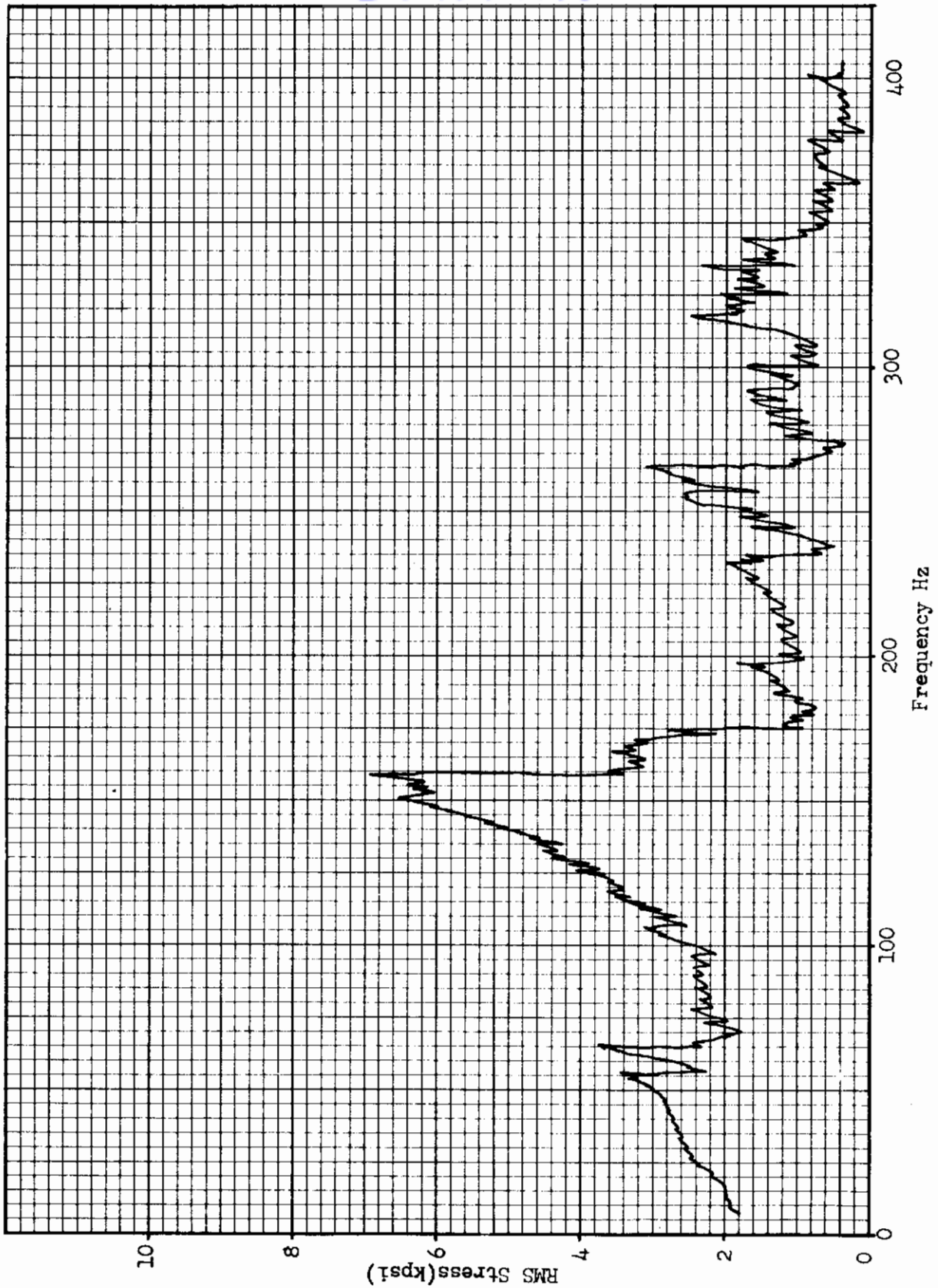


Figure 36. Typical Control Panel Stress vs. Frequency Response (145 db (Gage Position 2))

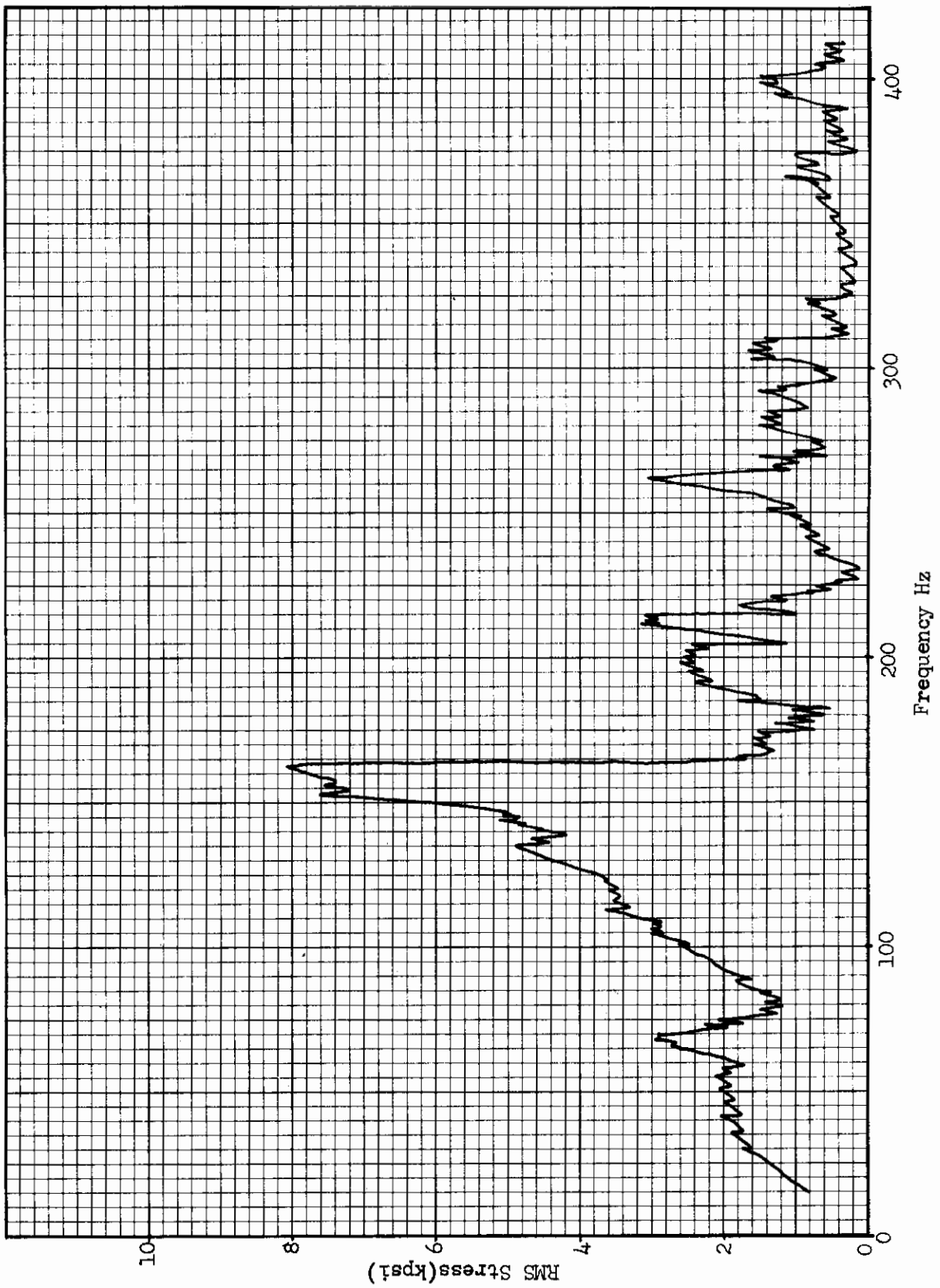


Figure 37. Typical Control Panel Stress vs. Frequency Response  
150 db (Gage Position 2)

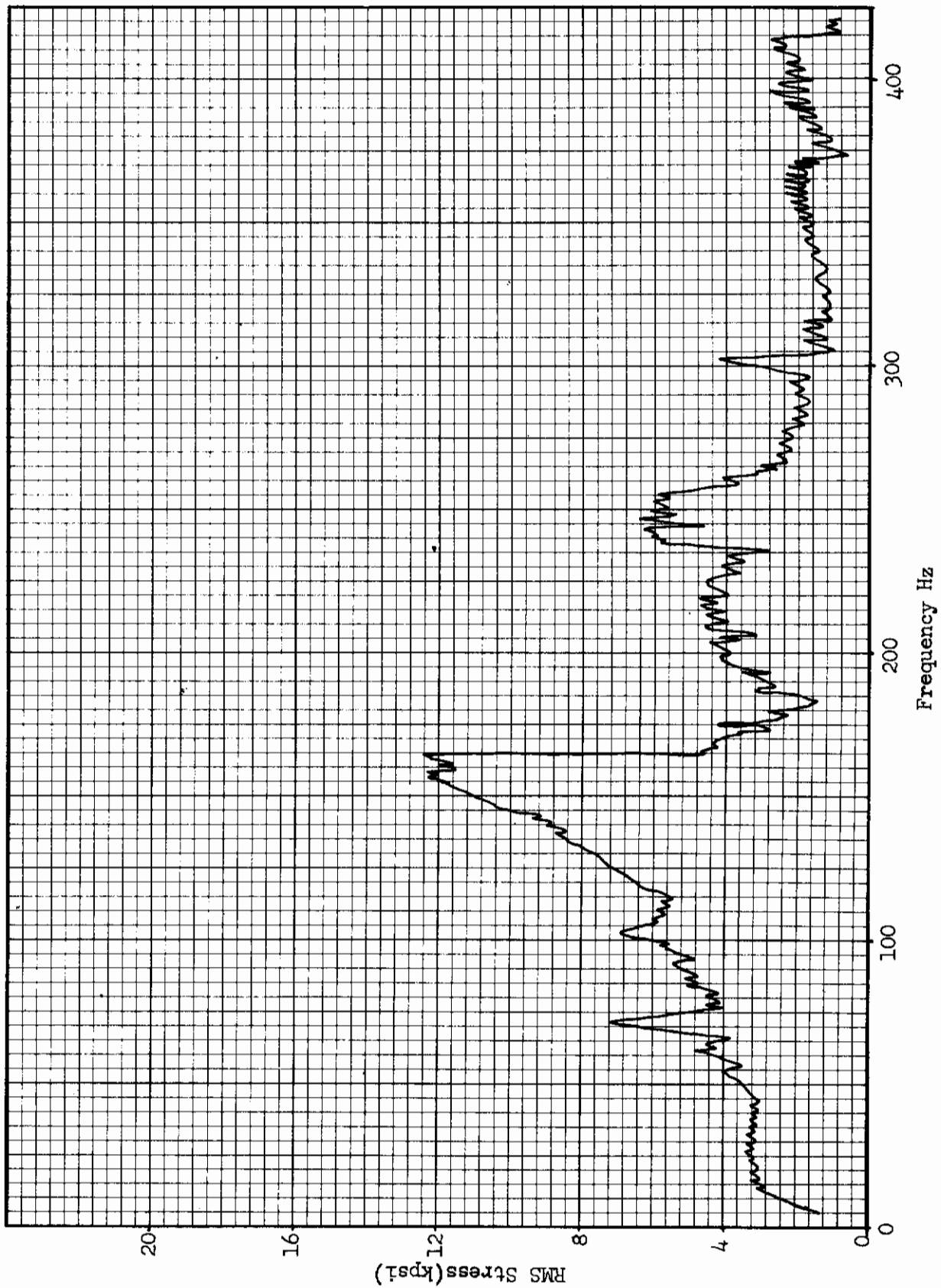


Figure 38. Typical Control Panel Stress vs. Frequency Response  
155 db (Gage Position 2)

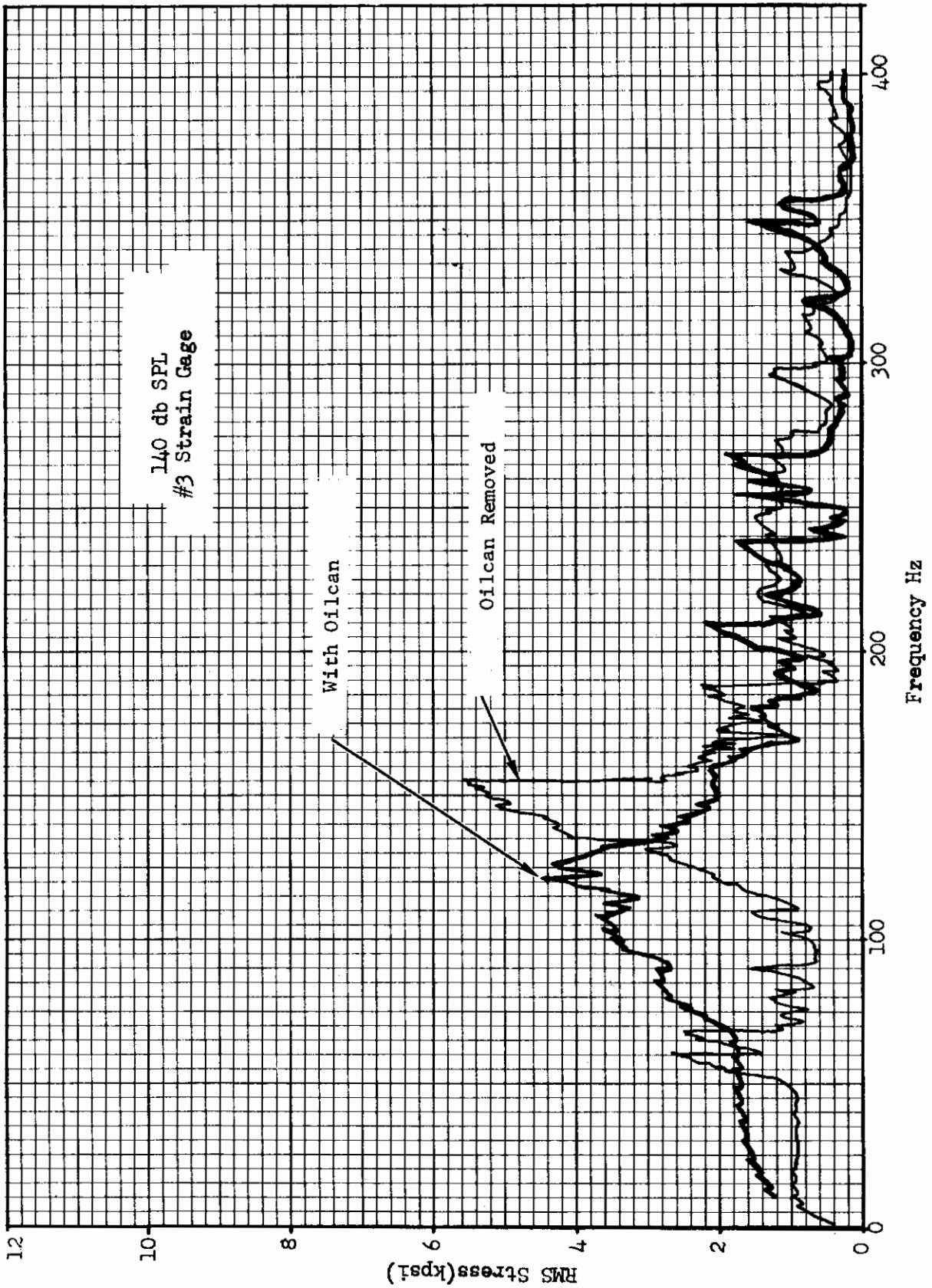


Figure 39. Stress Response Data Control Panel No. 25 - Effects of "Oilcan"

# Contrails

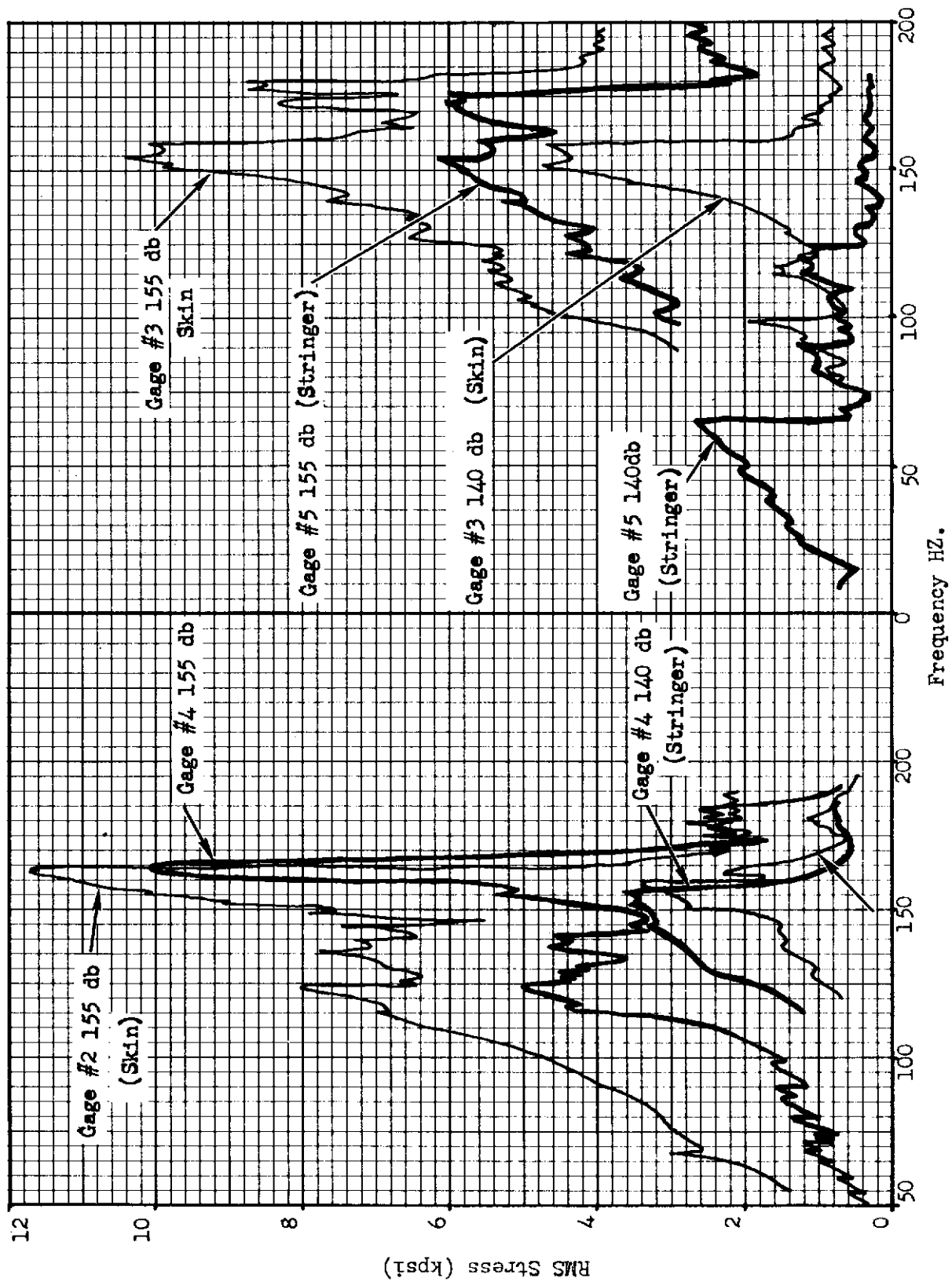


Figure 40. Control Panel Stress Response Showing Influence of Stringer Rotation

# Contrails

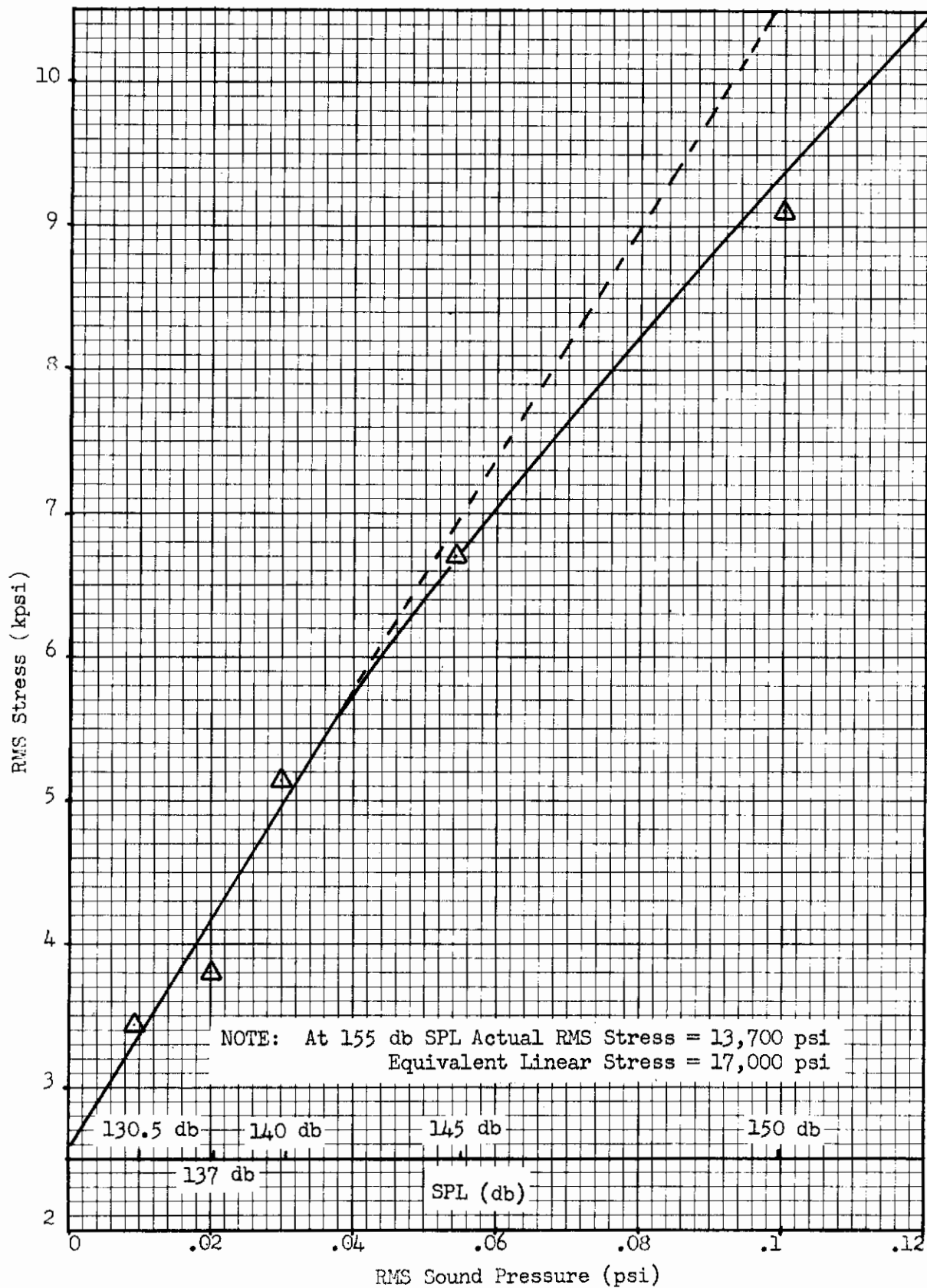


Figure 41. Control Panel Sound Pressure vs. RMS Stress (No. 2 Gage)

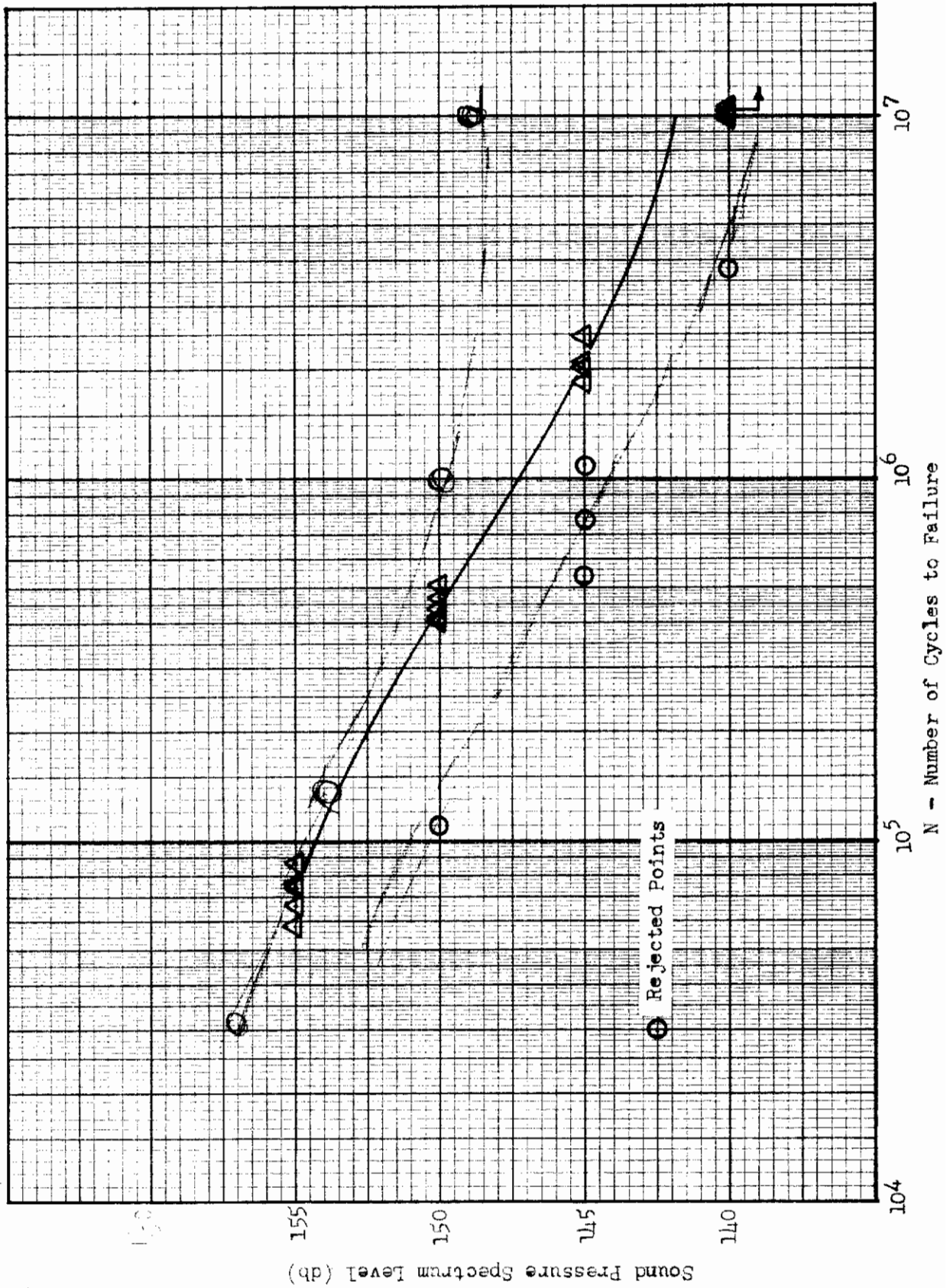


Figure 42. Aluminum Control Panels SPL vs. Cycles to Failure Plot

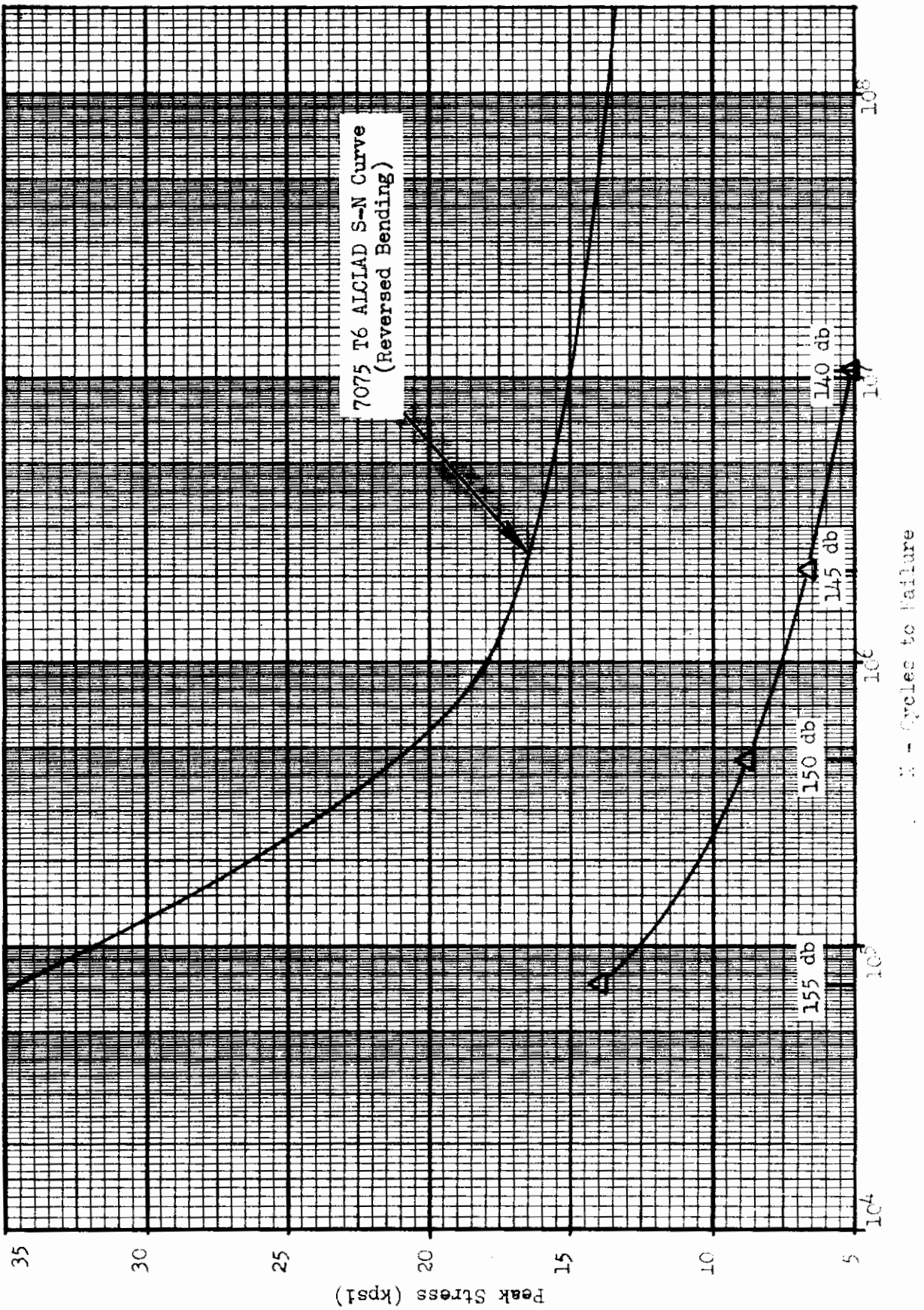


Figure 43. Control Panel Failing Stress vs. Cycles to Failure



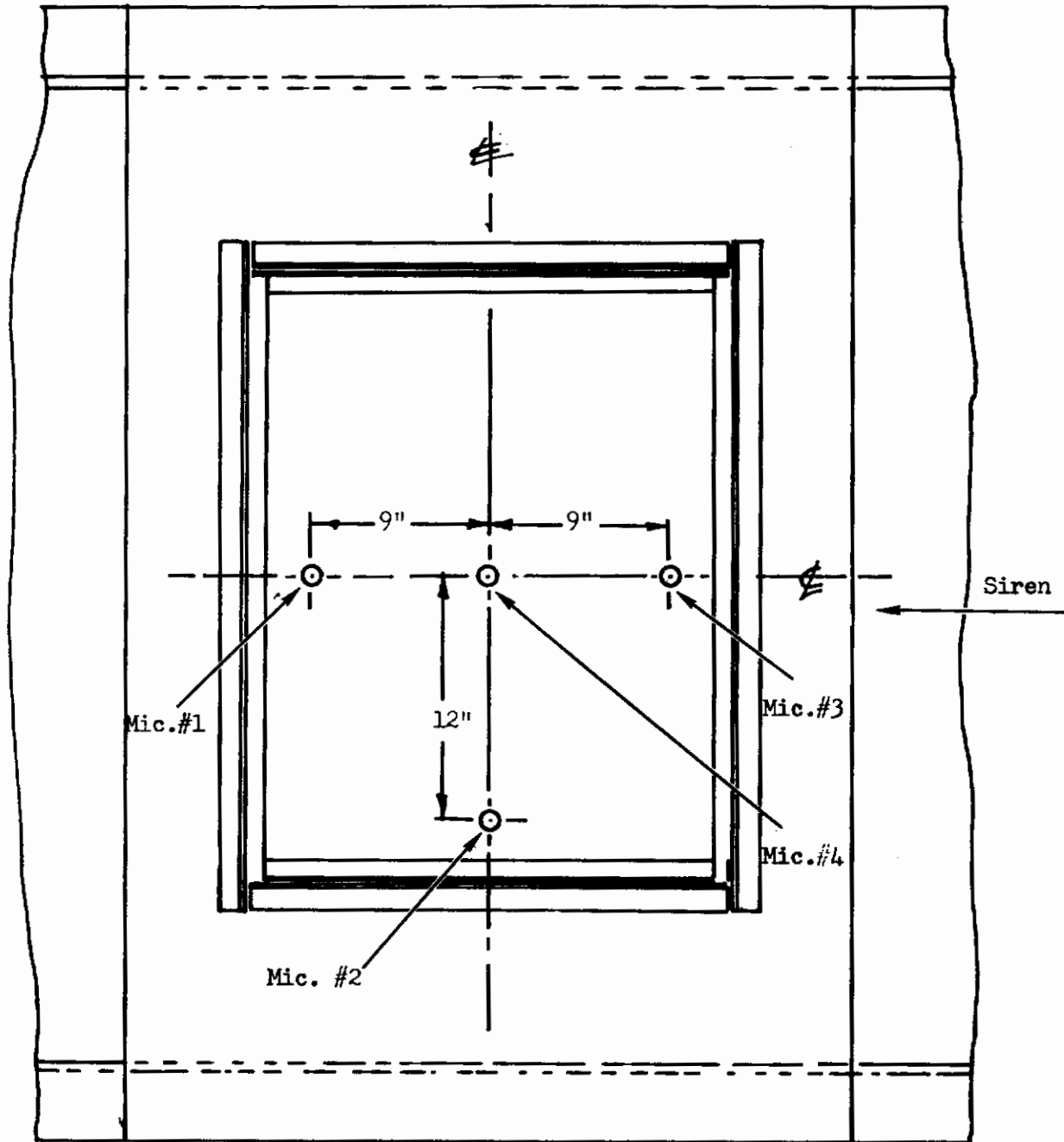
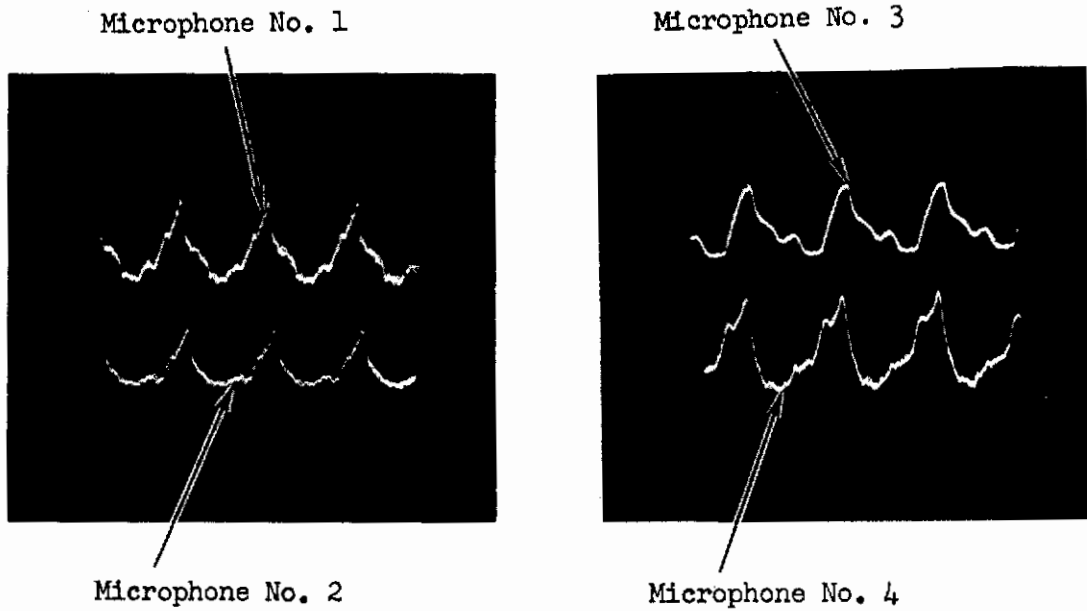


Figure 44. Microphone Locations in Siren Test Section

# Contrails



Control Panel No. 12 - 140 db SPL

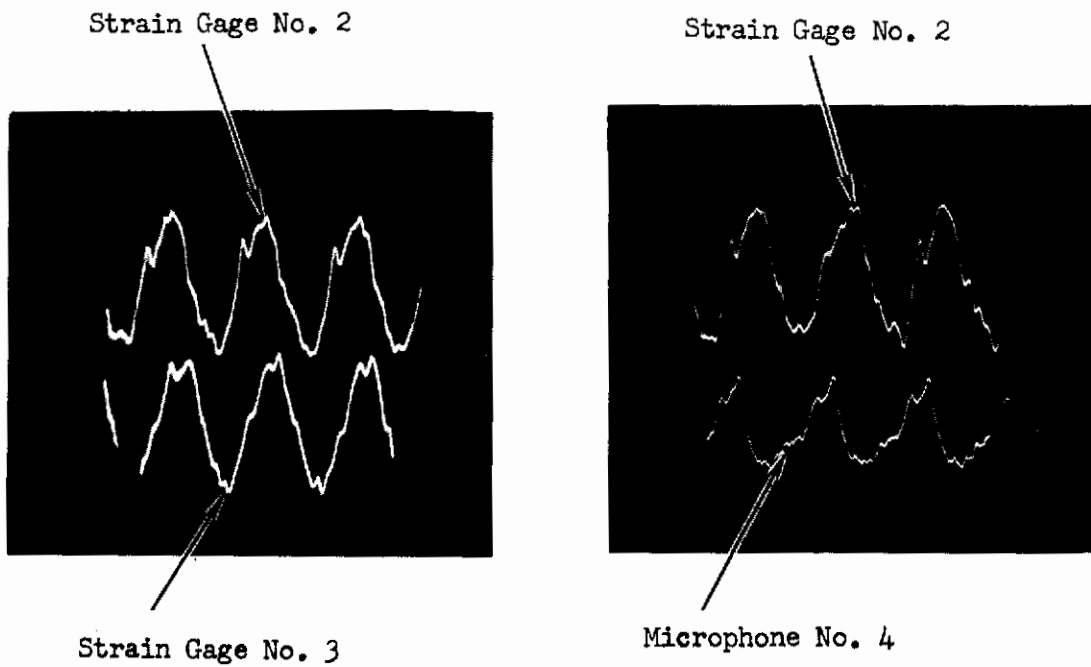


Figure 45. Typical Control Panel Microphone and Strain Gage Oscilloscope Traces

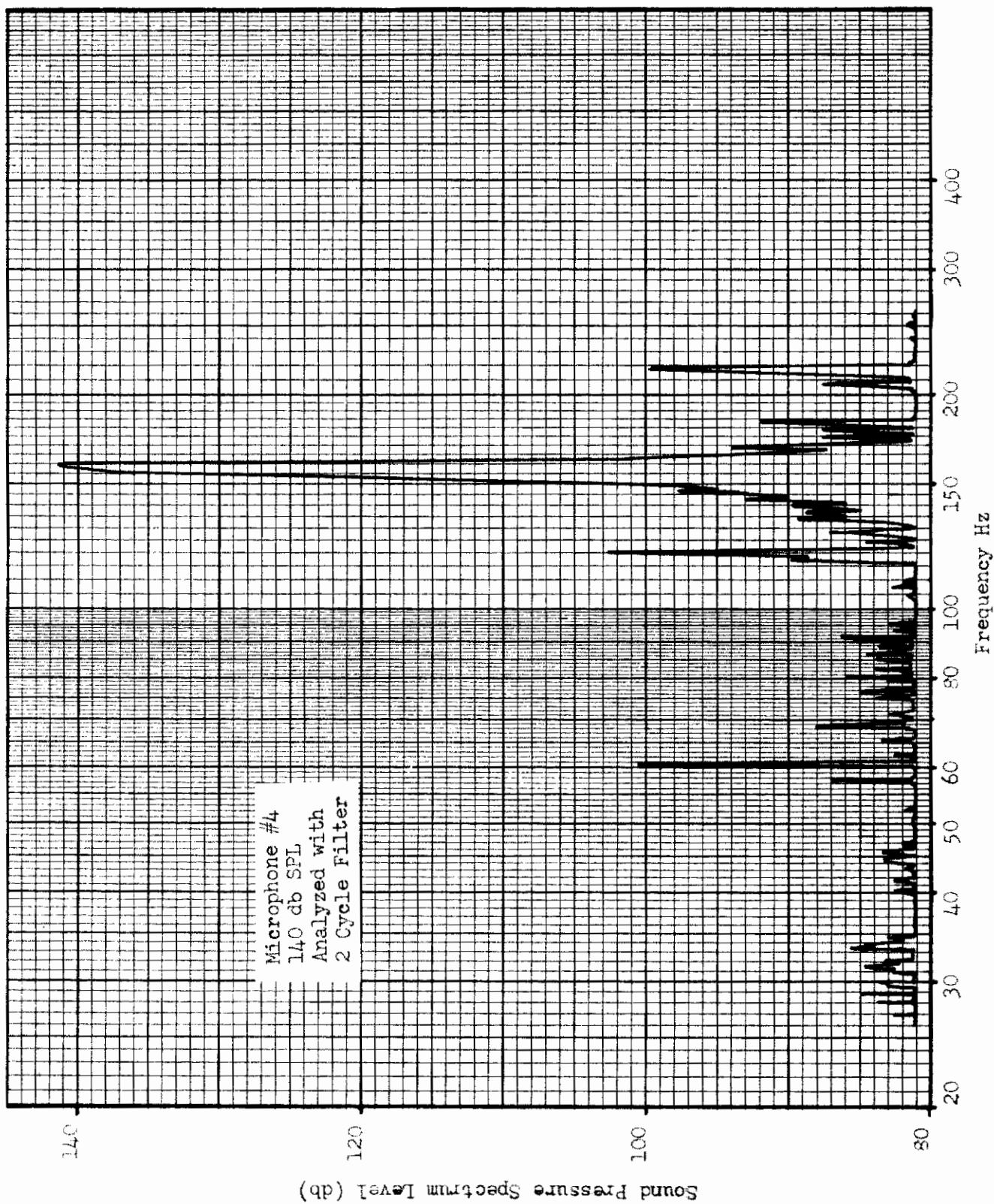


Figure 76. Narrow Band Analysis of #4 Microphone Noise (140 db)

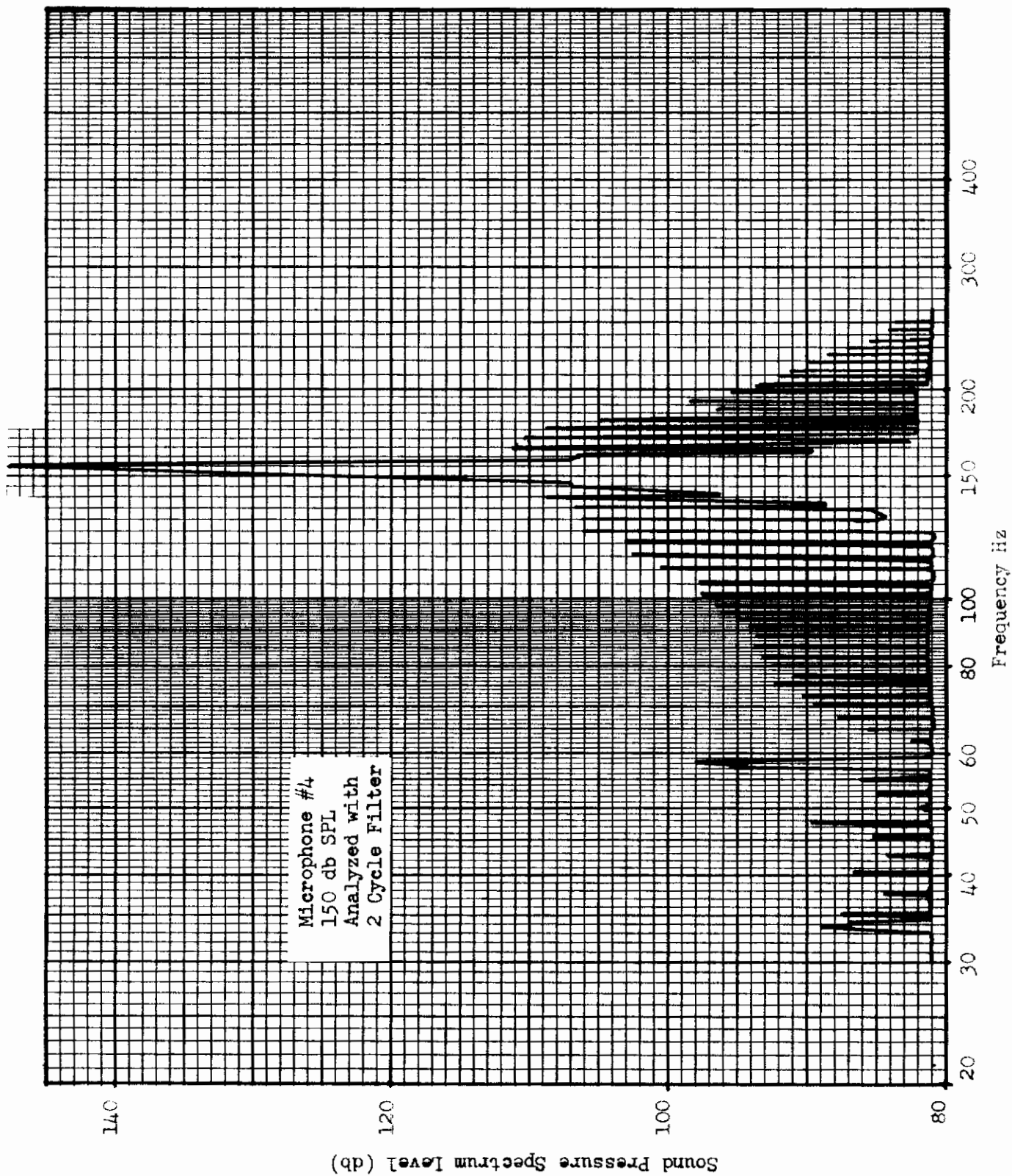


Figure 47. Narrow Band Analysis of #4 Microphone Noise (150 db)

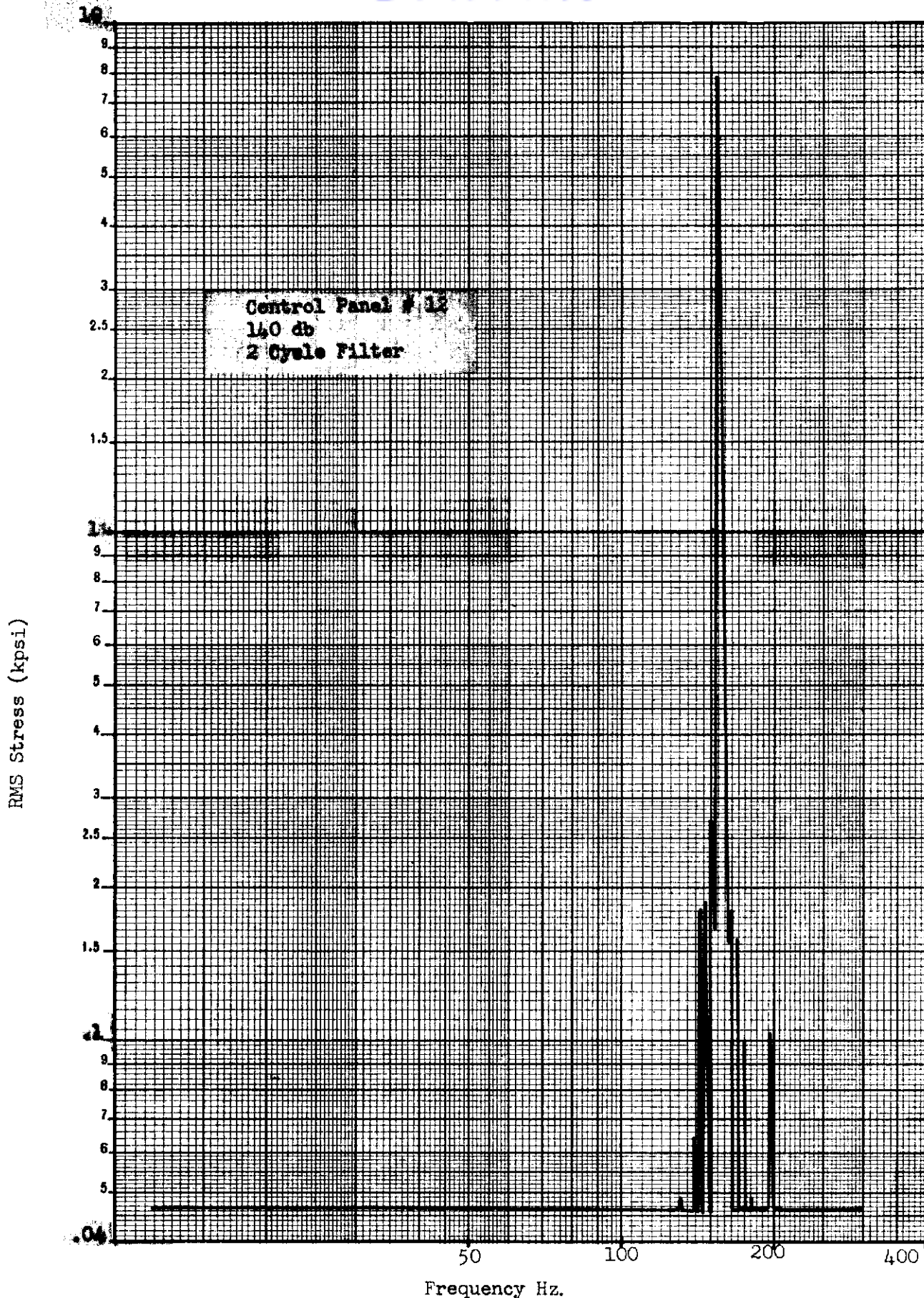


Figure 45. Narrow Band Analysis #2 Strain Gage Data (140 db)

# Contrails

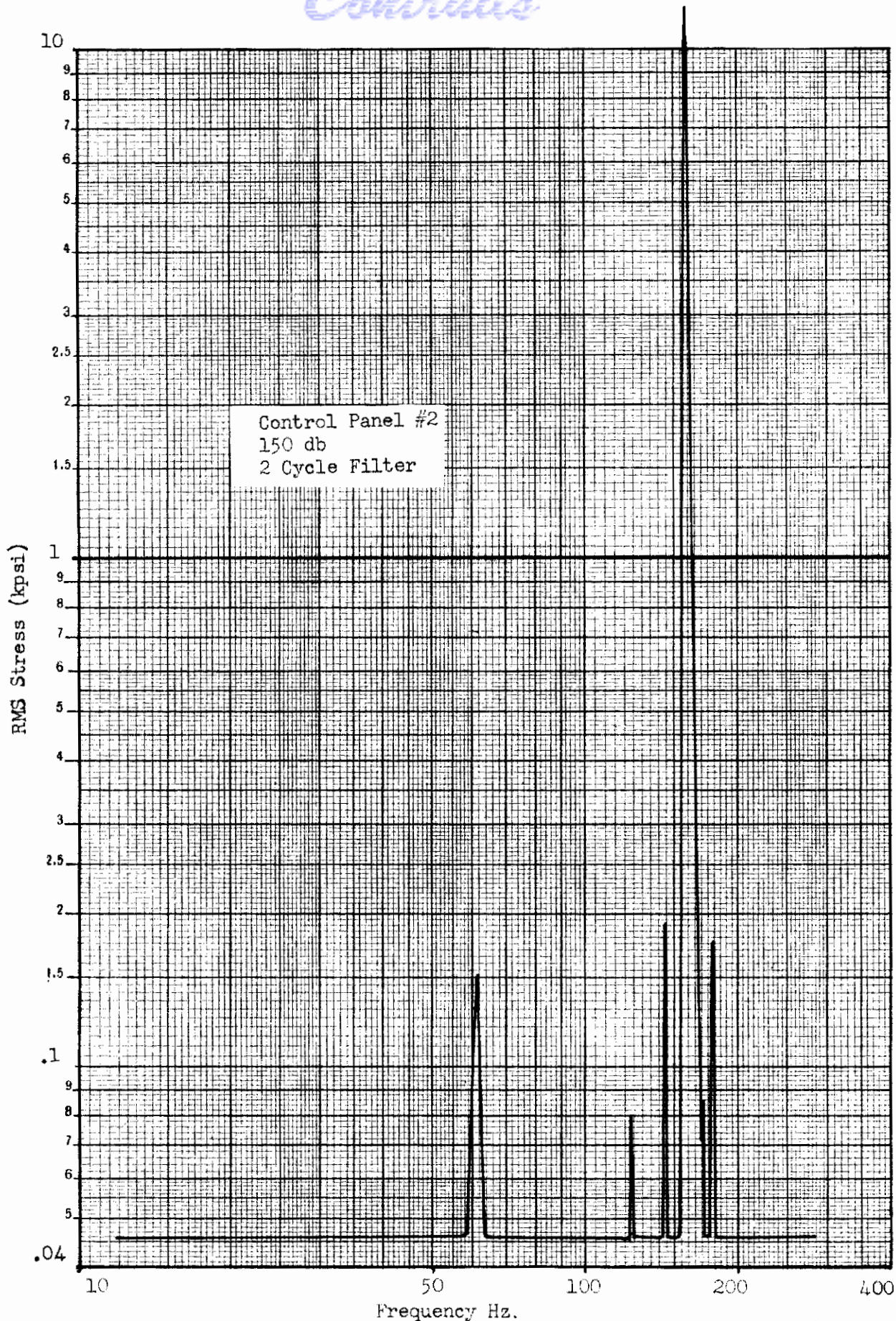
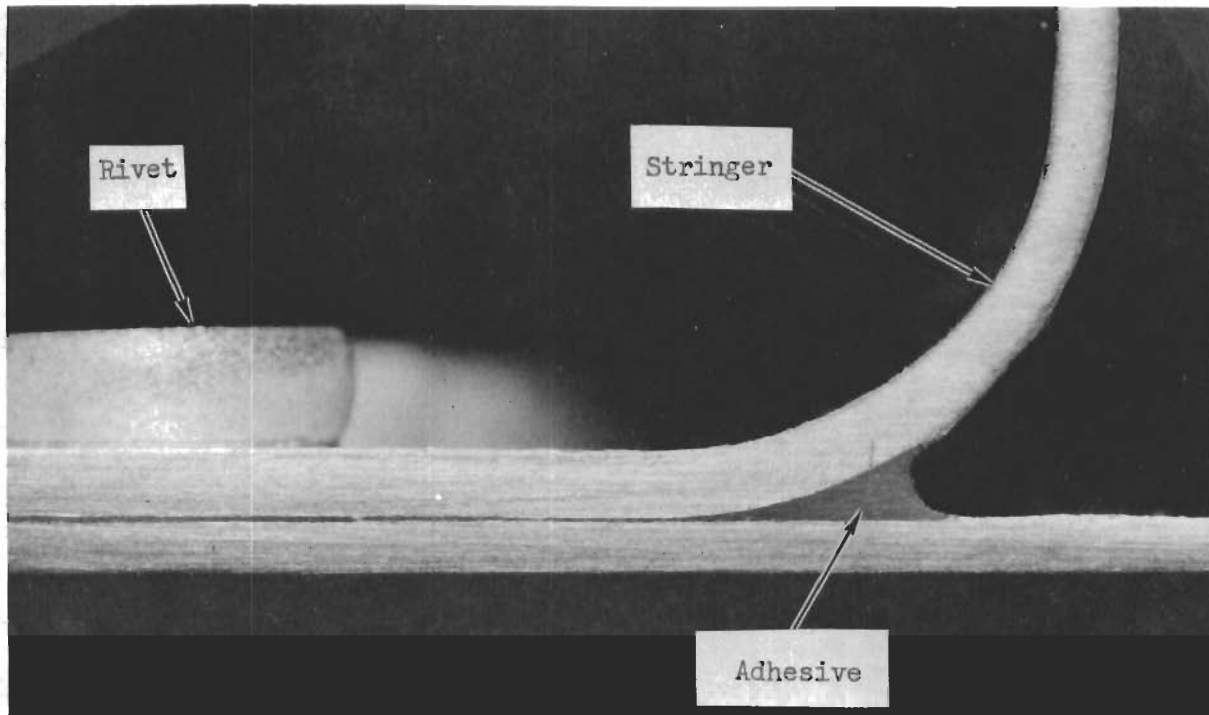
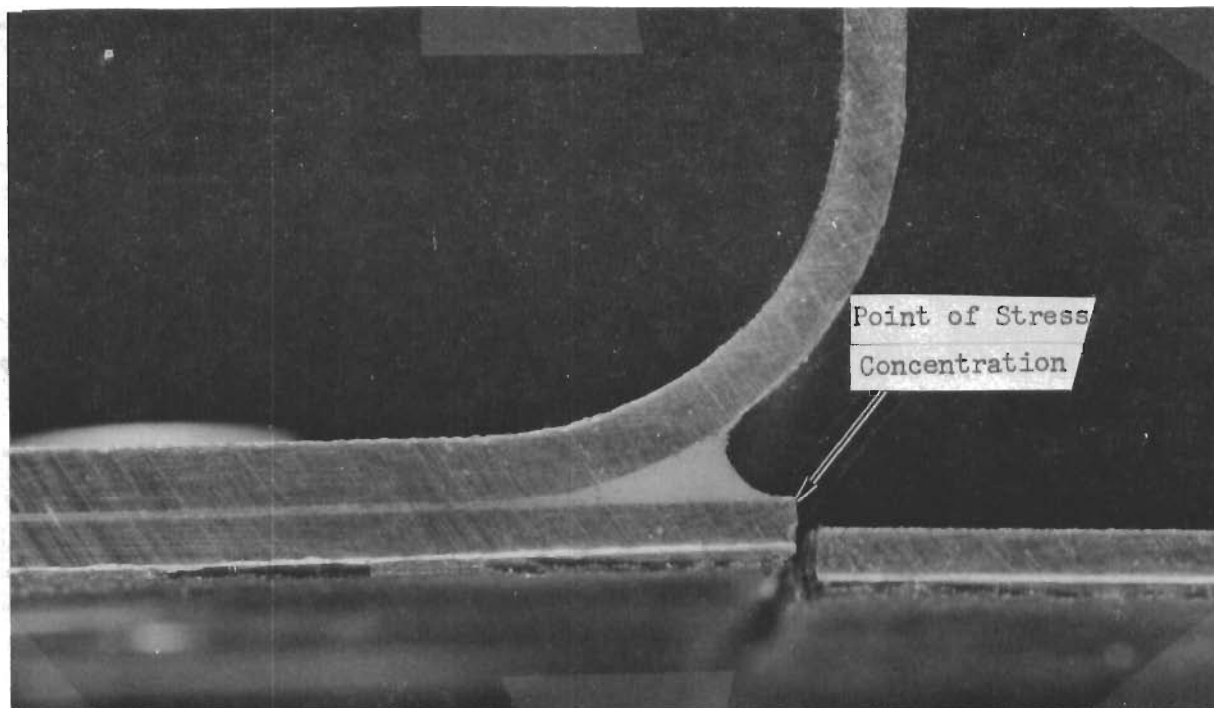


Figure 49. Narrow Band Analysis of #2 Strain Gage Data (150 db)

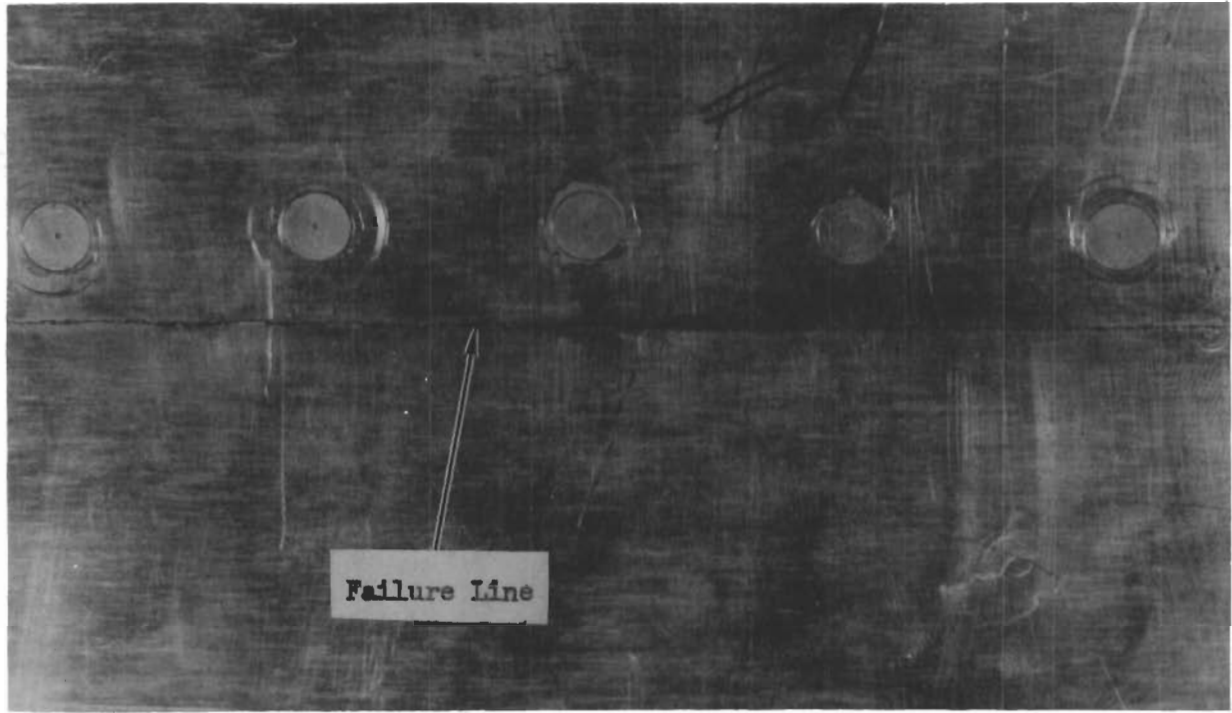


(a)

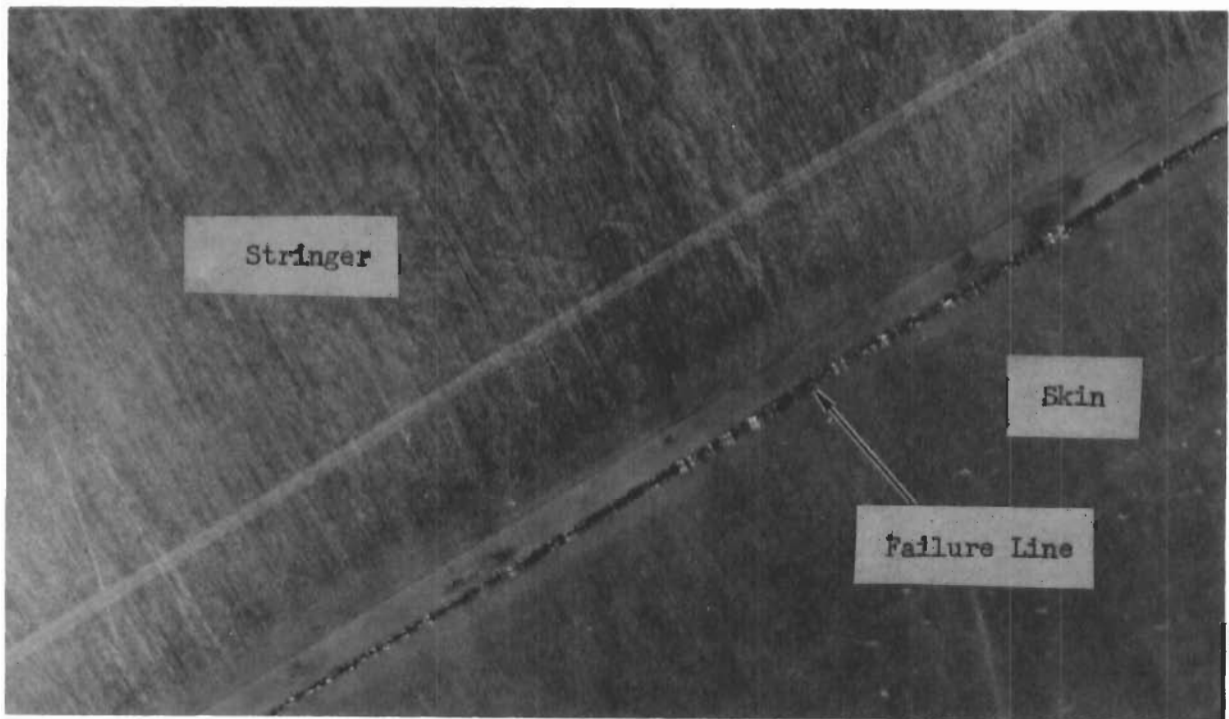


(b)

Figure 50. Cross-sectional View of Control Panel AF-111 Adhesive Bond Line



(a)



(b)

**Figure 51. Control Panel Typical Skin Failures**



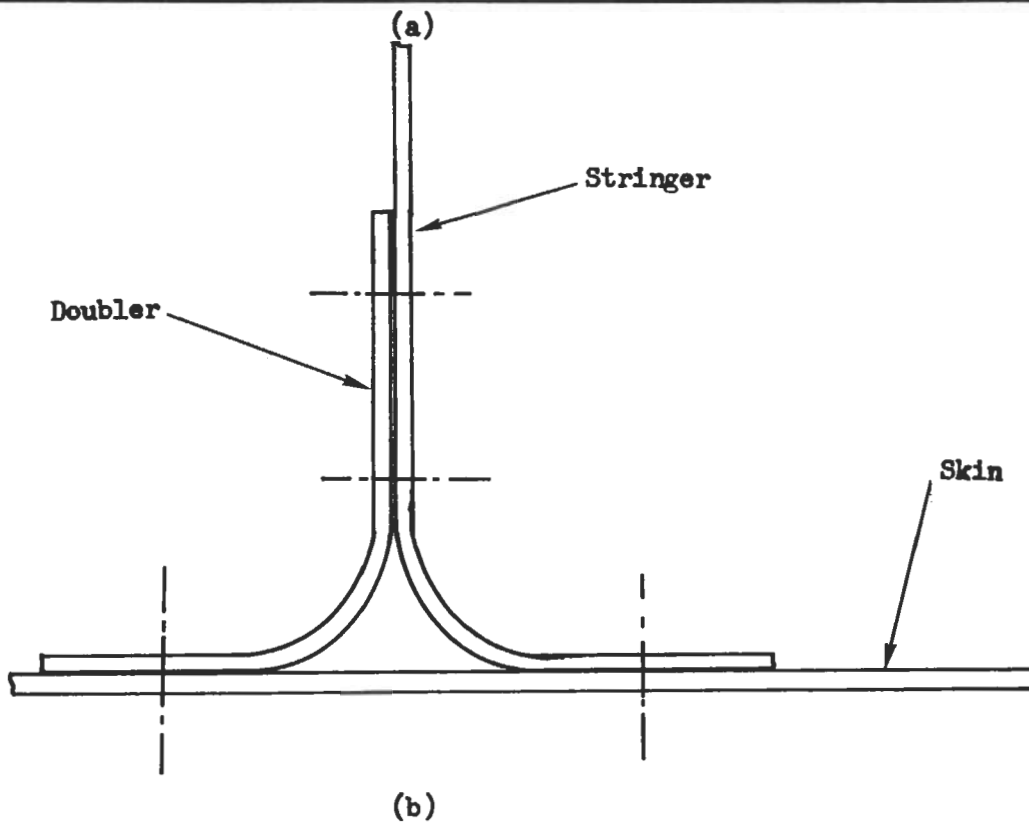
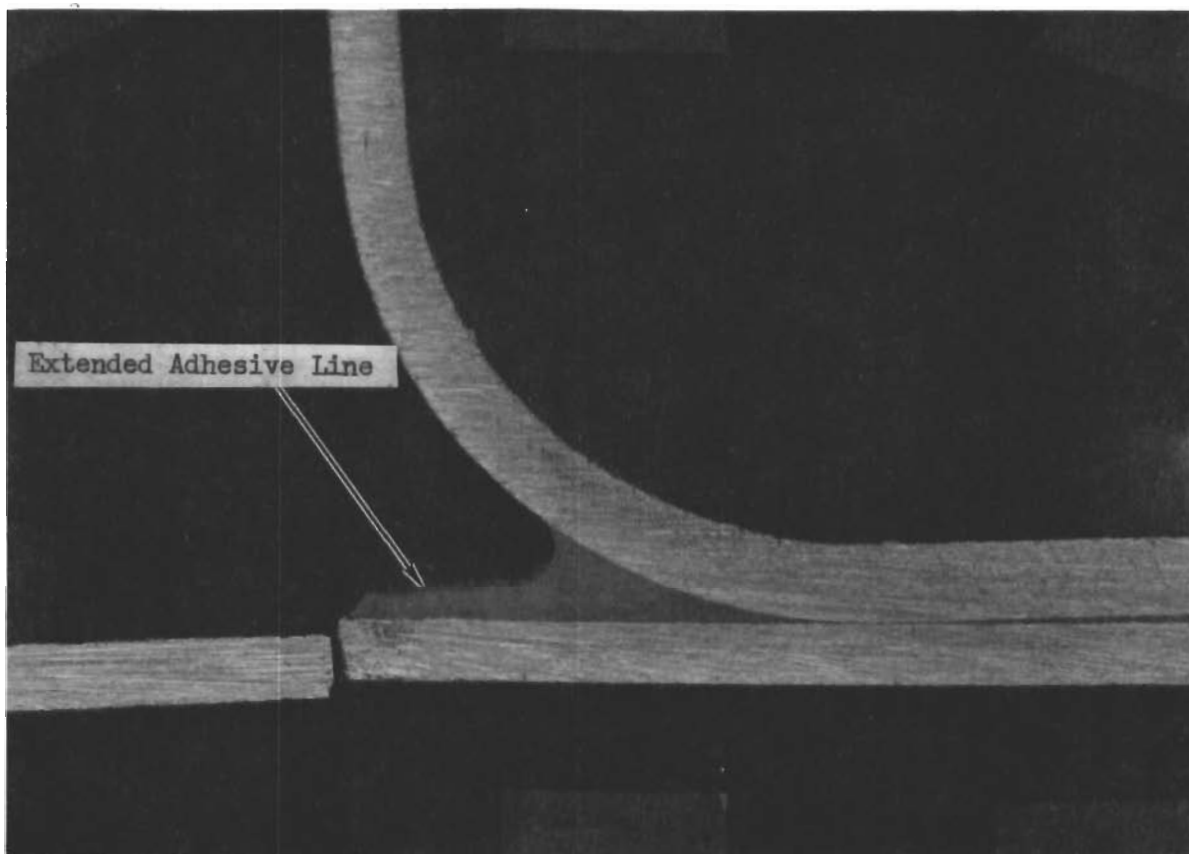


Figure 52. Skin-Stringer Attachment - Improved Design

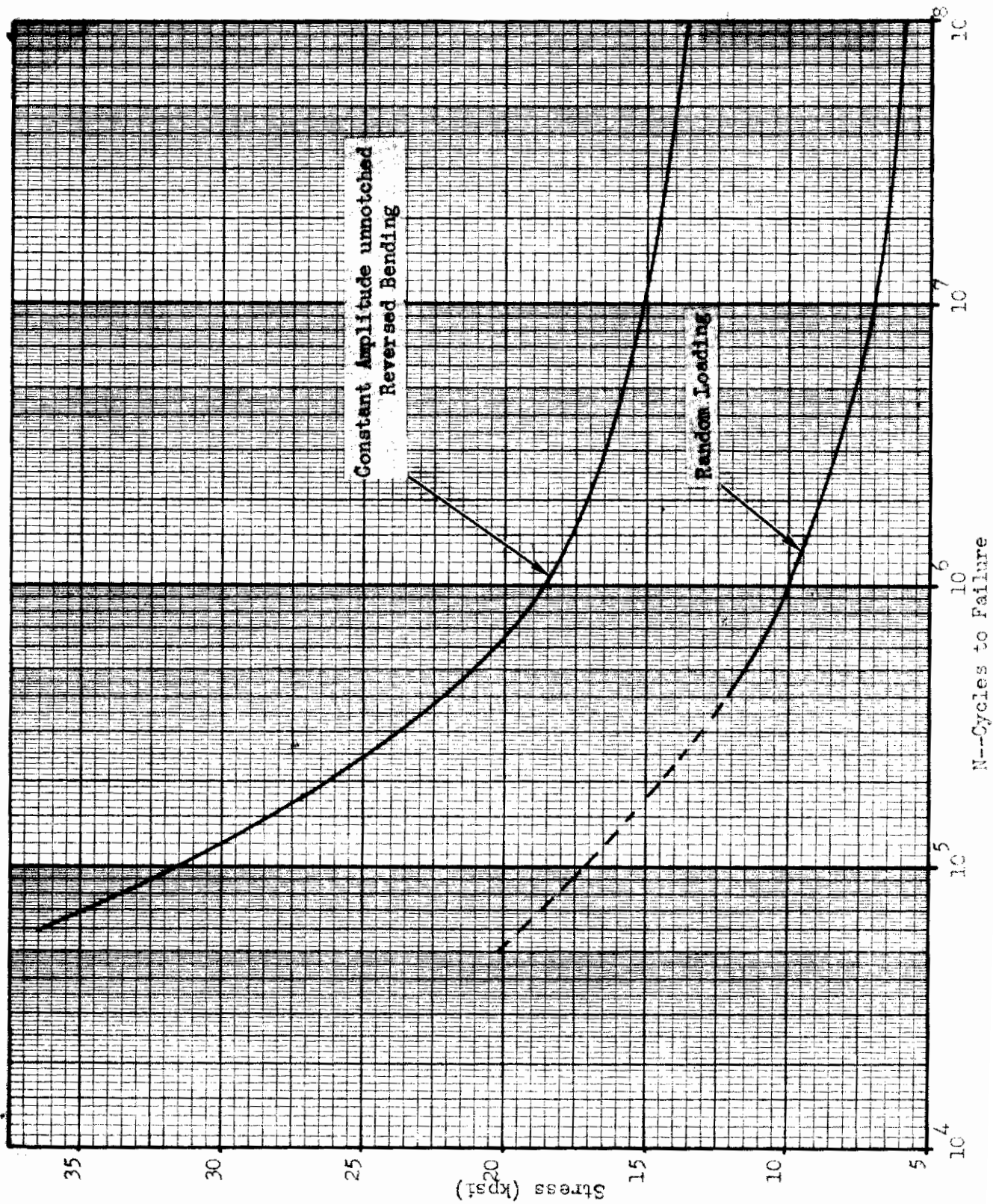
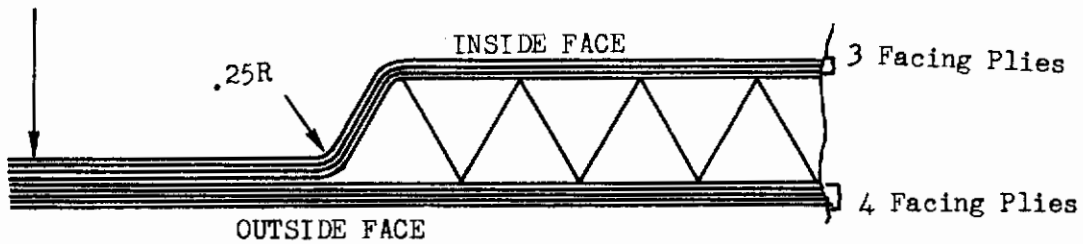


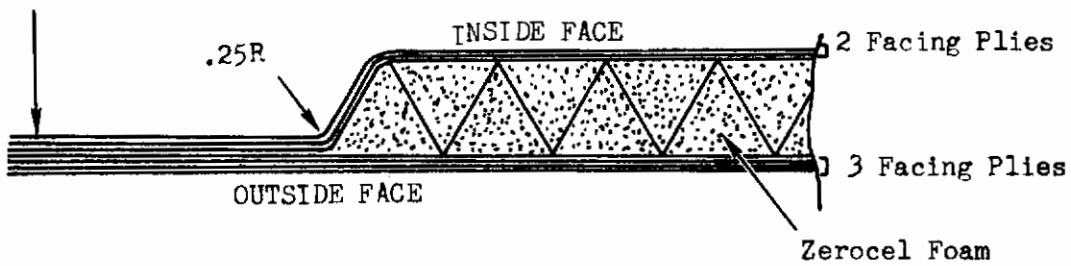
Figure 53.- Random S-N Curve for 7075-T6 Alclad

9 Plies 181-S Glass Fabric (.010 in.)



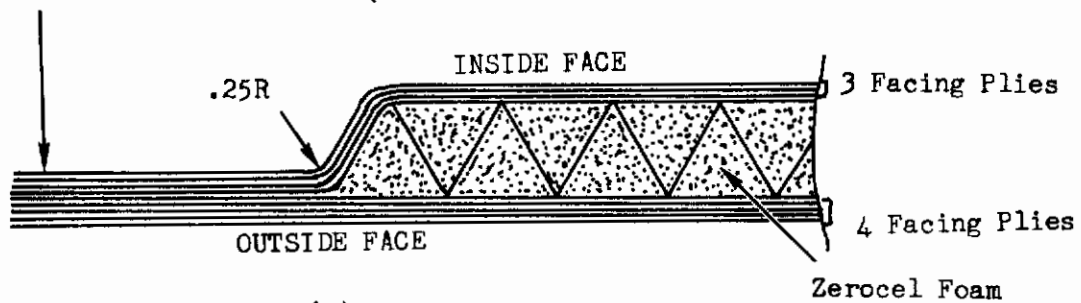
(a) TYPE I PANEL

7 Plies 181-S Glass Fabric (.010 in.)



(b) TYPE II PANEL

9 Plies 151-S Glass Fabric (.007 in.)



(c) TYPE III PANEL

Figure 54. Glass Fiber Production Test Panel Sectional Views

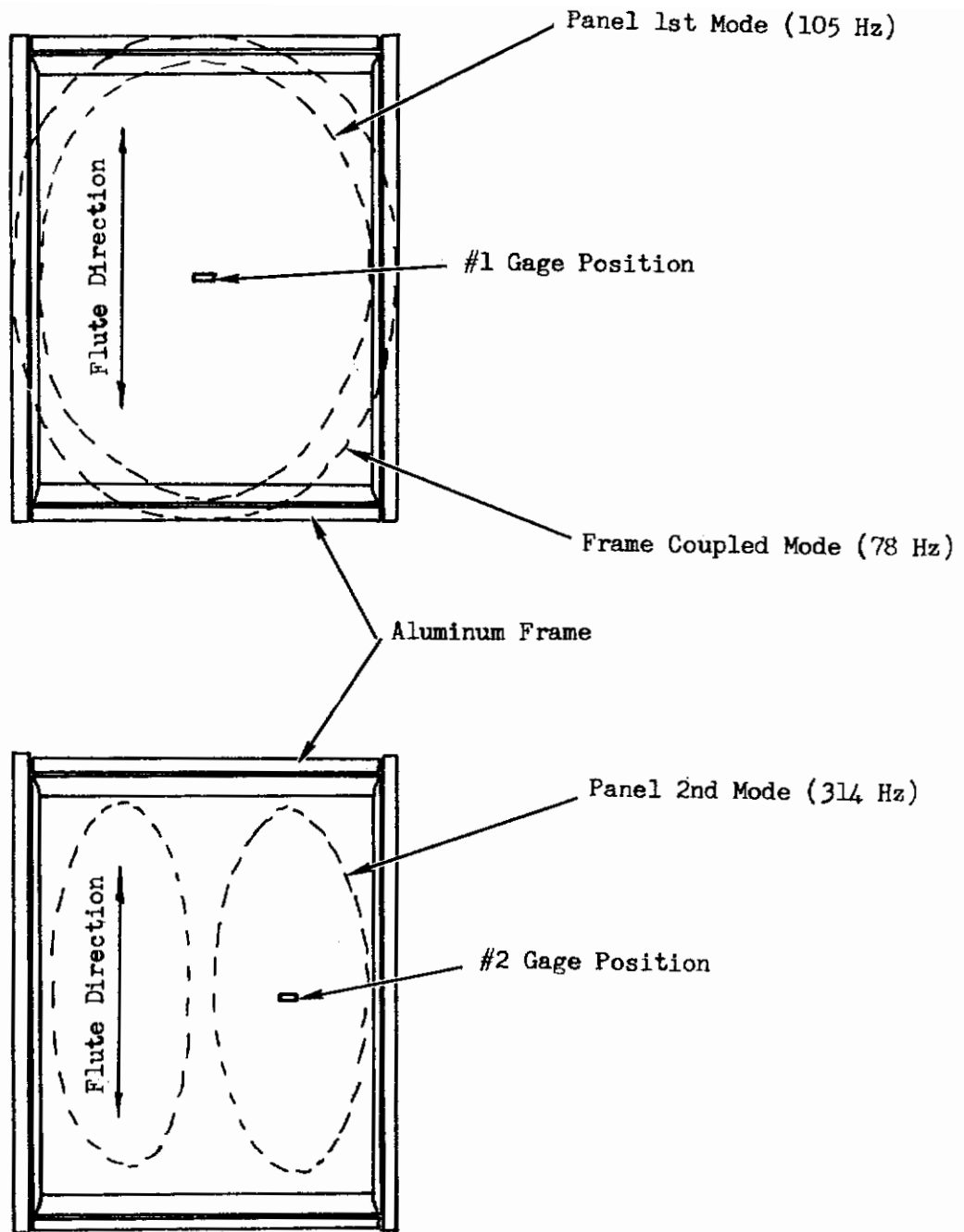


Figure 55. Type I Glass Fiber Panel Mode Shapes

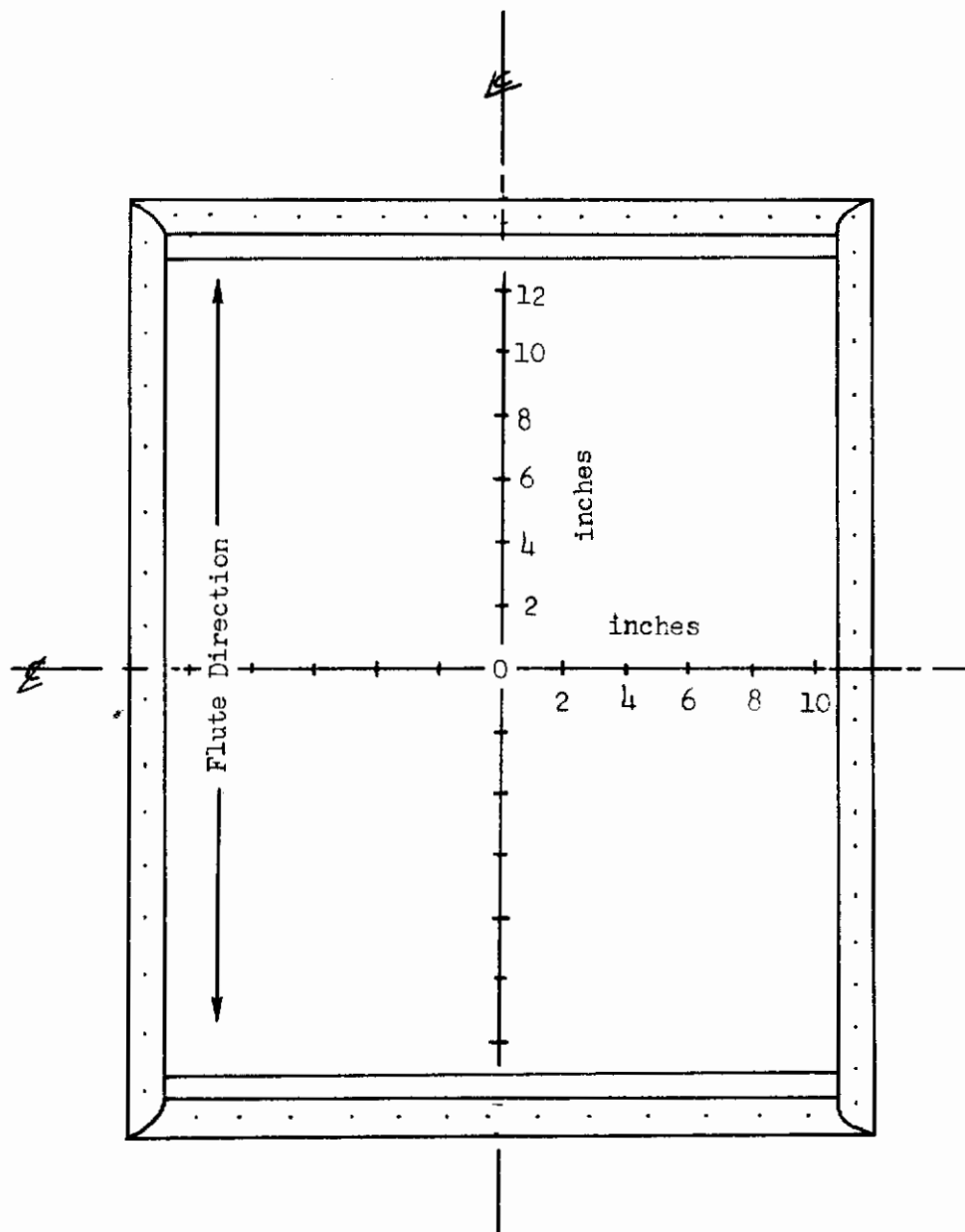


Figure 56. Accelerometer Locations for Panel Deflection Measurements

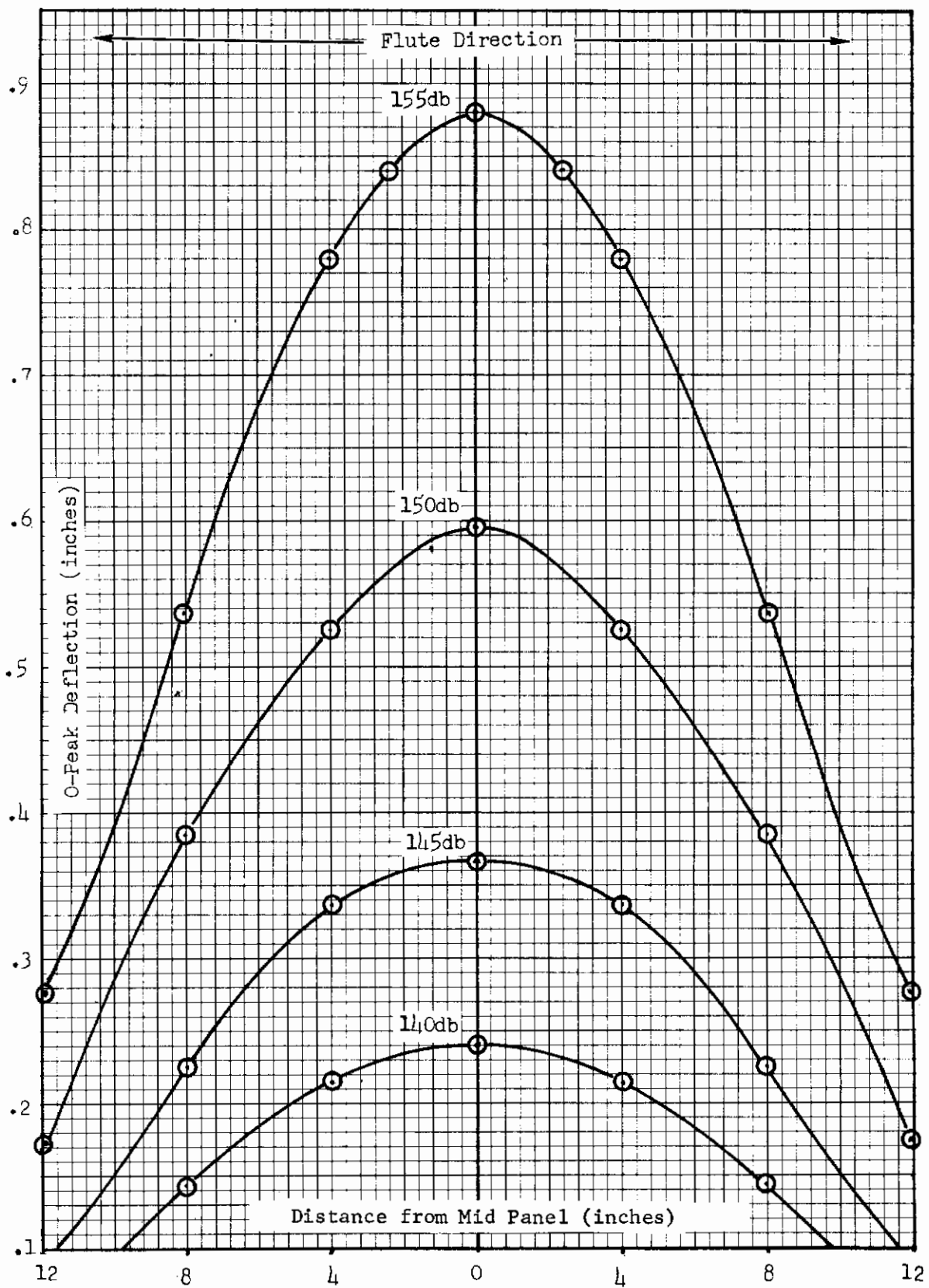


Figure 57. Type I Panel Deflection vs. SPL in Flute Direction

# Contrails

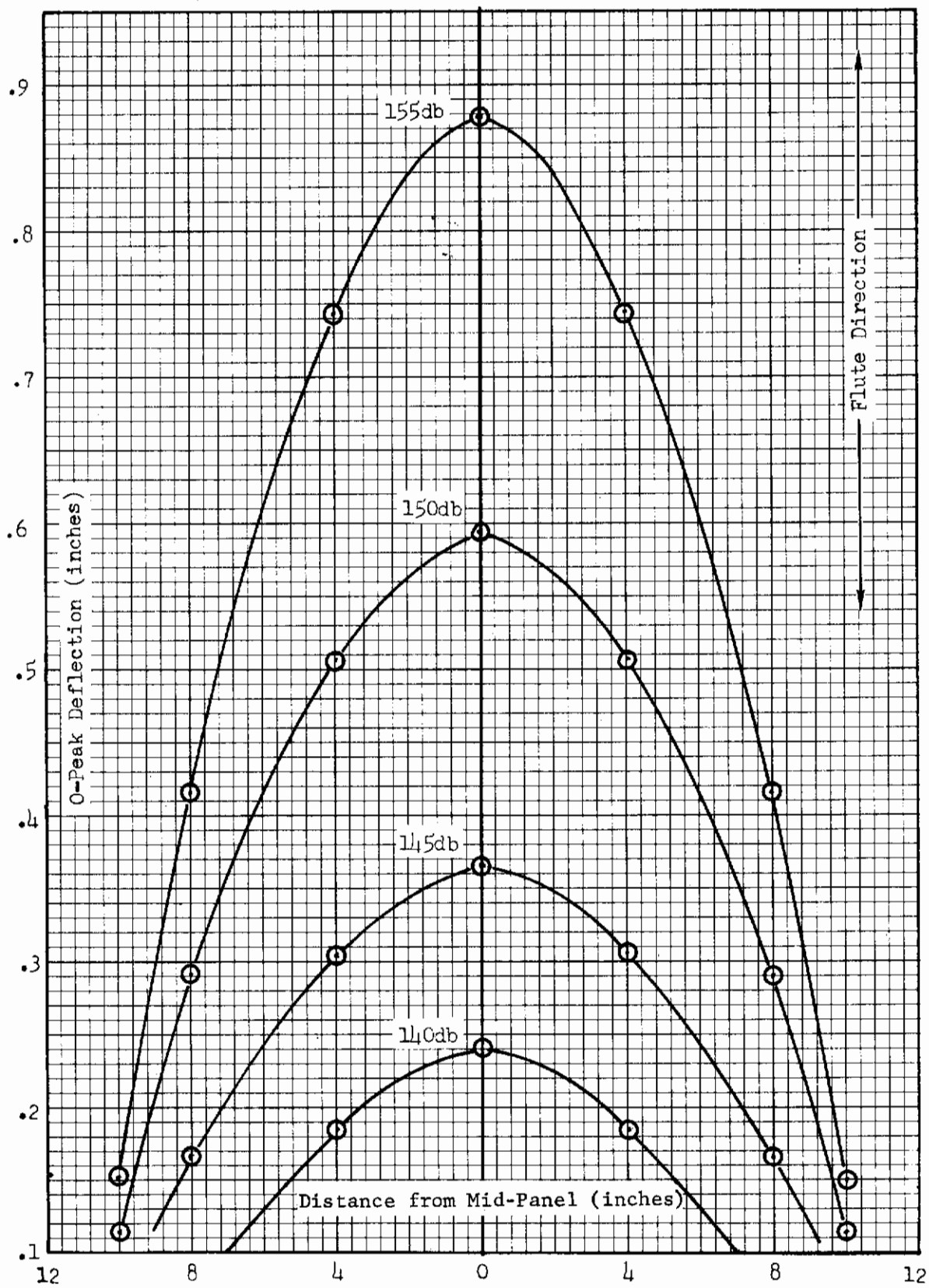


Figure 58. Type I Panel Deflection vs. SPL, Transverse Flute Direction,

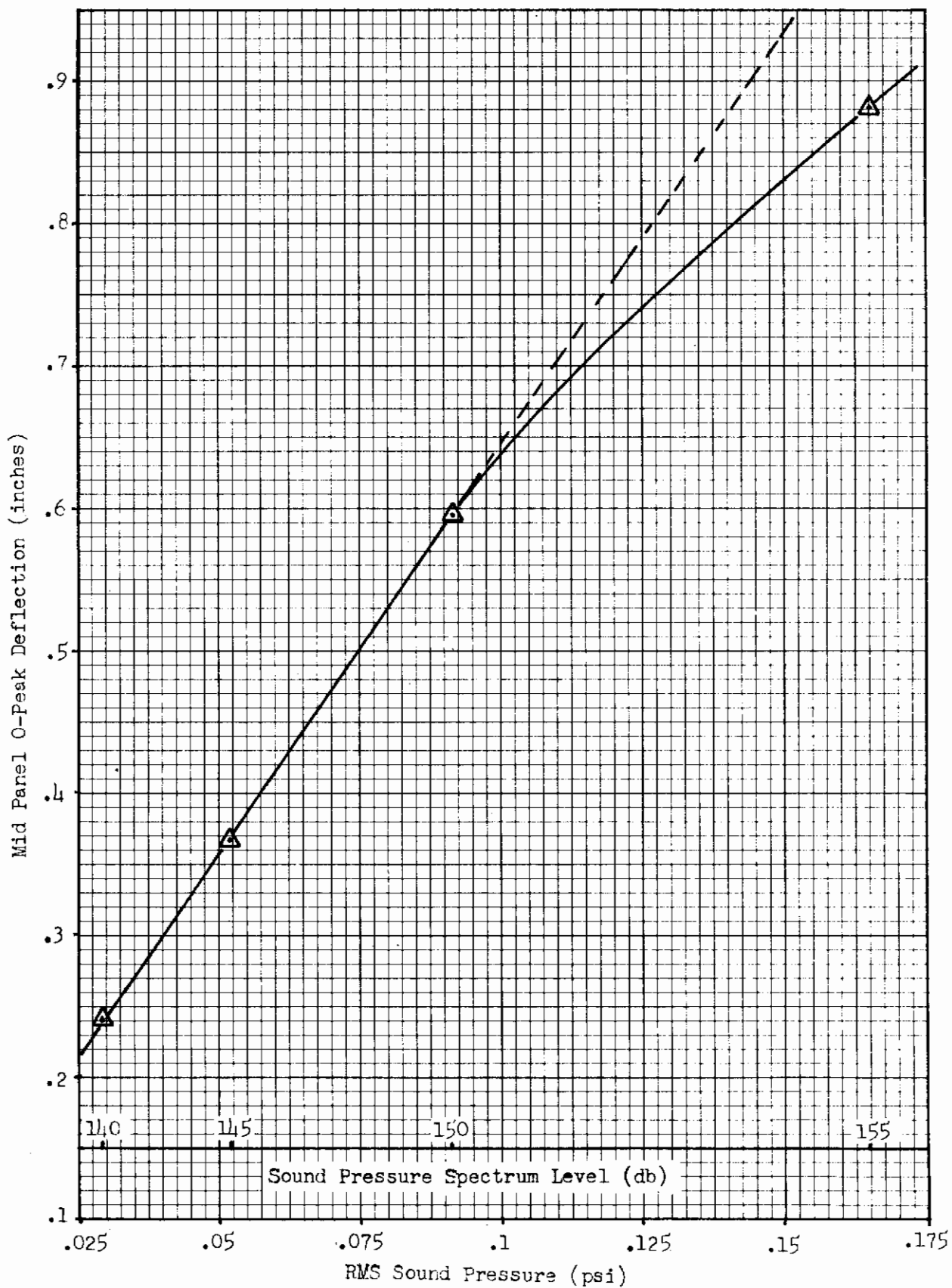
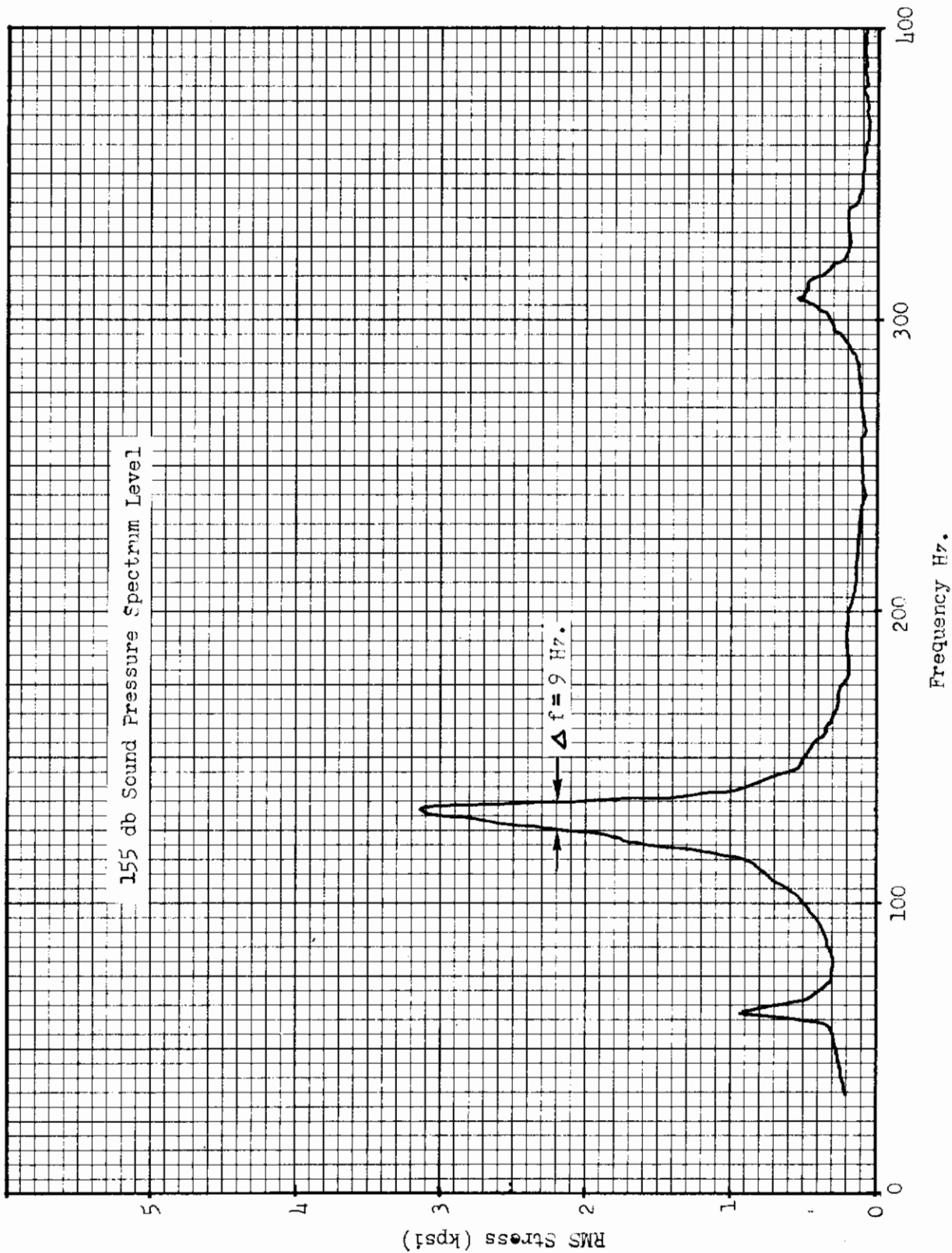


Figure 59 . Type I Panel-Mid Panel Deflection vs. SPL





8203

Figure 60. Type I Panel Frequency Response Characteristics (Gage Position #1)

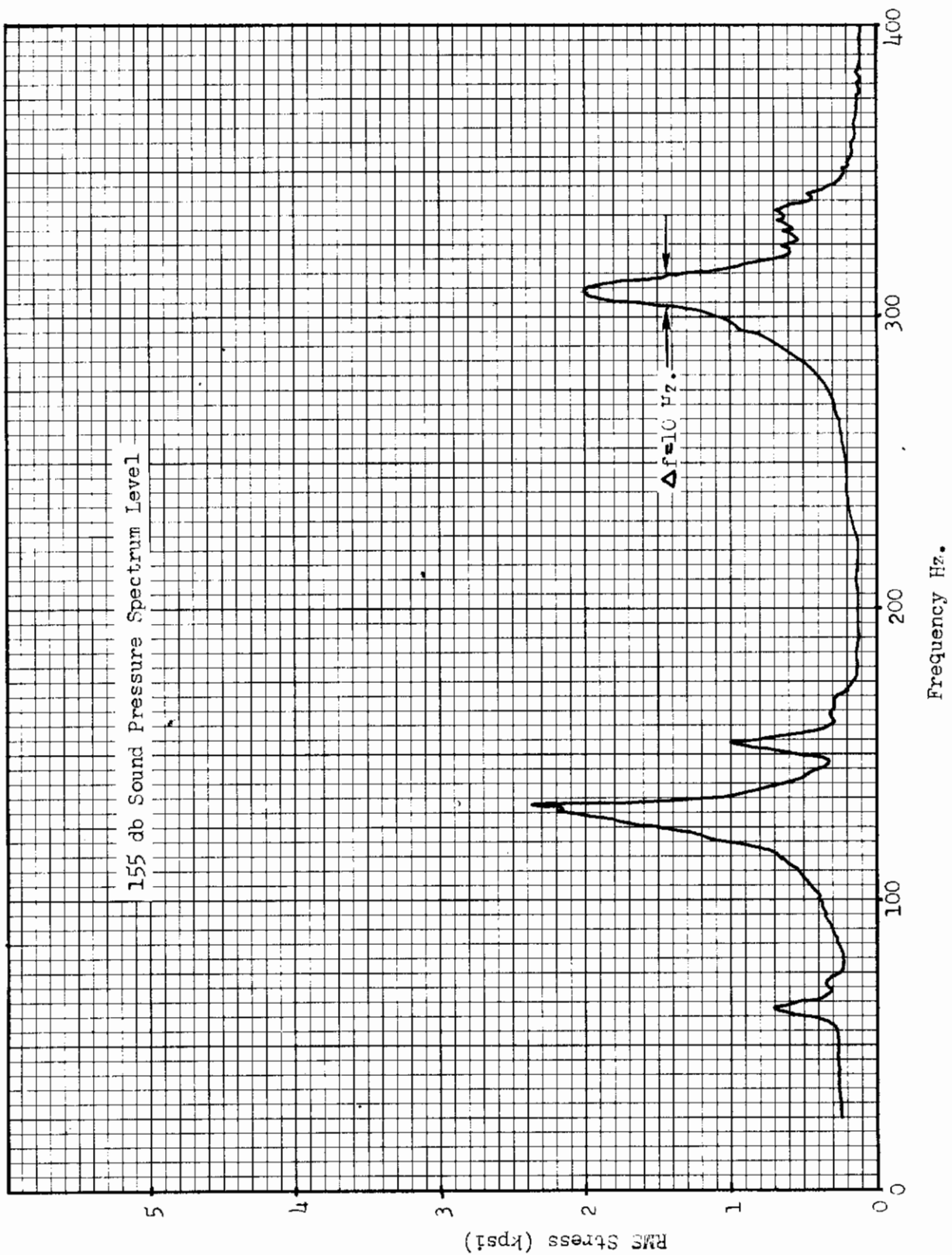
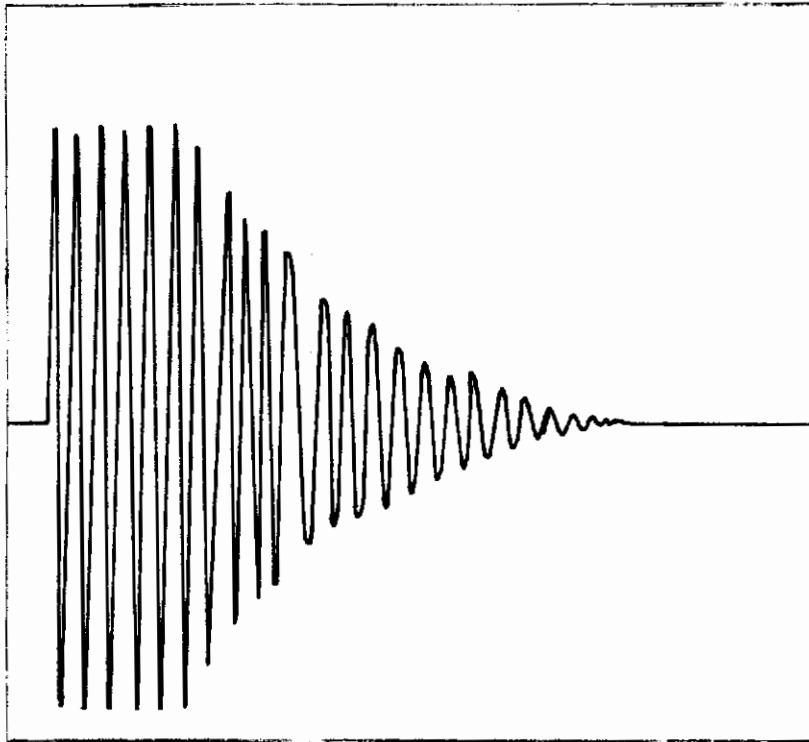


Figure 61. Type I Panel Frequency Response Characteristics (Gage Position#2)



Data Taken From Mid Panel Accelerometer  
Panel No. 13 1st. Mode 128 Hz.

No. Cycles to Half Amplitude=4.5

$$c/c_0 = .11/4.5 = .024$$

Figure 62. Typical Type I Panel Amplitude Decay Trace

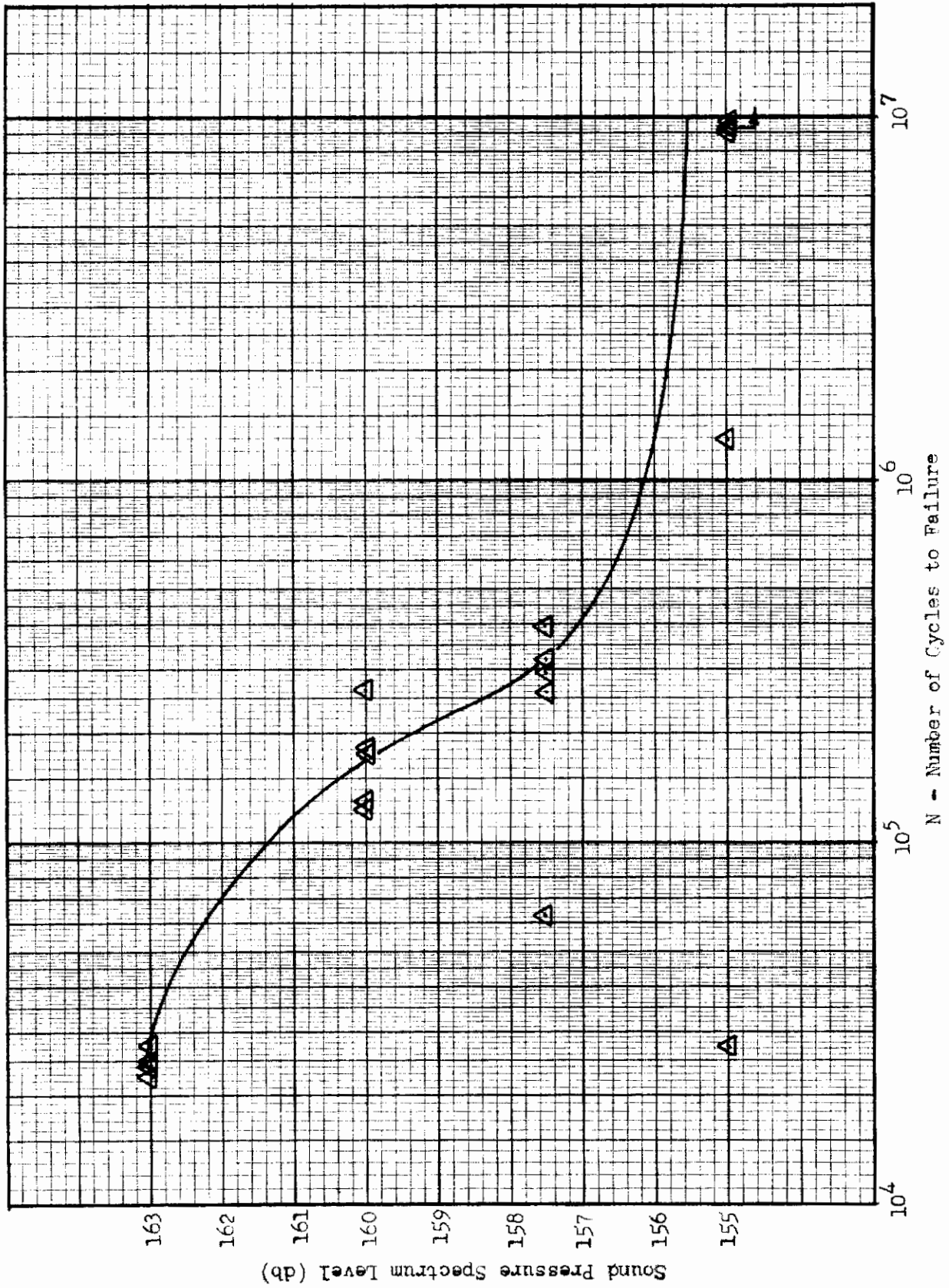


Figure 63. Type I Panels SPL vs. Cycles to Failure Plot

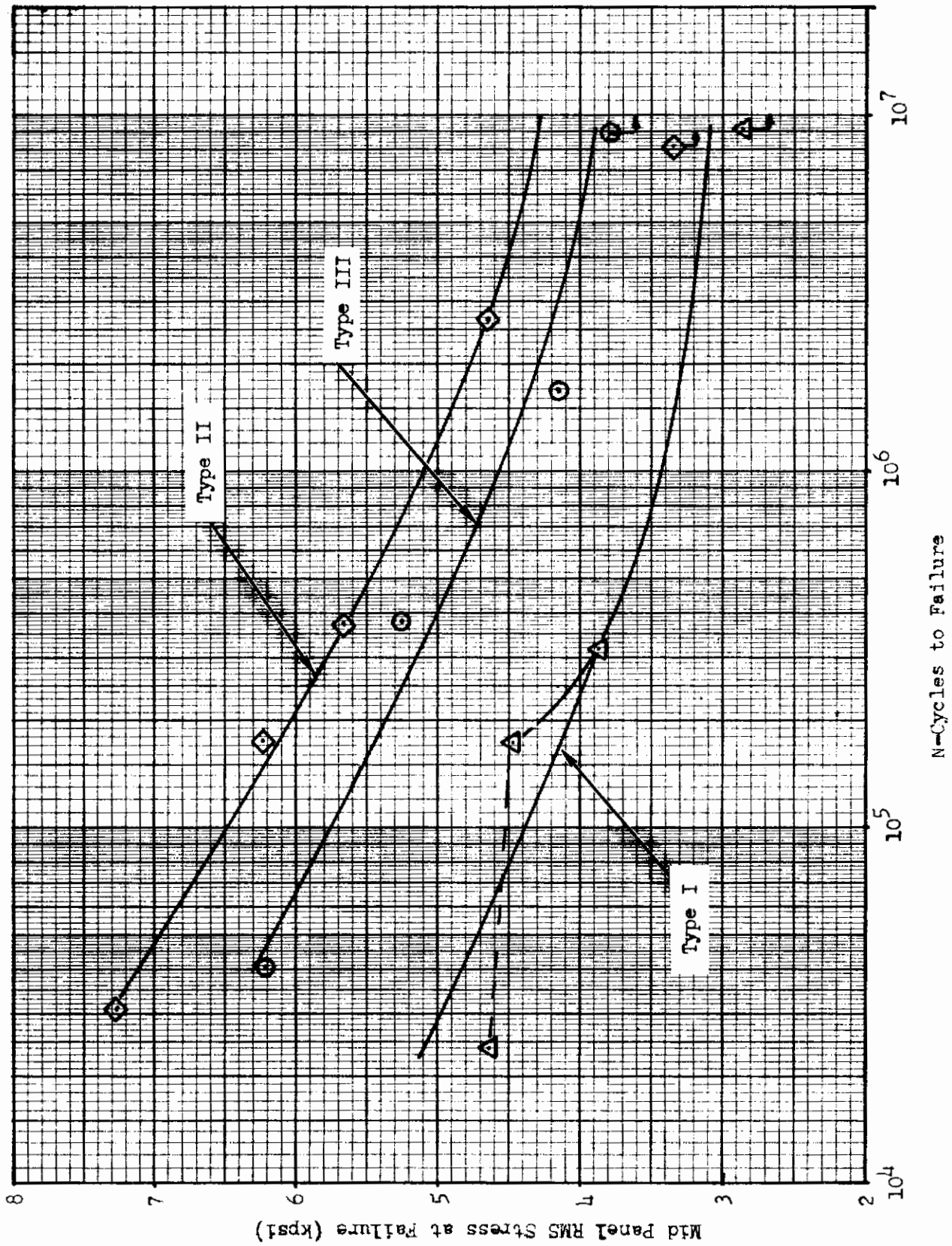
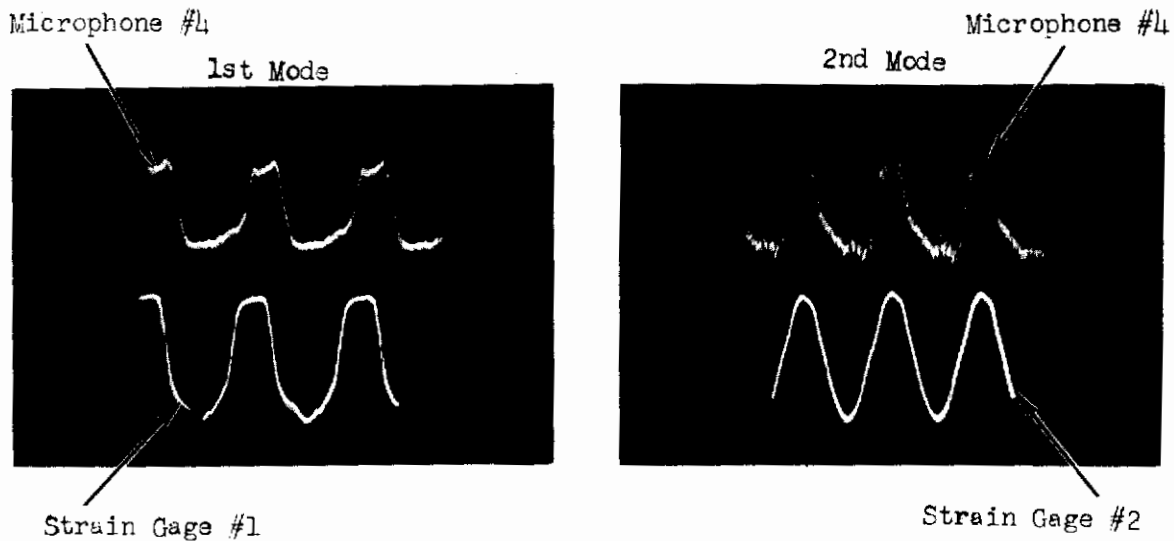
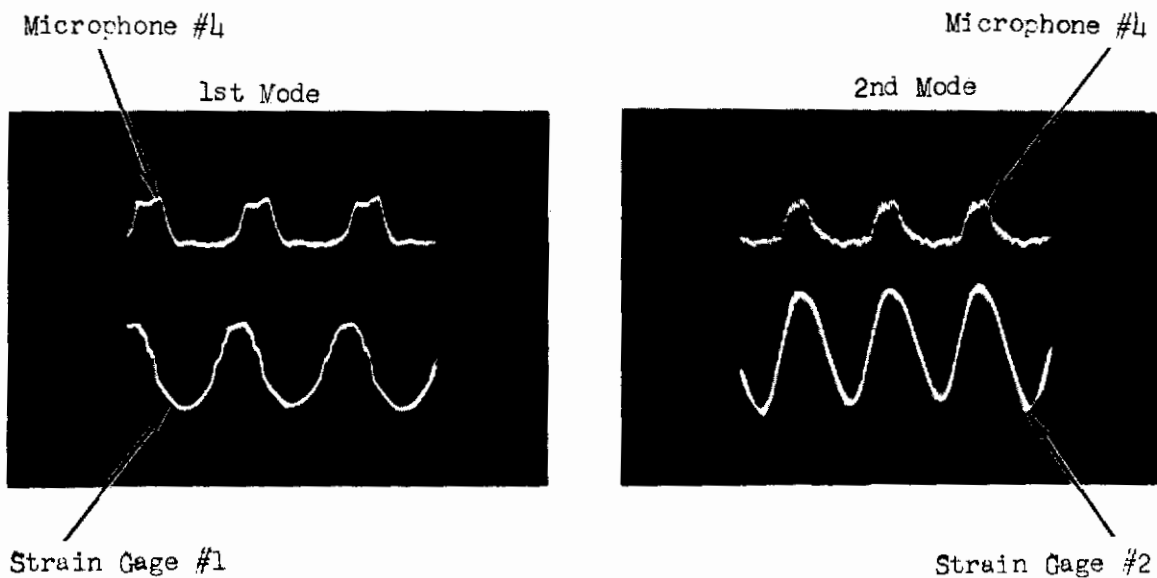


Figure 64 . Glass Fiber Panel S-N Curves

# Contrails



160db Sound Pressure Spectrum Level



155db Sound Pressure Spectrum Level

Figure 65 . Microphone and Strain Gage Oscilloscope Traces-Type I Panels

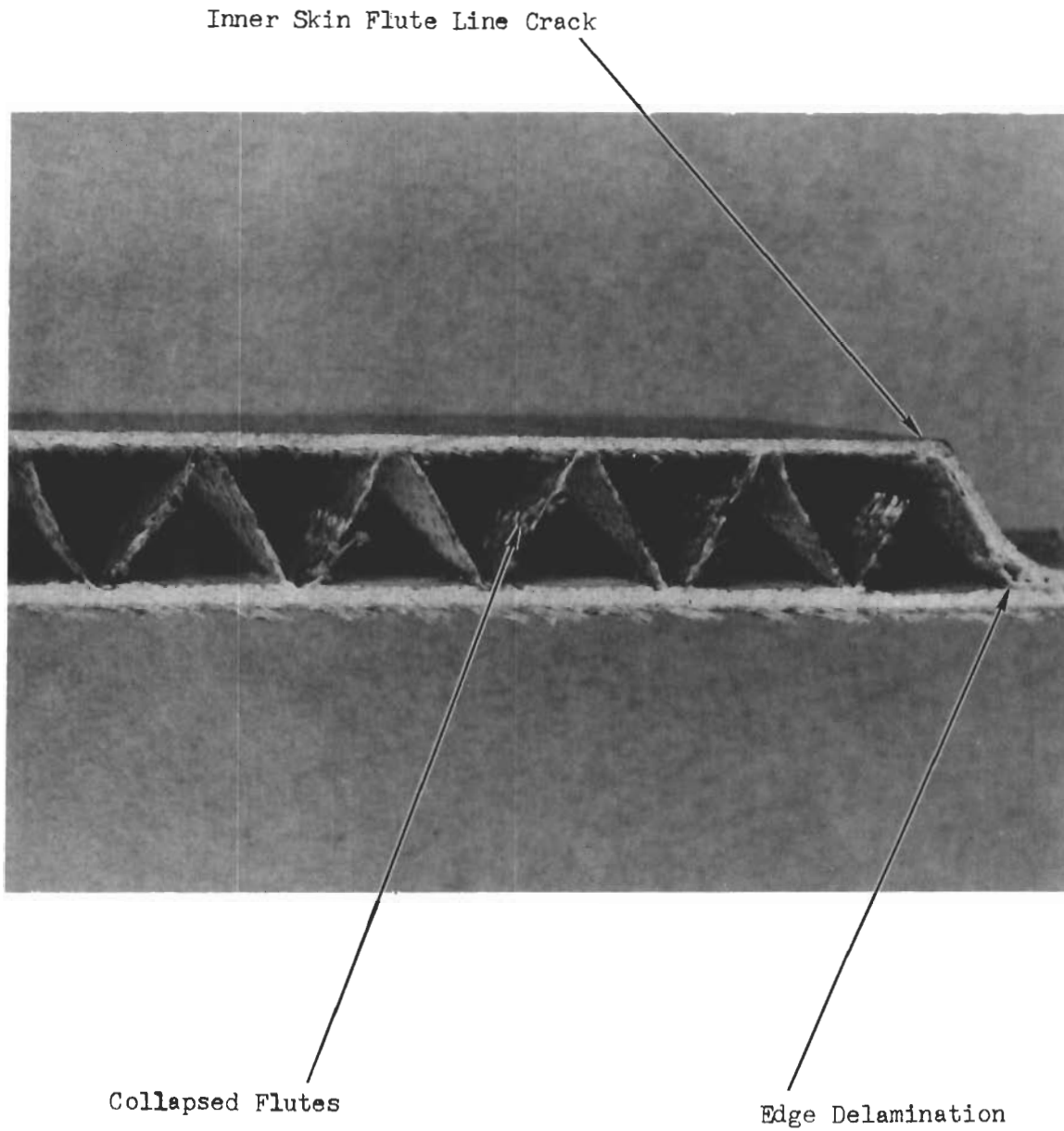


Figure 66. Type I Panel Cross-Section After Failure

# Contrails

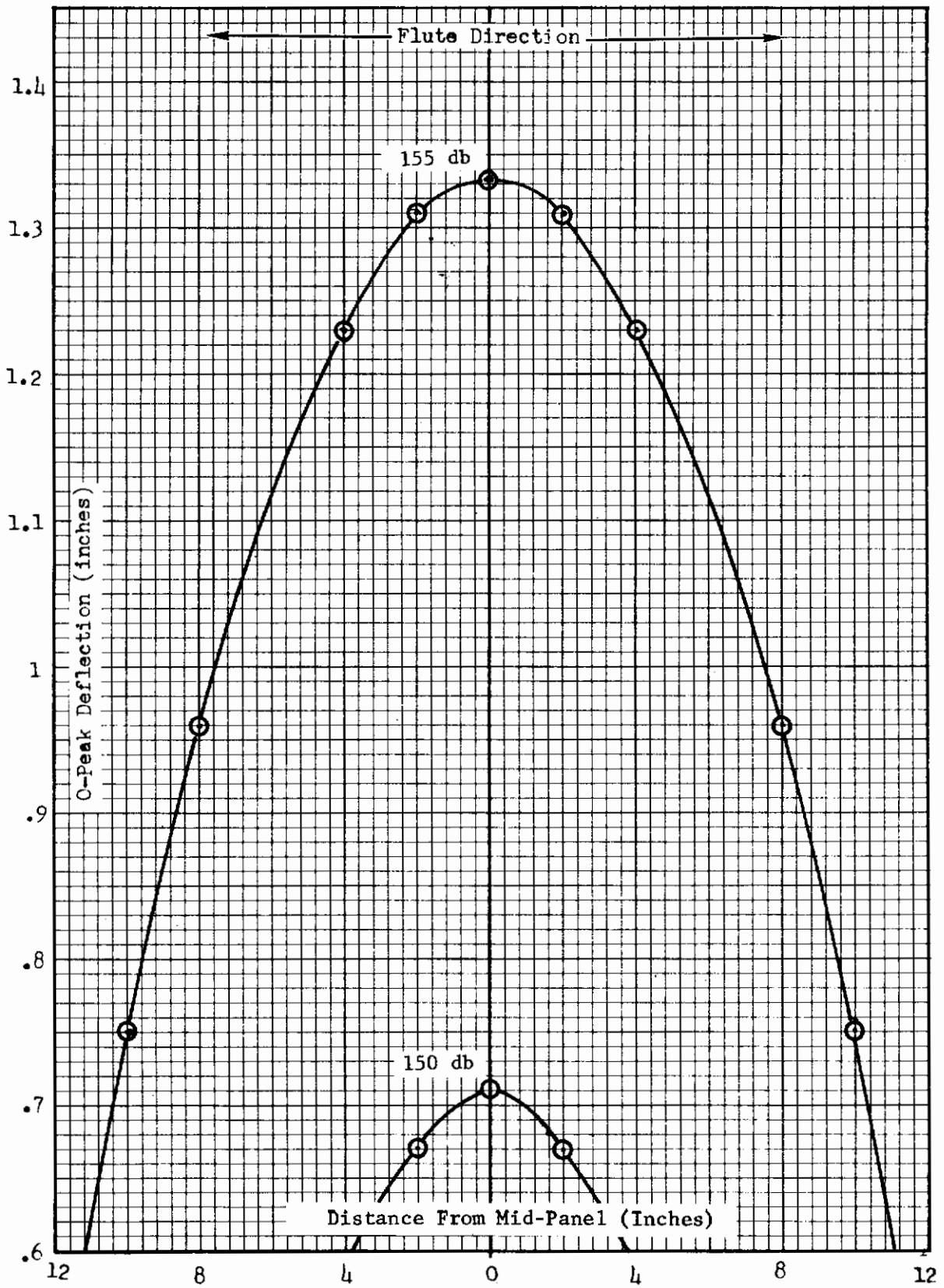


Figure 67. Type II Panel Deflection vs. SPL in Flute Direction



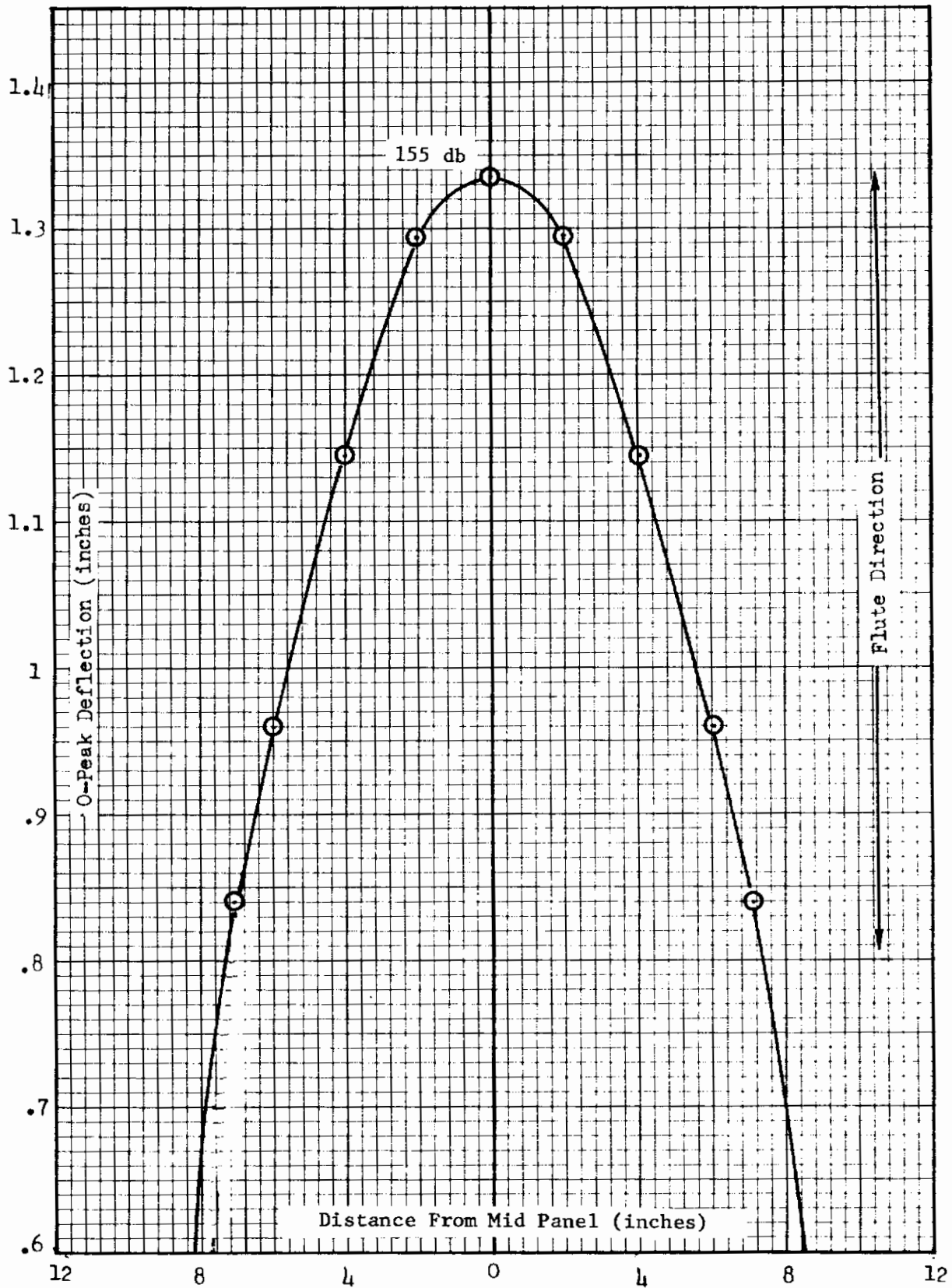


Figure 68. Type II Panel Deflection vs. SPL, Transverse Flute Direction

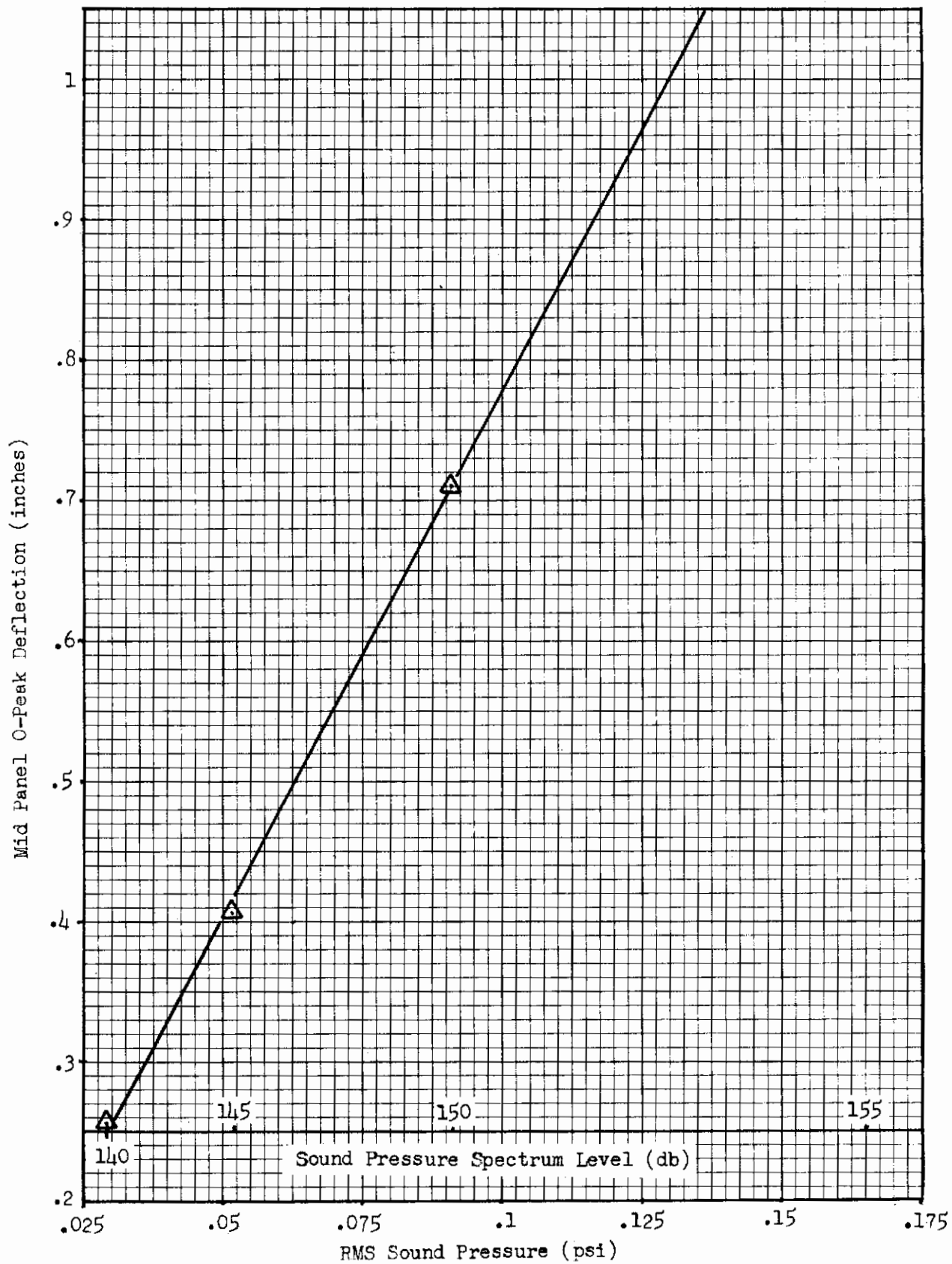


Figure 69. Type II Panel- Mid Panel Deflection vs. SPL

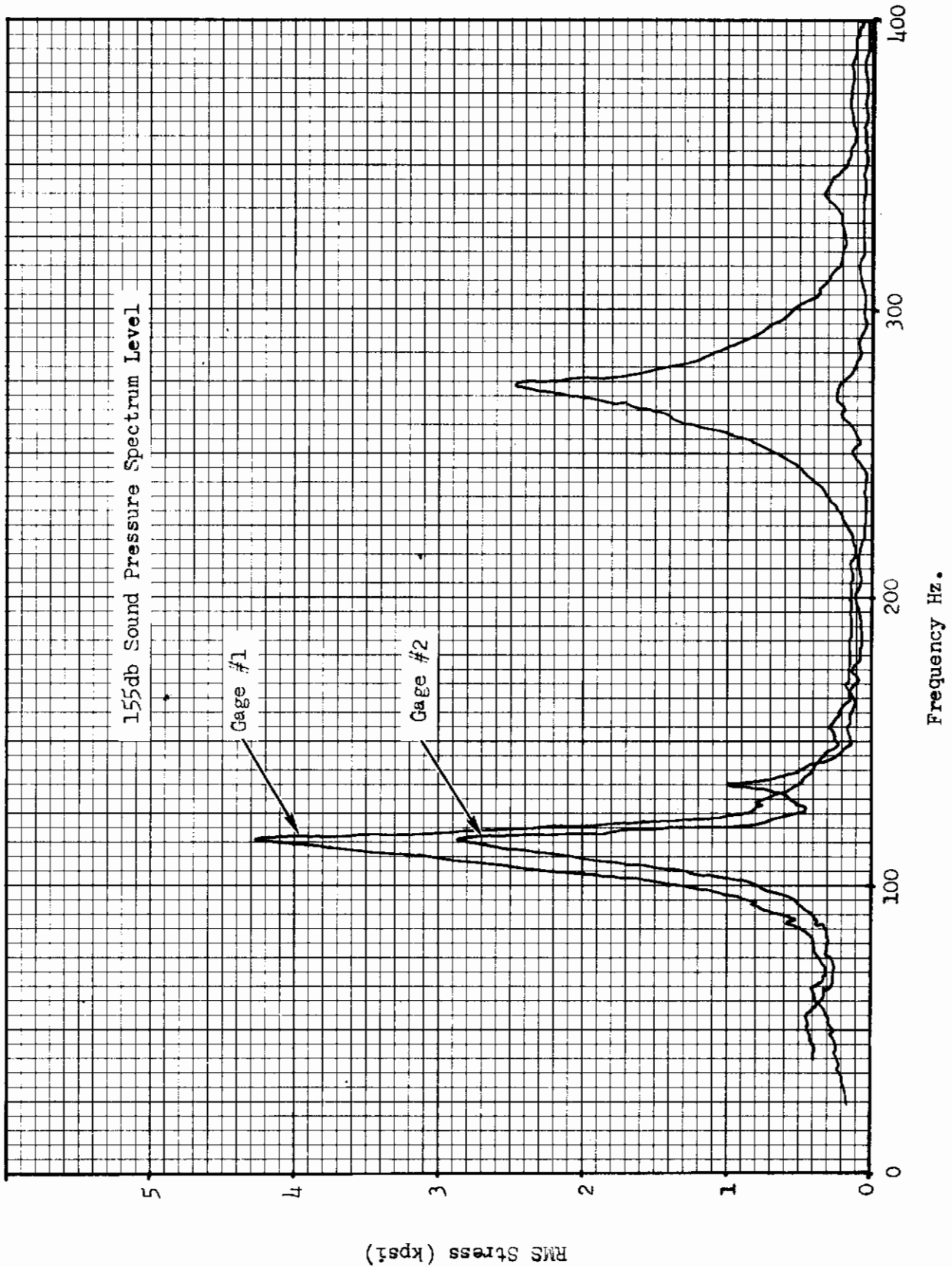


Figure 70. Type II Panel Frequency Response Characteristics

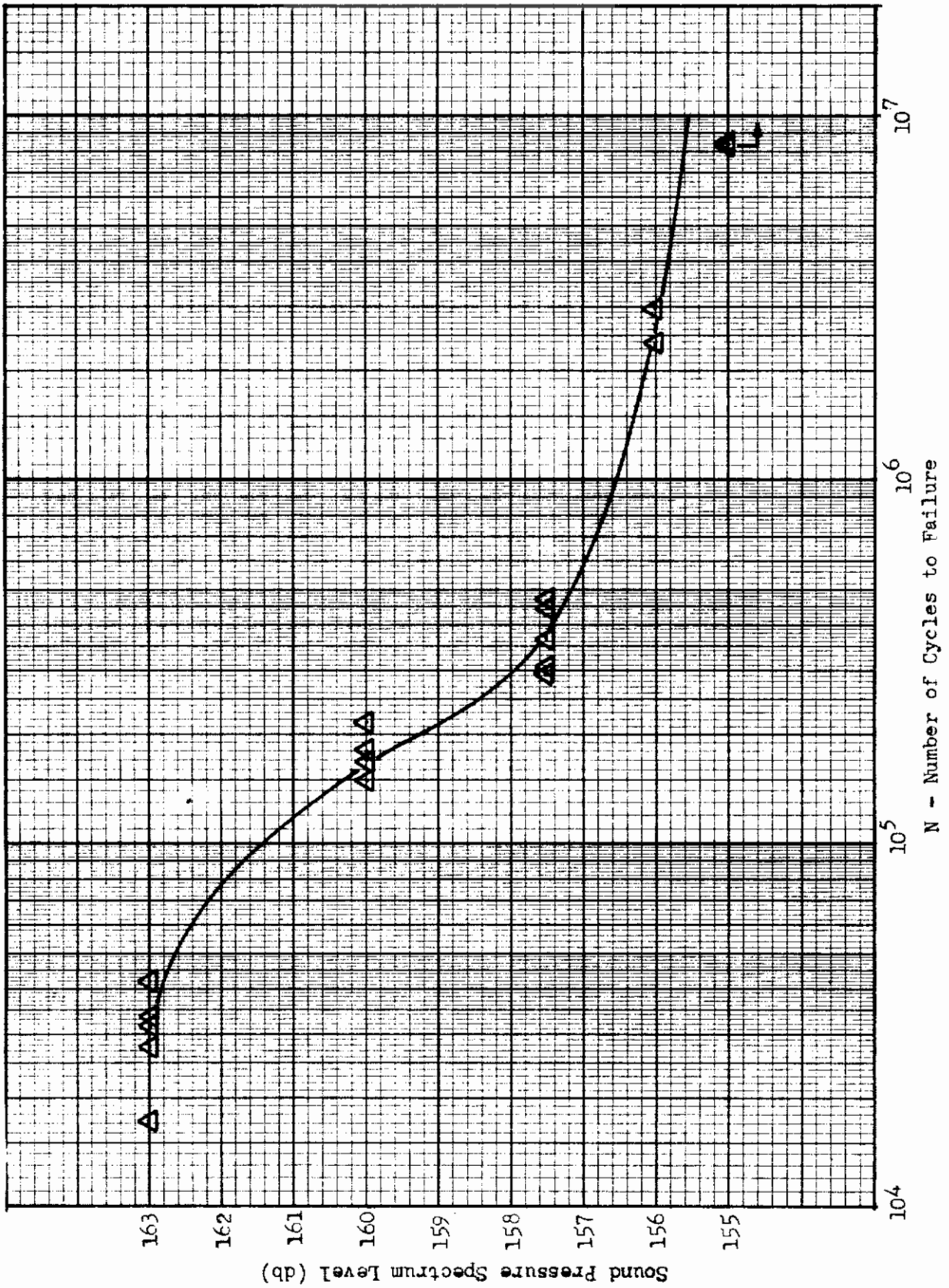


Figure 71. Type II Panels - SPL vs. Cycles to Failure Plot

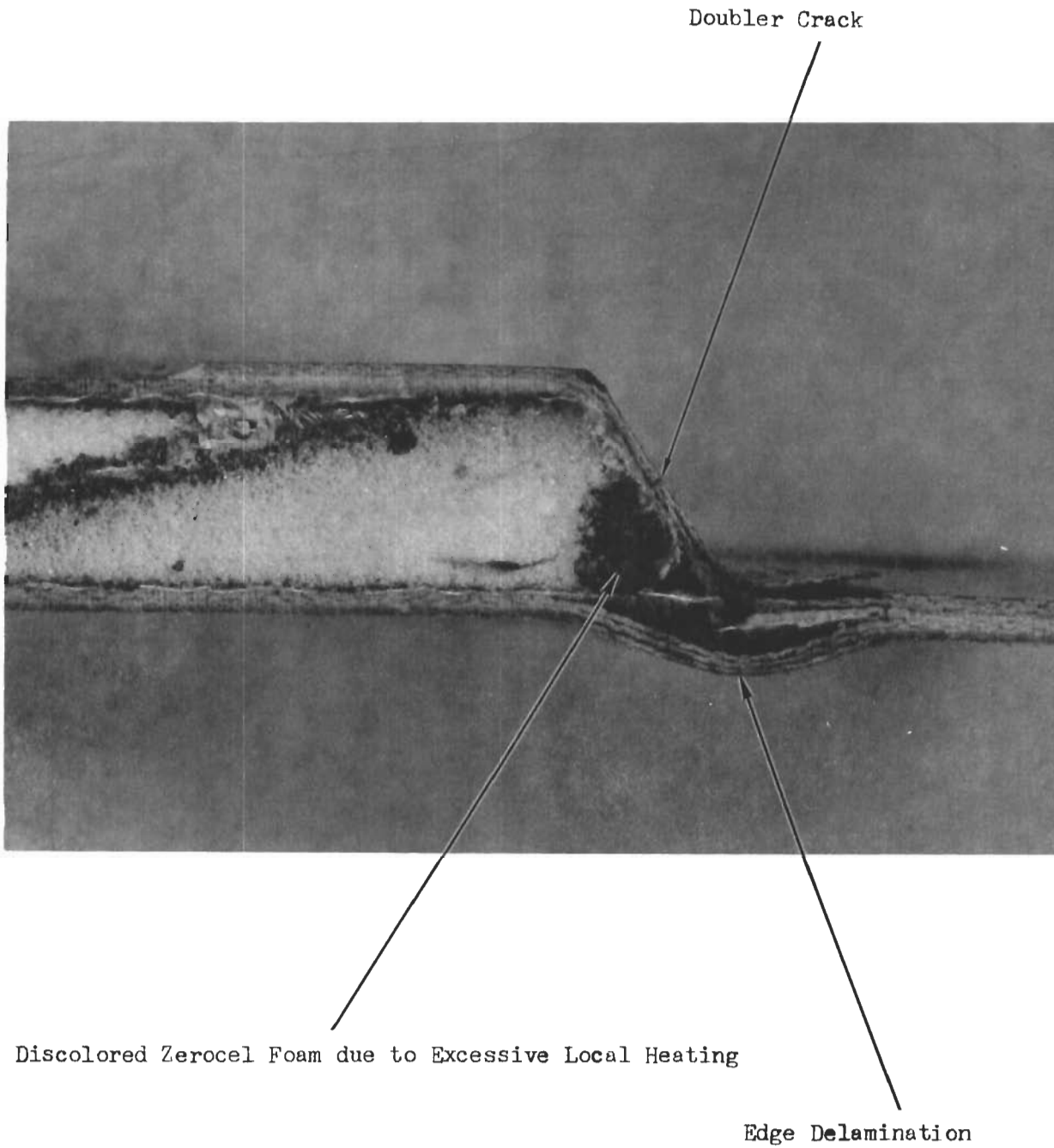


Figure 72. Type II Panel - Cross Section of Top Doubler Edge after Failure

# Contrails

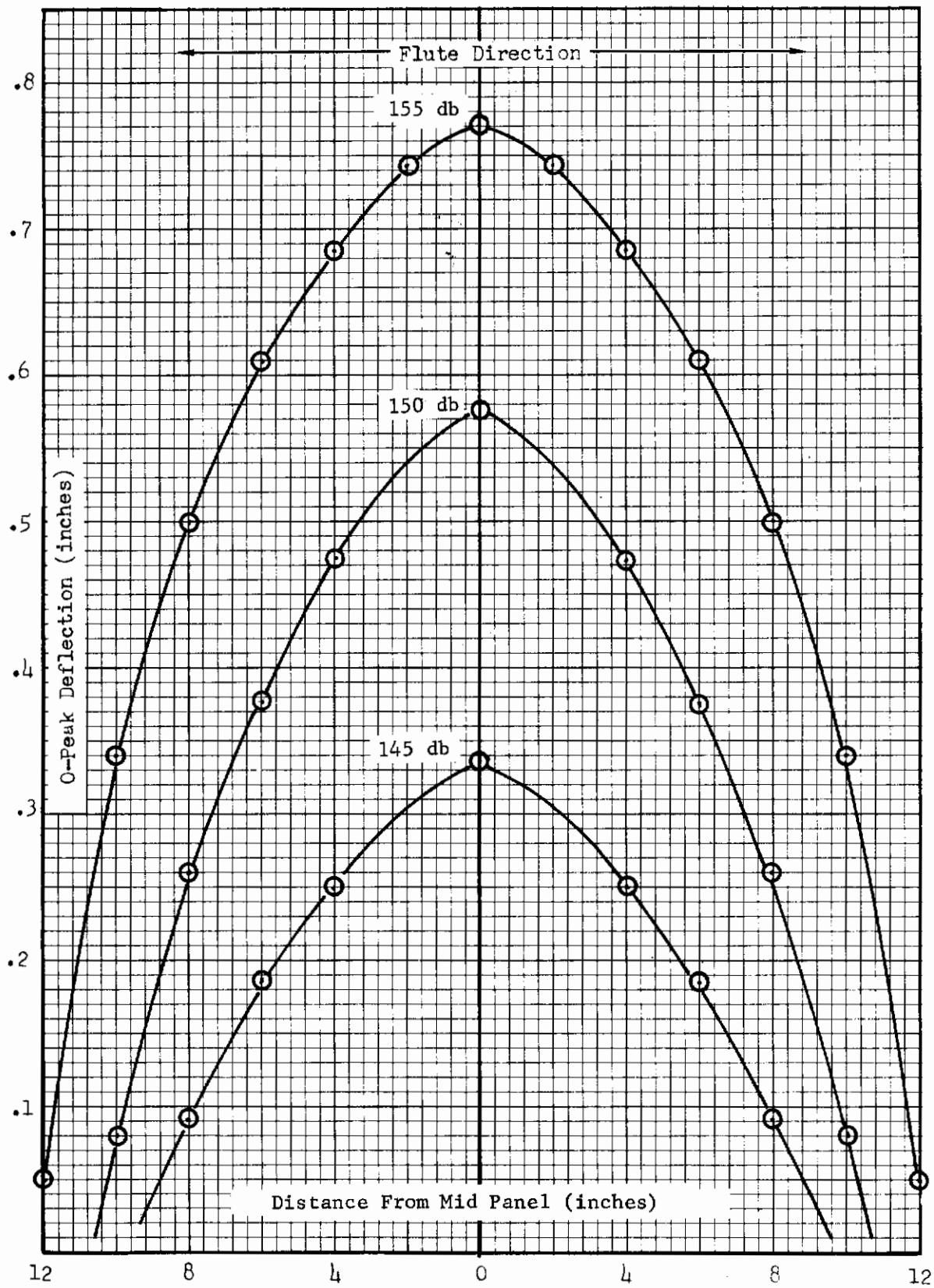


Figure 73. Type III Panel Deflection vs. SPL in Flute Direction

# Contrails

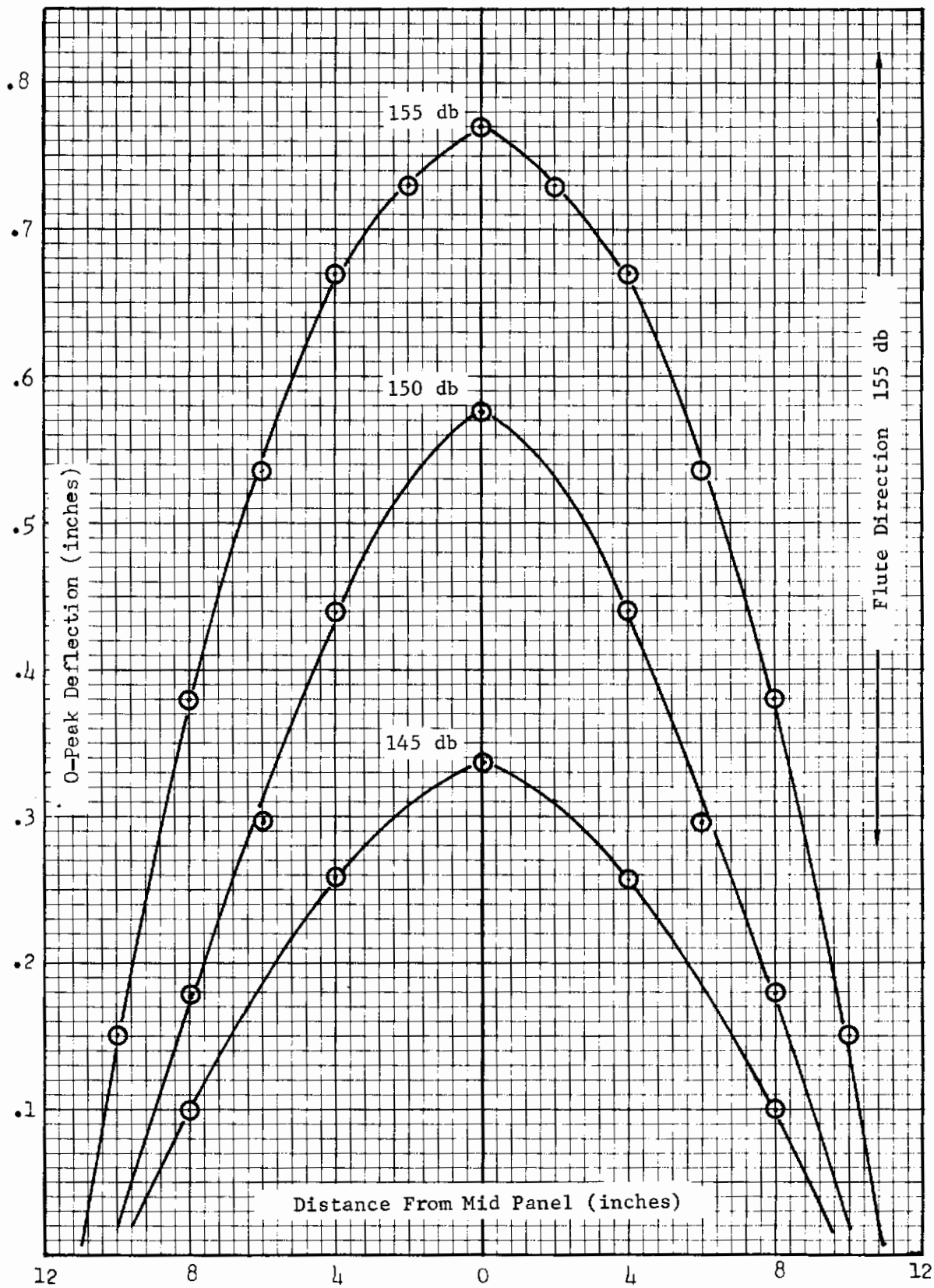


Figure 74. Type III Panel Deflection vs. SPL, Transverse Flute Direction

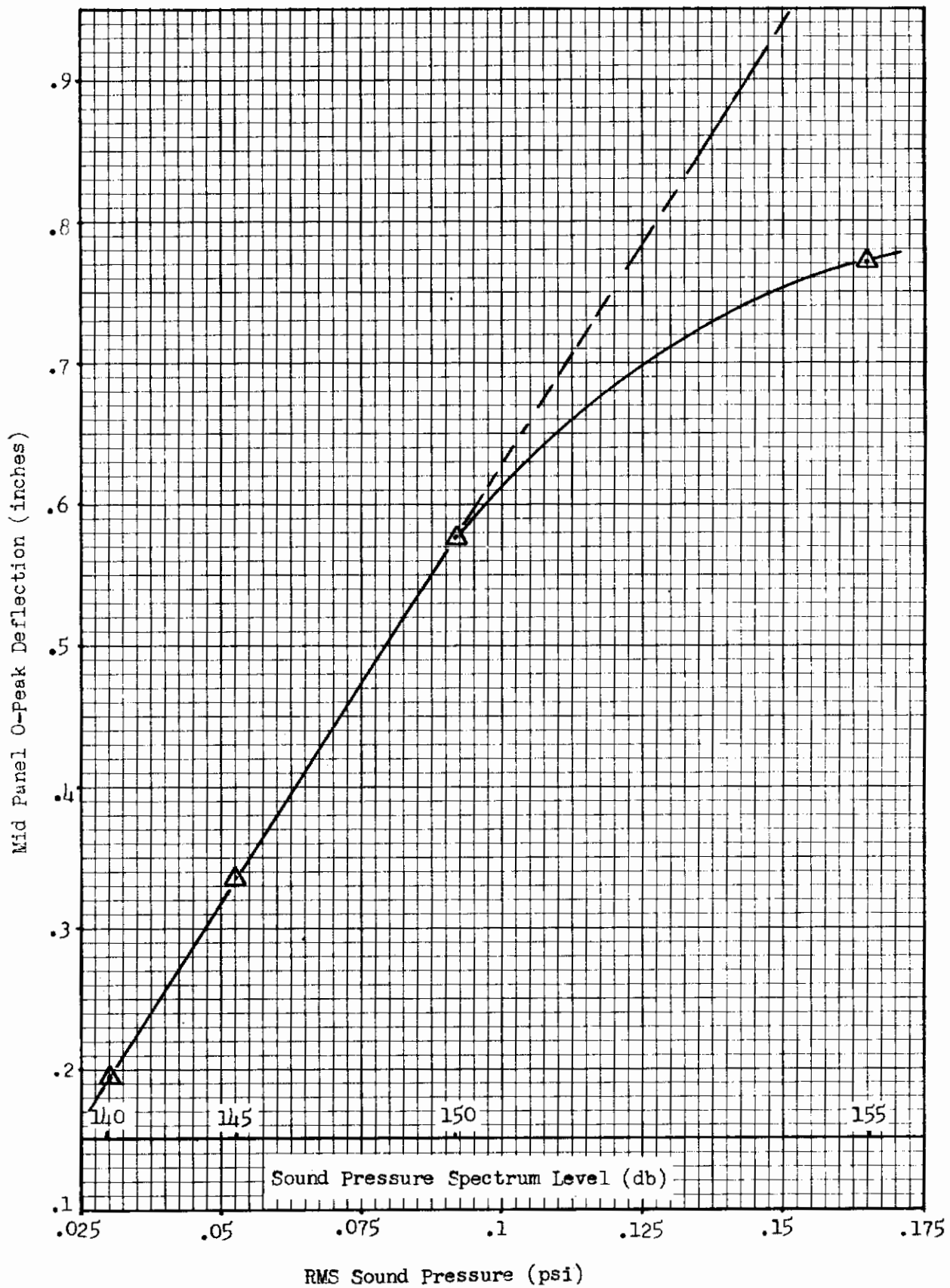


Figure 75. Type III Panel - Mid Panel Deflection vs. SPL



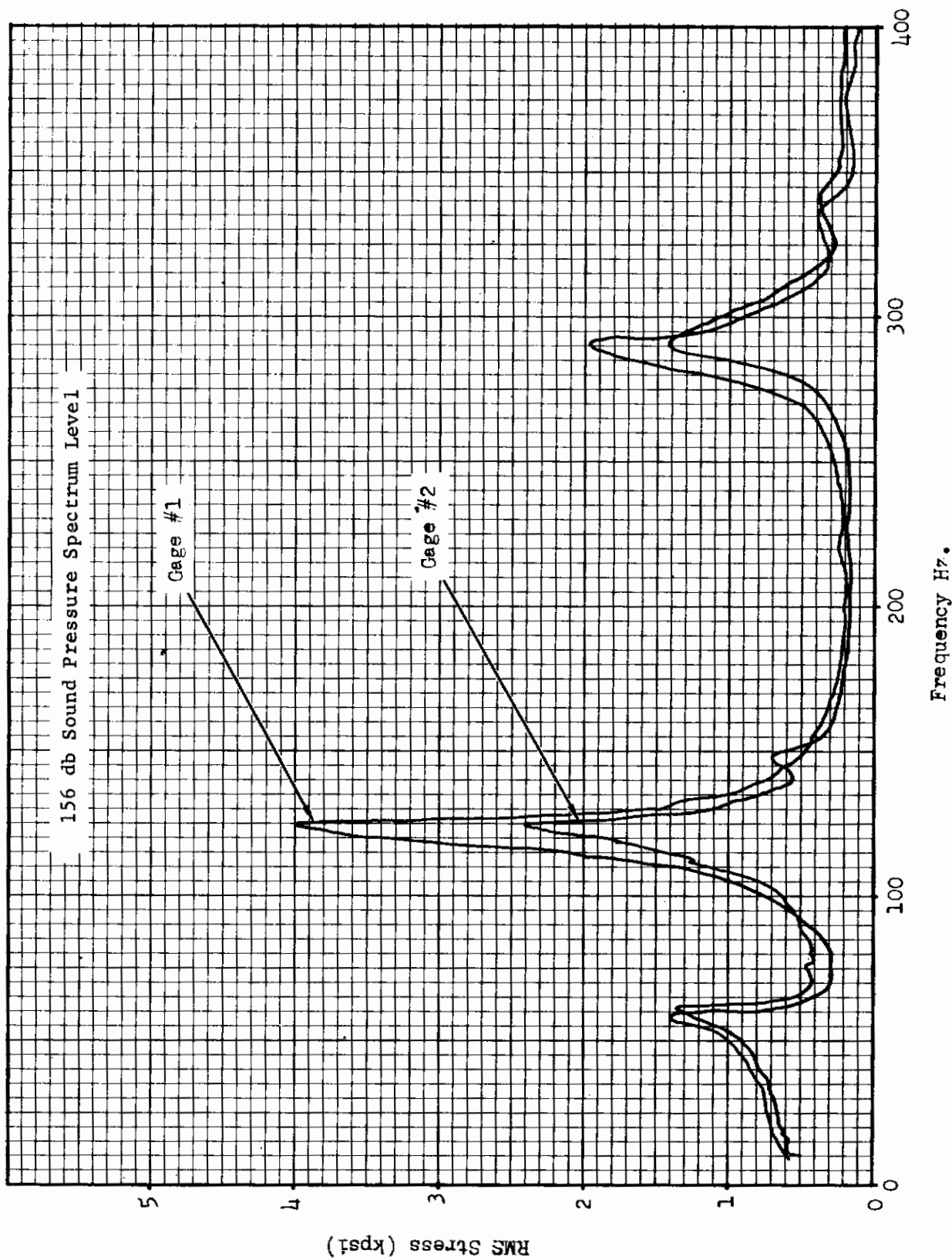


Figure 76. Type III Panel Frequency Response Characteristics

# Contrails

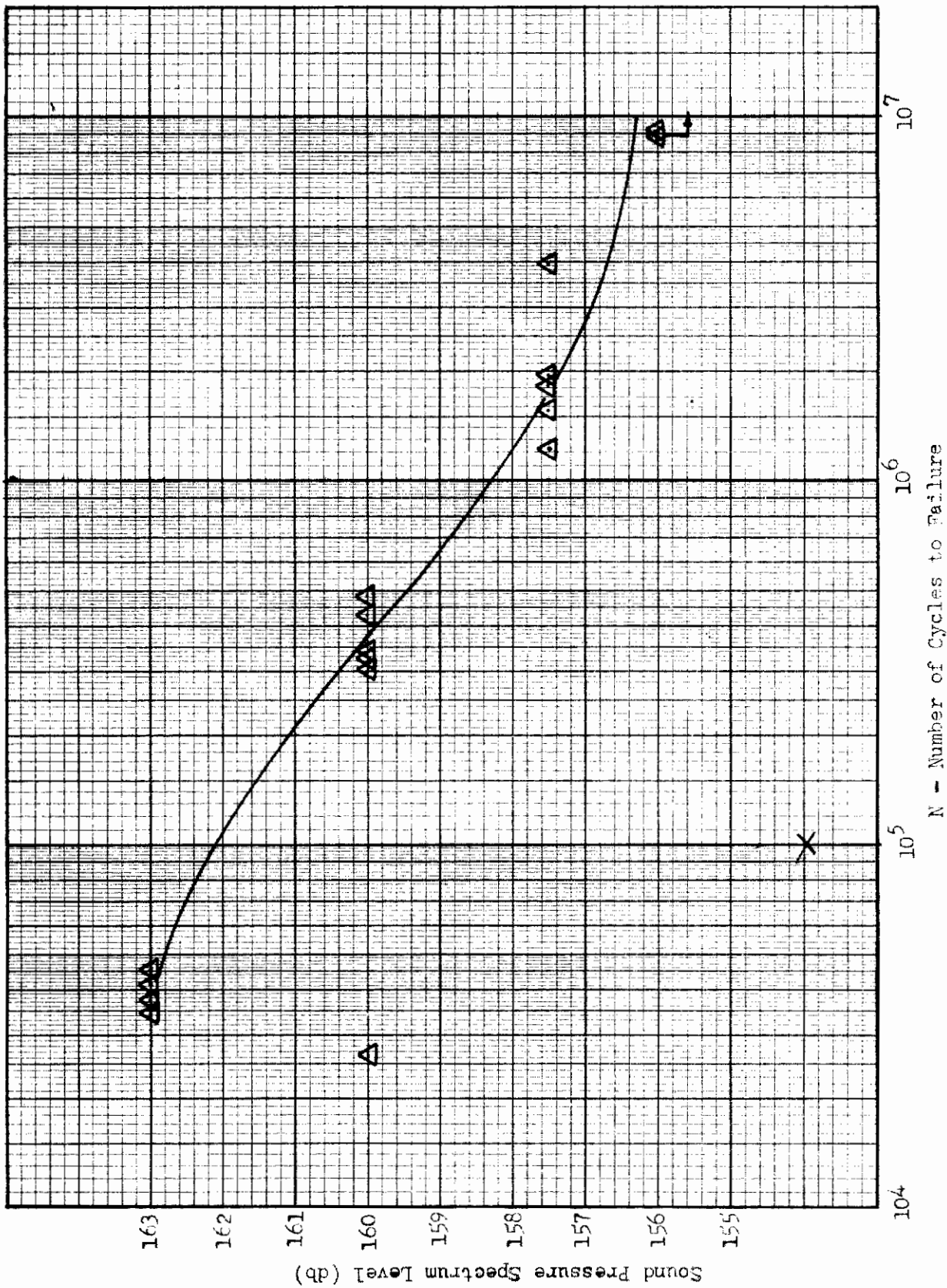


Figure 77 . Type III Panels SPL vs. Cycles to Failure Plot.

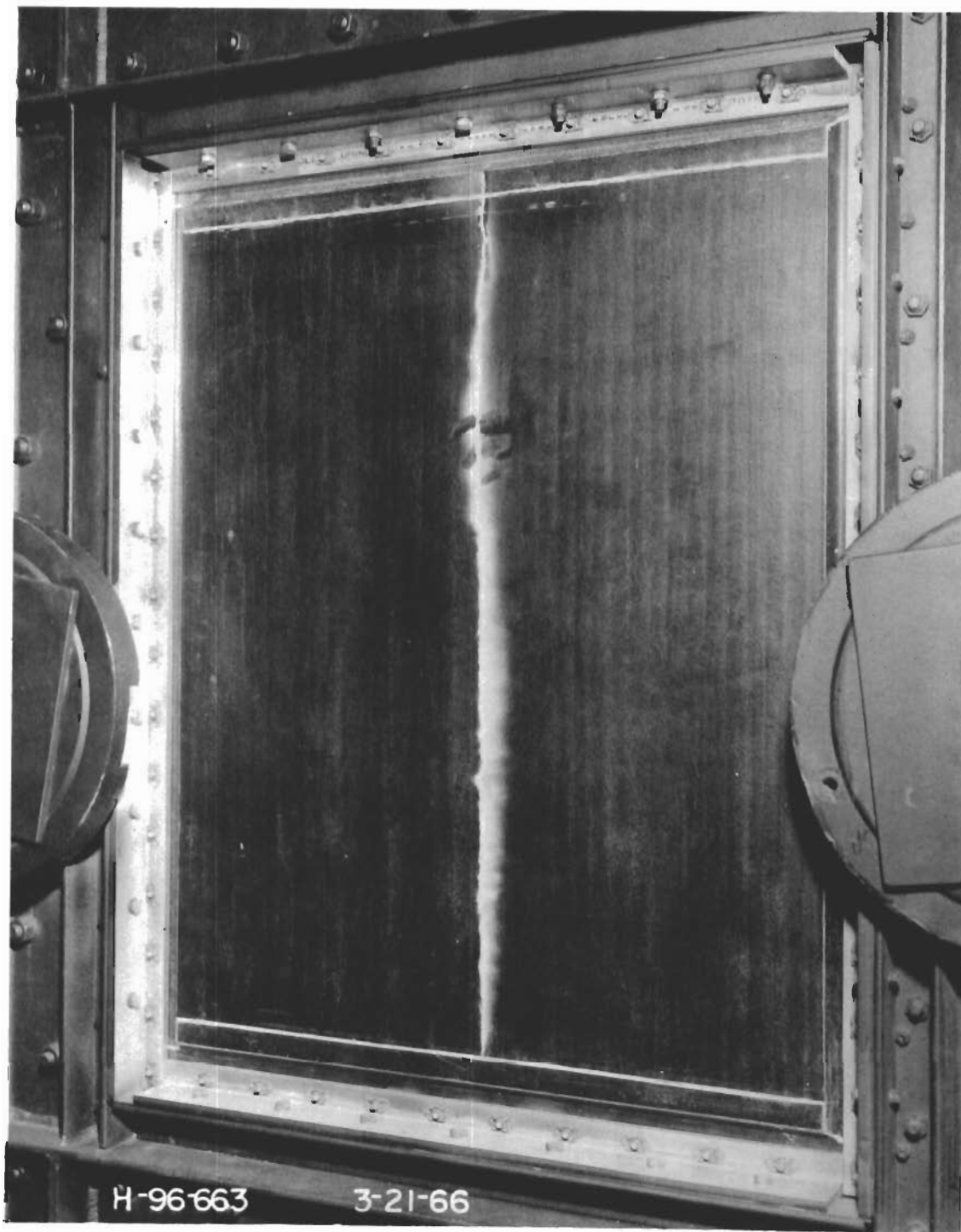


Figure 78. Typical Type III Mid Panel Failure

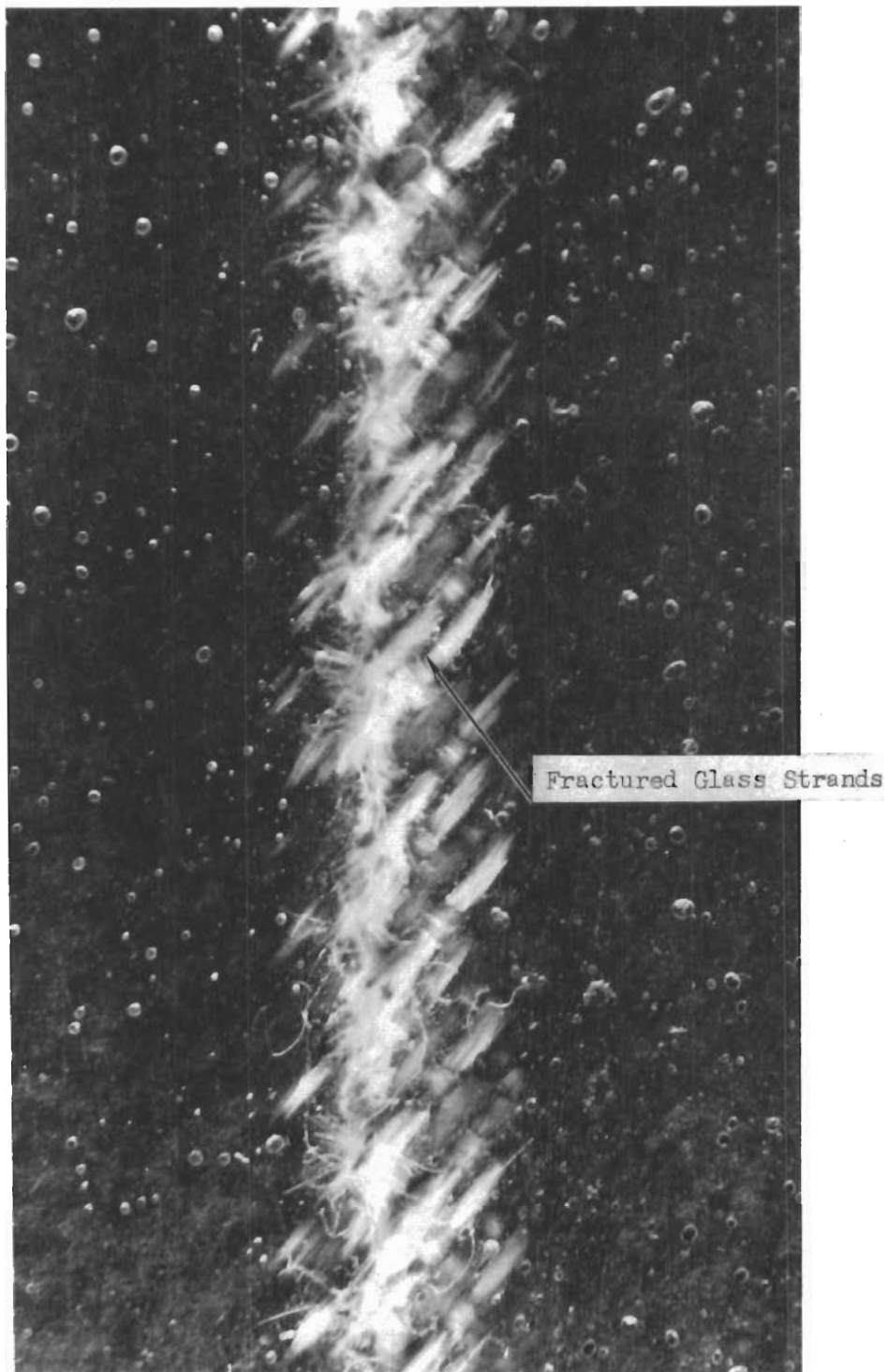


Figure 79. Type III Panel Flute Line Failure - Close-up View

TABLE I  
ALUMINUM CONTROL PANEL SONIC FATIGUE TEST RESULTS

Panel No.	SPL (db)	Frequency Hz	Mean Failing Stress (Kpsi)	Fail Time Hrs. Min. Sec.	No. Cycles to Failure	Panel Wt. Lb. (Grams)	Remarks
1	150	151	13,000	0 51 0	$4.62 \times 10^5$	5.25 (2387)	Failed on skin at stringer heel across #2 gage.
2*	145	142	7,800	2 8 0	$1.09 \times 10^6$	5.22 (2372)	Failed on skin at stringer heel across #3 gage.
3	155	162	15,600	0 6 0	$5.83 \times 10^4$	5.20 (2362)	Failed on skin at stringer heel across #2 gage.
4	155	155	12,000	0 7 0	$6.5 \times 10^4$	5.25 (2386)	Failed on skin at stringer heel across #2 and #3 gage.
5*	140	140	4,000	7 20 0	$3.7 \times 10^6$	5.22 (2371)	Failed on skin at stringer heel across #3 gage.
6	150	148	9,000	0 49 0	$4.35 \times 10^5$	5.23 (2376)	Failed on skin at stringer heel across #2 gage.
7	150	147	8,000	0 46 30	$4.1 \times 10^5$	5.22 (2371)	Failed on skin at stringer heel across #2 gage.
8	145	140	5,800	4 32 10	$2.2 \times 10^6$	5.23 (2373)	Failed on skin at stringer heel across #2 gage.
9	150	148	8,500	0 48 27	$4.3 \times 10^5$	5.23 (2381)	Combined adhesive and skin failure along rivet line, near #2 gage.
10	155	162	14,500	0 9 0	$8.7 \times 10^4$	5.22 (2372)	Failed on skin at stringer heel across #2 gage.
11*	145	150	8,000	1 0 0	$5.4 \times 10^5$	5.23 (2374)	Failed on skin at stringer heel across #2 gage.
12	140	148	6,000	20 0 0	$1.06 \times 10^7$	5.30 (2410)	Failed on skin at stringer heel across #2 gage after a further 14 mins. at 155 db.
13	145	130	5,800	4 28 0	$2.09 \times 10^6$	5.22 (2373)	Failed on skin across #2 gage. Some evidence of built in "oilcan".
14	155	155	12,000	0 8 0	$7.44 \times 10^4$	5.22 (2372)	Failed on skin at stringer heel across #2 gage.
15*	150	160	7,800	0 11 0	$1.05 \times 10^5$	5.22 (2370)	Failed on skin at stringer heel across #2 gage.
16	155	156	14,800	0 7 45	$7.25 \times 10^4$	5.22 (2371)	Failed on skin at stringer heel across #3 gage.
17	140	142	4,600	20 0 0	$0.99 \times 10^6$	5.23 (2375)	No failures after 20 hours of testing.
18*	145	165	8,500	1 20 21	$7.95 \times 10^5$	5.21 (2366)	Failed on skin at stringer heel across #2 gage.
19	140	145	5,100	20 0 0	$1.04 \times 10^6$	5.21 (2365)	No failures after 20 hours of testing.
20	145	143	5,000	3 55 0	$2.02 \times 10^6$	5.21 (2367)	Failed on skin at stringer heel across #3 gage.
21	150	163	7,000	0 52 30	$5.13 \times 10^5$	5.20 (2364)	Failed on skin at stringer heel across #3 gage.
22	145	157	8,600	4 20 0	$2.44 \times 10^6$	5.32 (2415)	Failed on skin at stringer heel across #3 gage.
23	145	158	8,000	3 15 30	$1.85 \times 10^6$	5.32 (2416)	Failed on skin at stringer heel across #3 gage.
24	140	159	4,000	20 0 0	$1.14 \times 10^6$	5.32 (2416)	No failures after 20 hours of testing.
25	140	145	5,600	20 0 0	$1.04 \times 10^7$	5.31 (2410)	No failures after 20 hours of testing.

\*REJECTED

TABLE II  
CONTROL PANEL HARDNESSES DATA

Panel	Rockwell "B"			
1	81.5	81.5	81.6	81.3
6	82.5	82.5	82.2	82.0
7	82.0	82.0	81.5	81.0
15	81.3	82.0	81.2	81.5

TABLE III  
CONTROL PANEL HARDNESSES DATA

SPEC.	PANEL		ANGLE		TOTAL			ALL THREE			ADHESIVE			
	R/H	Center	L/H	R/H	Center	L/H	R/H	Center	L/H	R/H	Center	L/H		
1	.031	.030	.030	.038	.038	.038	.069	.068	.068	.075	.074	.073	.006	.005
6	.029	.029	.029	.038	.038	.038	.068	.067	.067	.072	.075	.076	.005	.008
7	.029	.029	.029	.038	.038	.038	.067	.067	.067	.074	.074	.073	.007	.008
15	.029	.029	.029	.039	.039	.039	.068	.068	.068	.073	.074	.075	.005	.006

TABLE IV  
TYPE I GLASS FIBER PANELS - SONIC FATIGUE TEST RESULTS

TEST No.	FREQ Hz	MID-PANEL STRESS kpsi(RMS)	FAIL TIME		N	WT. LB. (GRAMS)	THICKNESS		REMARKS
			HR.	MIN. SEC.			EDGE	BODY	
1	155	---	0	35	0	2.73 x 10 <sup>4</sup>	5.22 (2376)	.095" .460"	Failure of edge flute left side. Marked temperature rise. (No cooling).
2	155	2.8	20	0	0	9.56 x 10 <sup>6</sup>	(2432) 5.35	.096" .465"	No failure.
3	157.5	4.4	0	33	0	2.6 x 10 <sup>5</sup>	5.50 (2498)	.099" .467"	Edge flute failure left side, outer skin crack.
4	160	4.8	0	15	0	1.22 x 10 <sup>5</sup>	5.29 (2403)	.093" .462"	Inner skin crack adjacent to edge flute right side.
5	160	4.3	0	33	10	2.62 x 10 <sup>5</sup>	5.31 (2411)	.093" .465"	Top and bottom bonded doubler cracks, no adhesive failure.
6	157.5	3.8	0	42	0	3.2 x 10 <sup>5</sup>	5.33 (2420)	.097" .460"	Inner skin crack along flute line left side.
7	163	4.5	0	3	0	2.39 x 10 <sup>4</sup>	5.40 (2454)	.098" .463"	Inner skin cracks adjacent to edge flute and 2 inches inboard left side.
8	163	4.75	0	3	5	2.46 x 10 <sup>4</sup>	5.57 (2531)	.095" .464"	Inner skin failure along flute approximately 3 inches from left edge.
9	155	----	2	50	0	1.30 x 10 <sup>6</sup>	5.48 (2488)	.103" .470"	Failed along edge flute and inner skin adjacent to right edge. (Aluminum frame failure)
10	157.5	4.2	0	8	10	6.26 x 10 <sup>4</sup>	5.63 (2588)	.096" .473"	Failure of internal flutes right side, inner skin swelling. Evidence of local resin starvation internally. (Premature gage failures)
11	157.5	3.8	0	38	0	2.97 x 10 <sup>5</sup>	5.50 (2498)	.096" .468"	Failure on inner skin flute apex right side. (Aluminum frame failure)
12	160	4.3	0	16	41	1.31 x 10 <sup>5</sup>	5.74 (2601)	.105" .475"	Inner skin flute line failure approximately 2" from lower right side.
13	163	4.8	0	3	16	2.51 x 10 <sup>4</sup>	5.9 (2691)	.110" .478"	Left inner skin flute line failure adjacent to edge flute.
14	163	---	0	3	38	2.76 x 10 <sup>4</sup>	5.68 (2591)	.108" .473"	Failure of top doubler left side.
15	157.5	3.2	0	52	12	3.98 x 10 <sup>5</sup>	5.68 (2591)	.106" .475"	Failure of inner skin along flute adjacent to right side.
16	155 (163)	2.2 4.8	20 0	0 2	0 7	9.22 x 10 <sup>6</sup> (1.65 x 10 <sup>4</sup> )	5.55 (2529)	.115" .482"	No failure. Failed along inner skin adjacent to right edge flute.
17	163	4.3	0	2	53	2.23 x 10 <sup>4</sup>	5.49 (2491)	.111" .500"	Right side inner skin flute line failure adjacent to edge flutes. Extreme local heating.
18	160	3.4	0	22	22	1.73 x 10 <sup>5</sup>	5.9 (2691)	.109" .483"	Inner skin flute line failure approximately 2 inches from lower left edge.
19	160	5.6	0	22	52	1.76 x 10 <sup>5</sup>	5.67 (2575)	.120" .505"	Inner skin flute line failure approximately 2 inches from lower left edge.
20	155	3.5	20	0	0	9 x 10 <sup>6</sup>	5.67 (2574)	.105" .500"	No failures.

TABLE V

TYPE I GLASS FIBER PANELS - DAMPING DATA

<u>PANEL NO.</u>	<u>C/C<sub>0</sub> 1st MODE</u>	<u>C/C<sub>0</sub> 2nd MODE</u>
1	.026	.011
2	.035	.015
3	----	----
4	.035	.020
5	.035	----
6	.034	.022
7	.039	----
8	.039	.028
9	----	----
10	.024	.016
11	.030	----
12	.024	.022
13	.020	.012
14	.032	.015
15	.031	.010
16	.027	.015
17	.023	.011
18	.035	.010
19	.032	----
20	.032	.016

Average 1st Mode  $C/C_0 = 0.030$

Average 2nd Mode  $C/C_0 = 0.016$

Note: All data obtained from Stress vs. Frequency Response Plots at 155 db. SPL.



TABLE VI

TYPE I GLASS FIBER PANELS STRESS SUMMARY

<u>PANEL NO.</u>	<u>SPL</u>	<u>MID PANEL STRESS*(kpsi)</u>	
1	155db	-	
2	155db	2.8	
9	155db	-	2.83 kpsi Avg.
16	155db	2.2	
20	155db	3.5	
3	157.5db	4.4	
6	157.5db	3.8	
10	157.5db	4.2	3.88 kpsi Avg.
11	157.5db	3.8	
15	157.5db	3.2	
4	160db	4.8	
5	160db	4.3	
12	160db	4.3	4.48 kpsi Avg.
18	160db	3.4	
19	160db	5.6	
7	163db	4.5	
8	163db	4.75	
13	163db	4.8	4.62 kpsi Avg.
14	163db	3.4(low)	
16	163db	4.8	
17	163db	4.3	

\*No. 1 Strain Gage Transverse-to-Flute Direction

TABLE VII  
TYPE II GLASS FIBER PANELS - DAMPING DATA

<u>PANEL No.</u>	<u>C/C<sub>0</sub> 1st MODE</u>	<u>C/C<sub>0</sub> 2nd MODE</u>
1	.030	0.020
2	.027	0.013
3	.035	0.018
4	----	-----
5	.026	0.014
6	.030	0.014
7	----	0.019
8	.030	0.018
9	.025	-----
10	.030	-----
11	.035	0.016
12	----	0.012
13	.027	-----
14	.035	-----
15	.041	.013
16	----	.013
17	.028	.011
18	.033	.015
19	.028	.015
20	.033	.015

Average 1st Mode C/C<sub>0</sub> = 0.031

Average 2nd Mode C/C<sub>0</sub> = 0.015

TABLE VIII  
TYPE II GLASS FIBER PANELS - SONIC FATIGUE TEST RESULTS

SPL NO.	TEST FREQUENCY Hz	MID-PANEL STRESS kpsi(RMS)	FAIL TIME		N	WT. LB.	THICKNESS		REMARKS
			HR.	MIN. SEC.			EDGE	BODY	
1	160	6.2	0	21 25	$1.5 \times 10^5$	5.07 (2304)	.079"	.446"	Mid-panel failure in flute direction extending from top to bottom.
2	160	6.9	0	31 0	$2.16 \times 10^5$	5.08 (2307)	.081"	.445"	Failure to bottom doubler across flute direction, right side.
3	157.5	6.0	0	51 10	$3.68 \times 10^5$	5.17 (2348)	.078"	.442"	Mid-panel inner skin failure along flute line and extending under bottom doubler.
4	155	3.1	20	0 0	$8.14 \times 10^6$	5.12 (2325)	.082"	.440"	No failure.
5	155	3.5	20	0 0	$8.36 \times 10^6$	5.30 (2408)	.078"	.452"	No failure.
6	157.5	5.1	1 5	43	$4.60 \times 10^5$	5.23 (2374)	.085"	.442"	Failure of bottom doubler across flute direction, right side.
7	155	3.4	20	0 0	$8.14 \times 10^6$	5.11 (2320)	.079"	.440"	No failure.
8	157.5	5.2	1 3	20	$4.49 \times 10^5$	5.07 (2301)	.080"	.440"	Top and bottom doubler failures across flute direction.
9	156	5.0	5 32	0	$2.39 \times 10^6$	5.40 (2452)	.085"	.456"	Top and bottom doubler failures across flute direction.
10	156	4.3	7 1	0	$2.98 \times 10^6$	5.31 (2415)	.082"	.460"	Top and bottom doubler failures across flute direction.
11	157.5	6.0	0 42	10	$2.94 \times 10^5$	5.14 (2336)	.080"	.443"	Top doubler crack in edge radius and edge hole tear out.
12	157.5	6.0	0 43	45	$3.05 \times 10^5$	5.48 (2488)	.078"	.450"	Bottom doubler crack in edge radius, hole tear out, frame failure.
13	163	7.6	0 4	5	$3.33 \times 10^4$	5.18 (2353)	.084"	.450"	Top doubler failure across flute direction right side.
14	160	6.6	0 25	0	$1.76 \times 10^5$	5.31 (2414)	.080"	.445"	Top doubler crack in edge radius.
15	163	7.3	0 5	38	$4.2 \times 10^4$	5.30 (2410)	.089"	.452"	Top doubler failure and edge delamination.
16	160	6.3	0 25	7	$1.75 \times 10^5$	5.49 (2493)	.088"	.450"	Delamination of outer skin top side.
17	160	5.1	0 23	47	$1.70 \times 10^5$	5.60 (2540)	.097"	.460"	Failed top and bottom doublers and inner skin in flute direction, approximately 3 inches from left ledge.
18	163	7.0	0 2	24	$1.71 \times 10^4$	5.40 (2458)	.089"	.450"	Failed on bottom doubler, also delamination of top edge.
19	163	7.2	0 4	24	$3.14 \times 10^4$	5.35 (2436)	.087"	.448"	Top and bottom doubler failures.
20	163	7.5	0 4	2	$2.78 \times 10^4$	5.23 (2376)	.094"	.452"	Top and bottom doubler failures.

TABLE IX

TYPE II GLASS FIBER PANELS STRESS SUMMARY

<u>PANEL NO.</u>	<u>SPL</u>	<u>MIDPANEL STRESS*(kpsi)</u>	
4	155 db	3.1	
5	155 db	3.5	Avg. 3.33
7	155 db	3.4	
9	156 db	5.0	
10	156 db	4.3	Avg. 4.65
3	157.5 db	6.0	
6	157.5 db	5.1	
8	157.5 db	5.2	Avg. 5.66
11	157.5 db	6.0	
12	157.5 db	6.0	
1	160 db	6.2	
2	160 db	6.9	
14	160 db	6.6	Avg. 6.22
16	160 db	6.3	
17	160 db	5.1	
13	163 db	7.6	
15	163 db	7.3	
18	163 db	7.0	Avg. 7.28
19	163 db	7.2	
20	163 db	7.5	

\*No. 1 Strain Gage Transverse-to-Flute Direction

TABLE X

TYPE III GLASS FIBER PANELS - DAMPING DATA

<u>PANEL No.</u>	<u>C/C<sub>0</sub>1st Mode</u>	<u>C/C<sub>0</sub>2nd Mode</u>
1	----	-----
2	.032	.025
3	.021	-----
4	.028	.013
5	.032	.020
6	.028	.017
7	.024	.025
8	----	-----
9	.035	.018
10	.032	-----
11	.033	.014
12	.025	-----
13	.028	.012
14	.028	.012
15	.032	-----
16	.032	.014
17	.037	-----
18	.028	-----
19	.038	.011
20	----	-----
21	.035	.015

Average 1st Mode C/C<sub>0</sub> = 0.030

Average 2nd Mode C/C<sub>0</sub> = 0.016

TABLE XI  
TYPE III GLASS FIBER PANELS SONIC FATIGUE TEST RESULTS

SPL No.	TEST FREQUENCY Hz	MID-PANEL STRESS kpsi(RMS)	FAIL TIME		N CYCLES TO FAILURE	WT. LB. (GRAMS)	THICKNESS		REMARKS
			HR.	MIN. SEC.			EDGE	BODY	
1	160	---	0	3 45	$2.64 \times 10^4$	5.10 (2315)	.086"	.453"	Inner skin failure in flute direction lower mid-panel (No cooling)
2	156	3.9	20	0 0	$8.86 \times 10^6$	5.03 (2285)	.088"	.460"	No failures.
3	160	5.3	0	40 0	$3.02 \times 10^5$	5.40 (2455)	.087"	.461"	Mid-panel failure in flute direction extending from top to bottom.
4	157.5	4.4	4	7 0	$1.84 \times 10^6$	5.16 (2346)	.082"	.457"	Upper right side doubler failure.
5	157.5	4.2	4	18 21	$1.95 \times 10^6$	5.12 (2326)	.088"	.452"	Horizontal failure line along top doubler.
6	157.5	4.2	2	39 30	$1.21 \times 10^6$	5.21 (2368)	.089"	.465"	Failure along flute direction mid-panel.
7	157.5	4.1	3	26 23	$1.56 \times 10^6$	5.21 (2367)	.080"	.452"	Failure along flute direction mid-panel.
8	163	6.6	0	5 42	$4.17 \times 10^4$	5.34 (2425)	.084"	.455"	Failure along flute direction mid-panel.
9	156	3.7	20	0 0	$9.15 \times 10^6$	5.24 (2380)	.082"	.470"	No failures.
10	157.5	3.9	9	0 0	$3.95 \times 10^6$	5.27 (2394)	.083"	.470"	Lower right side doubler failure.
11	163	6.2	0	5 30	$4.16 \times 10^4$	5.20 (2360)	.092"	.450"	Left side skin failure extending to edge flute.
12	156	3.4	20	0 0	$8.86 \times 10^6$	5.21 (2368)	.098"	.460"	No failures.
13	156	4.0	20	0 0	$8.92 \times 10^6$	5.06 (2300)	.089"	.461"	No failures.
14	160	5.3	0	58 0	$4.31 \times 10^5$	5.41 (2456)	.097"	.455"	Mid-panel failure along flute direction.
15	163	6.2	0	5 55	$4.54 \times 10^4$	5.43 (2467)	.100"	.475"	Left inner skin failure adjacent to edge flute.
16	163	5.8	0	4 54	$3.76 \times 10^6$	5.43 (2468)	.090"	.465"	Failure of top doubler across flute direction.
17	160	5.4	0	45 43	$3.35 \times 10^5$	5.50 (2497)	.091"	.460"	Failure of bottom doubler across flute direction.
18	163	4.5	0	4 40	$3.47 \times 10^4$	5.42 (2461)	.090"	.457"	Right edge failure through bolt hole due to aluminum frame failure.
19	160	5.3	1	5 38	$4.88 \times 10^5$	5.28 (2400)	.082"	.460"	Failure of bottom doubler across flute direction.
20	160	5.0	0	42 53	$3.21 \times 10^5$	5.14 (2323)	.093"	.462"	Failure of bottom doubler across flute direction and extending into body of panel.
21	156	3.8	20	0 0	$8.92 \times 10^6$	5.43 (2467)	.090"	.465"	No failures.

TABLE XIITYPE III GLASS FIBER PANELS STRESS SUMMARY

<u>PANEL No.</u>	<u>SPL</u>	<u>MIDPANEL STRESS*(kpsi)</u>	
2	156 db	3.9	
9	156 db	3.7	
12	156 db	3.4	Avg. 3.76
13	156 db	4.0	
21	156 db	3.8	
4	157.5 db	4.4	
5	157.5 db	4.2	Avg. 4.16
6	157.5 db	4.2	
7	157.5 db	4.1	
10	157.5 db	3.9	
1	160 db	---	
3	160 db	5.3	
14	160 db	5.3	Avg. 5.26
17	160 db	5.4	
19	160 db	5.3	
20	160 db	5.0	
8	163 db	6.6	
15	163 db	6.2	Avg. 6.20
16	163 db	5.8	
11	163 db	6.2	
18	163 db	4.5 (low)	

\*No. 1 Strain Gage Transverse-to-Flute Direction

## REFERENCES

1. "Light Armed Reconnaissance Airplane (COIN) Glass Fiber Reinforced Plastic Supplementary Proposal". North American Aviation, Columbus Division, unpublished report. North American Report No. NA64H-6-1, 9 March 1964.
2. "YAT-28E Glass Fiber Reinforced Plastic Aircraft Proposal". North American Aviation, Columbus Division, unpublished report. North American Report Number NA64H-366, 19 June 1964.
3. Lin, Y.K., "Free Vibrations of Continuous Skin Stringer Panels", Journal of Applied Mechanics, December, 1960.
4. Van Dyke, J.D., Fshleman, A.L., Structural Design for Acoustic Fatigue. Douglas Aircraft Co., Long Beach, California. Report No. ASD-TDR-63-820, October, 1963.
5. Jones, C.R., "Revised Lifting Surface Optimization Program". North American Aviation, Columbus Division, unpublished report. Report No. SMMR TM-21-62, Nov., 1962.
6. Stotler, C.L., "Optimization of Composite Fiberglass Laminates". North American Aviation, Columbus Division, unpublished report. Report No. AM-TM-15-64.
7. R.Roark, Formulas for Stress and Strain, McGraw Hill Book Company, Inc., 1954.
8. MIL-HDBK-17, Plastics for Flight Vehicles, 1 May 1964.



## APPENDIX A - TEST SET-UP AND INSTRUMENTATION

### Discrete Frequency Siren Test Set-Up

A simplified block diagram of the discrete frequency siren test set-up is shown on Figure 80. A view of the sonic fatigue test fixture with a glass fiber panel installed is shown on Figure 81. The nut plates employed for panel attachment were generally very satisfactory and only rarely failed. Each panel was installed using a power wrench which greatly reduced panel installation time. All microphones were calibrated regularly using Altec Type 12185 Acoustic Calibrator whose calibration is traceable to a secondary standard. Standard test instruments such as voltmeters were calibrated at least once each month during the test.

### Dynamic Strain Measurements

A simple two arm dynamic strain measuring bridge, Figure 82, was used for all strain gages.

If

$V_B$	=	Battery Voltage
$R_B$	=	Ballast Resistance ( $R_B = 120$ ohm)
$R$	=	Strain Gage Resistance ( $R = 120$ ohm)
$F$	=	Gage Factor ( $F = 2$ )
$E_O$	=	Gage Output (Volts)
$E$	=	Young's Modulus of Panel Material

We have: 
$$E_O = V_B \left[ \frac{R}{R + R_B} \right] \quad (1)$$

$$\frac{dE_O}{dR} = V_B \left[ \frac{R + R_B - R}{(R + R_B)^2} \right] = \frac{V_B R_B}{(R + R_B)^2} \quad (2)$$

Since for dynamic applications strain gages are used within their linear range,

$dE_O$  and  $dR$  may be replaced by  $\Delta E_O$  and  $\Delta R$ , respectively.  
By definition:

$$\text{Gage Factor } F = \frac{\Delta R}{R} \div \frac{\Delta L}{L}$$

where  $\frac{\Delta L}{L} = \epsilon = \text{strain} \quad (3)$

$$\epsilon F = \frac{\Delta R}{R} \quad (4)$$

$$\Delta R = \epsilon FR$$

# Contrails

From equation (2)

$$\Delta E_o = \frac{V_B F_B \Delta R}{(R + R_B)^2} = \frac{V_B R \epsilon F R}{(R + R_B)^2} \quad (5)$$

Setting  $R_B = R$

$$\Delta E_o = \frac{V_B R^2 \epsilon F}{4R^2} = \frac{V}{4} \cdot \epsilon \cdot F \quad (6)$$

Now strain  $\epsilon = \frac{\text{stress}}{E}$

$$\therefore \Delta E_o = \frac{V_B}{4} F \times \frac{\text{Stress}}{E} \quad (7)$$

$$\text{Stress} = \frac{4 \cdot \Delta E_o \cdot E}{V_B F} \quad (8)$$

Example:

For aluminum panels  $E \approx 10^7$  psi.

If  $V_B = 12$  volts  
and  $F = 2$

For 1 psi stress

$$E_o = \frac{12 \times 2}{4 \times 10^7} \times 1 \text{ volts.}$$

$$E_o = \frac{12 \times 2}{4 \times 10^7} \times 10^4 \text{ for 10,000 psi}$$

$$E_o = 6 \times 10^{-3} \text{ volts.}$$

If a gain of x 100 is used to amplify the strain gage signal, we have

$$E_o = 6 \times 10^{-1} = 0.6 \text{ volts} = 600 \text{ millivolts.}$$

For 10,000 psi on the aluminum panels

$$\text{Strain } \epsilon = \frac{\text{Stress}}{E} = \frac{10^4}{10^7} = 10^{-3} \text{ in/in.}$$

$$= 1000 \text{ microinches/in.}$$

For 5,000 psi on the glass fiber panels

$$\text{Strain } \epsilon = \frac{\text{Stress}}{E} = \frac{5 \times 10^3}{2.33 \times 10^6} = 2,150 \text{ microinches/in.}$$

The high strains in the glass fiber panels (over 20 percent for 5000 psi stress level) resulted in premature failures of the Budd C-12-141 5% elongation strain gages, which were employed for the aluminum panels. The Budd Type HE-141 high elongation strain gages (15% elongation) were a considerable improvement, however, they could only be considered marginal for the glass fiber panels in this program, since many premature gage failures were encountered, particularly at the higher sound pressure levels. A close-up view of a typical HE-141 gage failure is shown on Figure 83. It should be noted that the cracks through the grid of this gage are not visible to the naked eye.

### Damping Measurements

Damping measurements and panel mode shapes were investigated using a bungee cord-suspended frame driven by a pair of 50 lb. shakers, Figure 84. An alternate method using a large 18 inch loudspeaker to excite the panels in the siren test section gave much more satisfactory decay traces.

### Test Equipment List

Microphones:	Altec Lansing 21BR-180
Microphone Power Supply:	Altec Lansing, Model 525B
Microphone Calibration:	Altec Lansing, Model 12185
Console SPL Meter:	General Radio
Audio Frequency Spectrometer:	Bruel and Kjaer Model 3311
Tape Recorder:	Ampex FR 1100
True R.M.S. Voltmeter:	Ballantine Model 320
Harmonic Analyzer:	T.P.C. Model 625
Log Converter:	Moseley, Model 60D
X-Y Plotter:	Moseley, Model 2D-2
Accelerometers:	1 Glennite Model A3109
Accelerometer Amplifier:	Statham Model 270907
Shakers:	MB Model C.31 24 lb.
Signal Generator:	Hewlett Packard Model 201C
Counter:	C.M. C. Model 203A
Accelerometer Amplifier:	Statham Model 270907
Strain Gages:	Budd Type C12-141 and Budd Type HE-141
Decade Amplifier:	Ballantine Model 220B
Oscillograph:	C.E.C. Model 5-124 12 Channel
Oscilloscope:	Tektronix Model 502 Dual Beam

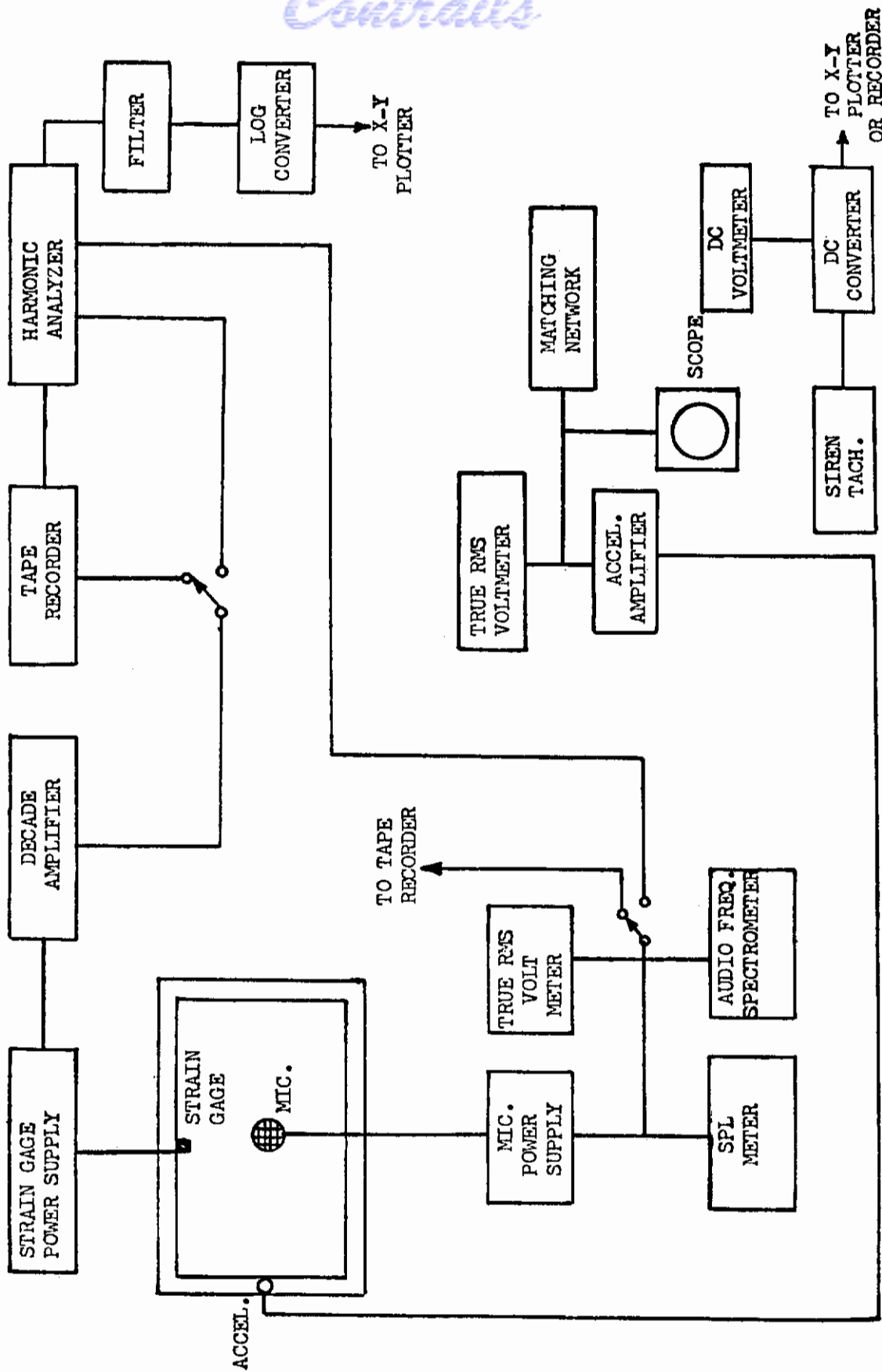


Figure 80. Simplified Block Diagram of Siren Test Set-up

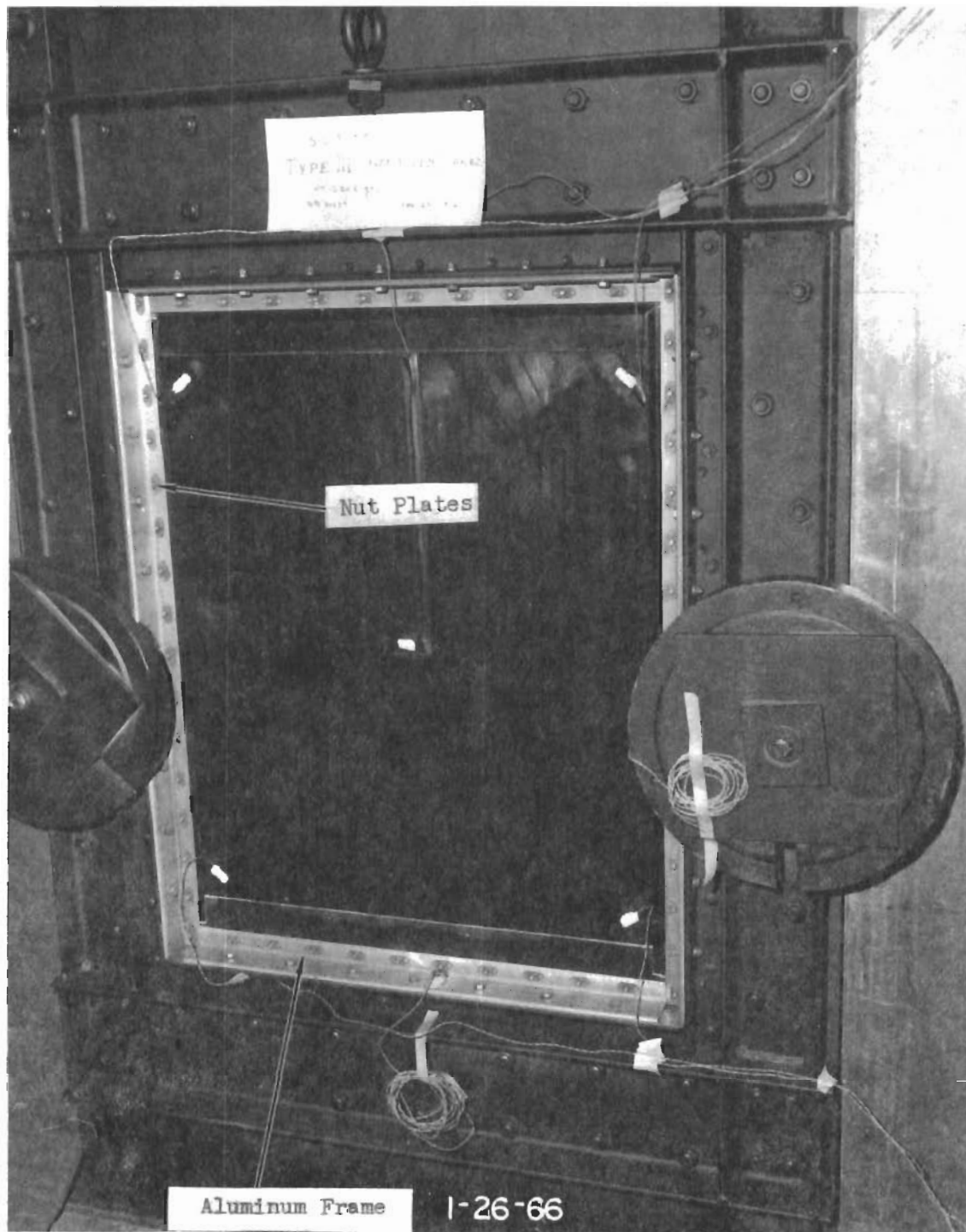


Figure 81. View of Sonic Fatigue Test Fixture with Glass Fiber Panel Installed

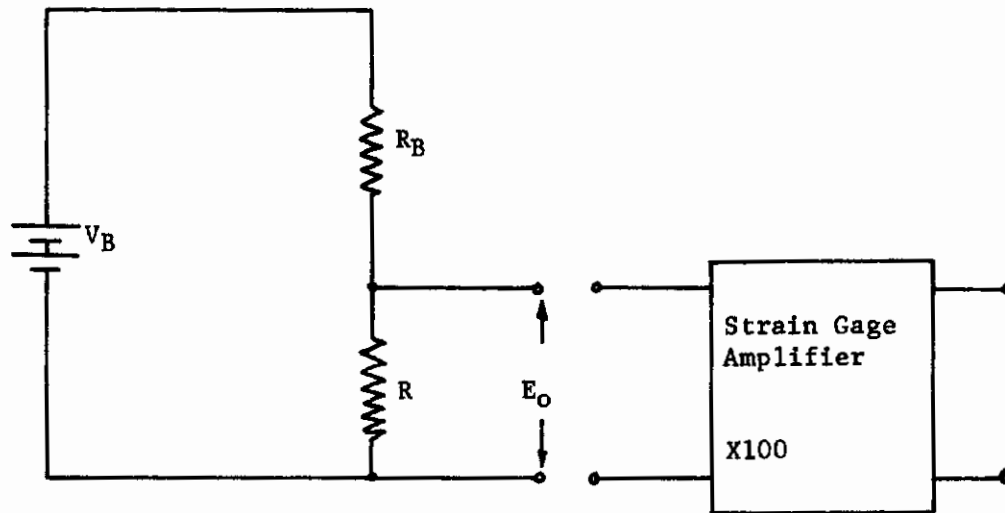


Figure 82. Dynamic Strain Gage Circuit



Figure 83. Typical HE-141 Strain Gage Grid Failure

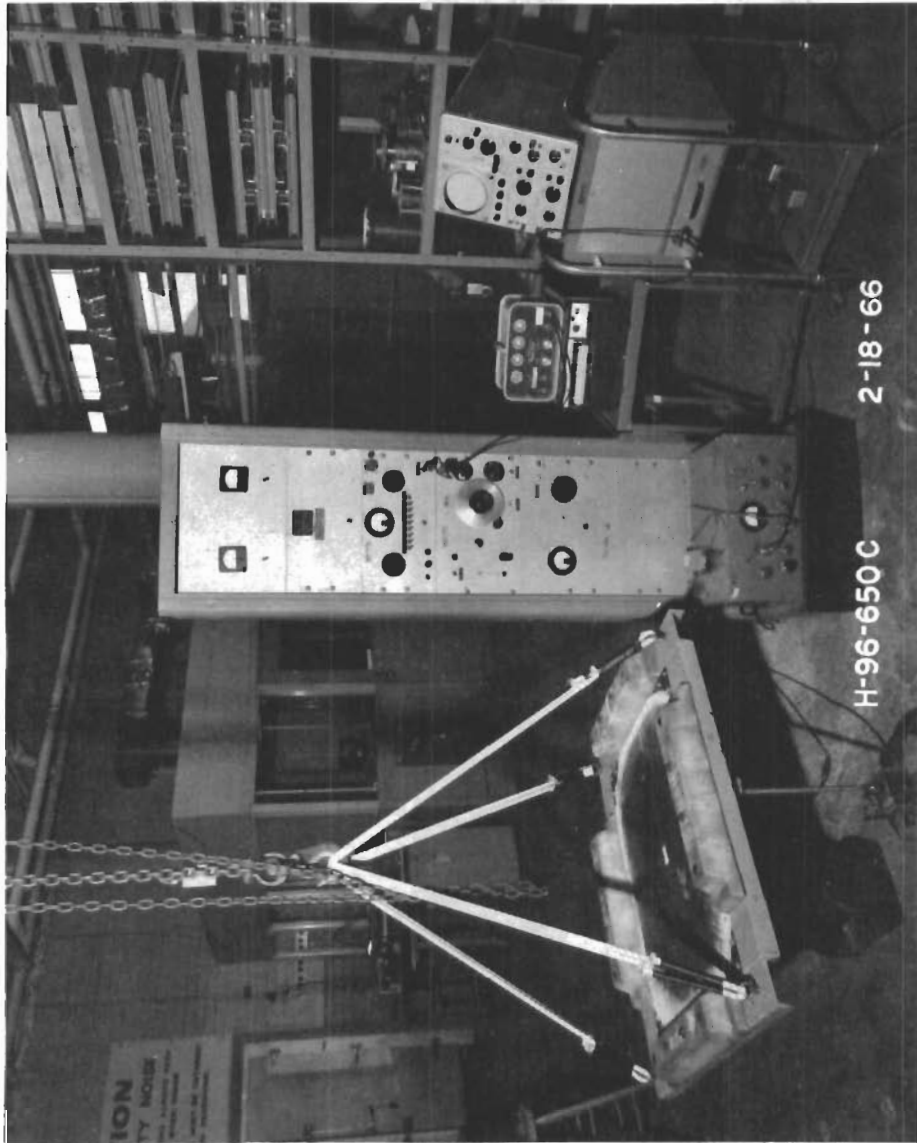


Figure 84. Test Set-up Panel Mode Shape and Damping Measurements



## APPENDIX B - GLASS FIBER PANELS STRUCTURAL OPTIMIZATION

### INTRODUCTION

A structural optimization study was undertaken in order to determine the optimum design configuration\* of each of the three fluted core sandwich sonic fatigue test panel designs, Type I, Type II and Type III. The aluminum control panel design, Figure 2, was used as a basis for determining bending moment requirements for the glass fiber panels. The results of the evaluation of the aluminum control panel design were used as a basis for the design of all three types of glass fiber panels in the program.

### DISCUSSION

Lifting Surface Optimization Program - The strength of the various panels described herein was established by means of the Revised Lifting Surface Design Optimization Program (Reference 5). This program optimizes, for input values of bending moment, the dimensions of the skin panels of a box beam. Since the panels used in the sonic fatigue program are established at 24" x 30" in size, these data served as fixed input. The program was then used to determine the required skin thickness or core depth versus bending moment. The box beam size chosen for the study is shown in Figure 85.

The loads input to the box beam optimization program are in the form of bending moments. The edge load per inch of chord of the beam shown in Figure 85 is given by

$$C = T = \frac{M}{24 \times 5}$$

where

C = Compression load per inch of skin on the upper panel

T = Tension load per inch of skin on the lower panel

In the actual testing of the sonic fatigue panels, the loading approximates a uniform pressure over the entire panel. Assuming a maximum sound pressure level of 170 db to be employed, this pressure will amount to approximately 1.4 psi peak. For this pressure, on the aluminum stiffened skin panel shown in Figure 86, the stress along the short side (Reference 7) is given by:

$$s = \frac{0.25 \text{ } wb^2}{t^2}$$

\*Optimum for end loading in the flute direction.

# Contrails

where

S = stress (psi)  
w = unit air pressure on the panel (psi)  
b = sub panel width (inches)  
t = panel skin thickness (inches)

For the case of a maximum uniform sound pressure the panel might conceivably see (approximate peak pressure at 170.8 db = 1.4 psi) the stress is:

$$S = \frac{0.25 (1.4) (6.33^2)}{(.032^2)} = 13,700 \text{ psi}$$

In terms of edge loading, this stress is equal to:

$$p = 13,700 (.032) = 439 \text{ \#/in.}$$

This load, in turn, results in a bending moment of

$$M = (24)(5)(439) = 52,800 \text{ in-lb.}$$

This bending moment represents, then, the static bending moment causing edge loading equivalent to that caused by the expected 1.4 psi normal pressure.

The approach to the problem was to establish the allowable bending moment for the aluminum panel and then to optimize a glass fiber panel on that bending moment. In order to determine the allowable strength of the aluminum panel, the existing gages of the panel were input to the program as minimum values. The program searches for optimum thicknesses, but will not attempt to optimize on any thickness below a minimum gage. Thus, as successively larger bending moments were supplied to the cross section, the optimization program supplied either the optimum gage for the panel or the minimum gage if the bending moment was so low as to cause the optimum gage to be less than the prescribed minimum gage. The highest bending moment for which the minimum gage was specified for the panel was then taken as the allowable bending moment for the aluminum panel.

Using bending moments in the range of the aluminum panel allowable bending moment as input, the desired configuration of the fiber glass panel was then input to the optimization program. The configuration chosen for the fiber glass panels was corrugated sandwich, with fluted core being the particular glass corrugation. The weaves chosen for the panel were 181 and 151. These are considered desirable weaves for a panel subjected to normal loading due to the near equality of strength in the orthogonal warp and woof directions.

Laminate Orientation Optimization Program - A second computer program, (Reference 6), was used to provide the optimum orientation of skin laminates for any value of edge loading on a panel. The program optimizes the direction of a laminate and then subtracts the strength of that laminate from the loads. This process is continued until the loads are accounted for. If the panel has a core, the strength of the core is input to the program and is accounted for by the program during the optimization process.

Panel Designs - The panel designs arrived at through use of the two optimization computer programs involve a combination of load capability. The core chosen was one which indicated a lesser bending moment capability than the aluminum panel allowable bending moment. The remainder of the load is then taken up by the necessary number of skin laminates prescribed by the laminate optimization program.

The panels\* designed by the procedures described in the preceding paragraphs are as follows:

- Type I - 181 weave, fluted core, non-foam filled.  
Two laminates of 181 weave on each surface of the panel, at angles of  $-45^{\circ}$  and  $+45^{\circ}$ .
- Type II - Identical to Type I except for being foam filled.
- Type III - 151 weave, fluted core, non-foam filled.  
Three laminates of 151 weave on each surface of the panel, at angles of  $-45^{\circ}$ ,  $+45^{\circ}$  and  $-90^{\circ}$ .

Panel Weights - The term "structurally equivalent" panel can be construed to mean "equal strength" or "equal weight". From the standpoint of sonic fatigue, it was felt that an equal weight equivalence should be established, with an eye toward the resulting strength to weight ratio. The aluminum panels, previously established in a study of aluminum sonic fatigue panel capabilities, all had a target weight of 1 lb./sq. ft. Thus, in a panel with an area of 2.0 ft. by 2.5 ft., the weight of the several aluminum panels should approximate 5 lb. Since weight is a factor in the optimization program, the weights of the various panels are known. Based upon the input data to the Lifting Surface Optimization Program, the computed weight is 4.67 pounds. This is based, of course, on an idealization of the panel. Some difference in weight is to be expected between the computed weight and the actual weight except in the case of a panel composed of a thick sheet without stiffeners. A second aluminum panel was also investigated to establish a comparison with the stiffened skin aluminum panel. This panel is a honeycomb sandwich panel and is available in three configurations varying in skin thicknesses. The computed weight of this panel is 3.45 pounds for a panel having the same strength as the stiffened skin panel. The allowable bending moment for the existing

\*These designs were later modified to meet surface weight requirements.

# Contrails

sandwich panel was computed to be 1.75 times higher than that of the skin-stringer panel. This was based upon stability considerations in the optimization program, however, and does not necessarily reflect a sonic fatigue strength comparison.

The weight of the Type I glass fiber panel was calculated by the optimization program to be 4.59 pounds, while the weight of the Type II glass fiber panel was 5.33 pounds. The difference here is the weight of 6 pound density Zerocel foam included in the Type II panel. The panel strengths are higher than the strength of the aluminum stiffened skin panel and are designed here for weight compatibility. Here again, the strengths are based upon panel buckling allowables. The weight of the Type III panel, constructed from 151 weave material at 0.007 inches per laminate rather than the 0.010 inches per laminate of the 181 cloth in the Types I and II panels, is 4.67 pounds. This panel is structurally equivalent, from panel buckling consideration, to the Types I and II panels.

The original intention of the optimization procedure was to produce glass fiber panels having the same strength as the existing aluminum control panel. This was decided upon so that some commonality would exist between the glass fiber and aluminum panels. There are currently no methods available which permit the design of a glass fiber panel to a desired sonic fatigue strength. Because of this, it is difficult to substantiate compatibility of the glass fiber and aluminum panels from a sonic fatigue standpoint based upon equivalence established on an equal strength basis.

During the evolution of the optimization process on the glass fiber panels, it was decided to make up panels which had the same weight as the aluminum panel rather than the same strength. Thus, the sonic fatigue comparison is reduced to a pound for pound situation. This has resulted in the construction of glass fiber panels which are, from a structural standpoint, only 2.4 times stronger than the existing aluminum test panel. The value of any data obtained in this manner must be questioned as to its usefulness. Certainly any future use of glass fiber to replace metal in structural applications must be based upon the advantages of the glass fiber, mainly weight savings. It would be unlikely that a metal component would be replaced by a glass fiber component of equal weight. The only likelihood of such an occurrence would be the replacement of a minimum gage metal panel by a glass fiber panel. This would imply the presence of a stability condition such as panel flutter. In general, the use of a glass fiber component to replace a metal component would result in a weight reduction. This is, of course, predicated on the use of the glass fiber in components which can employ the material efficiently. Thus, any comparison between a metal and a glass fiber component will not be made on a pound for pound basis, but on the basis of efficient structural design.

In order to have any grounds for comparison between the aluminum and the glass fiber panels, some common parameter must be chosen. From this

standpoint, it would appear that a strength/weight ratio comparison would be adequate. The comparison of the sonic fatigue life of aluminum versus glass fiber cannot, of course, be established from the one strength/weight ratio data point made available by these tests. Much more work is required to establish the entire range of strength/weight ratio variation for the materials. The number of parameters is high in such a study, and considerable time and effort will have to be devoted to this problem in the future to provide a systematic approach to design for sonic fatigue in composite structures.

## DESCRIPTION OF LIFTING SURFACE OPTIMIZATION PROGRAM

This optimization program consists of four sub-programs defining five different configurations. The configurations are:

- (a) Honeycomb Sandwich-Multispar Construction
- (b) Solid Skin Multispar Construction
- (c) Stiffened Panel Multi-rib Construction
- (d) Corrugation Sandwich Multispar Construction
- (e) Corrugation Sandwich Multi-rib Construction

The structural weight of each configuration is assumed, for optimization purposes to consist of (1) upper skin panel weight, (2) lower skin panel weight, and (3) weight of supporting structure, which may be ribs or spars depending on the specific structural configuration. Fixed inputs to the program include:

- (a) External section dimensions
- (b) Upward and downward section bending moments
- (c) Material properties
- (d) Supporting structure thickness

The structural design criteria for both the upper and lower skin panels include compression buckling failure at a stress level equal to or less than the allowable compression yield stress and also tension failure.

Output from the program includes the complete dimensional details of the optimized structural cross section, operating tensile and compressive skin panel stresses, section bending and torsional stiffness, and section weight per unit length.

A sample set of output data from the Lifting Surface Optimization Program is shown in Tables XIII through XV. This particular output is for 151 weave material. The box beam used in the analytical study is shown in Figure 85. The geometry of this box beam plus a set of bending moments representing various panel edge loads were input into the program. The output for the problem is given in Tables XIII through XV. In Table XIII is shown a tabulated resume of the input data. Material property data are

# Contrails

given above the table. Included in these data is the material minimum thickness, in this case 0.007, the thickness of one lamination of the woven fabric. The semi-span, 30 inches, is shown on Figure 87. The density  $\rho$  (rho), of the material is given, as well as the shear modulus, yield stress, ultimate stress, and elastic modulus. Also given are the end fixity coefficient (KC) of the panel, and the Ramberg-Osgood coefficient (small m) of the material. Table XIII gives a reading of the upward bending moment (M), the ratio (small k) of the downward to the upward bending moment, the box beam width (CS), the height (H) of the box beam, the thickness (TW) of the side beam, the thickness (TW) of the side beams of the box, the fixed distance, LO, between supporting ribs, and a case number describing the design parameters. The values are given for each of the eleven stations used in the problem.

Tables XIV and XV present dimensional data and stresses for the upper and lower box beam panels. In Table XIV is shown the skin thickness and the sandwich depth for the upper and lower panels. Also, the length of each panel is given. The values of weight per running inch of panel (ARHO) are also given. These values include the weight of the supporting structure.

The stresses, both tension and compression, in the upper and lower panels are given in Table XV. Also included are the stiffness values EI and GJ. The total weight (SUM ARHO DS) of the ten panels is also tabulated. Comparison of the results of the optimization procedures from the aluminum panel and the glass fiber panel allows for rapid equivalence. It can be seen from the print-outs that the dimensions are available for equal input loads and also, through use of the weight print-out, panels of equal weight can be chosen.

## DESCRIPTION OF LAMINATE ORIENTATION OPTIMIZATION PROGRAM

This computer program is used to determine the required number of laminates in a panel and to provide the optimum orientation of each laminate. The approach is to determine the axial and shear loads at all angles and then provide the required strength at these angles in the most efficient manner. The spanwise and chordwise loadings are resolved into normal and shear loads through 180 degrees in five degree increments, using the basic equations of the Mohr's circle technique. A basic reference axis system was chosen with X-axis in the spanwise direction and the Y axis in the chordwise direction. The spanwise and chordwise loadings are then resolved into normal and shear loads through 180 degrees in five degree increments, using the following equations from Reference 6.

$$P_s' = \left[ \frac{(P_x - P_y)^2}{2} + P_{xy}^2 \right]^{\frac{1}{2}} \quad (1)$$

# Contrails

$$\text{TAN } 2\theta_p = 2P_{xy} / (P_y - P_x) \quad (2)$$

$$P_N = \frac{P_x + P_y}{2} + P_s' \text{ COS } 2(\theta_p - \theta) \quad (3)$$

$$P_{xy} = P_s' \text{ SIN } 2(\theta_p - \theta) \quad (4)$$

where

$\theta_p$  = angle of principal axis measured CCW from the X axis

$\theta$  = angle CCW from X axis for which  $P_N$  and  $P_{xy}$  are being calculated

$P_x$  = spanwise loading in pounds per inch (plus is tension)

$P_y$  = chordwise loading in pounds per inch

$P_{xy}$  = shear flow in pounds per inch (plus is from right to left looking from the origin along the X-axis)

$P_N$  = load normal to plane inclined at an angle  $\theta$  from the X-axis

$P_s$  = shear load corresponding to  $P_N$

Since  $P_N$  is the normal load, it was shifted through 90 degrees to obtain the axial load. After the axial load diagrams are generated for each condition, two composite conditions are selected which represent the maximum tension and compression loadings for all input conditions.

Material properties are calculated at five degree intervals from the warp direction for each input material. The following equation was modified from those given in Reference (8).

$$\frac{1}{(F_x)^2} = \frac{\text{COS}^4\theta}{(F_\alpha)^2} + \frac{\text{SIN}^4\theta}{(F_\beta)^2} + K \left[ \frac{1}{(F_{\alpha\beta})^2} - \frac{1}{F_\alpha F_\beta} \right] \text{SIN}^2\theta \text{COS}^2\theta \quad (5)$$

where

$F_x$  = allowable axial stress at angle  $\theta$  from the warp direction

# Contrails

- $F_{\alpha}$  = allowable axial stress in the warp direction  
 $F_{\beta}$  = allowable axial stress in the woof direction  
 $F_{\alpha\beta}$  = allowable shear stress  
 $K$  = a constant dependent on the material

Note  $F_x$  will be either tension or compression depending on what values of  $F_{\alpha}$  and  $F_{\beta}$  are used.  $K$  is approximately 1 for woven materials but is very small (.01 to .04) for unweaved uni-directional materials.

For any common glass fiber material the greatest strength is in the warp direction for woven materials and in the fiber direction for uni-directional material. The angle of maximum applied load is determined from the composite load conditions and the warp of each material is located in turn in this direction. A pounds per inch allowable is determined for each laminate at five degree intervals and an applied load versus allowable load ratio is calculated for each of these angles. These ratios are summed up over 180 degrees for both tension and compression for each material. Each sum is divided by the appropriate laminate thickness to make the materials directly comparable from a strength-weight standpoint. The material which produces the smallest strength ratio sum is the most efficient. The allowable load diagram for this material is subtracted from the composite load diagrams and the above process is repeated until the composite laminate is sufficiently strong in all directions.

If a sandwich structure is to be used which has a core of some significant strength, such as an integrally woven fluted core, the major strength direction of the core is assumed to be in the spanwise direction. The allowable load for the core is calculated in the same manner as for any material laminate as previously described. This core allowable strength is subtracted out of the composite load diagrams and the procedure is then the same as described for a solid laminate.



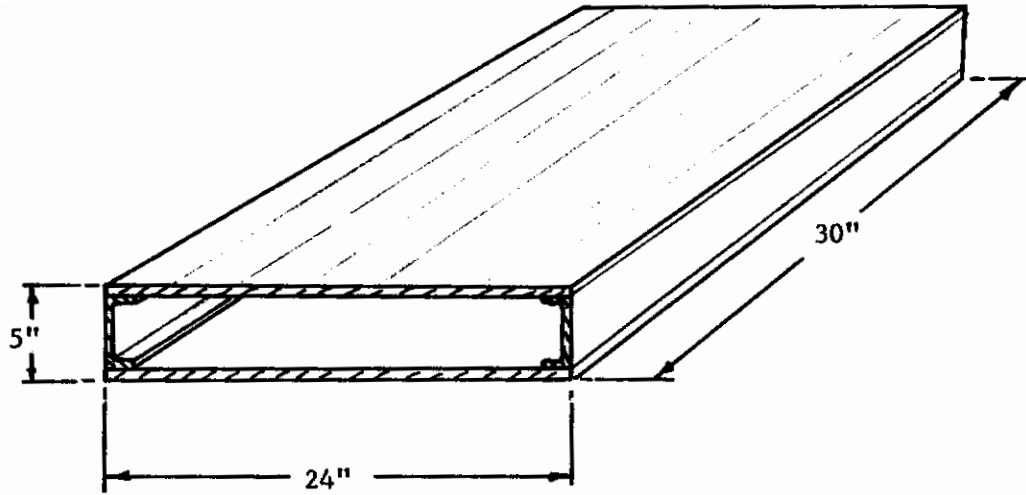


Figure 85. Lifting Surface Optimization Program Box Beam

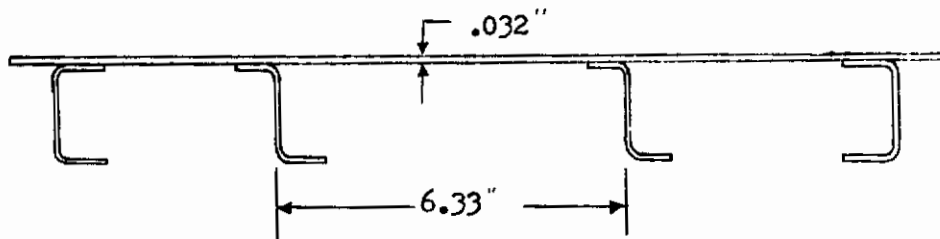


Figure 86. Aluminum Control Panel Cross Section

## Calculation of Edge Stresses

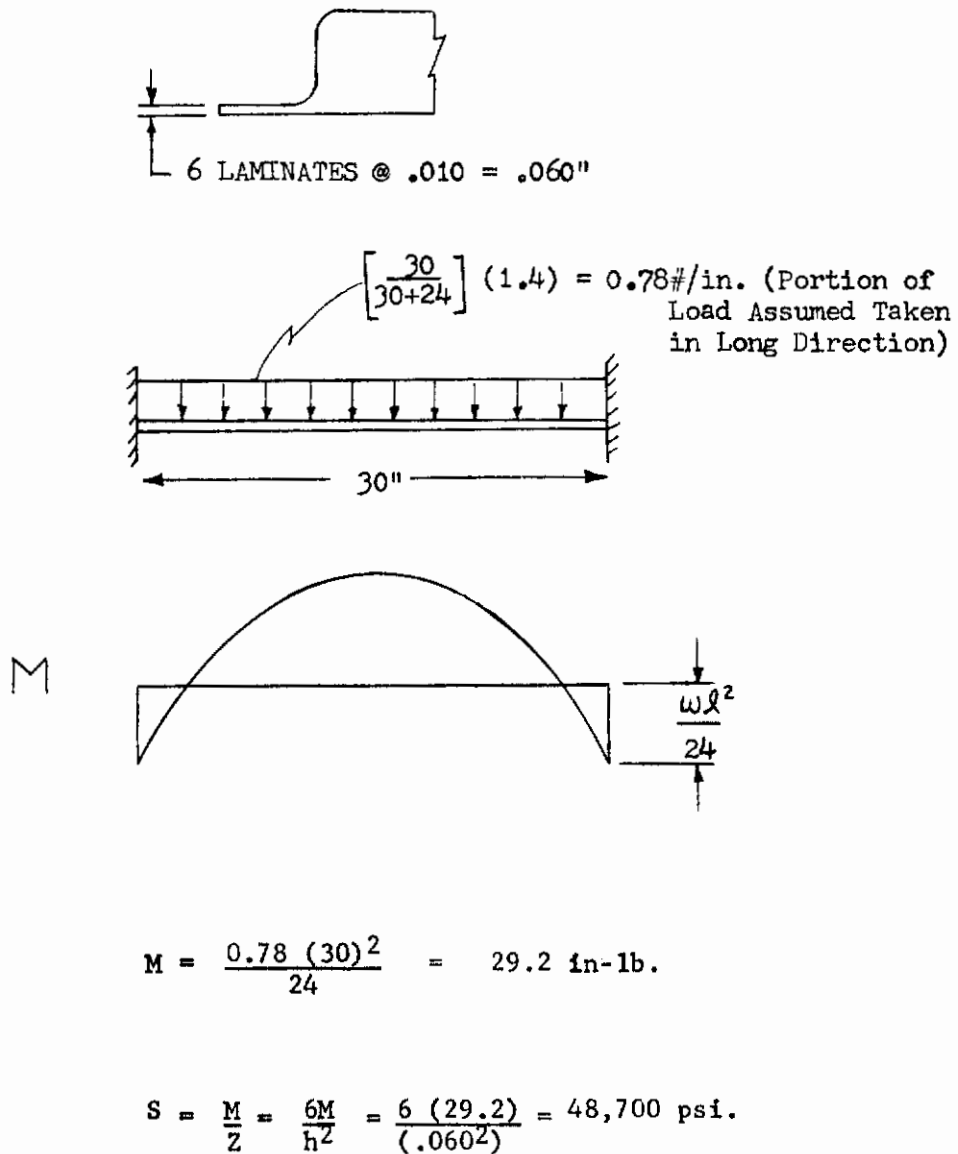


Figure 87. Box Beam Glass Fiber Panel, Load and Bending Moment Diagrams.

TABLE XIII

IBM 7090 LIFTING SURFACE OPTIMIZATION PROGRAM INPUT AND OUTPUT DATA

CORRUGATION SANDWICH MULTIR CONSTRUCTION

STATION	M	SMALL K	CS	H	TW	LO	CASE NO.
0	0.6000E 05	0.20000E-CC	0.2400E 02	0.5000E 01	0.1000E-00	0.3000E 02	01-01-10
1	0.9000E 05	0.20000E-CC	0.2400E 02	0.5000E 01	0.1000E-00	0.3000E 02	01-01-10
2	0.1200E 06	0.20000E-CC	0.2400E 02	0.5000E 01	0.1000E-00	0.3000E 02	01-01-10
3	0.1500E 06	0.20000E-CC	0.2400E 02	0.5000E 01	0.1000E-00	0.3000E 02	01-01-10
4	0.1800E 06	0.20000E-CC	0.2400E 02	0.5000E 01	0.1000E-00	0.3000E 02	01-01-10
5	0.2100E 06	0.20000E-CC	0.2400E 02	0.5000E 01	0.1000E-00	0.3000E 02	01-01-10
6	0.2400E 06	0.20000E-CC	0.2400E 02	0.5000E 01	0.1000E-00	0.3000E 02	01-01-10
7	0.2700E 06	0.20000E-CC	0.2400E 02	0.5000E 01	0.1000E-00	0.3000E 02	01-01-10
8	0.3000E 06	0.20000E-CC	0.2400E 02	0.5000E 01	0.1000E-00	0.3000E 02	01-01-10
9	0.3300E 06	0.20000E-CC	0.2400E 02	0.5000E 01	0.1000E-00	0.3000E 02	01-01-10
10	0.3600E 06	0.20000E-CC	0.2400E 02	0.5000E 01	0.1000E-00	0.3000E 02	01-01-10

TC	0.7000000E-02	RHO	=	0.6750000E-01	FCY	=	0.5619999E 05
SEMI SPAN	0.3000000E 02	KC	=	0.1500000E 01	CAPFU	=	0.1085000E 06
MATERIAL	0.1510000E 03	G	=	0.6930000E 06	E	=	0.4610000E 07
TEMPERATURE	0.7000000E 02	SMALL M	=	0.2000000E 01			

TABLE XIV

IBM 7090 LIFTING SURFACE OPTIMIZATION PROGRAM OUTPUT DATA

CCRRLGATION SANDWICH MULTIRIB CCNSTRUCTION

STATION	TU	TL	DU	DL	L	ARHO
0	C.16838E-01	C.74153E-C2	C.75151E C0	0.49885E-00	0.3C000E 02	0.18419E-00
1	C.2C743E-01	0.51119E-C2	C.83409E 00	0.55283E 00	0.3C000E 02	0.22046E-00
2	C.24066E-01	0.1C546E-C1	C.89845E C0	0.59474E 00	0.3C000E 02	0.25129E-00
3	C.27019E-01	C.11814E-C1	C.95176E 00	0.62950E 00	0.3C000E 02	0.27864E-00
4	C.297C8E-01	C.12965E-C1	C.99817E 00	0.65945E 00	0.3C000E 02	0.30353E-00
5	C.32196E-01	0.14C27E-C1	C.10391E C1	0.68593E 00	0.3C000E 02	0.32653E-00
6	C.34524E-01	C.15C19E-C1	C.10761E 01	0.70975E 00	0.3C000E 02	0.34804E-00
7	0.36723E-01	0.15953E-C1	C.11098E 01	0.73147E 00	0.3C000E 02	0.36834E-00
8	0.38813E-01	C.16838E-C1	C.11410E C1	0.75151E 00	0.3C000E 02	0.38762E-00
9	C.40P1CE-C1	0.17683E-C1	C.11700E 01	0.77012E 00	0.3C000E 02	0.40603E-00
10	C.42726E-01	0.18451E-C1	C.11971E 01	0.78753E 00	0.3C000E 02	0.42369E-00

TABLE XV  
IBM 7090 LIFTING SURFACE OPTIMIZATION PROGRAM OUTPUT DATA

CORRUGATION SANDWICH MULTIRIB CCNSTRUCTION

STATION	FCU	FCL	FTU	FTL	EI	GJ
0	C.74236C 04	0.32656E C4	C.14847F 04	0.16848E 05	0.56980E 08	0.19282E 08
1	C.9C393E 04	0.41155E C4	C.14079E C4	0.20577E 05	0.7C045E 08	0.23706E 08
2	C.10388E 05	0.47412E C4	C.20776E 04	0.23706E 05	0.81129E 08	0.27460E 08
3	C.11566E 05	C.529C2E C4	C.23132E 04	0.26451E 05	0.9C947E 08	0.30785E 08
4	C.12623E 05	C.57846E C4	C.25246E 04	0.28923E 05	0.99866E 08	0.33807E 08
5	C.13589E 05	0.62378E C4	C.27177E C4	0.31189E 05	0.1C810E 09	0.36597E 08
6	0.14483E 05	0.66583E C4	C.28965E 04	0.33291E 05	0.11580E 09	0.39204E 08
7	0.15317E 05	0.7C519E C4	C.30635E 04	0.35259E 05	0.12305E 09	0.41663E 08
8	0.16103E 05	0.74235E C4	C.32206E 04	0.37117E 05	0.12993E 09	0.43995E 08
9	C.16846E 05	0.7776CE C4	C.33693E 04	0.3888CE 05	0.13650E 09	0.46220E 08
10	0.17554E 05	0.8112CE C4	C.35107E 04	0.4056CE 05	0.14279E 09	0.48353E 08

SUM ARHO DS = 0.95832309E 01

## APPENDIX C. GLASS FIBER PANELS MANUFACTURING DATA

The principal steps in manufacturing the glass fiber fluted core panels for sonic fatigue testing are illustrated on Figures 88 through 92.

The process begins by laying the cut and trimmed glass fabric plies on the mould surface, and positioning the core material on top, Figure 88. The top plies are now positioned, Figure 89, ready for the caul tool, Figure 90. When the caul tool is in place, a polyvinyl alcohol sheet is placed over the entire mould, and the edges are sealed with a putty-like sealant, Figure 91. The resin-catalyst mixture is now poured on the mould surface at the end of the panel and the polyvinyl alcohol vacuum bag sheet extended to cover resin mixture and panel. A vacuum is now applied at the opposite end of the panel and the entire assembly is placed in an oven for the pre-cure cycle at approximately 170°F. for 60 minutes. The resin viscosity is lowered by this heating enabling the resin to flow through the core more easily. Excess resin is absorbed by hair felt placed around the panel edges. For the cure phase, the temperature is raised to 260°F. for a further 30 minutes, when post curing for 120 minutes at 325°F is commenced. The finished core is now removed and the polypropylene mandrels extracted (in the Type I, hollow flute panels). The polyurethane foam mandrels are retained in the Type II and III panels. The core ends are now trimmed and cut off at a 60° angle ready for bonding the end close out doublers.



Figure 88. Glass Fiber Panel - Lower Surface and Core Dry Fabric Lay-up



Figure 89. Glass Fiber Panel - Upper Surface Dry Fabric Lay-up





Figure 90. Glass Fiber Panel - Caul Tool

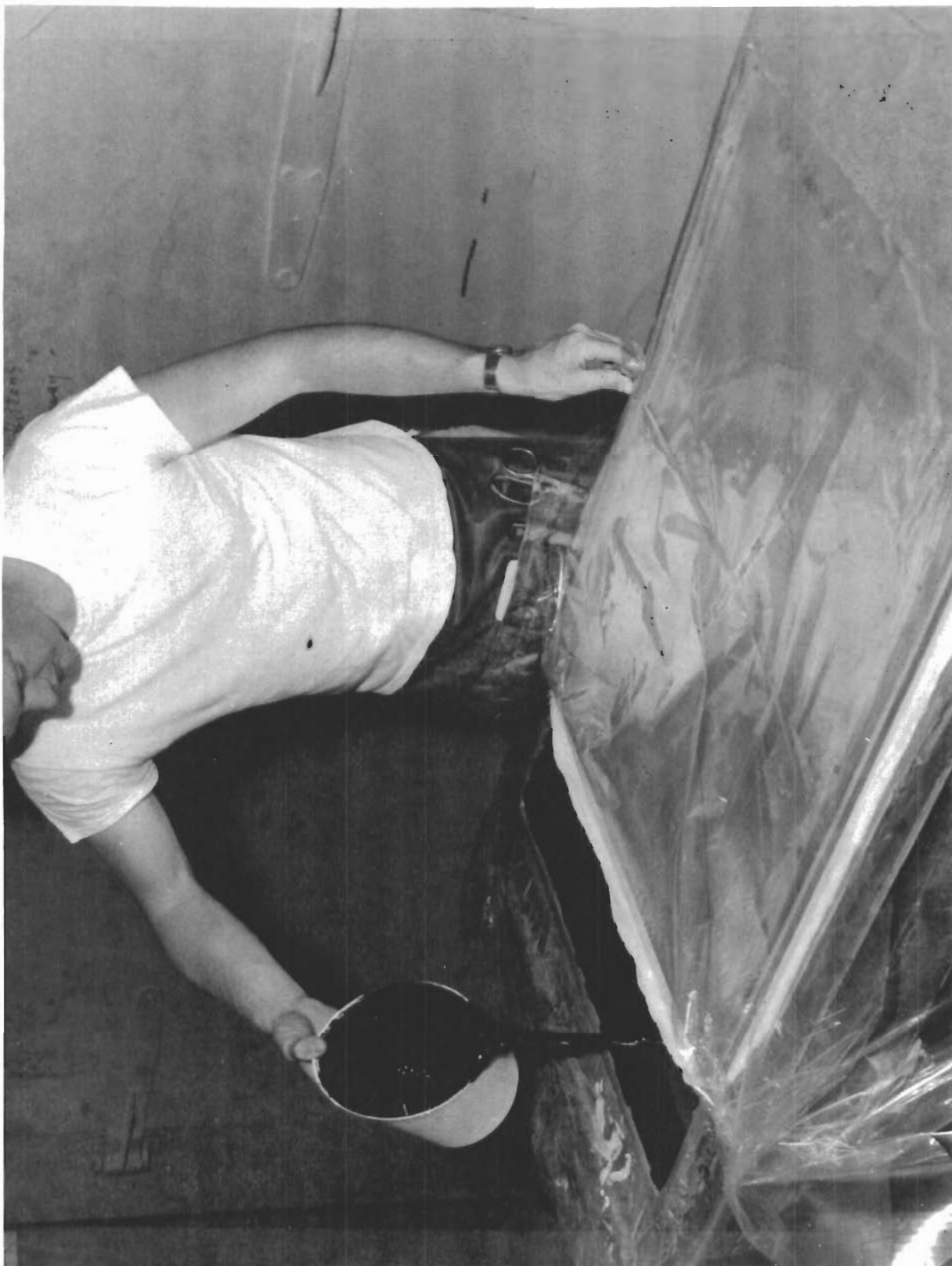


Figure 91. Glass Fiber Panel - Resin Pouring

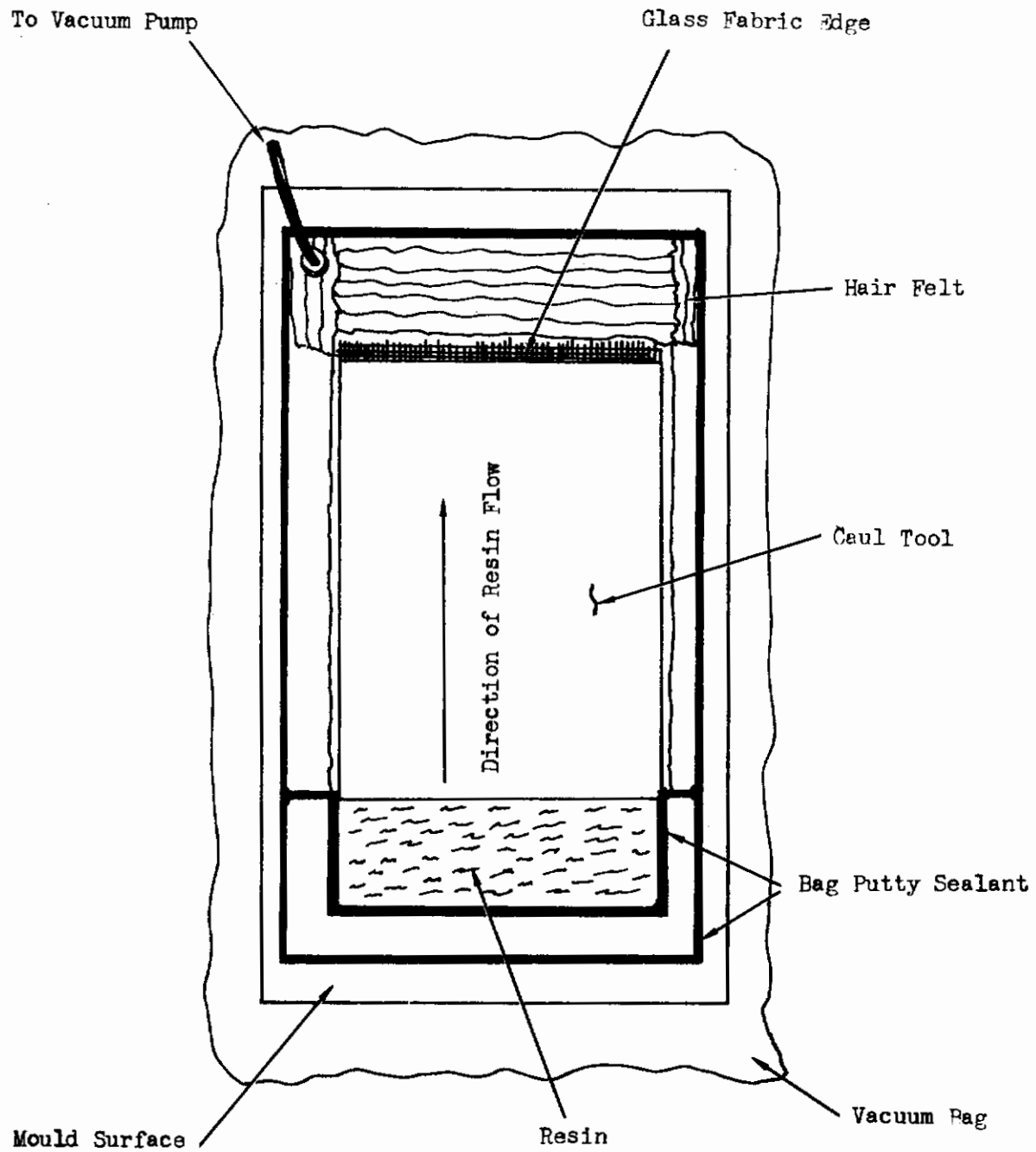


Figure 92. Diagram of Vacuum Impregnation System

## APPENDIX D

### FLUTED CORE GLASS FIBER FLIGHT VEHICLE STRUCTURAL APPLICATIONS

A number of proposals for use of fluted core glass fiber sandwich construction in aircraft, notably those in References (1) and (2), have been made in recent years. This type of construction was also included in a proposal for a glass-fiber-reinforced plastic version of the Convair Charger (COIN). Some typical structural applications of this type of construction are illustrated in Figure 93.

The wing section (OV-10A), Figure 93 uses secondary bonding for joining spars to outer skins. The tail boom section, Figure 93 is almost monocoque. This type of construction has also been proposed for fuselage structures. The outer skins may be woven glass fabric or filament wound.

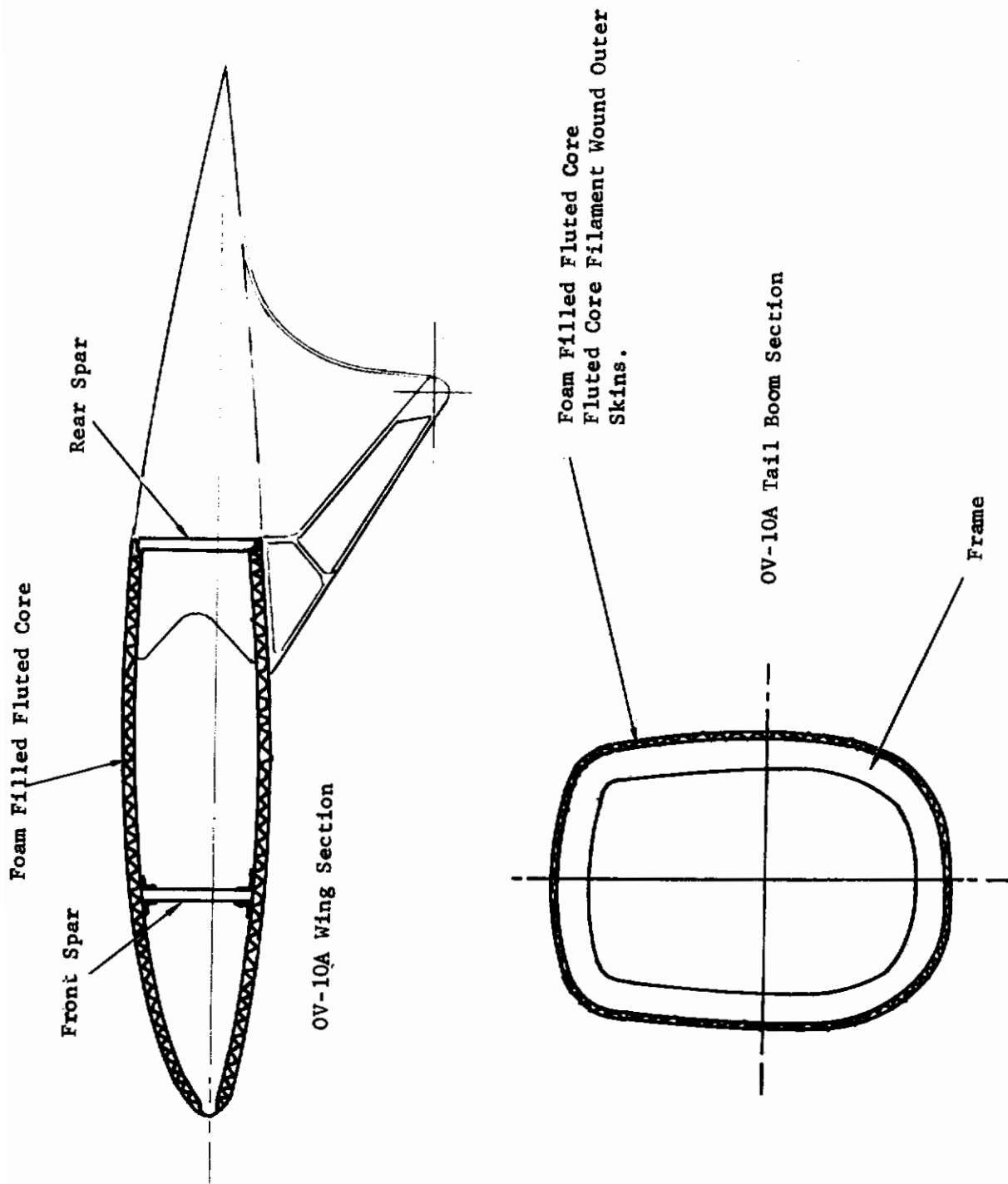


Figure 93 . Fluted Core Glass Fiber Wing and Tail Boom Sectional Views (OV-10A)

# *Contrails*

DOCUMENT CONTROL DATA - R&D

(Security classification of title, body of abstract and indexing annotation must be entered when the overall report is classified)

1. ORIGINATING ACTIVITY (Corporate author) North American Aviation, Inc. Columbus Division Columbus, Ohio		2 a. REPORT SECURITY CLASSIFICATION UNCLASSIFIED	
		2 b. GROUP N/A	
3. REPORT TITLE Sonic Fatigue Tolerance of Glass Filament Structure, Volume II Experimental Results			
4. DESCRIPTIVE NOTES (Type of report and inclusive dates) Final Report 15 May 1965 - 15 July 1966			
5. AUTHOR(S) (Last name, first name, initial)  Hayes, John A.			
6. REPORT DATE December 1966	7 a. TOTAL NO. OF PAGES 155	7 b. NO. OF REFS 8	
8 a. CONTRACT OR GRANT NO. AF33(615)-2863 b. PROJECT NO. 1471	8 a. ORIGINATOR'S REPORT NUMBER(S) AFFDL-TR-66-78,		
c. Task No. 147101 d.	8 b. OTHER REPORT NO(S) (Any other numbers that may be assigned this report)		
10. AVAILABILITY/LIMITATION NOTICES This document is subject to special export controls and each transmittal to foreign nationals may only be made with prior approval of Vehicle Dynamics Division (FDD) AF Flight Dynamics Laboratory, Wright-Patterson AFB, Ohio 45433			
11. SUPPLEMENTARY NOTES		12. SPONSORING MILITARY ACTIVITY Air Force Flight Dynamics Laboratory Wright-Patterson AFB, Ohio 45433	
13. ABSTRACT Sonic fatigue experimental test results on a series of sixty flat rectangular glass fiber sandwich test panels are presented and discussed. The panels were of the fluted core (corrugated) type, had nominal overall dimensions of 24" x 30" x 0.45", and a nominal surface weight of one pound per square foot. The fluted core glass fabric (I8I and I5IS glass) was of the integrally woven variety. A vacuum process was employed to impregnate the glass cloth with resin. Twenty each of three types of panels were sonic fatigue tested using a discrete frequency siren, five identical panels at four different sound pressure levels, to provide three S-N (Sound Pressure Level Vs. Cycles to Failure) plots. Twenty aluminum skin-stringer panels of the same overall dimensions and surface weight were similarly tested for control.			

Security Classification

14.	KEY WORDS	LINK A		LINK B		LINK C	
		ROLE	WT	ROLE	WT	ROLE	WT

**INSTRUCTIONS**

1. **ORIGINATING ACTIVITY:** Enter the name and address of the contractor, subcontractor, grantee, Department of Defense activity or other organization (*corporate author*) issuing the report.
- 2a. **REPORT SECURITY CLASSIFICATION:** Enter the overall security classification of the report. Indicate whether "Restricted Data" is included. Marking is to be in accordance with appropriate security regulations.
- 2b. **GROUP:** Automatic downgrading is specified in DoD Directive 5200.10 and Armed Forces Industrial Manual. Enter the group number. Also, when applicable, show that optional markings have been used for Group 3 and Group 4 as authorized.
3. **REPORT TITLE:** Enter the complete report title in all capital letters. Titles in all cases should be unclassified. If a meaningful title cannot be selected without classification, show title classification in all capitals in parenthesis immediately following the title.
4. **DESCRIPTIVE NOTES:** If appropriate, enter the type of report, e.g., interim, progress, summary, annual, or final. Give the inclusive dates when a specific reporting period is covered.
5. **AUTHOR(S):** Enter the name(s) of author(s) as shown on or in the report. Enter last name, first name, middle initial. If military, show rank and branch of service. The name of the principal author is an absolute minimum requirement.
6. **REPORT DATE:** Enter the date of the report as day, month, year, or month, year. If more than one date appears on the report, use date of publication.
- 7a. **TOTAL NUMBER OF PAGES:** The total page count should follow normal pagination procedures, i.e., enter the number of pages containing information.
- 7b. **NUMBER OF REFERENCES:** Enter the total number of references cited in the report.
- 8a. **CONTRACT OR GRANT NUMBER:** If appropriate, enter the applicable number of the contract or grant under which the report was written.
- 8b, 8c, & 8d. **PROJECT NUMBER:** Enter the appropriate military department identification, such as project number, subproject number, system numbers, task number, etc.
- 9a. **ORIGINATOR'S REPORT NUMBER(S):** Enter the official report number by which the document will be identified and controlled by the originating activity. This number must be unique to this report.
- 9b. **OTHER REPORT NUMBER(S):** If the report has been assigned any other report numbers (*either by the originator or by the sponsor*), also enter this number(s).
10. **AVAILABILITY/LIMITATION NOTICES:** Enter any limitations on further dissemination of the report, other than those

imposed by security classification, using standard statements such as:

- (1) "Qualified requesters may obtain copies of this report from DDC."
- (2) "Foreign announcement and dissemination of this report by DDC is not authorized."
- (3) "U. S. Government agencies may obtain copies of this report directly from DDC. Other qualified DDC users shall request through \_\_\_\_\_."
- (4) "U. S. military agencies may obtain copies of this report directly from DDC. Other qualified users shall request through \_\_\_\_\_."
- (5) "All distribution of this report is controlled. Qualified DDC users shall request through \_\_\_\_\_."

If the report has been furnished to the Office of Technical Services, Department of Commerce, for sale to the public, indicate this fact and enter the price, if known.

11. **SUPPLEMENTARY NOTES:** Use for additional explanatory notes.
12. **SPONSORING MILITARY ACTIVITY:** Enter the name of the departmental project office or laboratory sponsoring (*paying for*) the research and development. Include address.
13. **ABSTRACT:** Enter an abstract giving a brief and factual summary of the document indicative of the report, even though it may also appear elsewhere in the body of the technical report. If additional space is required, a continuation sheet shall be attached.  
  
It is highly desirable that the abstract of classified reports be unclassified. Each paragraph of the abstract shall end with an indication of the military security classification of the information in the paragraph, represented as (TS), (S), (C), or (U).  
  
There is no limitation on the length of the abstract. However, the suggested length is from 150 to 225 words.
14. **KEY WORDS:** Key words are technically meaningful terms or short phrases that characterize a report and may be used as index entries for cataloging the report. Key words must be selected so that no security classification is required. Identifiers, such as equipment model designation, trade name, military project code name, geographic location, may be used as key words but will be followed by an indication of technical context. The assignment of links, rules, and weights is optional